

UNIVERSITY OF SOUTHAMPTON
FACULTY OF MEDICINE, HEALTH & LIFE
SCIENCES
School of Medicine

Investigating the function of the retention /
retrieval, ERp57-binding and glycan-binding sites
of Calreticulin in MHC class I antigen presentation

Christopher Mark Howe

Thesis for the degree of Doctor of Philosophy

October 2007

UNIVERSITY OF SOUTHAMPTON

ABSTRACT

FACULTY OF MEDICINE, HEALTH AND LIFE SCIENCES

SCHOOL OF MEDICINE

Doctor of Philosophy

Investigating the function of the retention / retrieval, ERp57-binding and glycan-binding sites of Calreticulin in MHC class I antigen presentation

Christopher Mark Howe

Calreticulin (CRT) is an Endoplasmic Reticulum (ER) resident protein involved in intracellular calcium homeostasis and the folding of newly synthesised glycoproteins. CRT also forms part of the peptide loading complex (PLC) where it assists in Major Histocompatibility Complex (MHC) class I folding, maturation and peptide loading with the assistance of ERp57. CRT's localisation is kept in check through a C-terminal Lys-Asp-Glu-Leu (KDEL) sequence that retrieves it to the ER through the KDEL receptor.

The CRT $-/-$ mouse fibroblast cell line K42 loads MHC class I molecules and presents endogenous antigens to cytotoxic T lymphocytes inefficiently (Gao et al 2002). Importantly, the trafficking speed of the endogenous class I alleles (H-2K^b and H-2D^b) to the cell surface was shown to be faster in K42 than in its CRT $+/+$ counterpart K41; furthermore fewer MHC I were incorporated into the PLC in K42 (Gao et al., 2002), similar to a class I T134K mutant that fails to present antigen efficiently (Lewis et al., 1996). This suggests that CRT influences MHC I trafficking rate and may recruit MHC I to the PLC, ensuring efficient MHC I antigen presentation.

In this study, the role of CRT was further dissected using a series of mutant constructs that were expressed in K42 and their effects on MHC I antigen presentation determined. The mutants were designed to address three questions: the role of the c-terminus and KDEL in MHC I retention / retrieval; the importance of the interaction between CRT and ERp57; and the effect of mutation of CRT's glycan-binding site on MHC I antigen presentation.

Unexpectedly, the glycan-binding CRT mutant fully restored MHC I antigen presentation, suggesting that polypeptide interactions define CRT substrate specificity. However, efficient MHC I assembly with the PLC was shown to require an interaction between CRT and ERp57. The trafficking rate of MHC I was influenced not just by the KDEL sequence but also by the interaction between CRT and ERp57 and by undefined residues within the 11 c-terminal amino acids of CRT, consistent with a role in MHC I retention / retrieval. Cumulatively, results show that the CRT's c-terminus, KDEL sequence and ERp57 binding site, but not CRT's glycan-binding site, are obligatory for efficient MHC I antigen presentation.

Table of Contents

CHAPTER 1: INTRODUCTION.....	1
1.1 INNATE AND ADAPTIVE IMMUNITY.....	1
1.2 HUMOURAL AND CELLULAR IMMUNITY.....	2
1.3 MHC CLASS I STRUCTURE.....	4
1.4 MHC CLASS II STRUCTURE.....	6
1.5 MHC RESTRICTION.....	7
1.6 MHC POLYMORPHISM.....	8
1.7 ANTIGEN PROCESSING AND PRESENTATION.....	10
1.8 EXOGENOUS PATHWAY.....	10
1.9 CYTOSOLIC PATHWAY.....	10
1.10 ORIGIN AND GENERATION OF ANTIGENIC PEPTIDE DESTINED FOR THE CYTOSOLIC PATHWAY.....	14
1.11 CLASS I FOLDING.....	17
1.12 CLASS I ASSEMBLY.....	19
1.13 PEPTIDE LOADING COMPLEX COMPONENTS;.....	20
1.13.1 <i>Transporter Associated with Antigen Presentation</i>	20
1.13.2 <i>Tapasin</i>	21
1.13.3 <i>Calnexin</i>	22
1.13.4 <i>Calreticulin</i>	22
1.13.5 <i>ERp57</i>	25
1.13.6 <i>PDI</i>	25
1.14 MOLECULAR MODEL FOR ROLE OF PLC.....	26
1.15 THE AIMS OF THIS STUDY.....	29
CHAPTER 2: MATERIALS AND METHODS.....	30
2.1 ANTIBODIES.....	30
2.2 CELL LINES.....	33
2.3 RETROVIRAL TRANSDUCTION.....	33
2.4 BEAD PURIFICATION OF CELLS.....	34
2.5 CELL CLONING BY LIMITING DILUTION.....	34
2.6 PRODUCTION OF MUTANT CONSTRUCTS.....	35
2.6.1 <i>PCR</i>	35
2.6.2 <i>Restriction enzyme digest</i>	35
2.6.3 <i>DNA Ligation</i>	35
2.7 RETROVIRAL VECTOR.....	37
2.8 DNA SEQUENCING.....	37
2.9 FLOW CYTOMETRY.....	38
2.10 GFP-UB-SL8 ASSAY.....	38
2.11 IMMUNOBLOTTING.....	38
2.11.1 <i>Reagents common to sections 2.11-14:</i>	38
2.11.2 <i>Immunoblotting protocol</i>	39
2.12 IMMUNOPRECIPITATION (IP).....	39
2.12.1 <i>DETECTING ERP57 ASSOCIATED WITH TAP1</i>	39
2.12.2 <i>Detecting calreticulin associated with TAP1</i>	40
2.12.3 <i>The routine immunoprecipitation protocol</i>	40
2.13 PULSE-CHASE.....	40
2.14 PULSE CHASE THERMOSTABILITY ASSAY.....	41
2.15 K42CRTΔC SECRETION ASSAY.....	41
2.16 CTL ASSAY.....	41
2.17 CONFOCAL MICROSCOPY.....	42
2.18 NEM DISULPHIDE-BOND ALKYLATION.....	43
2.19 MMTS DISULPHIDE-BOND ALKYLATION.....	43
2.20 TCA DISULPHIDE TRAPPING EXPERIMENT.....	43
2.21 CELL SURFACE BFA DECAY OF H2-K ^B	44
2.21 CRT2 DETECTION BY PCR.....	44

CHAPTER 3: THE C-TERMINAL ER RETRIEVAL SEQUENCE.....	46
3.1 EFFECTS ON CLASS I ASSEMBLY AND ANTIGEN PRESENTATION.....	46
3.2 CRT-KNOCKOUT CELLS CAN STABLY EXPRESS RAT CALRETICULIN.....	46
3.3 A LOSS OF THE KDEL SEQUENCE CAUSES CRT TO BE SECRETED	51
3.4 CO-LOCALISATION WITH KDEL RECEPTOR.....	53
3.5 EFFECT ON CLASS I ASSEMBLY: C-TERMINAL CRT TRUNCATIONS IMPAIR H2-K ^B CELL SURFACE EXPRESSION	61
3.6 EFFECT ON CLASS I ASSEMBLY; TRANSDUCED CRT-DEFICIENT CELLS PARTIALLY RESTORE INTRACELLULAR MHC CLASS I CELL TRAFFICKING.	63
3.7 EXTENT OF OPTIMAL LOADING OF H2-K ^B MOLECULES THAT REACH THE CELL SURFACE IS UNAFFECTED IN THE MUTANT CONSTRUCTS.	70
3.8 LOADING OF EXOGENOUS PEPTIDE FOR PRESENTATION TO T-CELLS.....	72
3.9 ASSESSMENT OF H2-K ^B AND H2-D ^B THERMOSTABILITY	74
3.10 INTRACELLULAR PROCESSING AND PRESENTATION OF A MODEL ANTIGEN IS IMPAIRED IN CRT LACKING KDEL	77
3.11 INVESTIGATING THE REASONS FOR THE PARTIAL RESTORATION OF FULL LENGTH RAT CRT IN K42.....	79
3.12 SUMMARY	84
CHAPTER 4: THE CRT C-TERMINAL ER RETRIEVAL SEQUENCE.....	85
4.1 THE RETENTION / RETRIEVAL MECHANISM	85
4.1 PLC COMPOSITION.....	85
4.2 INTRACELLULAR TRAFFICKING OF MHC CLASS I AND CRT RETRIEVAL.	93
4.3 SUMMARY	101
CHAPTER 5: THE ERP57-BINDING AND GLYCAN BINDING SITES.....	103
5.1 THE CRT BINDING SITE FOR ERP57	103
5.2 MHC I ASSEMBLY IS IMPAIRED IN ERP57-BINDING DEFECTIVE CRT CELL LINES.....	106
5.3 PLC RECRUITMENT IS IMPAIRED IN ERP57-BINDING DEFECTIVE CRT CELL LINES.....	112
5.4 THE CRT GLYCAN BINDING SITE.....	115
5.5 SUMMARY	118
CHAPTER 6: DISCUSSION.....	119
APPENDIX 1.....	128
APPENDIX 2.....	129
APPENDIX 3.....	130
APPENDIX 4.....	131
MUTATIONAL ANALYSIS OF ERP57-CRT BINDING SITE BY MICHA HÄUPTLE, (HELENIUS LABORATORY, ZURICH).....	131
CLONING OF THE CRT(189-288)ΔEB MUTANT.....	131
EXPRESSION AND PURIFICATION OF CRT(189-288)ΔEB.....	132
STUDIES ON CRT(189-288)ΔEB.....	133
<i>Crosslinking experiments</i>	133
<i>Isothermal titration calorimetry</i>	134
<i>Interaction studies by ELISA</i>	135
REFERENCES	137

Table of Figures

Figure 1.1 The crystal structure of an MHC class I molecule.	4
Figure 1.2 The ribbon diagram shows the structure of an MHC II molecule	6
Figure 1.3 Simplified diagram of the human and mouse MHC	9
Figure 1.4: Diagram illustrating different cross-presentation mechanisms	12
Figure 1.5: Diagram illustrating the two classical antigen presentation pathways	13
Figure 1.6: Glycoprotein folding is driven by the continuous binding and release of incompletely folded glycoproteins from CNX/CRT; termed the CNX/CRT cycle	19
Figure 1.7: Ribbon structure superimposed onto a spacefilling model of the MHC I HLA-A*0201 peptide binding groove in complex with peptide	27
Table 2.1: Antibody information	31
Table 2.2: Antibody information	32
Figure 2.1: Schematic showing the four-step protocol used to generate each of the CRT constructs.	36
Figure 3.1: ClustalW protein sequence alignment of rat and mouse CRT	47
Figure 3.2: Schematic of the CRT constructs used in this study	49
Figure 3.3: Immunoblot comparing the expression of each rat CRT construct	50
Figure 3.4: K42 KDEL co-localisation with the KDEL-receptor	54
Figure 3.6: K42 HAKDEL co-localisation with KDEL-receptor	54-55
Figure 3.5: K42 HAKDEV co-localisation with the KDEL-receptor	56
Figure 3.6: K42 HAΔKDEL co-localisation with the KDEL-receptor	57
Figure 3.7: K42 HAΔ11 co-localisation with the KDEL-receptor	58
Figure 3.8: K42 HAΔ22 co-localisation with the KDEL-receptor	59
Figure 3.9: K42 HAΔ34 co-localisation with the KDEL-receptor	60
Figure 3.10: Reduced H-2K ^b cell surface expression in K42 transfected with c-terminally truncated CRT compared to HAKDEL	62
Figure 3.11: Pulse chase analysis to assess the trafficking rate of H-2K ^b to the cell surface	64
Figure 3.12: Quantitation of the H-2K ^b pulse chase experiment	65
Figure 3.13: Pulse chase analysis to assess the trafficking rate of H-2D ^b to the cell surface	66
Figure 3.14: Pulse chase analysis to assess the trafficking rate of H-2D ^b to the cell surface of K42 transfected with c-terminally truncated CRT	67
Figure 3.15: Quantitation of the H-2D ^b pulse chase experiment	69
Figure 3.16: H-2K ^b expressed on the cell surface by each K42 CRT transfectant has the same stability.	71
Figure 3.17: Assay to measure the efficiency of loading exogenous SL8 peptide for presentation to B3Z T-cell hybridomas	73
Figure 3.18: Assay to measure the efficiency of loading exogenous KAV peptide for presentation to 4D5 T-cell hybridomas.	74
Figure 3.19: Investigating intracellular H-2K ^b and H-2D ^b loading in c-terminally truncated CRT transfectants using a pulse-chase thermostability experiment	75
Figure 3.20: Time dependent peptide optimization of H-2K ^b and H-2D ^b	76
Figure 3.21: Intracellular loading assay of c-terminally truncated CRT transfectants.	78
Figure 3.22: CRT2 detection by PCR.	80
Figure 3.23: Cross-species CRT alignment	81
Figure 3.24: Intracellular loading assay of K42 transfected with rat and mouse CRT	83
Figure 4.1: The PLC remains intact in c-terminal truncated CRT mutants	86
Figure 4.2: PDI assembly with the PLC	88
Figure 4.3: NEM and MMTS alkylation of the ERp57-Tpn conjugate	90
Figure 4.4: An ERp57-HC conjugate forms in the absence of CRT	92
Figure 4.5: H-2D ^b leaves the ER in COPII vesicles of K41 at a faster rate than K42	94

transfected with CRT KDEL.	
Figure 4.6: The H-2D ^b COPII budding efficiency is higher in K42 than K42 transfected with CRT KDEL	95
Figure 4.7: Comparison of H-2D ^b budding efficiency against the Na ⁺ -K ⁺ -ATPase control	96
Figure 4.8: CRT is present in COPII vesicles	97
Figure 4.9: CRT accumulates in the cis-Golgi	98
Figure 4.10: CRT and MHC I co-localise at the cis-Golgi	99
Figure 4.11: MHC I expressed in K42 accumulates in the lysosome	100
Figure 4.12: Electroporation of high affinity H-2Db stabilizing peptide into K41 and K42 cells	101
Figure 5.1: Schematic of the ERp57-binding defective rat CRT mutant HAΔEB	104
Figure 5.2: Expression of HAΔEB is comparable to HAKDEL	104
Figure 5.3: HAΔEB is not secreted	105
Figure 5.4: HAΔEB does not restore the H-2Db trafficking rate compared to HAKDEL	106
Figure 5.5: Investigating intracellular H-2K ^b and H-2D ^b loading in HAKDEL and HA ^d EB using a pulse-chase thermostability experiment	107
Figure 5.6: Quantitation of the pulse chase thermostability experiments for H-2K ^b and H-2D ^b on HAΔEB	109
Figure 5.7: HAΔEB H-2K ^b surface expression is poorly restored relative to HAKDEL according to FACS analysis	110
Figure 5.8: Percentage loss of H-2K ^b from the cell surface of HAΔEB occurs at the same rate as K41 following BFA treatment	111
Figure 5.9: Intracellular loading assay of HAΔEB	112
Figure 5.10: anti-Tap1 antibody co-IP of the HAΔEB PLC	114
Figure 5.11: Trapping of the ERp57-Tpn conjugate from HAΔEB cell lysates	115
Figure 5.12: TAP1 co-IP of the HAΔEB PLC to identify PDI	116
Figure 5.13: Intracellular loading efficiency of the glycan-binding defective CRT mutants	118
Figure 5.14: Illustration of the intracellular peptide-loading defect in CRT HAΔEB	119
Figure 6.1: Construct summary; effects on MHC I antigen processing and presentation	121
Figure 6.2: Peptide binding complex assembly model	124
Figure 6.3: MHC I retention / retrieval model	126

Acknowledgements

I would like to thank the many people who have assisted me over the last four years. Firstly, I would like to thank Professor Tim Elliott for his continued enthusiasm, support and discussion, without which, getting to this stage of my project would not have been possible. Tim's constructive comments on all matters both personal and work-related were most helpful; particularly most recently for his comments and advice during the preparation of this thesis.

I would like to thank the people who helped me scientifically. I would like to thank Antony Antoniou (for his discussion, interest in my project and helpful advice during the preparation of this thesis, which was greatly appreciated), Tony Williams and Edd James (whose discussion and enthusiasm was a great motivational aid), Denise Boulanger, Andrew van Hateren and Helen North (for their comments and advice during the final stages of the write-up of this thesis) and the Elliott lab (for its great working environment).

Many thanks to James Bachelor for his invaluable technical and computer advice.

Deepest gratitude goes to my parents, grandparents and my sister Catherine for their encouragement, emotional support and friendship throughout, from which I have drawn inspiration and guidance. Without their support, this project would not have been possible.

Sincerest thanks to my friends Fernanda Castro, Fay Chinnery, Vivian Watson, Lena Fadda, Olivier Cexus, Nasia Kontouli & Soirée des Hommes for helping me to find ways to maintain my sanity and for providing a reassuring ear when times have been hard.

I would also like to thank the many other people who have not been mentioned for their help in many ways during my time in Southampton.

Definitions and Abbreviations

B ₂ m	Beta ₂ microglobulin	PAGE	Polyacrylamide Gel Electrophoresis
BFA	Brefeldin A		
cDNA	Complementary Deoxyribonucleic acid	PAS	Protein-A-Sepharose
CNX	Calnexin	PGS	Protein-G-Sepharose
CPRG	Chlorophenol red galactoside	PBS	Phosphate Buffered Saline
CRT	Calreticulin	PBST	Phosphate Buffered Saline + 0.2% Tween
Cys/Met	Cysteine/Methionine	PCR	Polymerase Chain Reaction
dH ₂ O	Distilled water	PDI	Protein Disulphide Isomerase
DMEM	Dulbecco's Modified Eagle's Medium	PFA	Paraformaldehyde
DMSO	Dimethyl sulphoxide	PLC	Peptide loading complex
dNTP	Deoxyribonucleotide triphosphate	PMSF	Phenylmethyl sulfonyl fluoride
DTT	1,4-dithioerythritol	RNA	Ribonucleic acid
EDTA	Ethylenediamine tetraacetic acid	RPMI 1640	Roswell Park Memorial Institute 1640 media
EndoH	Endoglycosidase H	SDS	Sodium dodecyl sulfate
FACS	Fluorescence Activated Cell Sorting	Tpn	Tapasin
FCS	Foetal Calf Serum	TBS	Tris Buffered Saline
HC	Heavy Chain	TAP	Transporter Associated with Antigen Presentation
HRP	Horseradish peroxidase	WB	Western Blot
IAA	Iodoacetamide		
IF	Immunofluorescence		
Ig	Immunoglobulin		
IP	Immunoprecipitation		
MgCl ₂	Magnesium Chloride		
MMTS	S-Methyl Methanethiosulfonate		
NEM	N-Ethylmaleimide		
NRLB	Non-reducing loading buffer		

Chapter 1: Introduction

1.1 Innate and Adaptive Immunity

The immune system can be dissected into two components: innate and adaptive immunity. The innate system provides the first barrier to infection, containing a repertoire of defensive components that are already present before the onset of infection. The cellular components comprise monocytes, macrophages, granulocytes and natural killer T cells. These circulate around the body and use pattern recognition receptors (PRR's) to recognise specific pathogenic features. In contrast, the adaptive immune system has the capacity to mount a highly specific response to an infection and generate a memory for it. This benefit of memory ensures that the host can rapidly respond to any subsequent re-infection. Adaptive immunity evolved more recently than innate immunity, approximately 400million years ago and is only present in cartilaginous and bony fish, amphibians, reptiles, birds and mammals (Fearon and Locksley, 1996; Thompson, 1995).

The innate immune system recognises molecular patterns common to frequently encountered pathogens, which are known as “pathogen-associated molecular patterns (PAMPS)” (Janeway, 1989). Although they are not unique to pathogens, they are produced by all microorganisms pathogenic or not (Medzhitov and Janeway, 2002). Lipopolysaccharide (LPS) of gram negative and Peptidoglycan of gram positive bacteria cell membranes are well known examples, but PAMPS are diverse. These include aldehyde-derivatised proteins, mannans, teichoic acids, denatured DNA, bacterial DNA (Clark and Kupper, 2005). These compounds are recognised by the innate immune system as signatures of infection and allow the host to distinguish between self and non-self, enabling the innate immune system to express a small number of receptors to recognise features common to many organisms.

Pattern recognition receptors (PRR) recognise PAMPS and initiate an immune response. Secreted PRRs, such as Mannose Binding Protein (Ikeda et al., 1987) and C-reactive protein (Wolbink et al., 1996) bind microorganisms and target them for destruction by phagocytic cells or complement, which is the major soluble protein effector of innate immunity (Fearon and Locksley, 1996). Toll-like receptors (TLR) are an important group of cell surface-expressed PRRs. They were originally identified in *Drosophilla* embryos by Nüsslein-Volhard and Wieschaus as a gene important for controlling dorsal-ventral polarity (Gay and Keith, 1991), but it was also shown to have connections with the immune system. For example, Lemaitre et al (Lemaitre et al., 1996) showed that their *Drosophilla* “toll” mutants were susceptible to *Aspergillus fumigatus* fungal infections but maintained normal anti-bacterial responses. This suggested that immune responses against bacteria and fungi could use different receptors or pathways that are pathogen-specific. To date, thirteen mammalian TLR

family members have been identified (10 in humans 12 in mice) that each recognise a distinct repertoire of conserved microbial molecules (Beutler, 2004). Binding of a TLR to its respective microbial ligand leads to a signalling cascade that triggers the activation of the transcription factor NF- κ B, which is an important instigator for the inflammatory response.

1.2 Humoural and Cellular immunity

Unlike innate immunity that has pre-existing pathogen-specific responses encoded into the genome, acquired immunity is more flexible and can adapt to provide a reaction that is specific and to the infection. The two cellular components of the adaptive immune system are B and T lymphocytes, which provide the humoral (antibody component) and cellular branches of adaptive immunity respectively. B lymphocytes (B cells) mature in the bone marrow and migrate into the peripheral lymph nodes, while T lymphocytes (T cells) migrate from the bone marrow to the thymus gland to mature. B cells express antibodies (also known as immunoglobulins; Ig) as their antigen receptor genes on the cell surface. Each Ig monomer is a “Y” shaped molecule that contains four polypeptide chains divided into two heavy and two light chains that are connected by disulphide bonds. There are 5 classes of immunoglobulin that the B cell can present IgA, IgD, IgE, IgG, and IgM, which differ according to the heavy chain type they express. These are denoted by the Greek letters α , δ , ϵ , γ , and μ . The γ , α and δ heavy chains contain 3 constant regions; the μ and ϵ heavy chains contain 4. They both contain a variable domain and hinge region. The light chains comprise two domains; one constant and one variable. Immunoglobulins have two functional regions; the F_{ab} (fragment antigen binding) region which is formed by the light chain and a variable and constant domain from the heavy chain, which bind to the antigen; the F_c (fragment crystallisable) region, which is formed by the remaining constant domains and are recognised by specific receptors such as the F_c receptor or can dimerise with other antibodies, such as IgA. B cells can express different classes of immunoglobulin but a single B cell clone can only express immunoglobulins with one pathogen specificity. B cell immunoglobulins recognise specific residues of proteins when in their folded, native state. Once the antibody has bound a specific antigen, the appropriate B cell expressing that antibody becomes activated, divides and starts secreting antibody, marking targets for destruction by effector systems such as complement or phagocytic cells (Sim and Reid, 1991; Wentworth et al., 2002). There is also evidence that antibodies may participate in generating reactive oxygen species of a type similar to those of activated neutrophils following inflammation, leading to efficient killing of bacteria regardless of the antigen specificity of the antibody (Wentworth et al., 2002).

T cells possess a T-cell receptor (TCR) that is structurally related to the B cell immunoglobulin but exists on the cell surface as a heterodimer comprising two subunits, either $\alpha\beta$ or $\gamma\delta$. Each subunit contains an N-terminal variable region and a single constant region, followed by a short membrane-spanning region at the C-terminal end. Most TCR in the human and mouse are of the type $\alpha\beta$ (Goldsby Richard A., 2003). $\alpha\beta$ TCR unlike antibodies, only recognise peptide fragments created from the proteolytic cleavage of antigens bound and presented by major histocompatibility complex (MHC) class I or class II molecules at the cell surface (Clark and Kupper, 2005). $\gamma\delta$ TCR however are slightly more unconventional and can recognise antigens in the form of intact proteins or non-peptide compounds (Allison et al., 2001). The variable domains for both the heavy and light chains in B and T cells contain 3 areas of hypervariability called complementarity determining regions (CDR), which interact with the antigen. During their development, B and T cells undergo rearrangements of the variable, diversity and joining (V(D)J) elements of the CDR genes early in their differentiation as a result of the activities of the recombination activating genes (RAG)1 and 2 (McBlane et al., 1995; Oettinger et al., 1990; Schatz et al., 1989). These have the capacity to generate as many as 10^{11} different cell clones that express distinct antigen receptors (Fearon and Locksley, 1996). This ability to recognise a large diversity of antigen gives adaptive immunity its strength but it also threatens to generate self-reactive clones that could create autoimmunity. In the case of T cells, the same process of subunit selection and junctional addition of nucleotides in the V(D)J elements to provide the wide repertoire of T cells, also generates “forbidden” clones able to recognise self-antigens and they need to be purged to prevent autoimmunity (Burnet, 1959; Siggs et al., 2006), which occurs in the thymus. On the other hand, B cells that express a defective and/or self-reactive receptor undergo a secondary Ig rearrangement while in the bone marrow to replace the receptor, rather than undergo default apoptosis (Edry and Melamed, 2004).

When the $\alpha\beta$ TCR interrogates the peptide cargo carried by the MHC, the T cell is either stimulated to perform its effector functions (cytokine release or cytotoxicity) or move onto the next MHC molecule presented to it (Garcia and Adams, 2005). Two types of T cell serve these effector functions and are distinguished by the co-receptors that they express, called cluster of differentiation (CD) proteins. CD4 expressing T cells ($CD4^+$ T cells), also known as T helper cells (T_H cells) only recognise MHC class II molecules and participate in activating B cells and produce inflammatory signals such as cytokines. CD8 expressing T cells ($CD8^+$ T cells), also known as cytotoxic T lymphocytes (CTL) / T cytotoxic cells (T_C), probe the repertoire of peptide-MHC class I complexes on the target cell surface for novel peptides that indicate expression of foreign or abnormal gene products (Shastri et al., 2002) and where necessary directly kill them.

1.3 MHC class I structure

MHC class I molecules consist of two polypeptide chains comprising a heavy chain (HC - Mr. 44kDa), which spans the membrane lipid bilayer and a smaller (12kDa) non-covalently bound β_2 -microglobulin (β_2 -m) domain (Figure 1.1). The HC contains 3 α domains, each of approximately 90 amino acids called α_1 , α_2 and α_3 (Bjorkman et al., 1987b; Malissen et al., 1982); a transmembrane domain of approximately 25 amino acids and a short cytoplasmic domain encoded on 7-8 separate exons. Exon 1 encodes the leader sequence; exons 2-4 code for the α_1 - α_3 chains; exon 5 codes for the transmembrane domain and exons 6-8 code for the cytoplasmic tail and 3' untranslated region. The β_2 -m domain interacts with all of the α domains and is essential for the class I molecule to reach its fully folded conformation (Goldsby Richard A., 2003). The α_3 domain contains a conserved sequence among class I molecules that interacts with the CD8 TCR (Goldsby Richard A., 2003), while 18 amino acids (3 of which are polymorphic (Bjorkman et al., 1987b)) interact with the α_1 α_2 domains.

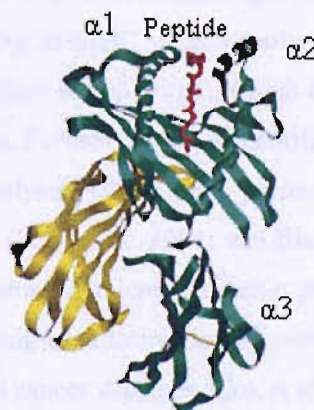


Figure 1.1: The crystal structure of an MHC class I molecule. The glycosylated heavy chain is shown in green, the beta2-microglobulin subunit in yellow and bound peptide in red. Adapted from: <http://biochemistry.utoroto.ca/williams/bch.html>

The membrane proximal α_3 and β_2 -m domains have tertiary structures resembling antibody domains and are paired by a disulphide bond. In contrast, the α_1 and α_2 domains are polymorphic and distal to the membrane, forming a platform composed of a single β -pleated sheet of 8 antiparallel strands, on top of which are two α -helices separated by a deep groove $\sim 25\text{\AA}$ long and 10\AA wide, lined with both polar and non-polar side chains.

During their studies, Bjorkman and co-workers observed a large continuous region of electron density in this groove that was attributed to the peptide antigen, which is usually between 8-9 amino acids

(Falk et al., 1991). Variations in the MHC class I binding groove allow the different class I molecules in the population to bind and present different portions of viral or other intracellular pathogens for immune targeting (Hildebrand et al., 2002). Class I molecules can bind a large range of peptides because they possess similar amino acid residues at defined locations in the peptide sequence. There are usually two allele-specific anchor residues located in a combination of either peptide positions 2/3/5 and 8/9. For example: 5 and 9 (H-2D^b), 2 and 9 (H-2K^d, HLA-A2) or 5 and 8 (H-2K^b). The amino acid anchor residue is also allele specific. For example H-2K^d usually binds peptides with Tyr at position 2 and Ile / Leu at position 9, while H-2D^b binds peptides with Asn at position 5 and Ile / Leu at position 9 (Falk et al., 1991). The N and C termini of the peptide are held in the A and F pockets of the MHC class I binding groove by conserved hydrogen bond, while the remaining residues interact with a hydrogen bond network along the length of the groove.

By virtue of their position in the middle of the trimolecular complexes made up of the T-cell receptor, peptide and MHC molecule, the rules defining the peptide have been central to understanding their role in the immune system (Falk et al., 1991). Townsend and co-workers demonstrated that specific peptides can confer increased stability to MHC class I molecules and form the basis of long-lived peptide-class I complexes *in vivo* (Elliott et al., 1991b), which is an important feature for maximizing antigen exposure to circulating T cells. Further more, the identification of peptides eluted from purified MHC class I alleles has been analysed using high performance liquid chromatography, mass spectrometry and protein sequencing (Falk et al., 1991; van Bleek and Nathenson, 1991). The defined peptide sequences can be used to search for microbe-specific proteins for use as potential antigens in vaccines. These strategies are also being used to fractionate peptide pools from tumours in the hope of defining tumour epitopes for potential cancer vaccines (Cox et al., 1994).

Of the many thousands of peptides encoded by a complex foreign antigen that can potentially be presented to T_C cells, only a small fraction induce measurable responses in association with any given major histocompatibility complex class I allele. To design vaccines that elicit optimal T_{CD8+} responses, a thorough understanding of this phenomenon, known as immunodominance is imperative (Yewdell and Bennink, 1999).

1.4 MHC Class II Structure

MHC class II molecules are highly polymorphic and are encoded by the HLA-DP, -DQ and DR loci in humans and H-2A and H-2E in mice. Each molecule consists of two protein chains; the α (light) and β (heavy) chains, which are encoded by two genes. The class II genes for the α domain are encoded by 5 exons, whereas the β domain has 6. The two proteins associate with one another to form heterodimeric structures that can bind peptide of between 13-25 amino acid residues in length (Chicz et al., 1992; Rudensky et al., 1991). Residues for the minimal peptide-binding motif were determined by high-performance liquid chromatography, mass spectrometry and microsequencing analyses for HLA-DR (Rudensky et al., 1991). Although the sequences were quite varied, they shared similar amino acid properties at key residues; position 1 was positively charged such as arginine, position 5 was a hydrogen-bond donor; tyrosine and position 9 was a hydrophobic residue; alanine. These were discovered before the 3D structure of HLA-DR had been determined by Brown et al using X-ray crystallography (Brown et al., 1993). MHC II heavy chains are approximately 30-34kDa and the light chains are between 26-29kDa. Both have a cytoplasmic and transmembrane region of approximately 25 amino acids. The α (light) and β (heavy) chains both contain two domains; α_1 and α_2 ; β_1 and β_2 . The α_1 and β_1 fold into one another to form the peptide binding cleft that is open ended to accommodate larger peptide antigen sizes, but unlike the MHC I binding cleft, class II molecules do not contain a disulphide bridge. The α_2 and β_2 domains have a similar structure to the α_3 domain of class I molecules and are adjacent to the plasma membrane (Figure 1.2).

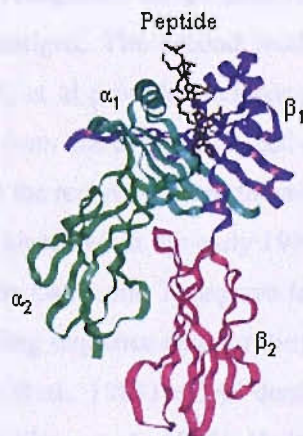


Figure 1.2: The ribbon diagram shows the structure of HLA-DR. The α_1 domain is shown in blue-green, the α_2 is green, the β_1 domain is purple and the β_2 domain magenta. The α_1 and β_1 domains form the binding groove that accommodates peptide fragments (shown in beige). The two chains associate without covalent bonds. Adapted from www.cryst.bk.ac.uk/.../coadwell/006.htm

1.5 MHC restriction

Both CD4⁺ and CD8⁺ T cells can only recognise antigen when bound to self-MHC molecules. Rosenthal and Shevach (Rosenthal and Shevach, 1973) used guinea pigs in their model and found that T_H cell proliferation in response to a specific antigen presented by macrophages could only occur when both were of the same haplotype. Macrophages derived from two guinea pig strains (2 and 13) were incubated separately with antigen and then mixed with T_H cells from the same, different or F₁ generation (2x13) animals. T_H cell proliferation was then measured. They found that strain-2 pulsed macrophages only activated strain-2 and F₁ but not strain-13 T cells. Conversely, strain-13 pulsed macrophages could only activate strain-13 and F₁ T cells but not strain-2. This demonstrated that the T_H cells had to share the same MHC class II allele as the antigen-pulsed macrophages to proliferate; in other words, they were MHC class II restricted. Doherty and Zinkernagel followed a year later with experiments demonstrating MHC class I restriction. They injected and immunised mice against lymphocytic choriomeningitis virus (LCMV) and took out the spleen cells; including the activated, viral-specific T_C cells; several days later. These were then incubated with LCMV-infected target cells that shared or differed in their haplotype and measured target cell killing. Their conclusions were that cytotoxic T cell activity in LCM was, as in the T helper effect, restricted (Doherty and Zinkernagel, 1975).

Initially, the precise mechanism for MHC restriction was unknown but two molecular models existed to potentially explain for it. The dual recognition model involved two TCRs, one binding to the MHC molecule, the other to the peptide antigen. The second model attributed both antigen and MHC specificity to the same TCR. Dambic et al provided evidence favouring the single receptor model, showing that by transfecting the TCR from one cytotoxic T cell clone of one specificity into a cytolytic T cell of a different specificity, caused the recipient T cell to have the same specificity as the donor cell (Dembic et al., 1986). The TCR was identified in the early 1980s (Allison et al., 1982; Haskins et al., 1983; Meuer et al., 1983), however the Davis and Tonegawa labs were the first to clone and identify the TCR at the molecular level, providing sequence data for the β (Hedrick et al., 1984a; Hedrick et al., 1984b; Yanagi et al., 1984), α (Chien et al., 1984) and γδ domains (Hayday et al., 1985; Saito et al., 1984; Samelson et al., 1985; van den Elsen et al., 1985). Hedrick et al (Hedrick et al., 1984b) noted how the β domain shared sequence similarity to the immunoglobulin receptors of B cells, which supported the body of evidence favouring the idea of clone specific TCR recognition of antigens. The nature of these antigenic peptides was reported by Babbitt and co-workers (Babbitt et al., 1985) who used CD4⁺ T cells restricted to MHC class II molecules on macrophages, which readily uptake, process and present the antigen (Babbitt et al., 1985). They used hen-egg lysosome (HEL), which has to be

processed in acidic intracellular vesicles (Allen and Unanue, 1984; Babbitt et al., 1985) to liberate the antigen and demonstrated that MHC class II molecules selectively bind such antigenic peptides. Townsend and co-workers showed a similar trend in CD8⁺ T cells when a specific peptide sequence from a library of synthetic influenza A nucleoprotein-derived peptides made target cells susceptible to influenza A-specific CD8⁺ T cell lysis. These studies suggested that the antigen was derived from the cellular degradation of antigenic proteins. Antigenic peptide therefore appeared to account for the unidentified cloud of electron density seen between the HLA-A2 α_1 and α_2 domains during crystal structure analysis (Bjorkman et al., 1987a). The antigenic peptide appeared to be stably bound to HLA-A2 because it remained during the purification and crystallisation procedures, consistent with a slow kinetic off-rate reported for peptides bound to MHC class II molecules. This implied that the peptides were also bound to MHC class I molecules and formed an essential feature of cellular immunity (Bjorkman et al., 1987a). This provided a molecular mechanism for MHC restriction, illustrating how the MHC molecule and antigen provided a composite ligand for the TCR.

1.6 MHC Polymorphism

The MHC is located in chromosome 17 in mice and chromosome 6 in humans (Figure 1.3). It spans a region of 3.6Mb in humans and is predicted to contain 128 expressed genes. Although the gene organisation is different between the two species, they can essentially be broken down into three regions: MHC class I, II and III. MHC I encodes the classical class I molecules designated human leukocyte antigen-A (HLA-A), -B and -C in humans and histocompatibility-2K (H-2K), -2D and -2L in mice. MHC II encodes the classical class II components designated DP, DQ and DR in humans and H-2A and H-2E in mice, while MHC III encodes other immune components such as complement (such as C2, C4a and C4b) and some cytokines, including TNF (tumor necrosis factor; α and β). Antigen processing molecules such as TAP: the transporter through which peptides from the cytoplasm enter the endoplasmic reticulum; TAPBP: the gene encoding tapasin, which is important for MHC I peptide-loading and LMP; genes for components of the proteasome, the enzyme complex that degrades proteins into peptides in the cytoplasm are encoded within this region alongside other non-classical MHC proteins such as HLA-E, -F and -G, which are relatively nonpolymorphic and may have functions other than the presentation of antigen to T cells. For example, HLA-G expression on melanoma cells has been shown to protect them against Natural Killer cell-mediated lysis (Paul et al., 1998).

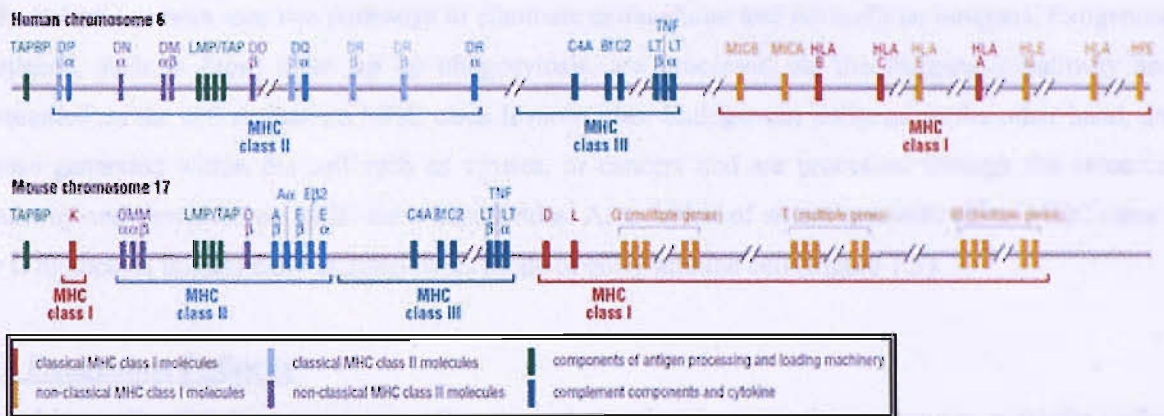


Figure 1.3: Simplified diagram of the human and mouse MHC. Only MHC class III genes with known immune functions are shown in figure 1.3. The gene for β_2 -microglobulin, which is encoded outside the MHC on human chromosome 15 and mouse chromosome 2, and five additional non-classical MHC class I genes – the CD1 genes, which are encoded outside the MHC on human chromosome 1 – are not shown. C4A, C4B, C2, Bf: genes for complement components; DN, DM, DO, M, O: non-classical class II genes; DP, DQ, DR, A, E: classical MHC class II genes; HLA-A, HLA-B, HLA-C, K, D, L: classical MHC class I genes; LMP; LT: genes for lymphotoxin; MICA, MICB, HLA-E, HLA-G, HLA-F, HFE, Q, T, M: genes for non-classical MHC class I molecules; TAP; TAPBP: gene for tapasin and TNF. Adapted from Immunity (Anthony L. DeFranco, 2007).

The highly polymorphic nature of the MHC is thought to have evolved by Darwinian selection to create genetic diversity against a growing number of infectious pathogens. To date (2007), nearly 2000 class I alleles and 900 class II alleles have been identified in humans (<http://www.ebi.ac.uk/imgt/hla/stats.html>). One individual can only express a limited set of different HLA molecules: up to 6 for MHC I and 12 for MHC II. With a limited repertoire of MHC molecules, how can an MHC molecule bind so many different peptides?

Analysis of MHC class I polymorphisms from a list of 22 human HLA-A2 sequences has shown that most variation exists in 17 amino acid positions of which 15 are located within the binding site region for processed antigen (Bjorkman et al., 1987a). 3 positions are thought to interact with the TCR and 12 with the antigenic peptide. Variations in these MHC class I amino acids are thought to be responsible for their antigen specificity, but less so to the TCRs that engage them. Limitations in the ability of a particular HLA molecule to associate with all antigens is thought to provide an explanation between the linkage of histocompatibility antigens to variations in susceptibility to human diseases (Bjorkman et al., 1987a, b; Zinkernagel and Doherty, 1974) and the immune system's responsiveness to particular antigens (Bjorkman et al., 1987b; McDevitt and Tyan, 1968).

1.7 Antigen Processing and Presentation

The immune system uses two pathways to eliminate extracellular and intracellular antigens. Exogenous antigens, such as those taken up by phagocytosis, are processed via the exogenous pathway and presented on the cell surface on MHC class II molecules. Endogenous antigens on the other hand, are those generated within the cell such as viruses, or cancers and are processed through the cytosolic pathway and presented on MHC class I molecules. Association of an antigen with either MHC class I or II molecules is classically dictated by its mode of entry into the cell (Figure 1.5).

1.8 Exogenous Pathway

Dendritic cells (DCs), macrophages, B-cells and the thymic epithelium comprise a family called Antigen Presenting Cells (APCs), which are responsible for internalising antigen. Once internalised, it is progressively degraded and cleaved by hydrolysing enzymes as it is processed through the increasing acidic compartments of the exogenous pathway where they are also presented onto MHC molecules. These compartments consist of an early endosome (pH 6-6.5), late endosome or endolysosome (pH 5-6) and a lysosome (pH 4-5). APCs can present both MHC class I and II molecules and systems have evolved to prevent them binding the same pool of antigenic peptides. When an MHC class II molecule is synthesised within the ER, it is pre-assembled with a trimeric protein called the invariant chain, which interacts with the peptide binding groove of the MHC class II molecule, preventing access to any endogenously-derived antigen. It also contains a sorting signal in the 12-15 N-terminal amino acids of its cytoplasmic tail that directs the transport of the MHC class II complex from the trans-Golgi network to the endocytic compartments (Bakke and Dobberstein, 1990). The invariant chain is progressively cleaved as it moves in complex with the MHC class II molecules through the increasingly acidic endosomal compartments, until a short fragment called CLIP (class II-associated invariant chain peptide) remains. This occupies the peptide binding groove until a molecule called HLA-DM catalyses the exchange of antigenic peptide in place of CLIP. A second molecule called HLA-DO (present only in B-cells) antagonises HLA-DM, however its ability to bind and inhibit HLA-DM decreases with the increased acidity, presumably swinging the reactions occurring within the exogenous pathway in favour of MHC class II binding peptide. MHC class II internalised from the cell surface may also be re-loaded with peptide in the endosome and recycle back to the cell surface for re-use (Chow and Mellman, 2005).

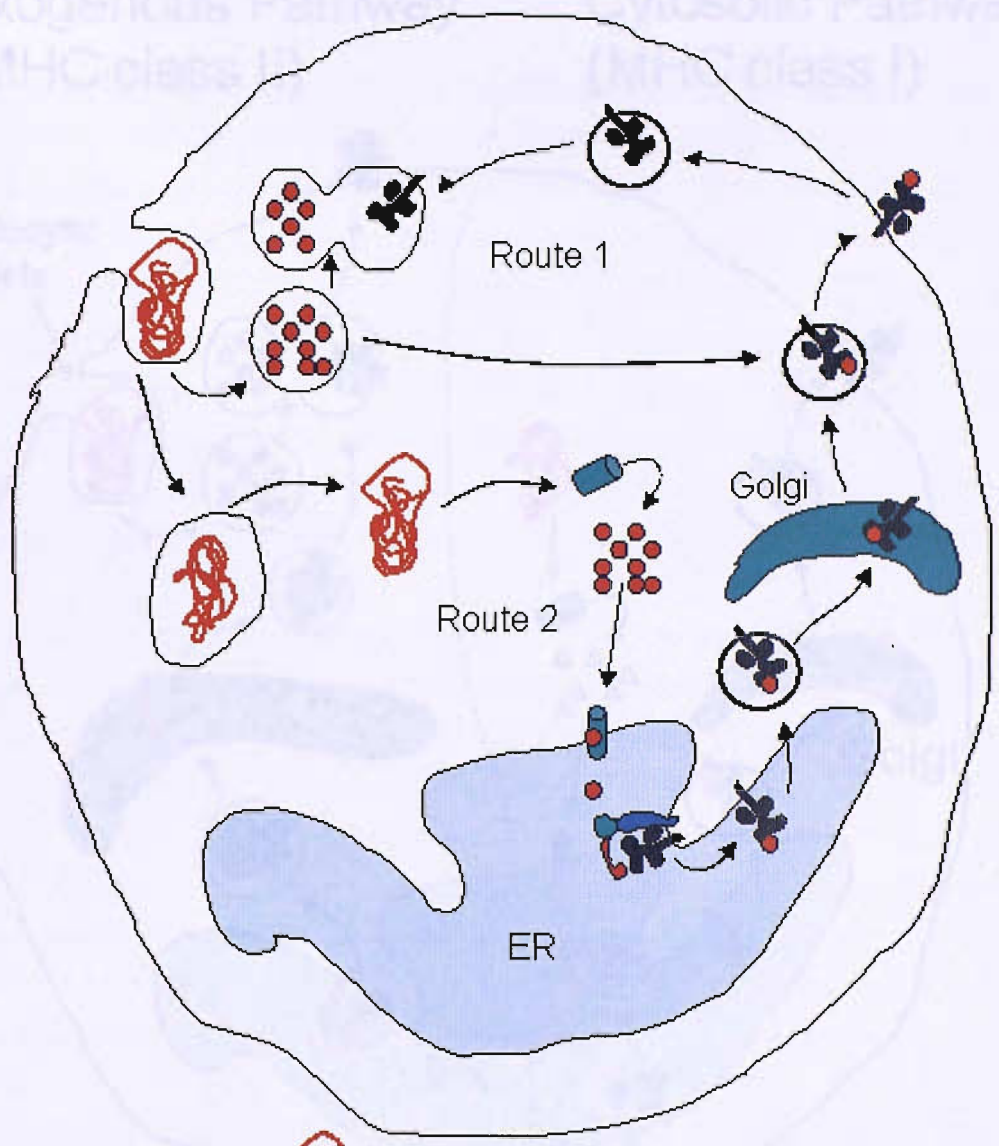
1.9 Cytosolic Pathway

In this pathway, intracellular-derived peptides are appropriately cleaved within either the cytosol or ER, where they subsequently bind MHC class I molecules within the lumen of the ER. Once

assembled, this complex is transported to the cell surface. Cells ensure that while class I molecules bound to high affinity peptide can leave, those that are empty are retained and for this to occur, the cooperative efforts of a multimolecular assembly called the MHC peptide loading complex (PLC), comprising the peptide transporter associated with antigen processing (TAP), the chaperones Tapasin (Tpn), Calreticulin (CRT) and the disulphide oxidoreductases Erp57 and possibly PDI are required. Since this pathway forms the core of the thesis, it will be described more comprehensively in its constitutive parts comprising; the origin of class I peptide, class I folding, assembly, and the PLC components below.

While the rules governing the endocytic and cytosolic pathway are generally true, they are not absolute and a process called cross-presentation has been reported recently, where exogenous peptide is able to load onto MHC class I molecules (which classically present endogenous peptide) and be presented to T_H cells. This occurs in APCs because they have the ability to express both MHC class I and II molecules, but dendritic cells are believed to be the dominant cell type that can perform this function (Cresswell et al., 2005). Material is taken up through phagocytosis, but may also occur using receptor-mediated or fluid phase endocytosis; also called macropinocytosis; and then presented onto MHC class I molecules. The mechanism responsible is still unclear, however, there are several ways that this could happen (Figure 1.4). Peptide generated after internalisation and digestion by lysosomal proteases may be able to bind MHC class I molecules recycling back into the cell or delivered to the endocytic pathway (Route 1). Alternatively, the internalised proteins could enter the cytosol and be degraded into peptides and then be delivered into the ER through TAP and loaded onto MHC class I molecules in the normal way (Cresswell et al., 2005) (Route 2). A third mechanism has also recently been suggested where soluble proteins can have direct access to the perinuclear ER after internalisation by DC's (Ackerman et al., 2005). The soluble proteins translocate into the cytosol by a common pathway established for ER associated degradation and derived peptides can then be transported back into the ER to bind MHC class I molecules.

Exogenous Pathway (MHC class II) Cytosolic Pathway (MHC class I)









- | | | | |
|-------------------|---|-------------------------------|---|
| Exogenous antigen |  | Peptide Loading Complex (PLC) |  |
| Antigenic peptide |  | TAP Peptide transporter |  |
| Proteasome |  | MHC class I |  |

Figure 1.4: Diagram illustrating different cross-presentation mechanisms. Route 1 involves the peptide loading of MHC I molecules recycling from the cell surface with lysosomal compartments containing antigen. Route 2 involves the generation of exogenous antigenic protein fragments by the proteasome which are then presented using the cytosolic pathway.

Exogenous Pathway (MHC class II)

Cytosolic Pathway (MHC class I)

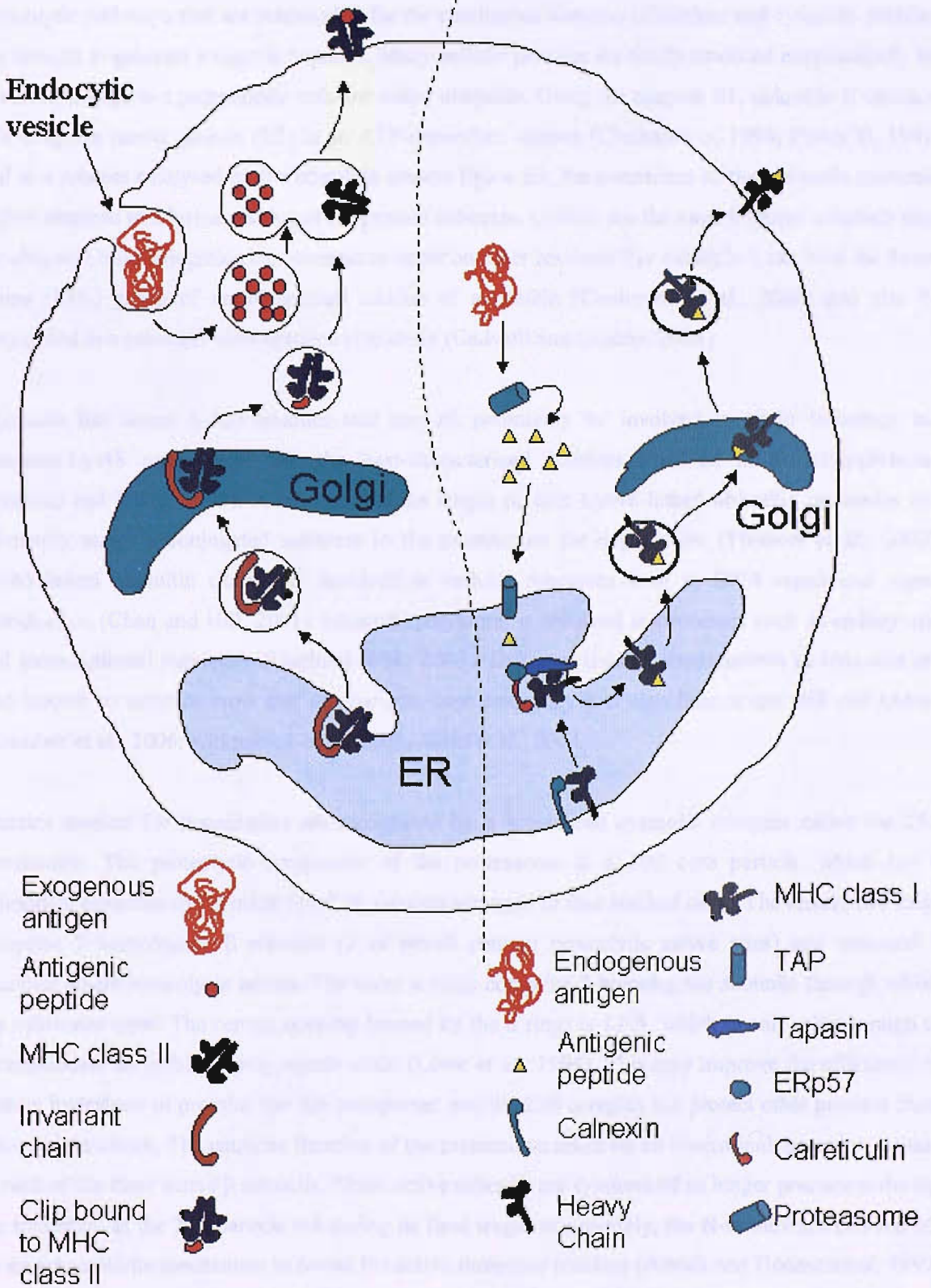


Figure 1.5: Diagram illustrating the two classical antigen presentation pathways.

1.10 Origin and Generation of Antigenic Peptide destined for the cytosolic pathway.

Proteolytic pathways that are responsible for the continuous turnover of nuclear and cytosolic proteins are thought to generate antigenic peptides. Many cellular proteins are firstly modified enzymatically by covalent linkage to a polypeptide cofactor called ubiquitin. Using the enzyme E1, ubiquitin is attached to a ubiquitin carrier protein (E2) in an ATP-dependent manner (Ciechanover, 1994; Finlay D, 1991) and in a process catalysed by the ubiquitin protein ligase E3, the c-terminus of the ubiquitin molecule is then attached to a lysine residue of the protein substrate. Lysines are the most frequent substrate sites for ubiquitin but conjugation can sometimes occur on other residues. For example it can bind the free-amine (NH₂) group of an N-terminal residue of a protein (Coulombe et al., 2004) and also be conjugated to a substrate via a cysteine side chain (Cadwell and Coscoy, 2005).

Ubiquitin has seven lysine residues that can all potentially be involved in chain formation but ubiquitin-Lys48 and -Lys63 are the best-characterized residues involved in polyubiquitylation (Haglund and Dikic, 2005). A minimum chain length of four Lys48-linked ubiquitin molecules can efficiently target a conjugated substrate to the proteasome for degradation (Thrower et al., 2000). Lys63-linked ubiquitin chains are involved in cellular processes such as DNA repair and signal transduction (Chan and Hill, 2001). Monoubiquitylation is involved in processes such as endocytosis and transcriptional regulation (Haglund et al., 2003). Different linkage combinations of ubiquitin are also known to exist *in vitro* and *in vivo* but their frequency and significance are still not known (Kerscher et al., 2006; Kirkpatrick et al., 2005; Saeki et al., 2004).

Proteins marked for degradation are recognized by a specialised cytosolic complex called the 26S proteasome. The proteolytic component of the proteasome is a 20S core particle, which has a cylindrical structure and is made up of 28 subunits arranged in four stacked rings. The central two rings comprise 7 homologous β subunits (3 of which contain proteolytic active sites) and surround a chamber where proteolysis occurs. The outer α rings comprise 7 homologous subunits through which the substrates enter. The central opening formed by the α rings is 13 Å, which is only wide enough to accommodate an unfolded polypeptide chain (Lowe et al., 1995). This may improve the efficiency of protein hydrolysis of proteins that are transported into the 20S complex but protect other proteins from non-specific attack. The catalytic function of the proteasome relies on an N-terminal threonine residue in each of the three active β subunits. These active subunits are synthesised as longer precursors during the formation of the 20S particle but during its final stages of assembly, the N-termini are cleaved off by an autocatalytic mechanism to reveal the active threonine residues (Arendt and Hochstrasser, 1997; Rock and Goldberg, 1999; Schmidtke et al., 1996). The N-termini of the 4 other β subunits are not

cleaved and remain inactive. The 20S complex is capped at either end by the 19S complex, which forms the lid and base of the central core (Glickman et al., 1998). It contains sites for tight binding of polyubiquitinated substrates as well as an ATPase component (Orino et al., 1991) within the base that presumably unfolds the polypeptide substrates to thread into the 20S core, generating fragments of between 4-24 amino acids (Kisselev et al., 1998; Wenzel et al., 1994). Another complex called PA28 can also cap the 20S core, however at present very little is known about it except that its expression can be induced by interferon- γ (IFN- γ) (Fruh and Yang, 1999) suggesting an importance in the immune system and a possible role in the generation of antigenic peptide (Kloetzel, 2004).

In mammalian cells, IFN- γ also induces the expression of three additional active β subunits called low-molecular weight proteins (or LMPs) 2 and 7 (encoded in the MHC)(Monaco and McDevitt, 1984, 1986) and MECL1 (Hisamatsu et al., 1996), which replace the constitutively expressed subunits in newly assembling 26S proteasomes. They are called immunoproteasomes to indicate their role in antigen presentation and show a preference for cleaving hydrophobic and basic amino acid peptide bonds. This is significant because it is consistent with the c-terminal peptide characteristics that an MHC class I prefers to bind.

Although studies have shown that the proteasome is key to the generation of peptide-MHC complexes, the addition of proteasomal inhibitors can in fact increase the presentation of some peptides (Shastri et al., 2002), suggesting that some peptide repertoires can be generated independently of the immunoproteasome. A reduction in the presentation of antigenic peptides by MHC class I through a loss of any of the immunoproteasomal units does not severely impair the immune system, suggesting that the constitutive proteasome and other proteases present within the cell are sufficient to generate a pool of antigenic peptides (Shastri et al., 2002). Therefore, the activities of multiple enzymes capable of generating different peptides seem to be required. The role of the immunoproteasome, however, may be to bias the generation of a specific set of peptides for incorporation into MHC class I molecules. Cytosolic proteases that could be candidates involved in generating peptides for MHC class I molecules include tripeptidylpeptidase II (TPPII)(Geier et al., 1999), leucine aminopeptidase (Beninga et al., 1998), which has the capacity to create actual antigenic peptides (and upregulates in expression following IFN- γ treatment), puromycin sensitive aminopeptidase and bleomycin hydrolase (Stoltze et al., 2000), which can trim the N terminus of synthetic peptide substrates.

It is not clear if these cytoplasmic proteases work alone, or in concert with one another, to generate the final peptides before they enter the ER, but lines of evidence now suggest that antigenic peptides can

be trimmed and generated in the ER itself (Hammer et al., 2006), an idea originally proposed by Falk et al (Falk et al., 1990). For example, TAP, which is involved in supplying the ER with a pool of antigenic peptide, is less efficient at transporting peptides containing proline at position 2 (Uebel et al., 1997), despite being an anchor residue for certain class I alleles such as H-2L. It is now known that N-terminally extended peptides can be transported through TAP and into the ER, where they are appropriately trimmed by an aminopeptidase called ERAAP (ER aminopeptidase associated with antigen processing in mice, human ortholog, ERAAP1), which has been linked to antigen processing following its upregulation in response to IFN- γ treatment (Serwold et al., 2002).

The antigenic peptide pool clearly represents a wide range of gene products, however their origin and the way that they are generated is still unclear. The traditional view has been that once a protein is no longer required to perform its function it is degraded and the fragments subsequently generated are used as antigenic peptides. For a cell to recycle and re-use parts of these proteins if they are no longer required makes economical sense.

Recent evidence suggests that the vast majority of antigenic peptides are from proteins degraded immediately after synthesis. Antigenic peptides obtained in this way would alleviate the need for a cell to retrieve proteins or their fragments from their different cellular compartments. Concomitant protein sampling and synthesis would provide an early detection mechanism of novel peptides generated by intracellular pathogens or mutations. If proteins were ear marked for degradation from failing to fold properly or being translated incorrectly, this mechanism would be just as economical as deriving antigenic peptides from normal protein turnover.

Shubert et al (Schubert et al., 2000) argued that if antigenic peptides destined for the cytosolic pathway came from newly synthesised proteins, then inhibiting the proteasome would cause them to accumulate. Having pulsed a cohort of proteins with ^{35}S , they measured the total amount of radioactivity in fractionated proteins of >14kDa following proteasomal inhibitor treatment. They saw an increase in high molecular weight proteins, of which a fraction were ubiquitinated. They calculated that 30% of newly synthesised proteins were degraded within 10minutes of translation and referred to these proteins as defective ribosomal products (DRiPS). They suggested that DRiPS formed a major pool of antigenic peptides and they proposed several ways from which they could be generated:

1. From the autonomous transcription of short DNA sequences called peptons by RNA polymerases,

2. Primary RNA transcripts could be mis-spliced, leading to the incorporation of intronic or peptide sequences out of frame with the primary AUG start codon,
3. Cryptic peptides could be generated by the ribosome from a conventional mRNA transcript but translated unconventionally.

Unconventional translation could arise if a ribosome; i) initiated translation at an AUG site downstream of the starting AUG codon; ii) if it bound to the AUG but started translating at an alternative codon; iii) started translating at the first AUG but frameshifted at some point during translation or iv) if it initiated translation at an alternative starting codon. Indeed, Malarkannan et al (Malarkannan et al., 1996) have implicated the CUG codon as a start codon, which translates to leucine instead of the conventional methionine. The mechanisms underlying how translation of these cryptic polypeptides arises still need to be determined, but evidently they would increase the diversity of peptides available in the antigenic pool for the immune system to choose from. Their immunological significance is also unclear because no one knows if they are exclusive to infected cells or to normal somatic cells too.

1.11 Class I folding

Proteins are synthesised by membrane-associated ribosomes and inserted co-translationally into the ER through a specialised structure known as the translocon. MHC class I assembly has much in common with that of other multisubunit glycoproteins within the ER, because it requires transient associations with the folding chaperones calnexin (CNX) and calreticulin (CRT) to help it fold properly. These folding enzymes facilitate protein folding by recognising signs of incomplete folding such as hydrophobic surfaces, mobile loops and a lack of compactness that may only be transiently observed in the dynamic luminal environment (Ellgaard et al., 1999). They also prevent the folding intermediates from premature degradation and expose them to ERp57, a thiol disulphide oxidoreductase, that helps them form the correct disulphide bonds during the folding process (Helenius and Aebi, 2004). Commonly to aid protein folding, N-linked oligosaccharides (in the form of a 14-saccharide core units, predominantly containing glucose and mannose residues $\text{Glc}_3\text{Man}_9\text{GlcNAc}_2$) are cotranslationally added to proteins. These oligosaccharides are then modified to create the preferred glycan ($\text{Glc}_1\text{Man}_7\text{-}_9\text{GlcNAc}_2$) substrate for CNX and CRT, which assist in protein folding through an alternating cycle of binding and release.

Both human and mouse MHC class I molecules have an N-linked, complex oligosaccharide attached at asparagine 86 (Asn 86), which is in the loop connecting the α_1 and α_2 domains (Bjorkman et al.,

1987b). The glycan is not necessary for HC to bind β_2 -m (Bjorkman et al., 1987b). The position and number of glycosylations may be important to determine whether glycoproteins bind to CNX or CRT. CNX is not detected in association with human class I bound to β_2 -m (Nossner and Parham, 1995; Ortmann et al., 1994; Sugita and Brenner, 1994), but is in mouse (Ahluwalia et al., 1992; Nossner and Parham, 1995; Sadasivan et al., 1996). The main difference is that human class I HC is only glycosylated at Asn 86 but mouse HC has a second site at Asn 176 (located in the α_2 domain) and H-2L^d, H-2D^b and H-2K^d alleles have a third at Asn 256 (located in the α_3 domain) (Bjorkman et al., 1987b). Zhang and Salter have shown that the addition of a second asparagine-linked glycan to the human class I allele A*201 at position 176, a site present in mouse, increased binding to CNX and decreased binding to CRT relative to a wild type A*201 molecule containing only one glycan at Asn 86 (Zhang and Salter, 1998). It is possible that CNX first associates with class I HC by virtue of its higher affinity than CRT for the glycan at position Asn 86 of the free class I HC. Wang et al demonstrated that CNX – assisted folding is important because only the fully disulphide-bonded class I HC can bind β_2 -m and peptide stably (Wang et al., 1994). It is possible that as disulphide bonds form, steric changes that then occur in the class I molecule, prevent CNX access to Asn 86, which would then favour an association with CRT.

BiP (Binding Protein), another ER chaperone, may also transiently support the folding of some proteins, since proteins containing a glycosylation site outside the first 50 residues probably bind BiP before interacting with CNX / CRT (Molinari and Helenius, 2000). Indeed, misfolding which can lead to ER-associated degradation (ERAD) has been associated with a prolonged association between HLA-B27 HC and BiP (Turner et al., 2005).

Glucosidase enzymes remove excess glucose molecules from the core oligosaccharide to promote CNX and CRT binding. Glucosidase II performs the central role of removing the innermost two residues, while glucosidase I removes the outermost. This trimming persists while the substrate is CNX/CRT-bound and once the innermost glucose residue has been removed, the protein substrate is then released. A second enzyme called uridine 5'-diphosphate (UDP)-glucose: glycoprotein glucosyltransferase (UGGT) replaces the glucose residues to promote CNX/CRT binding if the first round of folding has failed. Both enzymes drive a cycle of binding and release. UGGT works as the folding sensor, recognising exposed oligosaccharide and protein moieties of a misfolded glycoprotein (Gahmberg and Tolvanen, 1996)(Figure 1.6).

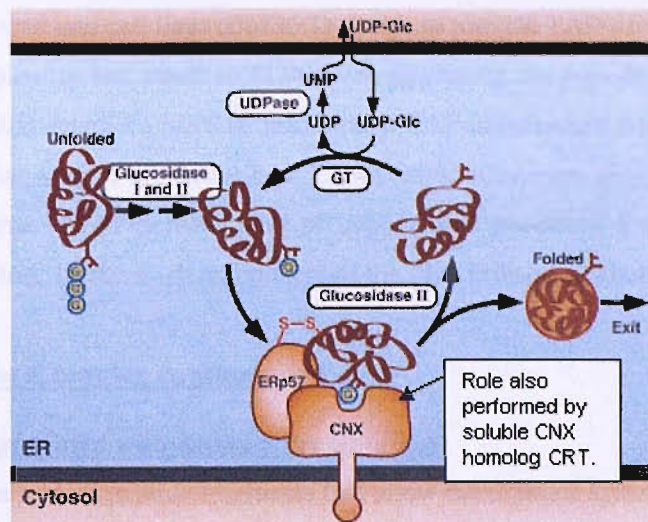


Figure 1.6: Glycoprotein folding is driven by the continuous binding and release of incompletely folded glycoproteins from CNX/CRT; termed the CNX/CRT cycle. Glucosidase I and II enzymes trim the glucose residues from the oligosaccharide chain, releasing it from CNX/CRT. Uridine 5'-diphosphate (UDP)-glucose: glycoprotein glucosyltransferase (GT) acts as a folding sensor, re-glucosylating the oligosaccharide chain if the glycoprotein is misfolded, promoting repeated CNX/CRT binding. Adapted from (Ellgaard et al. 1999)

1.12 Class I assembly

The assembly of the HC- β_2 -m complex and dissociation from CNX (Sugita and Brenner, 1994) marks the first stage in MHC class I assembly. In the presence of CNX, ERp57 appears to accelerate oxidative folding of the MHC class I heavy chain (Lindquist et al., 2001). The second step involves peptide loading of the heterodimer, which is unstable in the absence of peptide (Elliott et al., 1991a) and can promote the assembly of class I molecules *in vitro* (Townsend et al., 1990). There is evidence that the heterodimer can load with peptide prior to assembly with the peptide loading complex (Lewis and Elliott, 1998), which may serve to protect class I heterodimers from dissociating into free HC and β_2 -m before they encounter high affinity peptide in the PLC and can be sufficient to permit the egress of class I molecules from the ER. T134K HLA-A2.1 molecules contain a lysine in place of a threonine at position 134 and can access the secretory pathway in TAP-competent cells (Lewis et al., 1996) despite being in a predominantly peptide-receptive state, but delivery of a pre-processed epitope directly into the ER can overcome their peptide-loading defect (Lewis et al., 1996). A failure to bind the PLC appears to be the cause of T134K being transported to the cell surface more than three times faster than wild-type molecules expressed in the same cell, illustrating the importance of the PLC in peptide-loading. Observations on T134K have led to the suggestion of a two-step-binding model, where newly formed class I heterodimers bind peptide, which is subsequently optimized within the PLC. Key evidence for this model came from an experiment where wild type HLA-A2 and T134K

molecules were introduced into cell lines (BM36.1) unable to provide TAP-derived peptides because of a defective TAP complex, to test whether T134K was bypassing the peptide-loading step of antigen presentation. They would therefore have to load with a TAP-independent pool of peptide within the ER. The result was that very few HLA-A2 or T134K molecules were able to access the secretory pathway, suggesting that a TAP-derived pool of peptide was necessary for stable class I peptide-loading (Lewis and Elliott, 1998). Each component of the PLC is discussed below:

1.13 Peptide Loading Complex components;

1.13.1 Transporter Associated with Antigen Presentation

MHC class I molecules present peptide fragments that allow the immune system to monitor the protein repertoire being generated inside the cell. Protein fragments are generated in the cytosol but have to cross the ER membrane to have access to MHC I molecules and Townsend et al proposed that a specific mechanism could be responsible for peptide transport (Townsend et al., 1989). This was later to be called the Transporter Associated with Antigen Processing and has been extensively reviewed (Elliott, 1997b). Cell lines defective in MHC I antigen presentation were studied and revealed that TAP1 and TAP2 mutations encoded in the MHC class I genomic region were responsible for the defects (Deverson et al., 1990; Kelly et al., 1992; Kleijmeer et al., 1992; Spies et al., 1992). The transporter associated with antigen presentation (TAP) is an ATP-binding transporter (Deverson et al., 1990; Monaco et al., 1990; Trowsdale et al., 1990) that exists as a heterodimer (Velarde et al., 2001), supplying peptide to the ER ensuring the stable peptide-dependant assembly of MHC class I molecules (Lewis and Elliott, 1998). It exhibits some degree of peptide size and sequence specificity, transporting peptides of between 9-15 residues (Momburg et al., 1994a) into the lumen of the ER in an ATP-dependant fashion (Heemels et al., 1993; Shepherd et al., 1993), although longer peptides may be transported (Uebel and Tampe, 1999). Different MHC class I molecules can interact with TAP (Neisig et al., 1996). Human TAP prefers to bind hydrophobic or basic c-terminal residues compared to murine TAP that favours a hydrophobic c-termini (Momburg et al., 1994b; Schumacher et al., 1994) and it disfavours proline residues residing within the first 3 amino acids of the peptide (Neefjes et al., 1995). Each TAP heterodimer interacts with tapasin, calreticulin and MHC class I heavy chain/ β_2 -m dimers in a stoichiometric ratio of 1:4 (Bangia and Cresswell, 2005). Allelic variants of human and rat TAP have been described, but genetic polymorphism is limited in humans (Marusina et al., 1997), which instead have a high degree of polymorphism in their MHC I genes. Rat TAP is highly polymorphic and TAP2 alleles can vary in their affinity for class I molecules, which may cause their peptide-loading efficiency to vary. Rat class I and TAP genes appear to have co-evolved to maximize the supply of appropriate peptides to the presenting molecules (Joly et al., 1998). The genes encoding Chicken TAP and classical

class I are also thought to have co-evolved (Kaufman et al., 1999). Clinical studies have shown TAP to be important for the immune system, because in its absence patients display recurrent bacterial infections, but severe viral infections are absent. Patients also show necrotizing granulomatous skin lesions in the extremities and mid-face (Gadola et al., 2000). Viruses can also persist by blocking TAP, such as herpes simplex virus that expresses the protein ICP47 that binds TAP and inhibits peptide translocation (Fruh et al., 1995; Hill et al., 1995). Human cytomegalovirus prevents peptide translocation through TAP using protein U6 (Ahn et al., 1997; Hengel et al., 1997; Lehner et al., 1997). TAP downregulation or dysfunction has also been seen in tumours such as cervical carcinoma primary tumour tissue (Cromme et al., 1994a; Cromme et al., 1994b).

1.13.2 Tapasin

Tapasin was discovered as a protein associated with TAP (Ortmann et al., 1994) and was subsequently named TAP-associated glycoprotein, which was later shortened to tapasin (Tpn). It is an ER membrane spanning protein containing a single glycan chain in all species studied to date (except for chicken Tpn (Frangoulis et al., 1999), forming a bridge that brings TAP into close proximity with MHC class I molecules (Ortmann et al., 1997). Tpn influences the class I presentation machinery by improving TAP stability (Lehner et al., 1998), increasing TAP peptide transport into the ER and peptide binding to class I molecules (Li et al., 2000). Structurally, the first 50 N-terminal amino acids are important for class I assembly with TAP and Tpn-mediated peptide loading (Bangia et al., 1999). Tpn is a 48kDa protein that comprises an N-terminal ER luminal domain, a transmembrane region, a short cytoplasmic tail with a c-terminal retention sequence KKXX, where K represents Lysine and X represents any amino acid. Structural analysis has suggested that it is a member of the immunoglobulin superfamily (Herberg et al., 1998; Ortmann et al., 1997) and has two domains of 9kDa and 34kDa that are connected by a linker region (Chen et al., 2002).

Tapasin clearly seems important for MHC class I peptide loading, however there is allelic variability in Tpn dependence for different MHC class I molecules (Greenwood et al., 1994), which have been shown to have different levels of dependency for Tpn. For example, the MHC class I allele HLA-B*2705 has a low peptide-loading dependency on Tpn (Peh et al., 1998) but shows a dramatic improvement in its thermostability profile when Tpn is present (Williams et al., 2002b), suggesting that while a tapasin-mediated class I-TAP interaction is not essential for peptide loading of MHC class I molecules, MHC class I optimization can be maximised within peptide complex. Howarth et al studied the selection of the MHC class I peptide repertoire using a series of individual peptides with a wide binding affinity range to MHC class I molecules. An MHC class I peptide-specific antibody was used

to detect presentation of each minigene-expressed peptide variant. In wild-type cells, the hierarchy of presentation followed peptide half-life, however, this hierarchy broke down in cells lacking tapasin but not in cells deficient in calreticulin or in cells lacking PLC-associated ERp57 (Howarth et al., 2004). This demonstrated a key role for tapasin in determining MHC class I peptide repertoire that is perhaps analogous to HLA-DM which edits the peptides bound to MHC class II according to their binding stability (Brocke et al., 2002). Tpn is also known to interact with ERp57 through a disulphide bond (Dick et al., 2002). At steady state, all ERp57 molecules in the PLC are thought to be stably disulfide-linked to tapasin with a stoichiometry of 1:1 (Kienast et al., 2007), between the active site Cys57 of ERp57 and unpaired Cys95 of Tpn (Dick et al., 2002). Tpn is recognized as a unique substrate for ERp57, because it does not disengage from the oxidoreductase, unlike other protein substrates; trapping ERp57 in a stable disulfide complex (Peaper et al., 2005).

1.13.3 Calnexin

Calnexin is a 65kDa ER-resident chaperone that assists the folding of poorly folded proteins. One such substrate protein to be characterised is the MHC class I heavy chain (Anderson et al., 1993). Calnexin consists of a single transmembrane domain and a cytosolic tail, which contains an ER retention sequence (Bergeron et al., 1994). The crystal structure of the luminal domain reveals that the N and C termini form a globular domain with an extended proline-rich loop (P-domain) protruding from it (Schrag et al., 2001). The globular domain contains a carbohydrate binding site that recognizes an early oligosaccharide processing intermediate on folding glycoproteins, Glc₁Man₉GlcNAc₂ (Ware et al., 1995). Calnexin and its soluble homologue calreticulin have also been shown to be capable of binding proteins independently of their carbohydrate domain, suggesting that they are capable of peptide-peptide interactions (Ihara et al., 1999). The P-domain contains a tandem sequence repeat that comprises 4 copies of two sequence motifs arranged in the order 11112222.

1.13.4 Calreticulin

CRT is a 46.8kDa soluble lectin chaperone that shares homology with the membrane-bound calnexin ranging from 42% (residues 355-442) to 78% (residues 307-334) (Wada et al., 1991). The most striking and highly conserved segment contains two tandem repeat motifs, repeated four times each in CNX and three times each in CRT (David et al., 1993; Fliegel et al., 1989; Michalak et al., 1992; Wada et al., 1991). CRT's primary structure has been constructed into three domains using sequence prediction plots showing an N-domain, which comprises residues 1-180; the P-domain: 181-290 and the C-domain: 291-400.

The N-domain is currently thought to form a globular structure consisting of 8 anti-parallel β strands, with a short helical segment at residues 91-96. It also contains a low affinity, high capacity zinc-binding site (14 mol of zinc per mol of CRT) (Khanna et al., 1986; Li et al., 2001) as well as the lectin-binding site (Frickel et al., 2002) that specifically recognises the glycan processing intermediate $\text{Glc}_1\text{Man}_9\text{GlcNAc}_2$ described above.

The central proline-rich domain (P-domain) has been of particular interest, because it is thought to have three distinct functions; substrate binding (Peterson and Helenius, 1999; Vassilakos et al., 1998); containing a high affinity but low capacity calcium-binding site (1 mol calcium per mol CRT (Baksh and Michalak, 1991)); and potentially participate in protein-protein interactions (Peterson and Helenius, 1999; Vassilakos et al., 1998). The CRT P-domain contains three copies of two sequence repeats of 17 amino acids (repeat 1) and 14 amino acids (repeat 2), in the arrangement 111222.

To date, only the NMR-structure of the rat CRT P-domain has been solved (residues 189-288 (Ellgaard et al., 2001)). It is characterised by an extended hairpin fold, which loops back on itself, placing the N and C-termini next to one another. The structure is stabilized by three short anti-parallel β -sheets located at residues 189-192, 276-279, 206-209 and 262-265 and 223-226 and 248-251 and the tip of the hairpin contains a helical turn at residues 238-241 as well as a well-defined hydrophobic cluster of Lysine, Proline and Tryptophan amino acids. The p-domain then crosses over itself at each anti-parallel β -sheet. The proline clusters flanking the β -sheets have a low preference for folding into β -sheets and are thought to prevent them from growing longer. The high content of proline residues may also explain why the secondary structure computer programmes predicted very few secondary structure elements. Frickel et al (2002) analysed this domain and discovered that CRT and ERp57 interactions occur exclusively at the hairpin structure of CRTs P-domain, between residues 225-251 (Frickel et al., 2002). Their analyses suggested that ERp57 binding at the distal end of this domain is likely to generate a partially solvent-shielded cavity surrounded by the lectin domain. This is thought to restrict access of other folding chaperones and intermediates and ensure that aggregation and formation of non-native intermolecular disulphides with other newly synthesized proteins is repressed (Frickel et al., 2002).

The C-domain is characterised by a high number of acidic residues, which is consistent with the location of a low-affinity, high-capacity calcium-binding site (~20 mol calcium per mol CRT) (Baksh and Michalak, 1991). Removal of bound calcium abrogates oligosaccharide binding (Vassilakos et al.,

1998). It also contains the ER COOH-terminal retention and retrieval Lys-Asp-Glu-Leu (KDEL)(Fliegel et al., 1989; McCauliffe et al., 1990; Smith and Koch, 1989) amino acid sequence that ensures that it is returned via the KDEL receptor in COPI vesicles in the retrograde pathway if it escapes (Pelham, 1989). The KDEL sequence is only functional when present at the extreme c-terminus (Lewis and Pelham, 1990; Pelham, 1989). Recently, a study on *Dictyostelium* PDI has shown that when a chimera made from GFP was fused to the c-terminal 57 amino acids of PDI, the resultant fusion protein was retained with similar efficiency to the *Dictyostelium* tetrapeptide sequence HDEL-GFP chimera (Monnat et al., 2000), suggesting that c-terminal regions may also complement KDEL-mediated retrieval. Indeed, the acidic c-terminus has been implicated in CRT retention in the ER (Sonnichsen et al., 1994). The spatial organisation of the three domains has not yet been identified but sedimentation analysis has shown that it adopts an elongated shape in solution (Li et al., 2001), possibly attributed due to the extended hairpin structure adopted by the P-domain. This strongly suggests that the protein is characterised by high intrinsic structural plasticity, which may be an attribute required for its chaperone function (Bouvier and Stafford, 2000).

The suboptimal loading properties and trafficking rate of the T134K MHC class I molecule are strikingly similar to those of class I molecules studied in the CRT-deficient cell line K42 (Gao et al., 2002). MHC class I molecules are poorly peptide loaded, which may be as a result of an increased trafficking rate to the cell surface compared to CRT-competent cells and are unable to efficiently process and present antigen to elicit an efficient CTL response. There is also the suggestion that class I may have impaired PLC binding, but this was not a major conclusion of the paper. These effects could implicate CRT in several key roles in MHC class I peptide-loading, which may include MHC class I PLC recruitment, retaining poorly peptide loaded class I molecules in the ER or retrieving them from the secretory pathway to the ER using its KDEL ER retrieval sequence. MHC class I molecules do not contain a retrieval sequence, so it is possible that CRT could constitute part of an ER-Golgi quality control mechanism. This model would require CRT to sense the difference between incompletely folded class I molecules and those stably loaded with peptide and competent to proceed past this checkpoint. Li et al observed that CRT predominantly associated with empty class I molecules, while Tpn interacted with both empty and loaded class I molecules (Li et al., 1999). Whether CRT operates independently or in collaboration with another co-factor in the model is unclear, however a good candidate would be ERp57, considering their mutual reliance in glycoprotein folding and the formation of the PLC.

1.13.5 ERp57

ERp57 is a 54kDa protein and member of protein-disulphide isomerase (PDI) enzyme family responsible for promoting disulphide bond formation in glycoproteins. It has a domain structure written schematically as **a-b-b'-a'** to differentiate their functions; the a and a' correspond to the thioredoxin-like domains, each containing two active site C-X-X-C motifs; the b and b' appear to be important for isomerisation reactions (Ferrari and Soling, 1999). It is retained within the ER through a QEDL retrieval sequence present in its C-terminus. ERp57 has been shown to form transient intermolecular disulphide bonds with glycoprotein substrates bound to CNX and CRT during viral glycoprotein folding in the ER of living cells (Frickel et al., 2002; Molinari and Helenius, 1999). When the glucosidase inhibitor castanospermine is used to block glycoproteins from binding CNX and CRT, intermolecular disulphide bonds formation is abrogated (Frickel et al., 2002). These observations would suggest that ERp57-protein interactions can only be mediated through CNX and CRT but recently, ERp57 has been shown to interact directly with the α_2 disulphide-bond within the peptide binding groove of the class I alleles HLA-A*0201 (Antoniou et al., 2007) and HLA-B*4402 (Kienast et al., 2007). ERp57 is connected to peptide loading complex through Tpn by a disulphide bond between cysteine 57 and 95 of the N-terminal domain of Tpn and forms a bridge connecting CRT with Tpn (Wright et al., 2004). ERp57 $-/-$ cells show impaired CRT and HC recruitment to the PLC, poor class I peptide-loading and accelerated class I trafficking to the cell surface compared to ERp57 $+/+$ cells, suggesting that it plays an important role in class I antigen presentation.

1.13.6 PDI

Like ERp57, PDI (Protein Disulphide Isomerase) is a 55kDa member of the thioredoxin superfamily. Its structure consists of two double cysteine and redox-active sites, organized into a similar domain structure to ERp57 of **a-b-b'-a'-c**; the additional "c" domain, which is absent in ERp57 is a putative low affinity but high capacity Ca^{2+} binding site (Macer and Koch, 1988). It shares an overall identity of 33% with ERp57 (Ferrari and Soling, 1999). Alongside its redox/isomerase activities as a chaperone, PDI's can also interact with incorrectly folded polypeptides through two peptide binding sites; one in the b' domain and the other in the c-terminal 57 residues after the a' domain (Klappa et al., 1998; Noiva et al., 1993). The binding affinity increases with increasing length of the substrate backbone, but for peptides of similar length, those containing Cys residues enhance PDI binding (Klappa et al., 1997; Morjana and Gilbert, 1991). Recently, Park et al demonstrated that PDI was part of the MHC class I antigen processing machinery within the PLC and interacts with the α_2 disulphide bond in the peptide-binding groove. It promotes oxidization of the disulphide bond, which appears to be required for optimal peptide selection (Park et al., 2006). The importance of PDI in antigen presentation has yet to

be widely accepted in the field because there are irregularities in the literature; Santos et al have shown that it is present in the PLC (Santos et al., 2007) while other groups have not (Wearsch and Cresswell, 2007).

1.14 Molecular model for role of PLC

MHC class I peptide-loading in close proximity to TAP appears to be an important feature for antigen presentation, because it places class I molecules near a direct source of peptide, reducing the likelihood of peptide being the rate limiting factor for class I assembly. Indeed, MHC class I assembly in the absence of TAP leads to unstable class I molecules that are not exported from the ER (Cerundolo et al., 1990; Van Kaer et al., 1992). MHC class I molecules can show different levels of TAP-dependency (Neisig et al., 1996). For example, generating an HLA-B7 molecule containing an amino acid substitution from tyrosine to aspartic acid at position 116 correlates with better TAP association. It can also be seen in naturally occurring class I alleles, such as HLA-B*1510 that differs from B*1518 by a tyrosine to serine residue at position 116. This difference appears to be the cause of B*1510 associating well with TAP and displaying a greater proportion of stable class I molecules at the cell surface compared to B*1518, which associates with TAP poorly and is more unstable (Turnquist et al., 2000).

Tpn is also thought to be important for MHC class I peptide-loading and single amino acid substitutions can profoundly effect whether a class I allele is Tpn dependent or not. Three residues in the β -sheet floor of the class I peptide binding groove at residues 114 (Park et al., 2003), 115 (Beissbarth et al., 2000) and 116 (Neisig et al., 1996) seem to be principally responsible for this. For instance, position 114 contains an acidic residue in Tpn-dependent alleles, such as aspartic acid in HLA-B*4402, but is basic in Tpn-independent alleles, such as hisidine in B*2705. To illustrate the subtle differences that can occur between Tpn-dependent and independent alleles, a tyrosine (Y) to aspartic acid (D) substitution at residue 116 distinguishes HLA-B*4402 from -B*4405. This makes -B*4402 dependent on Tpn to load peptides compared to -B*4405 which is independent (Williams et al., 2002b).

Structural considerations within the MHC class I peptide binding groove may also contribute to the differences between Tpn-dependent and independent alleles (Figure 1.7). The groove termini have quite different characteristics; the peptide N-terminus is quite rigid because hydrogen bonds that interact with the groove cannot exchange with water (Zacharias and Springer, 2004), while the C-terminal region shows a greater conformational variation (Smith et al., 1996) that can. Peptide-binding

is thought to induce a conformational shift in the C-terminus (Elliott, 1997a), which is the same region implicated in Tpn binding (Harris et al., 2001; Yu et al., 1999). It is possible that Tpn binding may induce a shift in the geometry of the groove to one favouring peptide-binding. The “venus fly-trap” model (Williams et al., 2002a) is thought to describe these differences by proposing that MHC class I heterodimers may have two conformations that differ in their affinities for peptide (Williams et al., 2002a; Zacharias and Springer, 2004)(see Discussion). In summary, Tpn-dependent alleles are thought to require Tpn assistance to adjust the binding groove toward a peptide receptive conformation, compared to Tpn-independent alleles that have a more rigid structure that does not.

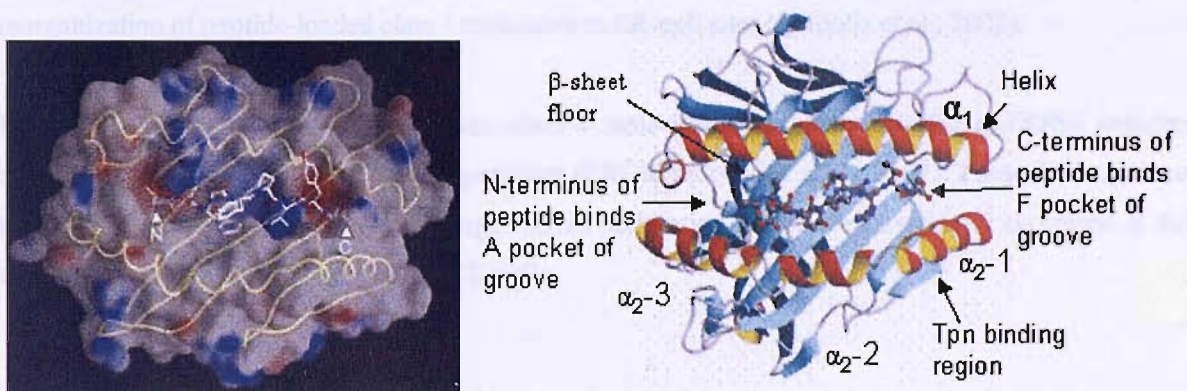


Figure 1.7: Ribbon structure superimposed onto a spacefilling model of the MHC I HLA-A*0201 peptide binding groove in complex with peptide. Adapted from bio.dfci.harvard.edu/Tool/rankpep_help.html. This is displayed alongside an annotated schematic of the peptide binding groove. Adapted from Zacharias and Springer, 2004.

Disulphide isomerases may also contribute to peptide binding, but the evidence for PDI has yet to be accepted by the wider antigen presenting community for the reasons described above. Oliver et al developed an *in vitro* assay that demonstrated how recombinant ERp57 could act as a reductase on a partially folded pool of MHC class I molecules that reacted to the HC antibody HC10 (Oliver et al., 1999). It has since been shown to interact with the class I peptide binding groove (Antoniou et al., 2007; Kienast et al., 2007) and form a HC-ERp57-Tpn conjugate (Santos et al., 2007). The current working model proposes that both PDI and ERp57 have access to the peptide-binding groove of MHC class I molecules during their assembly within the PLC, where they may play complementary roles in regulating the peptide-binding groove redox state so that only optimally loaded molecules egress to the cell surface.

Cooperative binding with CRT is thought to increase Tpn's affinity to the class I heterodimer and its ability to stabilize the open, peptide-free conformation, since they are both linked together through ERp57 (Bangia et al., 1999; Harris et al., 2001; Turnquist et al., 2000; Yu et al., 1999). This would further add to the stringency of peptide editing. Whether the Tpn-CRT bond has to be broken before a class I molecule can dissociate is unclear, but a rescue mechanism has been proposed (Walker and Gilbert, 1997) in which ERp57 could use an internal cysteine (e.g. Cys-60) to liberate the adjacent Cys-57 from the Cys-95 disulphide bond with Tpn. This would have the effect of destabilizing the PLC, causing it to dissociate. Other factors may also contribute to class I dissociation from the PLC, such as ATP hydrolysis and depletion in the vicinity; possibly mediated by TAP; but also the spatial reorganization of peptide-loaded class I molecules to ER-exit sites (Spiliotis et al., 2002).

Following transport to the ER exit sites, class I molecules are transported in COPII vesicles towards the ER-Golgi intermediate compartment (ERGIC) (Spiliotis et al., 2002). These then continue through the secretory pathway and undergo further maturation before they are finally expressed at the cell surface for presentation to activated T_c cells.

1.15 The aims of this study

Efficient CTL cell responses require MHC class I molecules to be loaded with high affinity peptides. Elucidating the mechanisms involved in MHC class I processing and presentation will help towards the development of CTL-mediated vaccination strategies against tumours and viruses such as Hepatitis C Virus (HCV) and Human Immunodeficiency Virus (HIV), which constantly escape T-cell and antibody responses (Zinkernagel, 2003). The effects of the ER chaperones calreticulin, ERp57 and tapasin on MHC class I assembly and cell surface presentation have been investigated, but we still do not understand the individual contribution of each chaperone and how this leads to the efficient loading and peptide optimisation of MHC class I molecules. The intracellular behaviour and cell surface expression of the MHC class I molecules H-2K^b and H-2D^b in calreticulin-deficient cells was reported in Gao et al (Gao et al., 2002). The aim of this study is to investigate the mechanism behind the phenomenon that Gao et al reported. The possible roles, consequences and biological mechanisms are then discussed. Specifically, objectives of this study are to investigate:

- The function of the KDEL sequence and c-terminus of CRT,
- The function of ERp57 binding to CRT and
- The function of the CRT glycan binding site.

Chapter 2: Materials and methods

2.1 Antibodies.

Details listed in Table 2.1 and 2.2.

- Primary antibodies used:

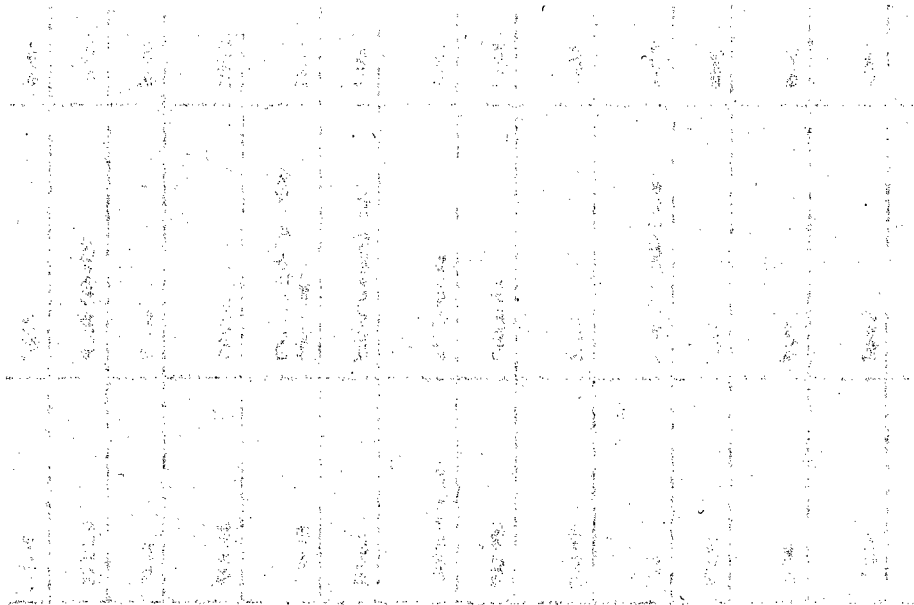
Y3 (Hammerling et al., 1982), B22.249 (B22) (Lemke et al., 1979), 25-D1.16 (D1) (Porgador et al., 1997), BB7.2 (Parham and Brodsky, 1981), PA3-900 (Affinity Bioreagents, Inc. Golden USA), PA3-009 (Affinity Bioreagents, Inc. Golden USA), anti-HA-probe (Santa Cruz Biotechnologies Inc. USA (Chen et al., 1993)), anti-glyceraldehyde-3-phosphate dehydrogenase (GAPDH)(Abcam), anti-Tapasin antiserum (Li et al., 1999), T18 antiserum (Rigney et al., 1998), anti-rat TAP1 antiserum (Powis, 1997), 24/94 antiserum (Carreno et al., 1995), anti-calnexin SPA-860 (Stressgen), PDI antiserum (Benham et al., 2000), anti-KDEL receptor (Calbiochem).

- Fluorophore-conjugated antibodies used:

Alexa Fluor® 546 anti-mouse IgG, Alexa Fluor® 488 anti-rabbit IgG, Alexa Fluor® 647 anti-mouse IgG, anti-mouse IgG phycoerythrin (PE), anti-mouse IgG fluorescein isothiocyanate (FITC).

- HRP-conjugated antibodies used:

anti-mouse IgG, anti-rabbit IgG.



at the end of the document. The text is very faint and illegible.

Table 2.1: Antibody information: IP, Immunoprecipitation, FACS; Fluorescence Activated Cell Sorting, WB, Western Blot, IP, Immunofluorescence.

Antibody	Specificity	Derived Species	Type	Isotype	Working dilution	Company / Source	Details
Y3	H-2Kb	Mouse	Monoclonal	IgG2a	IP and FACS: 10µg/ml	Hammerling et al., 1982	recognises a conformation-sensitive epitope on the alpha domain of murine H2-Kb.
B22.49	H-2Db	Mouse	Monoclonal	IgG2b	IP and FACS: 10µg/ml	Lenke et al., 1979	recognises a conformation sensitive epitope on the alpha domain of murine H2-Db.
25-D1.16	H-2Kb-SIINFEKL	Mouse	Monoclonal	IgG1	FACS: 20µg/ml	Porgador et al., 1997	recognises H2-Kb in complex with the SIINFEKL peptide residues 257-264 ovalbumen.
BB7.2	HLA-A2	Mouse	Monoclonal	IgG2b	IP: 10µg/ml; FACS: 10 to 20µg/ml	Parham and Brodsky, 1981	anti HLA-A2 antibody and was a human isotype control in experiments involving Y3, B22 and D1
SPA-860	Calnexin	Rabbit	Polyclonal	IgG	WB: 1:10,000	Stressgen	generated against a synthetic peptide derived from canine calnexin residues 575-593. Supplied as a 50µl aliquot.
GAPDH	Glyceraldehyde 3 phosphate dehydrogenase	Mouse	Monoclonal	IgG2b	WB: 1ng/ml	Abcam	Anti-glyceraldehyde-3-phosphate dehydrogenase antibody. Recognises a 30-40kDa subunit of the 140kDa protein
HA-tag	Influenza hemagglutinin	Rabbit	Polyclonal	IgG	WB: 1µg/ml; IP: 1.5µg/ml	Santa Cruz Biotechnologies Inc. USA	raised against amino acids 98-108 of influenza hemagglutinin (HA); YPVD VPD YASL
αKDEL-receptor	KDEL-receptor	Rabbit	Polyclonal	IgG	IP: 1:200	Calbiochem	clone KR-10, raised against a synthetic peptide corresponding to amino acids 192-212 of the bovine KDEL receptor
P A3-900	Calreticulin	Rabbit	Polyclonal	IgG	WB: 1:1000	Affinity Bioreagents, Inc. Golden USA	raised against human recombinant calreticulin, supplied as 100µl of diluted reagent
P A3-009	ERp57	Rabbit	Polyclonal	IgG	WB: 1:3000	Affinity Bioreagents, Inc. Golden USA	raised against amino acid residues 490-505 of human ERp57 and is supplied as 100µl of diluted reagent
PDI	Protein Disulphide Isomerase	Rabbit	Polyclonal	IgG	WB: 1:1000	Benham et al., 2000	raised against purified PDI protein; gift to Adam Benham from Dr P Klappa, University of Canterbury, UK.
αTAP1	TAP1	Sheep	Polyclonal	IgG	IP: 1:500	Powis, 1997	anti-rat TAP1 antiserum
24/94	TAP1	Rabbit	Polyclonal	IgG	WB: 1:500	Carrero et al., 1995	reacts against the c-terminal sequence CKRGCGYRAMVEALAAPAD of murine TAP-1
αTapasin	Tapasin	Rabbit	Polyclonal	IgG	WB: 1:1000	Li et al., 1999	antibody maps to the peptide sequence CATAASLTTPRMSKKSQ and recognises mouse Tapasin. Supplied as serum.
T18	H2-Kb and H2Db Heavy chain	Rabbit	Polyclonal	IgG	WB: 1:1000	Rigney et al., 1998	raised against H2-Db residues 1-193 inclusion bodies. It recognises epitopes on both Db and Kb α1 and α2 heavy chains which are lost upon β2-m binding but remain when heavy chains bind to peptides in the absence of β2-m. Supplied as Ascites

Table 2.2: Antibody information

Antibody	Specificity	Derived Species	Type	Isotype	Working dilution	Company / Source	Details
Fluorophore-conjugated antibodies							
Alexa Fluor® 546	Antimouse IgG heavy and light chain	Goat			FACS; 2µg/ml (i.e. 1:1000 dilution).	Molecular Probes	
Alexa Fluor® 488	Anti-rabbit IgG	Goat			FACS; 2µg/ml (i.e. 1:1000 dilution).	Molecular Probes	
Alexa Fluor® 647	Antimouse IgG	Goat			FACS; 1µg/ml (i.e. 1:2000 dilution)	Molecular Probes	
Ab7002 - Phycoerythrin (PE)	Antimouse IgG.	Goat			FACS; 3.3µg/ml (i.e. 1:150 dilution)	Abcam	
Fluorescein Isothiocyanate (FITC)	Antimouse IgG.	Goat			FACS; 1:100	Sigma	Supplied as 1ml aliquot.
HRP-conjugated antibodies							
Anti-mouse IgG	Fc specific.	Goat			WB; 1:10,000	Sigma	Supplied as 1ml aliquot.
Anti-rabbit IgG	Fc specific.	Goat			WB; 1:10,000	Sigma	Supplied as 1ml aliquot.

2.2 Cell lines.

Cells were grown in either **R10**; RPMI 1640 (Biowhittaker no L-glutamine)/10% heat inactivated Fetal Calf Serum (Globepharm, UK)/50U/ml penicillin & 50µg/ml (final) streptomycin mix (Biowhittaker)/2mM (final) L-glutamine (Biowhittaker), **D10**; Dulbecco's Modified Eagle's Medium (DMEM; Biowhittaker 4.5g/l glucose, no L-glutamine)/10% Fetal Calf Serum (Globepharm, UK)/50U/ml penicillin & 50µg/ml (final) streptomycin mix (Biowhittaker) and 2mM (final) L-glutamine (Biowhittaker) or **Hybridoma media**; R10/1mM pyruvate [Sigma]/50µM β-mercaptoethanol [Sigma] at 37°C with 5% CO₂. Adherent cells were harvested using Trypsin (500mg/l) EDTA (200mg/l)(Biowhittaker).

Mouse fibroblast cell-lines were cultured in R10. K41 is CRT competent while K42 is a CRT knock-out fibroblast line that was generated by homologous recombination (as described (Mesaeli et al., 1999)). K42 were engineered to contain a variety of CRT constructs. These included; K42 transfected with a 34 amino acid c-terminally truncated gene encoding rabbit CRT (K42CRTΔC)(gift from Marek Michalak); K42 transduced with a retrovirus to contain rat CRT ± HA tag (HA probe sequence TACCCATACGATGTTCCGGATTACGCTAGCCTC (Chen et al., 1993)) immediately 5' of the KDEL sequence for wild-type rat CRT and the predicted Erp57 binding mutant; or 3' of the c-terminal truncated mutants. Cells were designated by their CRT modification (KDEL, HAKDEL, HAKDEV, HAKDQL, HAAKDEL, HAΔ11aa, HAΔ22aa, HAΔ34aa or HAΔEB).

R10 cultured RMA-S (H-2^b) were generated by Ethyl Methanesulphonate mutagenesis of the Rauscher virus-induced T cell lymphoma cell RMA and selection for low surface MHC class I expression by antisera to MHC class I and complement (Ohlen et al., 1989). RMA-S cells have a defective TAP2 gene (Powis et al., 1991).

Phoenix-Ecotropic is a retroviral packaging cell-line based on the human fibroblast cell-line 293T, stably expressing Moloney Murine Leukaemia Virus gag, pol and env. These were grown in D10.

2.3 Retroviral Transduction.

Phoenix cells express the gag, pol and env structural gene products required to generate Moloney Murine Leukemia Virus. RNA containing a packaging signal and long terminal repeats, derived from plasmid transfection of these cells, is packaged into the newly generated virus particles. These then bud from the Phoenix cells and accumulate in the cell culture media. This is then harvested and used to infect target cells. Once infected, the viral RNA is reverse-transcribed into DNA and inserted into the host genome. Viral particles do not contain any structural genes as a safety measure, so cannot be produced by the target cell. Ecotropic phoenix cells will only infect mouse cells.

2×10^6 cells were plated o/n in wells of a 6-well plate and transfected the following day (day1) at a density of approximately 70-80% using Lipofectamine 2000 (Invitrogen), according to manufacturers instructions (1 μ g DNA). On day 2, cells were given 3ml fresh D10 medium and incubated at 32°C o/n. On day 3, cell media was harvested and centrifuged at 1500rpm for 5min to pellet any cell debris. Cells to be transduced were resuspended in this supernatant, which contained the retroviral particles, 5 μ g/ml polybrene (Hexadimethrine bromide; Sigma) and 25mM HEPES (Sigma) and centrifuged at 2500rpm for 2hr at 32°C. This retroviral supernatant could be snap-frozen in dry ice/methanol and stored at -80°C for transduction at a later date. After centrifugation with retroviral supernatant, the cells were incubated at 37°C and resuspended in fresh medium the next day. Details of the Phoenix cell line and retroviral transduction can be found on the Dr. Gary Nolan webpage (www.stanford.edu/group/nolan/).

CMV-bipep- Δ NGFR (Appendix 1) has been previously described (Tolstrup et al., 2001) and has the ability to express Δ NGFR from the same promotor as the CRT gene, via an internal ribosomal entry site (IRES). Δ NGFR is a form of the p75 Nerve Growth Factor Receptor with most of the cytoplasmic tail truncated and is used as a selection marker gene. Δ NGFR-expressing cells were purified once using antibody-coated CELlection Pan Mouse IgG Dynabeads (DynaL Biotech) and then clones established using limiting dilution.

2.4 Bead Purification of Cells.

300 μ l RPMI 1640 and 1% FCS (called R1) was added to 20 μ g anti- Δ NGFR antibody and 100 μ l CELlection Pan Mouse IgG Dynabeads (DynaL Biotech). This was rotated for 30min at 4°C. Free antibody was removed by washing twice with 1ml R1, using a Dynal MPC-S magnet and resuspending in 100 μ l R1. These antibody-coated beads could be stored for several months at 4°C. Transduced cells were washed in R1 and then resuspended in 300 μ l R1 with 7 μ l antibody-coated beads. Cells were incubated for 10min at r/t, with frequent suspension. The beads were washed four times with 1ml R1, pipetting up and down several times to remove cells not bound to the beads. Cells were then incubated in a 24-well plate. The beads did not appear to impair growth of the cells.

2.5 Cell Cloning by Limiting Dilution.

1ml from 10ml R10 containing 1×10^5 cells was transferred into 9ml R10 to give 1×10^4 cells/10ml. This was repeated again to give a dilution of approximately 1×10^3 cells/10ml. For a dilution of 1, 0.5 or 0.3 cells/well of a 96-well plate, 100 μ l, 50 μ l or 30 μ l, was then transferred to 10ml of R10. 100 μ l of this suspension was then loaded per well of a 96-well plate. Fibroblast clones could not grow well alone and needed approximately 3×10^6 of 30min γ -ray-irradiated K42 cells per 96-well plate. 100 μ l of these cells were added per 96-well.

2.6 Production of Mutant Constructs.

2.6.1 PCR

A four-step method was used to generate the expression constructs; illustrated in Figure 2.3 mutant rat CRT constructs were PCR amplified from a pCR3 vector containing wild type rat CRT (kind gift from Antony Antoniou) using the appropriate combination of primers shown in section 2.7. PCR conditions: 5µl 1x pfu DNA polymerase buffer (promega), 4% DMSO (Dimethyl sulphoxide, SIGMA), 0.2µM forward and reverse primers, 1µl (approximately 100ng) template DNA, 1µl Pfu DNA polymerase (Promega), dH₂O made up to 50µl. PCR programme used: 95°C 2 min initial step followed by 30 cycles of 95°C for 1 min, annealing at 53.2°C for 30 sec and extending at 72°C for 4 min. The programme was completed with a final extension at 72°C for 10 min. The PCR products were PCR purified using a Qiagen kit and eluted in 30µl ddH₂O.

2.6.2 Restriction enzyme digest

The purified PCR product was digested with XhoI and HincII for 2 hours at 37°C. Digest conditions: 20µl PCR product, 1x buffer B (Promega), 1µl XhoI (10u/µl Promega), 1µl HincII (10u/µl Promega) and dH₂O made up to 50µl. This was Qiagen PCR purified.

A Qiagen midi-prep of CMV-bipep-ΔNGFR was made from an existing bacterial stock. 10µl was taken for a restriction enzyme digest. Digest conditions: 1x buffer B (Promega), 1µl XhoI (10u/µl Promega), 1µl HincII (10u/µl Promega), dH₂O made up to 50µl incubated at 37°C for 2 hours. The digested product was separated on an agarose gel and the band of correct size was excised and purified using a Qiagen gel purification kit.

2.6.3 DNA Ligation

Optimal ligation of the digested PCR product and CMV-bipep-ΔNGFR vector was undertaken by mixing at ratios of 3:1, 1:1 and 1:3 for 5 min at r/t followed by Qiagen PCR purification. Ligation conditions: 1x T4 DNA ligase buffer (Promega), 1-3u/µl T4 DNA ligase (Promega), 1µl digested CMV-bipep-ΔNGFR, PCR product volume varied according to the above ratio, dH₂O made up to 20µl. Following transformation into DH5α cells, colonies were PCR screened on a 1% agarose gel for the presence of the insert. Procedure: a p10 disposable Gilson tip was used to pick part of the bacterial colony from an agar Petri dish inoculated with 100µg/ml ampicillin (Sigma). Material taken by the p10 tip was mixed with 20µl dH₂O, boiled for 5 min and centrifuged at 13krpm for 15 min to generate a bacterial lysate. PCR conditions: 0.2µM dNTPs (Promega), 5u/µl Taq DNA polymerase (Promega), 1.5mM MgCl₂ (Promega), 1x MgCl₂-free Tag Polymerase buffer, 5µl bacterial lysate, 0.2µM CMV F and CMV R primers (see section 2.8), dH₂O to make up to 25µl. The same PCR programme used to generate the above mutant CRT PCR products was used. Plasmid DNA was purified and sequenced.

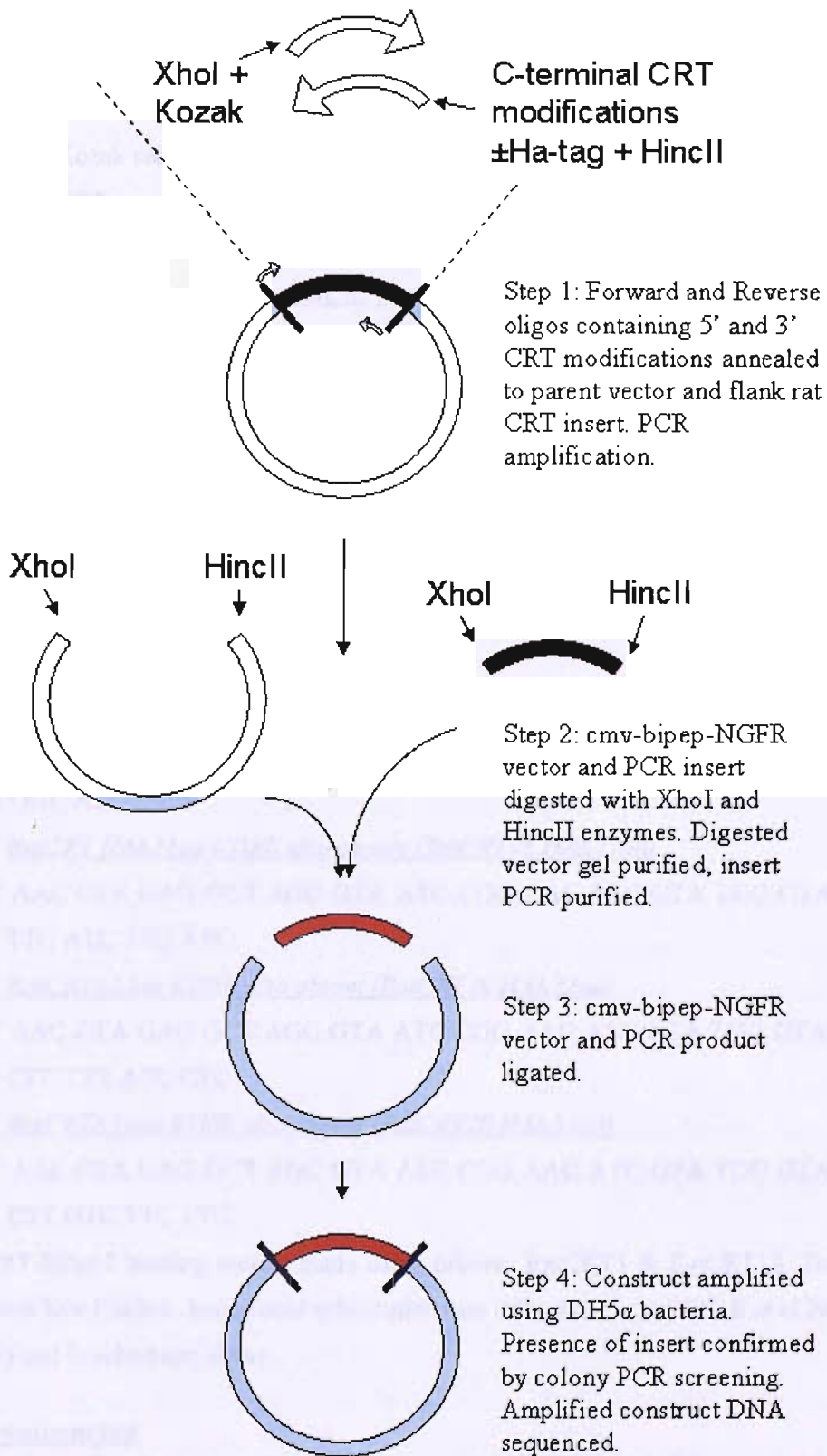


Figure 2.1: Schematic showing the four-step protocol used to generate each of the CRT constructs.

2.7 Retroviral Vector

CMV-bipep-ΔNGFR primer and restriction enzymes used are shown below:

CTC GAG – 5' Xho I restriction enzyme sequence

GTT AAC – 3' Hinc II restriction enzyme sequence

GCC ACC A – Kozak sequence

Forward 5' Rat CRT sequence (RatCRT3)

CCA CTC GAG GCC ACC ATG CTC CTT TCG GTG CCG

Reverse 3' RatCRT KDEL sequence (RatCRT10 KDEL)

GGT GTT AAC CTA CAG CTC ATC CTT GGC TTG

Reverse 3' RatCRT HAKDEL sequence (RatCRT11 HA KDEL)

GGT GTT AAC CTA CAG CTC ATC CTT GAG GCT AGC GTA ATC CGG AAC ATC GTA
TGG GTA GGC TTG GCC AGT GGC ATC

GAG-TGGGTA = HA Tag

Reverse 3' RatCRT HAKDEV sequence (RatCRT15 HA KDEV)

GGT GTT AAC CTA CAC CTC ATC CTT GAG GCT AGC GTA ATC CGG AAC ATC GTA
TGG GTA GGC TTG GCC AGT GGC ATC

Reverse 3' RatCRT HAΔKDEL (RatCRT17 HAΔKDEL)

GGT GTT AAC CTA GAG GCT AGC GTA ATC CGG AAC ATC GTA TGG GTA GGC TTG
GCC AGT GGC ATC

Reverse 3' RatCRT HAΔ11aa KDEL also absent (RatCRT18 HAΔ11aa)

GGT GTT AAC CTA GAG GCT AGC GTA ATC CGG AAC ATC GTA TGG GTA CTT CTC
ATC CTC TTC ATC TTC ATC

Reverse 3' RatCRTΔ22aa KDEL also absent (RatCRT19 HAΔ22aa)

GGT GTT AAC CTA GAG GCT AGC GTA ATC CGG AAC ATC GTA TGG GTA GTC ATC
CTC ATC CTC TTT ATC CTC

Reverse 3' RatCRTΔ34aa KDEL also absent (RatCRT20 HAΔ34aa)

GGT GTT AAC CTA GAG GCT AGC GTA ATC CGG AAC ATC GTA TGG GTA CTC TTT
ACG CTT CTT GTC TTC TTC

HAE EB CRT-ERp57 binding mutant made using primers RatCRT3 & RatCRT10. Template was obtained from Eva Frickel. Amino acid substitutions are referenced in Frickel, E et al 2002 (Frickel et al., 2002) and in schematic above.

2.8 DNA sequencing.

The DNA Sequencing Facility, Oxford University, OX1 3QU was used for sequencing (website address: polaris.bioch.ox.ac.uk/dnaseq/). 3.2pmol/ul primer and at least 0.4ug/ul plasmid template were supplied for analysis. CMV-bipep-ΔNGFR was sequenced using the primers:

CMV F 5' TAT CTG GCG GCT CCG TGG 3'

CMV R5' CCG GCC TTA TTC CAA GCG 3'

2.9 Flow Cytometry.

Cells were trypsinised at r/t and immediately transferred to 4°C to minimize loss of fast decaying class I complexes from the cell surface, washed in FACS wash (10mM Phosphate buffer, 2.7mM KCl₂, 137mM NaCl₂ (PBS pH7.4), 2% Fetal Calf Serum, 0.02% NaN₃) and incubated in a saturating concentration of 1° antibody for approximately 30mins (Y3; 10µg/ml, B22; 10µg/ml, D1; 20µg/ml). Cells were washed twice in FACS wash and resuspended in Fluorescein-labelled Goat anti-mouse IgG (Sigma, UK), Phycoerythrin-labelled goat anti-mouse IgG or Alexa Fluor® 642 anti-mouse IgG for approximately 30mins. Cells were washed 3 times (optional fixation at third wash in 1% formaldehyde, followed by 10min incubation), resuspended in FACS wash and then transferred to FACS tubes for analysis on a FACScan flow cytometer (Becton Dickinson, US) using CellQuest software. At least 10,000 events were collected and a minimum of 5000 viable cells were gated by forward and side scatter.

2.10 GFP-ub-SL8 assay.

Adapted from (Neijssen et al., 2005):

2x10⁶ cells were harvested and subsequently electroporated according to the AMAXA nucleofection protocol (www.amaxa.com). Briefly, cells were resuspended in 100µl of AMAXA nucleofection "V" solution and mixed with 3µg DNA. A Nucleofector I machine (AMAXA) was then set to programme T-30 and electroporation cuvettes placed inside. Disposable syringes supplied with the kit were used to resuspend the electroporated cells in pre-warmed R10 media, which was then dispensed into a 6-well plate containing 1.5ml pre-warmed R10. These cultures were left for approximately 24hr. Cells were harvested by trypsinisation and prepared for flow cytometry (see method) – the only modification involved 10min 1° D1 and 2° Alexa Fluor® 642 anti-mouse IgG antibody incubations. Analysis was undertaken on a FACS Canto (Becton Dickinson, US) using FACS Diva software with at least 40,000 events being collected. Samples were gated against low, medium and high GFP fluorescence to which the corresponding D1 fluorescence could be correlated.

2.11 Immunoblotting

2.11.1 Reagents common to sections 2.11-14:

Nonidet P-40 (Sigma) lysis buffer; 150mM NaCl [Sigma], 5mM EDTA (ethylenediamine tetraacetic acid; calcium chelator)[Fisher], 20mM Tris-HCl pH7.4 [Sigma], 2mM Phenylmethyl sulfonyl fluoride (PMSF; an inhibitor of serine proteases such as trypsin and chymotrypsin) [Sigma], 2mM Iodoacetamide (IAA; also protease inhibitor) [Sigma], 0.5% Nonidet P-40.

3xNon-reducing loading buffer (NRLB); 2.4ml glycerol [BDH] (12% final), 1ml 1M Tris pH6.8 (50mM final), 8ml 10% SDS [Fisher] (0.5% final), 8.6ml H₂O, 0.05% Bromphenol Blue (Sigma).

3xReducing loading buffer (RLB); add 1:10 dilution of 1M stock 1,4-dithioerythritol (DTT)[Sigma] to NRLB.

2.11.2 Immunoblotting protocol

Cells were harvested, washed once in PBS and lysed in 0.5% Nonidet P-40 lysis buffer for a minimum of 20min at 4°C. Nuclei and other cell debris were spun down at 13krpm for 10min and the supernatant collected. This was mixed with either RLB or NRLB at 95°C ~5min and run on a 9, 10 or 12% SDS-PAGE gel at 200v for approximately 60min. Proteins were transferred to a Hybond-C Super nitrocellulose membrane (Amersham, UK) overnight by electrophoresis (12v) and blocked with blocking solution (BS); PBS, 0.2% Tween (PBST) and 5% fat free milk (Marvel) for 60min. The membrane was washed 3 times for 10min under gentle agitation in PBST and then incubated in 1° antibody diluted in BS for 60min. The antibody could be used repeatedly if stored at -20°C in the presence of 0.02% sodium azide (Sigma). The membrane was then washed a further 3 times in PBST and incubated in a horseradish peroxidase-conjugated 2° antibody diluted in BS for 45-60min. The membrane was washed a further 3 times in PBST and developed with SuperSignal West Pico Chemiluminescent Substrate (Pierce, UK) and imaged with a Fluor-S Multi-imager (Biorad, UK). In figures where bands for a particular protein are being compared in different samples, the images are all derived from the same exposure and blot.

2.12 Immunoprecipitation (IP).

2.12.1 Detecting ERp57 associated with TAP1

7×10^6 cells were washed once in PBS. The cells were then pelleted and lysed on ice in 700µl 1% digitonin (WAKO), 2mM PMSF, 5mM IAA, Tris Buffered Saline (TBS: 151mM NaCl, 10mM Tris) pH7.4, containing 3µl sheep anti-rat TAP1 antibody and rotated at 4°C for 15-20min. The lysates were clarified by microcentrifugation at 13krpm for 15min. A 50:50 mixture of Protein A- and G-Sepharose (PAS and PGS) beads was made and resuspended in TBS pH7.4 (per IP; 10µl PAS, 10µl PGS, 20µl TBS). This was again rotated at 4°C for 1hr. The beads were washed three times in 0.1% digitonin, briefly giving the samples a vortex pulse followed by a 7.5krpm pulse in a tabletop microcentrifuge to pellet the beads. TBS and excess liquid was aspirated from the beads using a 25G hypodermic needle. Beads were then mixed with 40µl NRLB and the proteins were eluted at room temperature for 20-30min. 25µl of sample was loaded into each well of a 12-well 10% SDS-PAGE cassette. Proteins were transferred o/n at 12v onto Protran nitrocellulose paper (Amersham) and a West Pico Chemoluminescent reagent (Pierce, UK) was used to detect HRP-conjugated 2° antibodies. If this was not sensitive enough, nitrocellulose membranes were washed briefly in PBST and a West Femto Chemoluminescent reagent (Pierce, UK) was used instead.

2.12.2 Detecting calreticulin associated with TAP1. Procedure 2.12.1 was followed.

2.12.3 The routine immunoprecipitation protocol. Cells were harvested, washed in ice cold PBS, then lysed in Nonidet P-40 lysis buffer at 4°C for a minimum of 20min. Cell debris was spun to a pellet at 13krpm for 15min and the supernatant pre-cleared with 100µl 10% PAS beads on a rotor at 4°C for 30min. Beads were pelleted using a 7.5krpm pulse in a tabletop microcentrifuge. The supernatant was then transferred to 100µl 10% PAS beads mixed with the appropriate concentration of antibody on a rotor at 4°C for 1-2hr. Methods for washing samples, aspirating residual liquid and sample preparation are described 2.12.1.

2.13 Pulse-chase.

These were carried out as described in Lewis et al (1996)(Lewis et al., 1996). Cells (2×10^6 per well) were starved in cysteine/methionine-free (cys/met are required to initiate protein synthesis) medium (Sigma), for 30-60min and then radioactively labelled for 10min using 10µCi cys/met Promix (Amersham) per 10^7 cells. Labelling was quenched in the presence of R10 supplemented with 2mM cysteine (from 100x stock dissolved in dH₂O) and 2mM methionine (from 100x stock dissolved in dH₂O). This was used for the duration of the chase. Cells were aliquotted into 1.5ml eppendorf tubes on ice at each time point. Cells were pulsed at 10krpm to a pellet using a microcentrifuge, washed once in PBS, pulsed again and lysed in Nonidet P-40 lysis buffer at 4°C in a volume equivalent to 2×10^6 cells per 200µl. Cell lysates were centrifuged at 13krpm for 15min and cell supernatants pre-cleared at 4°C with 100µl 10% protein-A-Sepharose beads (Sigma) for 30min. Immunoprecipitation with 10µg/ml B22 (for D^b) or 10µg/ml Y3 (for K^b) was undertaken for 1hr with 100µl 10% protein-A-Sepharose beads on a rotor at 4°C. Cells were then washed and residual TBS removed according to 2.12.1. Samples were then resuspended in 19µl Endoglycosidase H (EndoH) buffer (50mM Sodium Citrate, 0.2% SDS, pH5.5) and 1µl Endoglycosidase H_f (EndoH_f; NEB) at r/t o/n. Samples were mixed with NRLB and placed at 95°C ~5min before being loaded onto a 9% SDS-PAGE gel.

EndoH_f is a recombinant protein fusion of Endoglycosidase H and maltose binding protein (MBP), which was engineered to help in the purification of the enzyme. The fusion protein was noted to have identical activity to the non-fusion clone. Endo H_f cleaves the core of high mannose oligosaccharides bound to N-linked glycoproteins (See fig NEB; <http://www.neb.com>). It provides a useful tool to identify the location of N-linked glycoproteins within the secretory pathway, by giving proteins different apparent molecular weights on SDS-PAGE gels according to whether they are EndoH sensitive or resistant. Between the ER and cis-golgi, the mannose oligosaccharide chain is susceptible to EndoH digestion, however beyond this point, complex sugar addition to the oligosaccharide chain renders the protein EndoH resistant. The disappearance of the susceptible

and appearance of the resistant bands can be used to calculate the trafficking rate. Lab convention dictates that the glycoprotein trafficking rate is determined from the time that it takes for 50% of the proteins to acquire EndoH resistance.

2.14 Pulse Chase Thermostability assay

The pulse chase was carried out according to 2.13 using only two time points; 0min and 60min. Cells were washed in ice cold PBS and lysed in Nonidet P-40 lysis buffer at 4°C in a volume equivalent to 2×10^6 cells per $200 \mu\text{l} \pm 50 \mu\text{M}$ SIINFEKL (SL8; H2-K^b-specific peptide) or ASNENMDAM (ASN; H2-D^b-specific peptide). SL8 is an ovalbumen-derived 8mer (residues 257-264) that provides the source of model antigen, representing an optimal, high affinity H2-K^b binding peptide. ASN is an Influenza A H3N2 nucleoprotein-derived 9mer (residues 366-374) representing an optimal high affinity H2-D^b binding peptide. Cell lysates were centrifuged at 13krpm for 15min and cell supernatants pre-cleared at either 4°C or r/t with $100 \mu\text{l}$ 10% protein-A-Sepharose beads (Sigma) o/n. Immunoprecipitation then conducted according to 2.13.

2.15 K42CRTΔC secretion assay.

Day 0, 3x T25 culture flasks were seeded with 2×10^6 cells in Opti-MEM® I medium (Sigma). On the same day, 10ml of Opti-MEM® was concentrated in a centrifuge at 2000g for approximately 20min to $\sim 250 \mu\text{l}$ in an Amicon concentrating falcon tube (Mw cut-off 30,000; Millipore). Cells were harvested, washed once in PBS and lysed to the equivalent of 1×10^7 cells per 1ml in Nonidet P-40 lysis buffer for a minimum of 30mins. Nuclei and other cell debris were spun down at 13krpm for 15min and the supernatant collected. For each day of the three-day time course, cells were harvested and lysed as described above. Cell culture media was filtered through a $0.45 \mu\text{m}$ syringe filter to remove cell debris before being transferred to the Amicon concentrating falcon tube. Cell lysates and concentrated culture media was mixed with RLB and heated to 95°C for 5min and run on a 10% SDS-PAGE reducing gel.

2.16 CTL assay.

Assays were conducted with the H2-K^b-SL8 specific T cell hybridoma B3Z (Karttunen et al., 1992), a kind gift of Dr. Nilabh Shastri (Berkley, CA) or an H2-D^b-KAV specific T-cell hybridoma 4D5 (KAV9 DbL), a kind gift of Dr Denise Boulanger. 4D5 recognises the lymphocytic choriomeningitis virus (LCMV) 9mer KAVYNFATM, which binds H2-D^b with high affinity. 1×10^5 target cells/well were resuspended in hybridoma media and seeded across rows 2-12 of a 96-well plate containing $100 \mu\text{l}$ /well media. 2×10^5 target cells were seeded in well 1 in $200 \mu\text{l}$ media. A peptide titration was undertaken using a 1:2 dilution of SL8 peptide, which was added exogenously starting at 1nM (this worked out at $2 \mu\text{l}$ of a 100nM SL8 peptide stock in the first well) or KAV starting at 100nM ($2 \mu\text{l}$ of a 10,000nM KAV peptide stock in the first well). $100 \mu\text{l}$ of cell suspension starting from well 1 was sequentially transferred into each neighbouring well, leaving

number 12 devoid of peptide as a control. The excess 100µl peptide dilution in well 11 was discarded. Between $0.5-1 \times 10^5$ B3Z / 4D5 cells/100µl were seeded per well of the 96-well plate, and this was left o/n at 37°C. Cells were then centrifuged at 1500rpm for 3min and the media discarded. This was replaced with 100µl/well of chlorophenol red galactoside (CPRG; 91mg CPRG [Roche]/1.25ml NP-40 [Sigma] /9ml 1M MgCl₂ [Sigma] per 1litre PBS) and incubated at r/t. T_c cells produce the cytokine IL-2 upon stimulation and in the case of B3Z / 4D5, an additional β-galactosidase enzyme (LacZ) gene is driven off the same promotor. A colorimetric assay is then used to determine the level of B3Z / 4D5 stimulation, which is directly proportional to the number of H2-K^b-SL8 / H2-D^b-KAV complexes presented on the cell surface. CPRG provides a yellow substrate for LacZ, which turns to increasing intensities of red when degraded. A Biorad 680 microplate reader was used to measure the CPRG intensity at A595nm. An addition wavelength of A695nm was used to subtract background from the result.

2.17 Confocal microscopy.

Coverslips were sterilised prior to adding cells, using 70% ethanol to sterilise, then PBS to wash them. They were then placed in a 24-well plate and blocked with 1ml R10 while cell counting was underway. 2×10^5 cells per well were seeded and incubated at 37°C o/n. The following day, cells were washed in 1ml PBS, then fixed in 400µl/well 4% Paraformaldehyde (Preparation; 400mg Paraformaldehyde (PFA) [Sigma], 10ml PBS, 31µl 4M NaCl [Sigma] heated to 56°C until PFA dissolved, then cooled to r/t before use) for 7min. The PFA was removed and cells washed in 1ml PBS. Cell membranes were permeabilised using 500µl of 0.1% Triton-X-100 (Sigma), PBS for 7min at r/t. This was removed and cells were washed with 1ml PBS. They were then blocked using 500µl of 3% BSA (Sigma), PBS and incubated at r/t for 60min and washed 1ml of PBS. 250µl 1^o antibody diluted in PBS was added to the cells and incubated for 60min. The antibody could be used repeatedly if stored at 4°C in the presence of 0.02% sodium azide (Sigma). Cells were washed with 1ml PBS. At this point, cells were protected from light to minimise fluorophore photobleaching. 250µl of the 2^o antibody were added to each well and incubated at r/t for 60min. Cells were washed twice in 1ml PBS. If staining the nuclear compartment, a further 500µl of 1µg/ml DAPI (Roche) was added to each well and incubated for 10min at r/t. Coverslips were washed quickly in nuclease-free water and blotted away with tissue. Coverslips were then mounted onto microscope slides using 5µl of Mowiol mountant containing 0.1% Citifluor. Slides were left to dry before visualising – for storage, samples were stored at 4°C.

2.18 NEM Disulphide-bond alkylation

Harvest and wash 1×10^6 cells in PBS then incubate in 100µl of pH6.8 PBS containing fresh 20mM N-Ethylmaleimide (NEM; Sigma made from a 100mM stock), PBS pH6.8 for 20min. Lyse cells in Nonidet P-40 lysis buffer supplemented with 20mM NEM for 15-20min at 4°C at an equivalent of 50µl per 1×10^6 cells. Cell debris was pelleted at 13krpm for 15min at 4°C and 40µl NRLB then

added to supernatants before freezing at -20°C . Reduced and non-reduced samples were run on a 9% SDS-PAGE gel at 100v for 2-3hr.

2.19 MMTS Disulphide-bond alkylation

Harvest and wash 1×10^6 cells in PBS then incubate in $100\mu\text{l}$ of pH7.4 PBS containing fresh 10mM S-Methyl Methanethiosulfonate (MMTS; Pierce made from 100mM stock) for 20min. Lyse cells in Nonidet P-40 lysis buffer supplemented with 10mM MMTS for 15-20min at 4°C at an equivalent of $100\mu\text{l}$ per 1×10^6 cells. Cell debris was pelleted at 13krpm for 15min at 4°C and $40\mu\text{l}$ NRLB then added to supernatants before freezing at -20°C . Reduced and non-reduced samples were run on a 9% SDS-PAGE gel at 100v for 2-3hr.

2.20 TCA disulphide trapping experiment.

Outline;

Tube 1	Tube 2	Tube 3	Tube 4
- AMS	+AMS	+AMS	+AMS
		DTT	Diamide

Harvest 2×10^6 cells and resuspend in 4ml R10. Split into 4 x 1ml eppendorf tubes and add the reducing reagent 5mM 1,4-dithioerythritol (DTT; Sigma) or oxidising reagent 0.5mM diamide (Sigma) to the appropriate tube as illustrated above for 15min at 37°C . Pellet cells at 10krpm on a tabletop microcentrifuge and remove all the supernatant. This may require a second spin to remove the residual media. Resuspend in $200\mu\text{l}$ ice cold 10% trichloroacetic acid (TCA; Sigma), PBS for 10-15min and pellet the precipitated protein 14krpm for 10min. Meanwhile, thaw out 4-acetamido-4'-maleimidylstilbene-2,2'-disulphonic acid disodium salt on a 37°C heat block (AMS; 1mg in $100\mu\text{l}$ NRLB; Cambridge Biosciences, Molecular Probes). Remove TCA and keep the pellet. Wash off excess TCA with $400\mu\text{l}$ acetone (VWR) and remove. Repeat the 14krpm spin for 2min and remove residual acetone (helps when Gilson p1000 tip connected into p200 tip) before leaving the pellets to air dry for 5min. Add $50\mu\text{l}$ NRLB to untreated AMS samples or $25\mu\text{l}$ AMS to treated samples and rotate the pipette tip through the cell pellet to dislodge. Incubate at 37°C for 5min, add $25\mu\text{l}$ NRLB to the AMS-treated samples and freeze at -20°C o/n. Thaw and dissolve pellet using a G25 hypodermic needle, being careful not to suck up too much material, because it will be lost in the dead-space of the needle. Multiple freeze thaw cycles can facilitate this procedure. Continue pipetting until the sample no longer sticks to the needle. Load onto a 9% SDS-PAGE gel and run at 100v for approximately 2-3hr. TCA protonates the intracellular environment, while AMS binds the free thiols. It has a large enough molecular weight (0.5kDa) to allow proteins possessing different redox states to be distinguished from one another (Antoniou and Powis, 2003).

2.21 Cell surface BFA decay of H2-K^b

The fungal metabolite brefeldin A (BFA) inhibits guanine nucleotide exchange for ARF-1 (ADP-ribosylation factor)(Donaldson et al., 1992; Helms and Rothman, 1992), causing the golgi to fuse with the ER, while the trans-golgi network fuses with the recycling endosomal system (Lippincott-Schwartz et al., 1991). It was used to prevent the expression of new class I molecules at the cell surface to allow the stability of class I molecules already present at the cell surface to be analysed. 5×10^5 cells were seeded per well of a 6-well plate for 0, 1, 2, 4, 6 and 18hr time points in R10. 5ug/ml Brefeldin A was added to each well in reverse chronological order. At the end of the time-course, the decay of cell surface H2-K^b for each cell line was measured by FACS using the flow cytometry protocol. The primary antibody Y3 was used at 10µg/ml.

2.21 CRT2 detection by PCR

Primer sequences were kindly provided by Anna Åkesson (Department of Plantbiochemistry, Lund University, Getingevägen 60, S-222 41, Sweden) for both human and mouse CRT2. These were individually screened by an NCBI Blast analysis showing that they specifically anneal to CRT2.

Forward and reverse sequences:

Human:

HsCRT2 F – AAG CAG AGC GAC TGG AAC

HsCRT2 R – CCA ATG GCA CCA ATG TT

Mouse:

mCRT2 F – CAC TGG ACT CTA GGG ACT GG

mCRT2 R – CAT CCT CAT ATG GTG GCT TC

RNA was extracted from K41 and K42 cells according to manufacturers' instructions (Qiagen). This included the optional step of using Qiagen DNase treatment, to remove DNA contamination of the sample. A Superscript III first strand cDNA synthesis kit (Invitrogen) was then used. Conditions; 8µl RNA, 1µl oligo dTs, 1µl 10mM dNTP mix. Mix at 65°C for 5min, then place on ice for 1min. This was then mixed with the cDNA synthesis mix: 2µl 10x Reverse Transcriptase (RT) buffer (Invitrogen), 4µl 25mM MgCl₂ (Invitrogen), 2µl 0.1M DTT (Invitrogen), 1µl 40u/µl RNase out (Invitrogen), 1µl 200u/µl Superscript III (Invitrogen) and placed in a Biorad PCR thermocycler at 50°C for 50min. cDNA synthesis was terminated at 85°C for 5min, chilled on ice. 1µl of RNase H was then added and incubated at 37°C for 20min. cDNA was then stored at -20°C.

PCR was used to look for cDNA encoding mCRT2. PCR conditions per reaction; 5µl Go Taq buffer (Promega), 0.9µl 25mM MgCl₂ (Promega), 0.15µl 10mM dNTPs (Promega), 0.75µl Dimethyl sulphoxide (DMSO; Sigma), Go Taq Polymerase (Promega), 1µl cDNA preparation, 1µl

25mM mCRT2 forward (F) primer, 1µl 25mM mCRT2 reverse (R) primer, 4.45µl ddH₂O. PCR strand denaturation set at 94°C for 2min, followed by 30 cycles of 94°C for 30sec, annealing at 56°C for 30sec, extension at 72°C for 30sec with the programme terminated at 72°C for 10min.

The PCR products were purified using a PCR purification kit (Qiagen) and then sequenced using the mCRT2 forward and reverse primers. The sequencing reaction was performed using BigDye 3.1 sequencing chemistry (Applied Biosystems) and the products were purified using a BigDye 3.1 sequencing kit (Applied Biosystems). The sequencing products were then analysed using an ABI3130XL DNA sequencer (Applied Biosystems). The sequencing data were analysed using the Geneious software package (Biomatters). The sequencing data were then compared to the mCRT2 reference sequence (GenBank accession number: J01422.1) using the Geneious software package. The sequencing data were then compared to the mCRT2 reference sequence (GenBank accession number: J01422.1) using the Geneious software package.

The sequencing data were then compared to the mCRT2 reference sequence (GenBank accession number: J01422.1) using the Geneious software package. The sequencing data were then compared to the mCRT2 reference sequence (GenBank accession number: J01422.1) using the Geneious software package. The sequencing data were then compared to the mCRT2 reference sequence (GenBank accession number: J01422.1) using the Geneious software package. The sequencing data were then compared to the mCRT2 reference sequence (GenBank accession number: J01422.1) using the Geneious software package.

The sequencing data were then compared to the mCRT2 reference sequence (GenBank accession number: J01422.1) using the Geneious software package. The sequencing data were then compared to the mCRT2 reference sequence (GenBank accession number: J01422.1) using the Geneious software package. The sequencing data were then compared to the mCRT2 reference sequence (GenBank accession number: J01422.1) using the Geneious software package.

Chapter 3: The C-terminal ER retrieval sequence

3.1 Effects on class I assembly and antigen presentation.

Constructs were generated to investigate whether CRT is involved in recycling newly synthesised but incompletely loaded class I molecules from the ERGIC/Golgi to the ER (Gao et al., 2002; Hsu et al., 1991). Recycling of other glycoproteins has been attributed to the recognition of either a cytoplasmic KKXX motif or a c-terminal KDEL motif and because class I molecules have neither, Gao et al proposed that recycling could be mediated through a binding to a protein that does. Previous studies have shown that a mutant class I molecule (T134K), which fails to bind the PLC and loads poorly with peptide. This is a similar phenotype to endogenous class I molecules in K42, making CRT a possible candidate for this role. The c-terminal modifications used in this study were aimed at removing the ability of CRT to retrieve class I molecules to the ER. To investigate the precise role of CRT in the regulated folding of MHC class I molecules, the assembly and antigen presenting function of MHC class I alleles H2-K^b and H-2D^b was assessed. The c-terminal mutations were in either the KDEL ER retrieval sequence or c-terminus of rat CRT. They were stably expressed in mouse embryonic fibroblasts containing a homozygous deletion of the CRT gene (K42) following transduction by a moloney murine leukaemia retrovirus (see chapter 2, materials and methods).

To date, most work has been undertaken on CRT using the CRT-positive K41 and CRT-negative K42 mouse embryonic fibroblasts. These are independently derived cell lines and may differ in expression of genes other important for generating epitopes and assembling MHC class I molecules. Indeed, by semi-quantitative western blot, levels of Tpn and class I HC differ by greater than a factor of 4, CNX by a factor of approximately 2, but both express a similar amount of Erp57 (Gao et al., 2002). To investigate the function of CRT in MHC class I assembly it was therefore necessary to establish a system in which CRT and CRT variants could be reliably and stably expressed in K42. K42 transfected with CRT was therefore made as an appropriate control and was predicted to be sufficient to restore MHC I assembly to that of K41.

3.2 CRT-knockout cells can stably express rat calreticulin

Rat CRT was chosen because attempts to create the appropriate constructs in mouse CRT from murine cDNA had repeatedly failed and rat CRT was available in the lab and already cloned into a vector. Sequence analysis revealed that mouse and rat share approximately 98% homology at the amino acid level. The 7 amino acid differences between the two species are all conservative; positions 60

(Mouse>Rat; L>Q), 80 (K>R), 115 (S>G), 388 (D>E) and 407-408 (ES>DA); except for one non-conservative substitution at position 409 from P>T, but all are thought to be outside of the functionally relevant regions (Figure 3.1). These include the glycan binding site in the CRT globular region formed by the N and C-termini comprising residues Y109, K111, Y128, and D317 (Kapoor et al., 2004; Thomson and Williams, 2005), the low affinity but high capacity calcium binding site in 37 of the last 57 residues (Breier and Michalak, 1994), the p-domain, which is thought to have a peptide-binding function (Peterson and Helenius, 1999; Vassilakos et al., 1998) and the KDEL ER retention sequence at the c-terminus (Pelham, 1989).

```

98.3% identity in 416 residues overlap; Score: 2242.0; Gap frequency: 0.0%

CRTC_MOUSE 1 MLLSVPLLLGLLGLAAADPAIYFKEQFLDGDAWTNRWVESKHKSDFGKFLVSSGRFYGDL
CRTC_RAT    1 MLLSVPLLLGLLGLAAADPAIYFKEQFLDGDAWTNRWVESKHKSDFGKFLVSSGRFYGDL
*****

CRTC_MOUSE 61 EKDKGLQTSQDARFYALSARFEPFSNKGQTLVVQFTVKHEQNIDCGGGYVKLFPGLDQK
CRTC_RAT    61 EKDKGLQTSQDARFYALSARFEPFSNKGQTLVVQFTVKHEQNIDCGGGYVKLFPGLDQK
*****

CRTC_MOUSE 121 DMHGDSEYNIIFGPDICGPGTKKVHVIFVYKGNVLIINKDIRCKDDEFTHLYTLIVRPDN
CRTC_RAT    121 DMHGDSEYNIIFGPDICGPGTKKVHVIFVYKGNVLIINKDIRCKDDEFTHLYTLIVRPDN
*****

CRTC_MOUSE 181 TYEVKIDNSQVESGSLEDDWDFLPPKKIKDPDAAKPEDWDERAKIDDPTDSKPEDWDKPE
CRTC_RAT    181 TYEVKIDNSQVESGSLEDDWDFLPPKKIKDPDAAKPEDWDERAKIDDPTDSKPEDWDKPE
*****

CRTC_MOUSE 241 HIPDPDAKKPEDWDEEMDGEWEPVVIQNPEYKGEWKPRQIDNPDYKGTWIHPEIDNPEYS
CRTC_RAT    241 HIPDPDAKKPEDWDEEMDGEWEPVVIQNPEYKGEWKPRQIDNPDYKGTWIHPEIDNPEYS
*****

CRTC_MOUSE 301 PDANIYAYDSFAVLGLDLWQVKSQTIFDNFLITNDEAYAEFGNETUGVTKAAEKQMKDK
CRTC_RAT    301 PDANIYAYDSFAVLGLDLWQVKSQTIFDNFLITNDEAYAEFGNETUGVTKAAEKQMKDK
*****

CRTC_MOUSE 361 QDEEQLKEEEEDKKRKEEEEAEDKEDDDRDEDEDEDEKEEDEEESPGQARDEL
CRTC_RAT    361 QDEEQLKEEEEDKKRKEEEEAEDKEDDDRDEDEDEDEKEEDEEDATGQARDEL
*****

```

Figure 3.1: ClustalW protein sequence alignment of rat and mouse CRT (<http://www.ebi.ac.uk/clustalw/index.html>). Percentage homology between the two species was calculated by the clustal algorithm. Identical amino acids are represented by an asterisk.

To investigate the role of KDEL-mediated ER retention / retrieval, PCR was used to generate the appropriate mutant constructs consisting of a point mutation of L>V in the KDEL sequence, which was chosen because it has been used to inhibit KDEL function before (Andres et al., 1990; Haugejorden et al., 1991; Tang et al., 1992) and a complete deletion of KDEL. To investigate the role of any additional residues required for CRT-mediated retention / retrieval, truncations of 11, 22 and 34 amino acids were created at the c-terminus (Figure 3.2). An epitope tag was constructed by inserting an oligonucleotide sequence corresponding to the influenza hemagglutinin (HA) peptide sequence (amino acids 98-108), YPYDVPDYASL, immediately downstream of the mutated CRT sequence. In constructs where KDEL was present, the HA-tag was inserted immediately upstream of it. A wild type rat CRT \pm HA-tag was also generated to control for the mutant constructs as well as any negative effects associated with the HA-tag. Transfectants were positively selected using the cell surface expression of a truncated nerve growth factor receptor (Δ NGFR)(Appendix 1), which was translated from an internal ribosomal entry site (IRES) located 3' of the rat CRT gene, allowing both to be transcribed from the same promoter. Δ NGFR should have been detected concomitantly in a 1:1 ratio with the gene of interest, however, in the presence of rat CRT, an inverse correlation between the expression of Δ NGFR and rat CRT was found (Appendix 2). The reason for this is unknown and was not investigated in detail, but it is possible that high CRT expression was toxic to the cells, creating a natural selection bias towards the lower CRT-expressing cells. It is also conceivable that the 5' and 3' ribosomal docking sites may compete against one another for the same ribosome, with one construct being favoured to the other. Whatever the reason for this difference, the selection system was impractical to use, so cells were cloned by limiting dilution and selected for their CRT expression using western blot. K42 CRT transfectants were renamed according to their c-terminal modification (Figure 3.2).

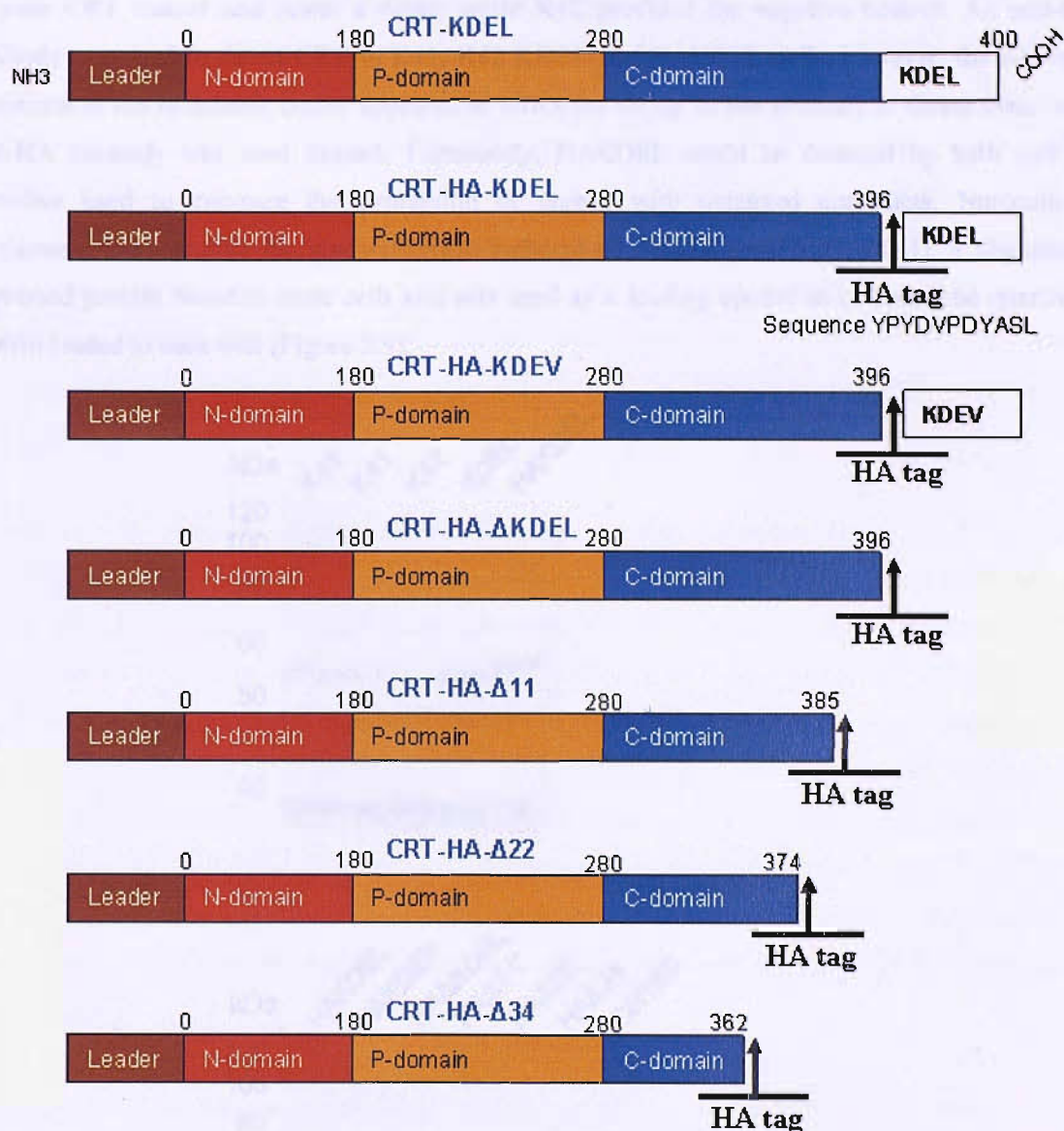


Figure 3.2: Schematic of the CRT constructs used in this study. The haemagglutinin (HA)-tag and c-terminal truncation sites are shown.

All constructs were sequenced prior to use. K41 (CRT positive) were used to compare the expression of each CRT mutant and select a clone, while K42 provided the negative control. An anti-CRT antibody was used to detect CRT in K41, K42 KDEL and HAKDEL cells, however, the c-terminal mutations of the remaining clones appeared to affect the ability of the antibody to detect them, so an anti-HA antibody was used instead. Fortunately, HAKDEL could be detected by both and was therefore used to compare the expression of tagged with untagged constructs. Nitrocellulose membranes were probed for glyceraldehyde-3-phosphate dehydrogenase (GAPDH), a ubiquitously expressed protein found in most cells and was used as a loading control to compare the quantity of protein loaded to each well (Figure 3.3).

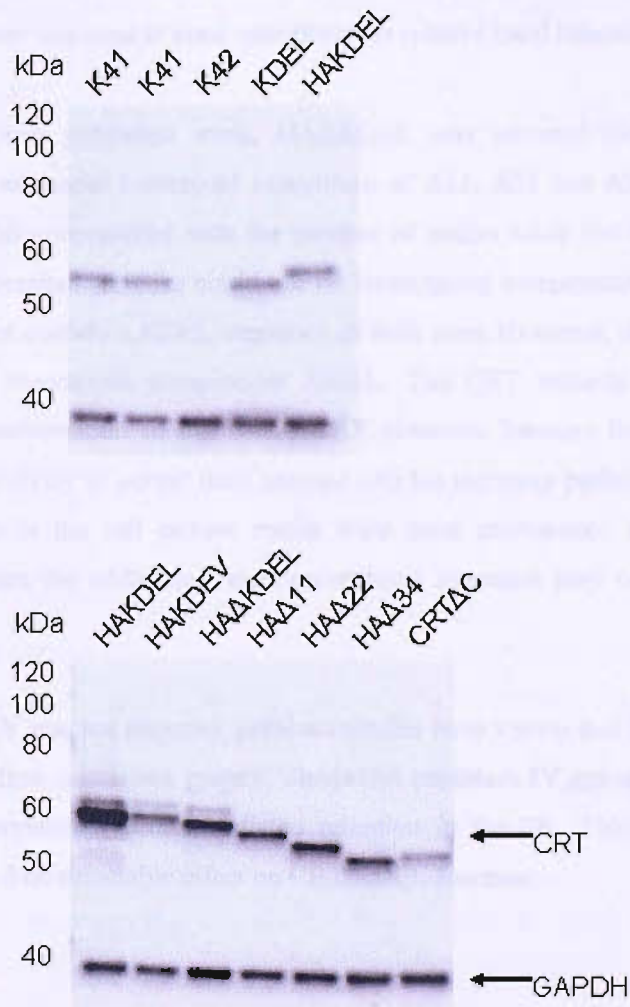


Figure 3.3: Immunoblot comparing the expression of each rat CRT construct following transduction and subsequent cloning into CRT^{-/-} K42 cells. Upper immunoblot used an anti-CRT antibody. Lower immunoblots used an anti-HA-tag antibody.

3.3 A Loss of the KDEL sequence causes CRT to be secreted

The level of CRT secretion into the surrounding cell culture media was measured to provide a simple indirect measurement of protein accumulation over time and test whether the CRT modifications impaired their ability to be retained / retrieved to the ER. K41, KDEL and HAKDEL were used as wild type controls to compare the normal accumulation of CRT against that for the mutant CRT constructs. Each day for the two day duration of the experiment, a sample of culture media was taken and probed for the presence of CRT by western blot using either anti-CRT or anti-HA antibodies depending on whether the construct was tagged or not (Figure 3.4). A sample of cell lysate (5 μ l/well) was also made at each time point to control for any variations in cell density during the experiment. This made it easier to normalise the band intensities when the different cell lines were compared to one another. Biorad imaging software was used to semi-quantitate the relative band intensities

Consistent with previous published work, HA Δ KDEL was secreted (Sonnichsen et al., 1994). Interestingly, further sequential c-terminal truncations of Δ 11, Δ 22 and Δ 34 amino acids showed a rising level of secretion concomitant with the number of amino acids lost from the c-terminus. The precise role of the c-terminal residues could not be investigated independently of the KDEL because these constructs did not contain a KDEL sequence of their own. However, the results suggest that the sequential c-terminal truncations complement KDEL. The CRT mutants are also likely to have acquired a similar conformation to the native CRT structure, because the protein quality control machinery would be unlikely to permit their passage into the secretory pathway if not. The differences in CRT accumulation in the cell culture media were most pronounced between HA Δ KDEL and HA Δ 11, suggesting that the additional retention/retrieval sequence may exist in the c-terminal 11 amino acids.

Surprisingly, HAKDEV was not secreted: previous studies have shown that the same change at the c-terminus of a cell surface membrane protein, dipeptidyl peptidase IV appended with a KDEV motif (Tang et al., 1992) prevented KDEL-mediated retention in the ER. This indicated that the point mutation from L>V had no detectable effect on CRT KDEL function.

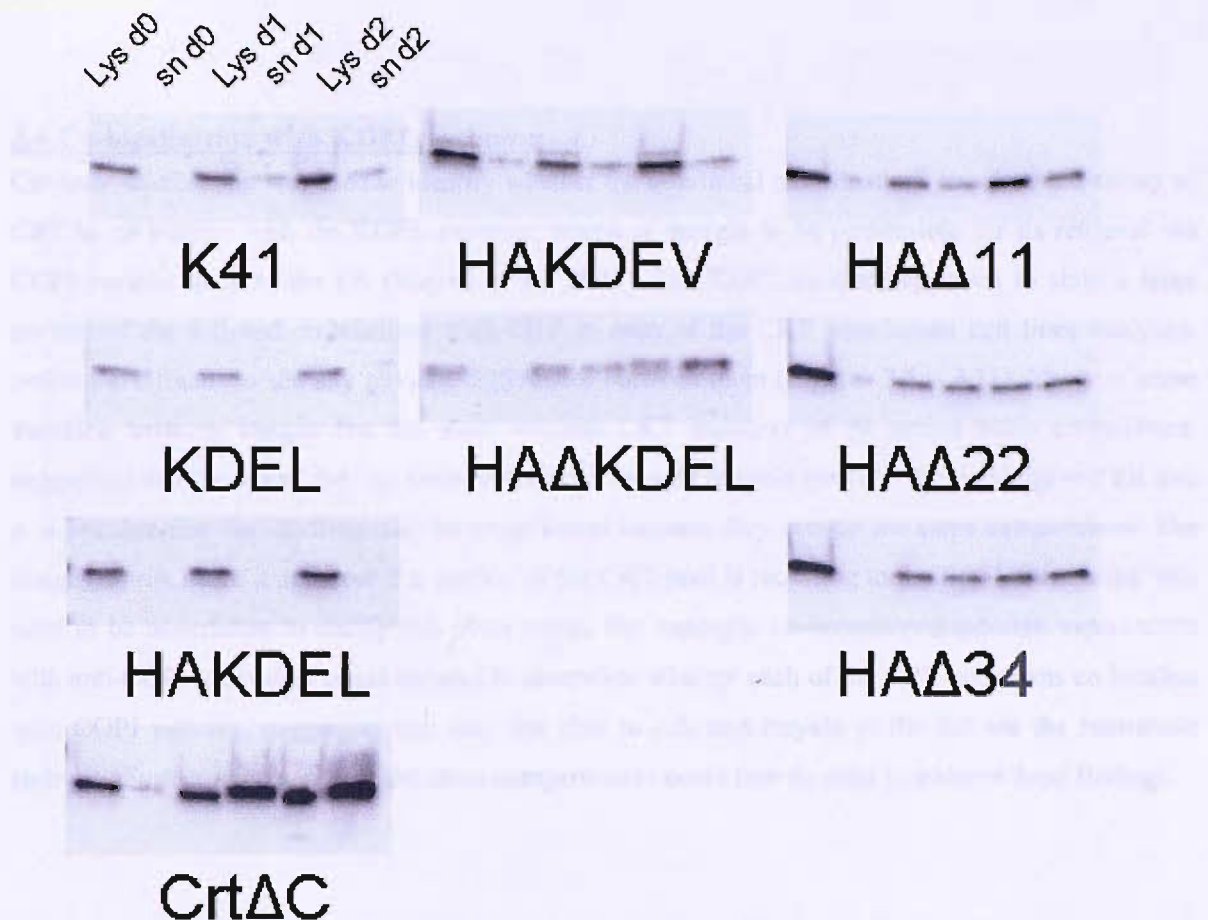


Figure 3.4: A secretion experiment was undertaken to establish whether the rat CRT mutations affected their ability to be retained within the cell. Cell lysate and media were collected over a two day period and analysed by western blot using either the anti-CRT or anti-HA-tag antibodies depending on whether the constructs were HA-tagged or not.

The secreted CRT control cell line was based on a rabbit CRT construct called CrtΔC obtained from Marek Michalak and was used to provide a K42 full length CRT transfectant control. Initial tests showed that it migrated with a lower apparent molecular weight than K41 CRT and was secreted into the cell culture media at much higher levels than K41, which doubted its authenticity.

Further investigation revealed that CrtΔC had a truncation of 38 amino acids from its c-terminus, which included a deletion of KDEL. This had been replaced by 21 novel amino acids derived from the original pcDNA3 cloning vector. It was unknown whether CrtΔC was secreted because of the 21 novel c-terminal amino acid addition or the absence of KDEL and / or other additional c-terminal residues within the deleted 38 amino acids. It is for this reason that constructs containing sequential c-terminal deletions of Δ11, Δ22 and Δ34 amino acids without a KDEL were included in this study.

3.4 Co-localisation with KDEL receptor

Confocal microscopy was used to identify whether the c-terminal modifications impaired the ability of CRT to co-localise with the KDEL receptor, which is thought to be responsible for its retrieval via COPI vesicles back to the ER (Majoul et al., 2001). The KDEL receptor appeared to stain a large portion of the cell and co-localised with CRT in each of the CRT transfectant cell lines analysed, making it difficult to see any obvious differences between them (Figures 3.5 – 3.11). There is some variation between images but the most extreme CRT mutation of 34 amino acids co-localised, suggesting that the others did too. Both proteins are thought to cycle between the cis-Golgi and ER and it is possible that the labelling may be coincidental because they occupy the same compartment. The images do not make it apparent if a portion of the CRT pool is recycling to the ER. Further work will need to be undertaken to clarify this observation. For example, co-immunoprecipitation experiments with anti-COPI antibodies could be used to determine whether each of the CRT constructs co-localise with COPI vesicles, suggesting that they are able to exit and recycle to the ER via the retrograde pathway. Further microscopy of the same compartments could then be used to endorse these findings.

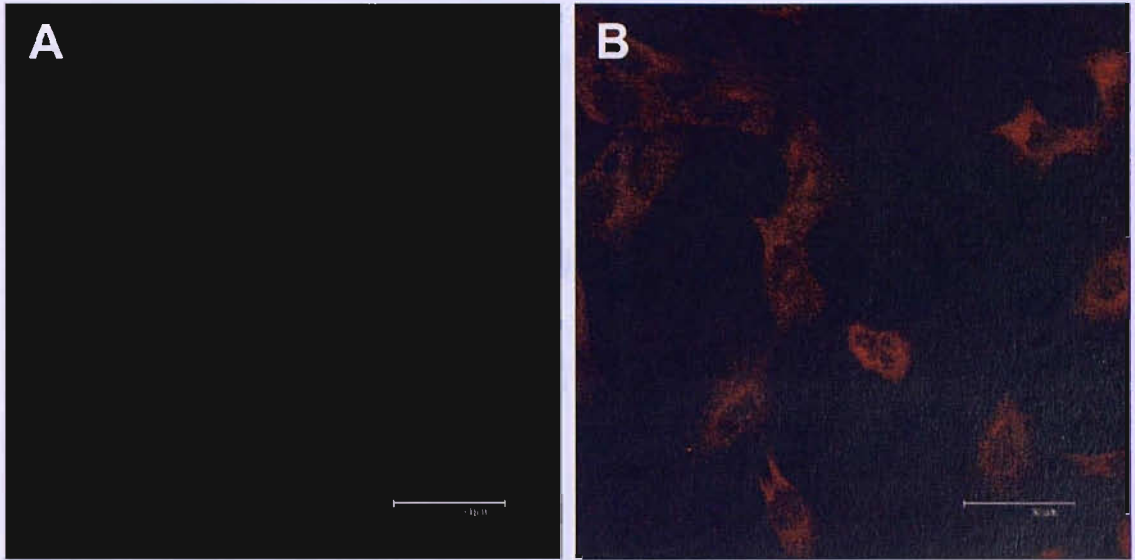


Figure 3.5: K42 KDEL co-localisation with the KDEL-receptor. Confocal microscopy was used to determine the level of co-localisation between the c-terminal CRT mutants and the KDEL-receptor. An anti-HA antibody was used against CRT (green), anti-KDEL-receptor (red). KDEL was used as a control to show the specificity and background detected for the anti-HA antibody. Panels A and B show individual labeling of (A) CRT and (B) KDEL-receptor at 100x magnification.

Figure 3.6 (also refers to Figures 3.7 – 3.11): K42 HAKDEL co-localisation with KDEL-receptor. Panels A & B show individual labelling of (A) CRT and (B) KDEL-receptor at 100x magnification. (C) is an adobe photoshop magnified merge of a cluster of cells in D. (D) is a merge of panels (A) and (B). (E) Cytofluorogram analysis software allowed a co-localisation quadrant to be drawn from a dot plot comparing HA v KDEL-receptor labelling. (F) Regions of co-localisation are represented in white. Cytofluorogram software uses a user-defined gate to surround regions of co-localisation on a voxel (3D pixel) scale on a dot plot. The intensity of each fluorophore is measured in arbitrary units on the X and Y axis and the dot plot depicts regions of co-localisation in yellow. These regions are gated manually and correspond to areas of white on the confocal image overlays.

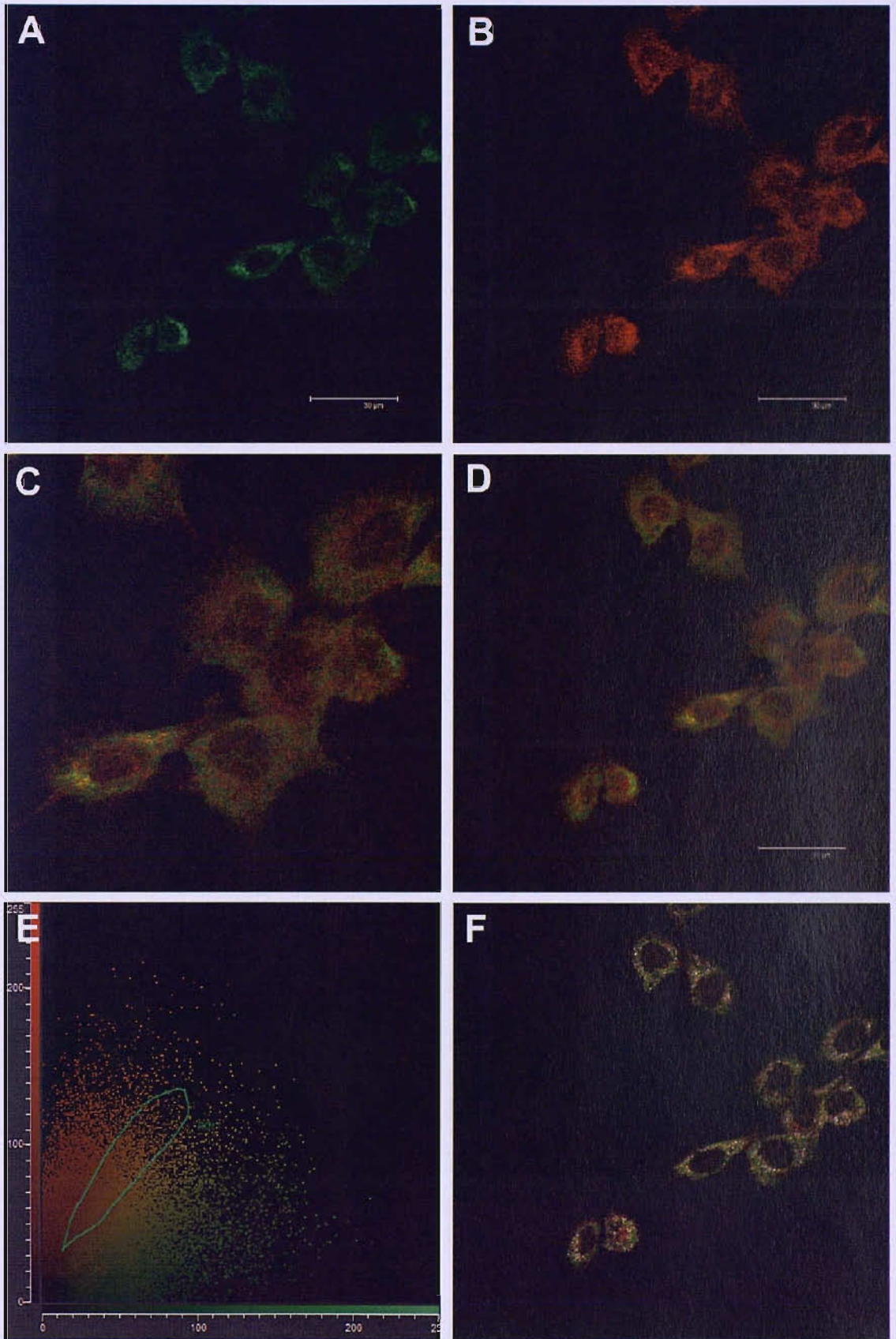


Figure 3.6: HAKDEL co-localisation with the KDEL-receptor

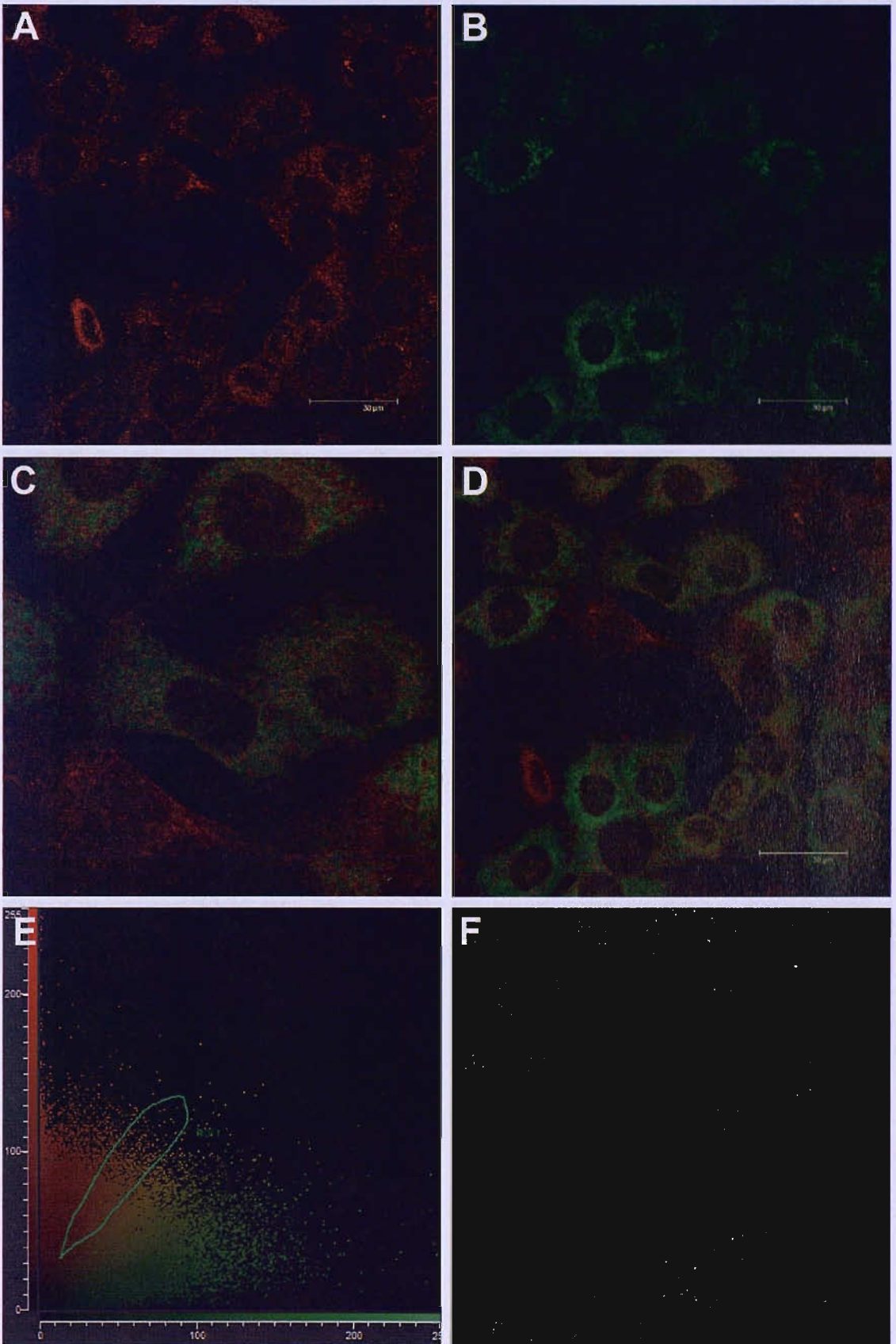


Figure 3.7: K42 HAKDEV co-localisation with the KDEL-receptor

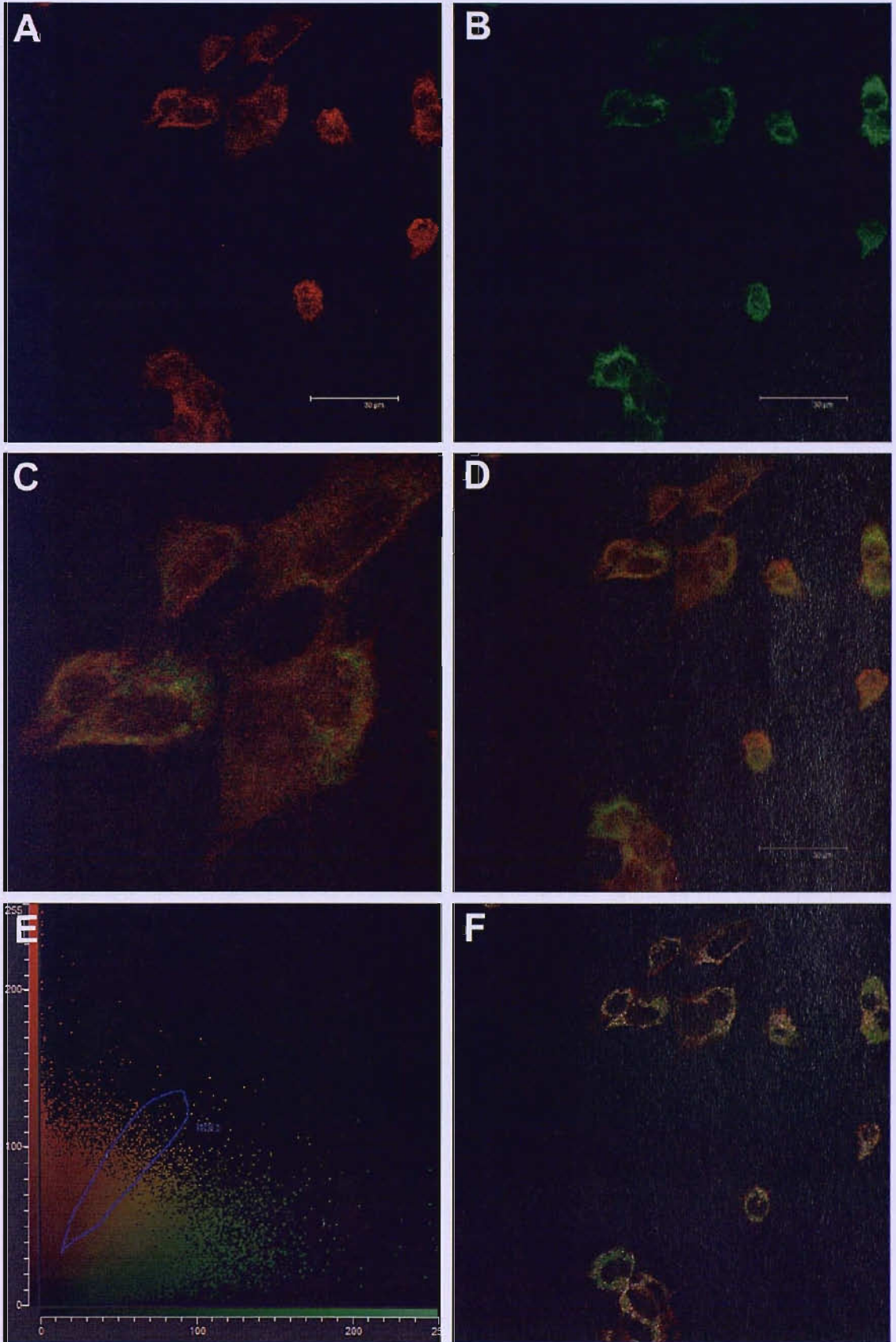


Figure 3.8: K42 HA Δ KDEL co-localisation with the KDEL-receptor

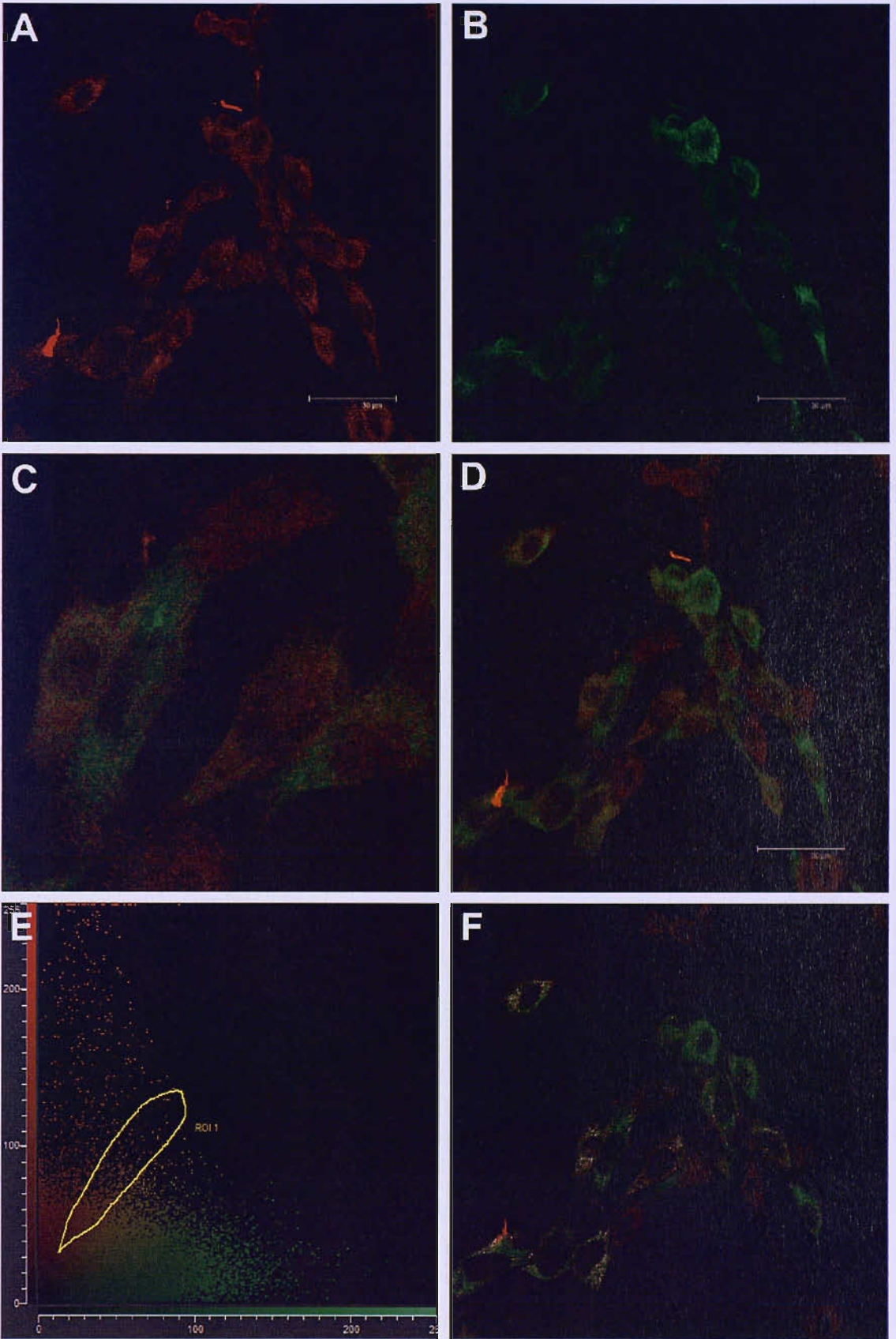


Figure 3.9: K42 HAΔ11 co-localisation with the KDEL-receptor

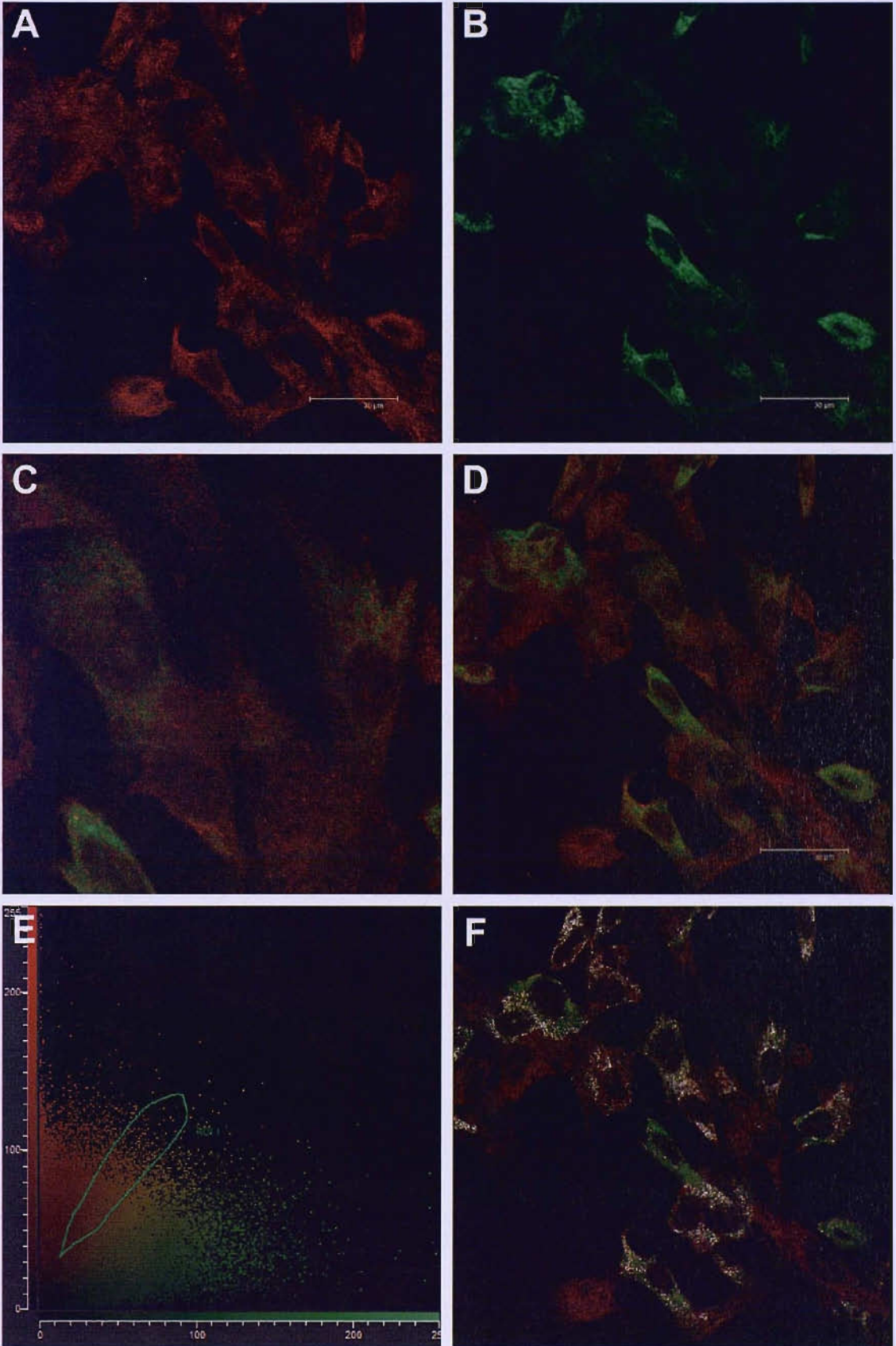


Figure 3.10: K42 HA Δ 22 co-localisation with the KDEL-receptor

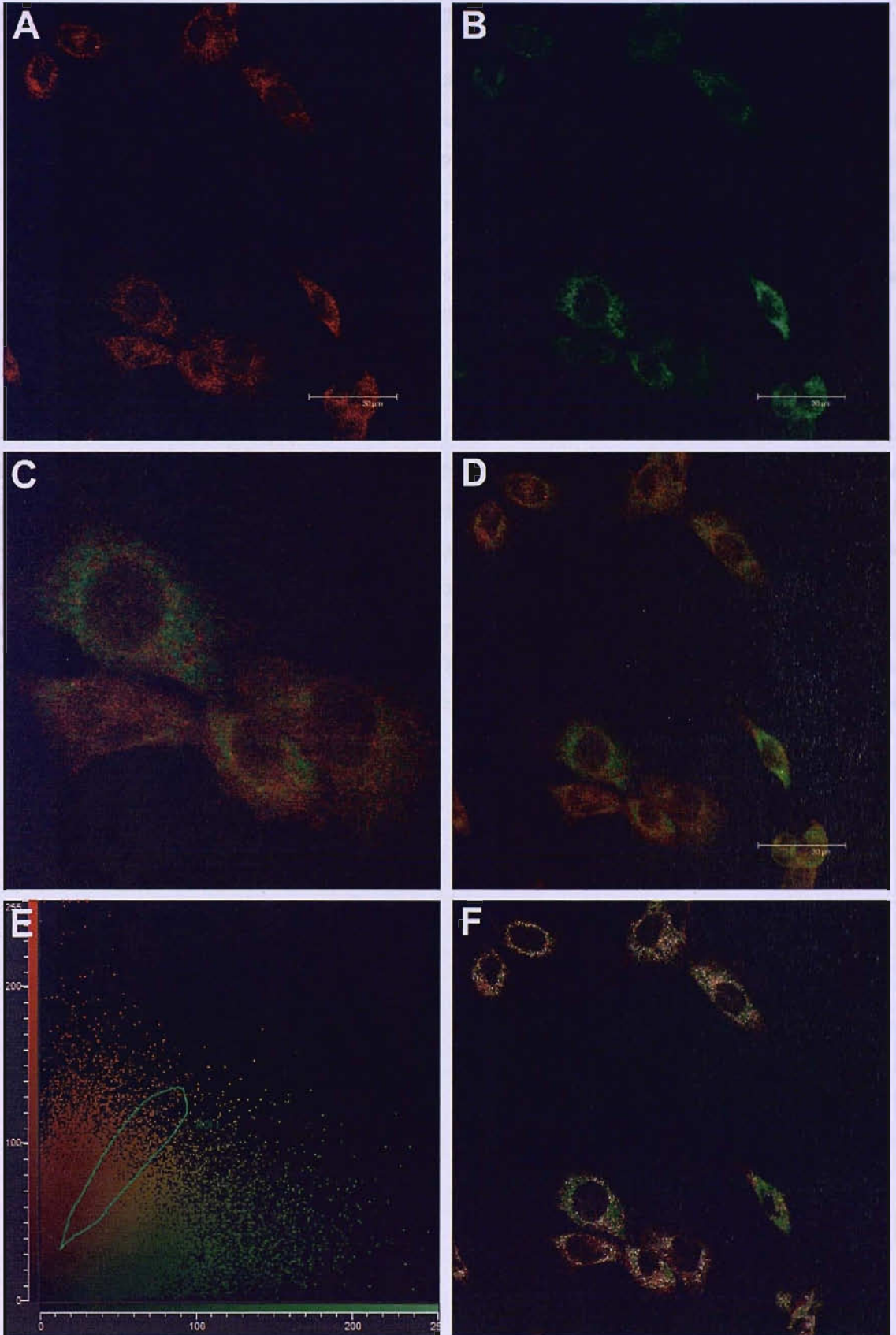


Figure 3.11: K42 HA Δ 34 co-localisation with the KDEL-receptor

3.5 Effect on Class I assembly: C-terminal CRT truncations impair H2-K^b cell surface expression

To determine the effects of each CRT mutant on class I assembly, H2-K^b cell surface expression was analysed by FACS. Embryonic fibroblasts have been noted to condition the cell culture media with an as yet unknown factor that induces class I expression (Mark Howarth, unpublished and David Williams, personal communication). Consequently, before studying class I expression, cells were split to a similar density and given fresh media the day before an experiment. An acid strip step was also incorporated to denature the cell surface proteins, serving to bring the class I expression of all mutant constructs to the same baseline at the beginning of the assay.

The results show that K42 transfected with CRT HAKDEL increases H-2K^b cell surface expression by a factor of 3 in the absence of peptide compared to K42, consistent with published data showing that CRT restores class I assembly (Gao et al., 2002). HAKDEL fails to restore class I expression above K42 (Figure 3.12). Both HAA Δ 22 and HAA Δ 34 failed to restore class I expression above the level for K42. HAKDEV restored (partially) the cell surface class I expression compared to HAKDEL. These results suggest that KDEL is required for restoration of class I at the cell surface of K42 compared to HAKDEL. This is supported by the observation that KDEV is retained (see section 3.3) and restores class I cell surface expression relative to HAKDEL. The HAKDEL transfectant was used as the positive control instead of K41, because it was better suited at comparing class I restoration for the different transfectants.

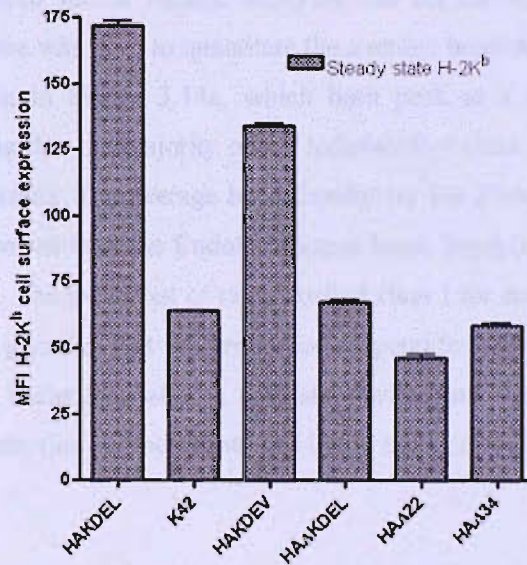
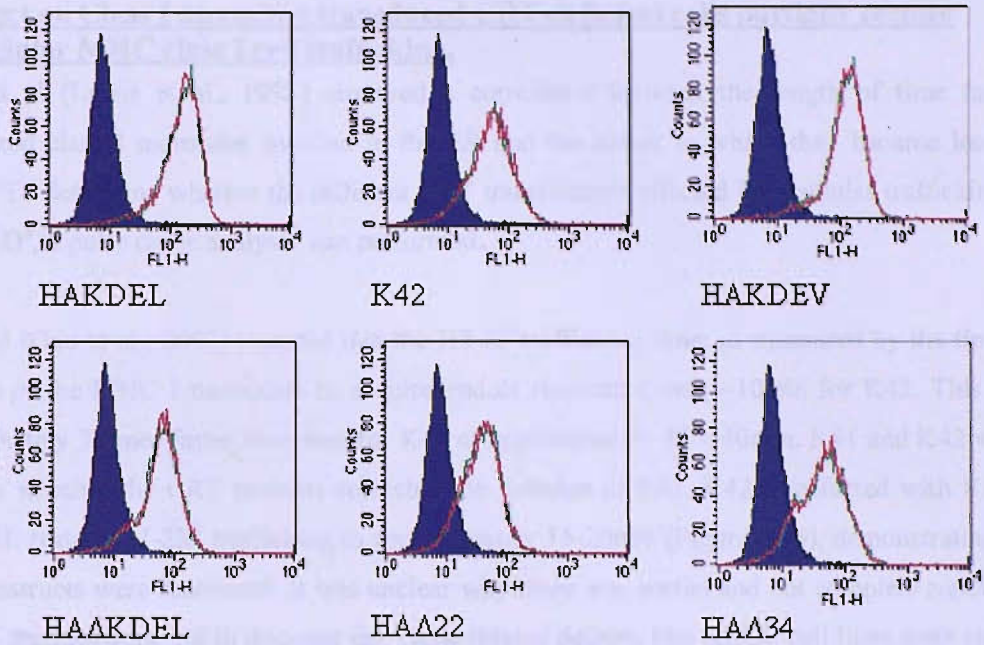


Figure 3.12: Reduced H-2K^b cell surface expression in K42 transfected with c-terminally truncated CRT compared to HAKDEL. An acid strip was used 4-6hr prior to analysis to denature cell surface MHC I and bring their expression to the same baseline at the start of the assay. Red and green lines represent sample duplicates as do the error bars.

3.6 Effect on Class I assembly; transduced CRT-deficient cells partially restore intracellular MHC class I cell trafficking.

Lewis et al (Lewis et al., 1996) observed a correlation between the length of time that newly synthesised class I molecules dwelled in the ER and the extent to which they became loaded with peptide. To determine whether the different CRT transfectants affected intracellular trafficking of H2-K^b and -D^b, a pulse chase analysis was performed.

Gao et al (Gao et al., 2002) reported that the H2-K^b trafficking time; as measured by the time it took for 50% of the MHC I molecules to acquire endoH resistance; was ~10min for K42. This rate was approximately 3 times faster than seen for K41 of approximately 30 – 40min. K41 and K42 were used to gauge whether the CRT mutants corrected the deletion in K42. K42 transfected with KDEL and HAKDEL restored H-2K^b trafficking to approximately 15-20min (Figure 3.13), demonstrating that the CRT constructs were functional. It was unclear why there was partial and not complete restoration for the CRT transfectants, but to discount any clone-related defects, two KDEL cell lines were chosen; B2 and F10. These produced similar results, implying that the calculated trafficking rate was genuine. Biorad imaging software was used to quantitate the average band density for the EndoH sensitive and resistant bands, shown in Figure 3.14a, which both peak at a similar band density in the K42 transfectants, indicating that the majority of the radiolabelled class I molecules are permitted to leave the ER for the cell surface. The average band density for the EndoH sensitive class I cohort in K41 reaches a higher maximum than the EndoH resistant band, implying that some class I molecules are retained and degraded. The total pool of radiolabelled class I for each cell line diminishes at a similar rate (Figure 3.14b), suggesting that the proportion of peptide-loaded class I molecules recognised by the IP antibody have a similar stability, consistent with data showing that a hierarchy of peptide affinities for class I molecules can be maintained in the absence of CRT (Howarth et al., 2004).

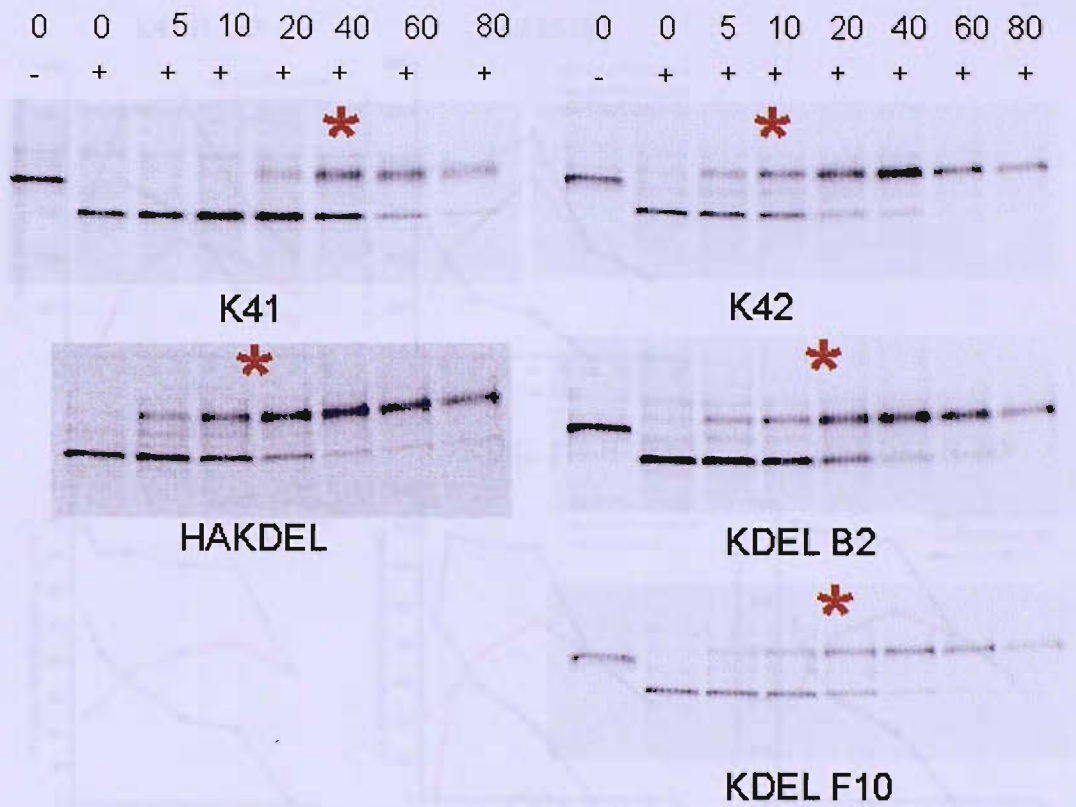


Figure 3.13: Pulse chase analysis to assess the trafficking rate of H-2K^b to the cell surface. Cells were labeled in ³⁵S cysteine/methionine for 10min. Aliquots of the cell culture were taken at the above indicated time during the chase, lysed in N-P40 lysis buffer and immunoprecipitated using the Y3 antibody (see chapter 2). Asterisks indicate the time taken for the MHC I molecules to acquire 50% EndoH resistance.

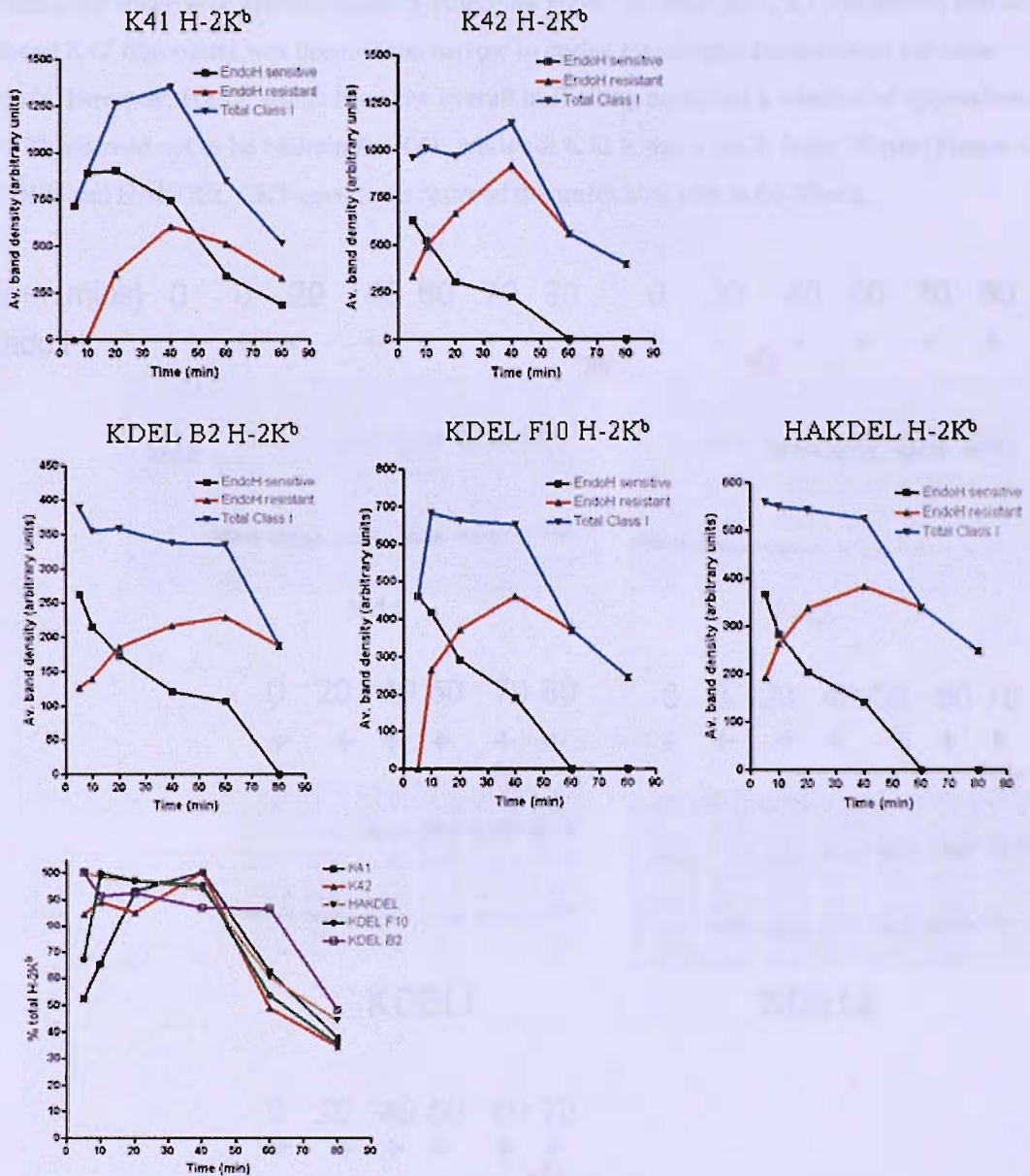


Figure 3.14: Quantitation of the H-2K^b pulse chase experiment (upper 5 panels). Biorad band analysis software was used to semi-quantitate the pulse-chase experiment for each cell line. EndoH sensitive H-2K^b (black), EndoH resistance H-2K^b (red) and total H-2K^b (blue). Lower panel; Decay rate of total H-2K^b (calculated as a percentage of maximum ³⁵S labeling).

The trafficking window of approximately 5-10min for H2-K^b between the CRT transduced and non-transduced K42 fibroblasts was deemed too narrow to derive meaningful comparisons between constructs. However, H2-D^b which has slow overall trafficking permitted a window of approximately 50min. This turned out to be >80min for K41, while for K42 it was a much faster 30min (Figure 3.15). The KDEL and HAKDEL CRT constructs restored the trafficking rate to 60-70min.

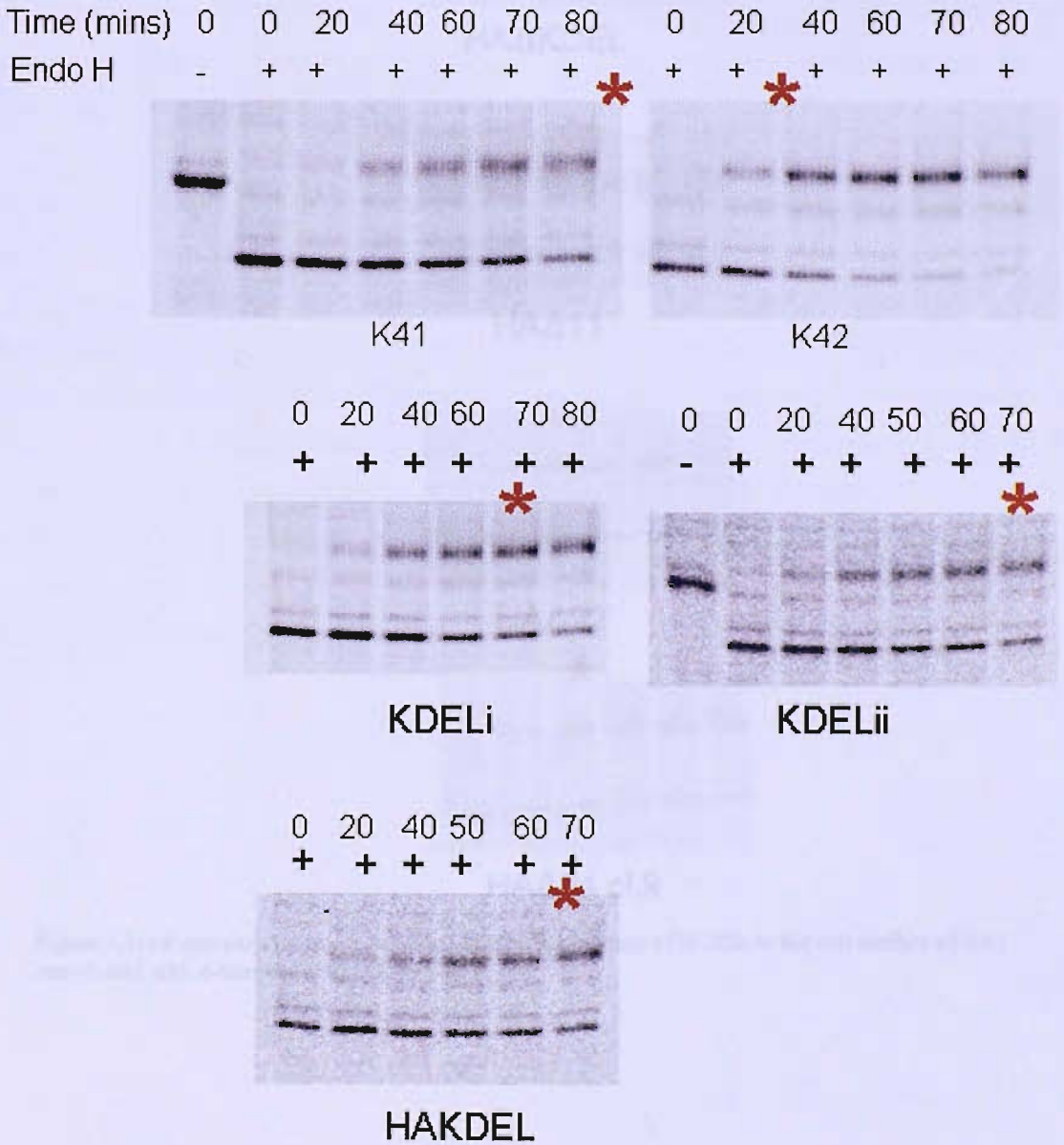
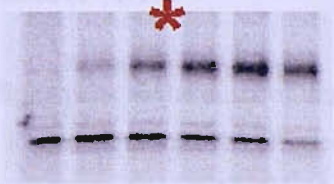


Figure 3.15: Pulse chase analysis to assess the trafficking rate of H-2D^b to the cell surface (for method see chapter 2). A duplicate experiment using KDEL B2 cells is shown to illustrate the reproducibility of the results.

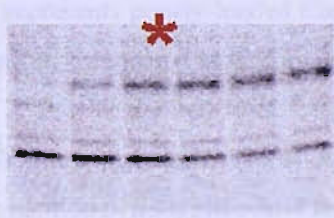
Time	0	20	40	50	60	70
EndoH	+	+	+	+	+	+



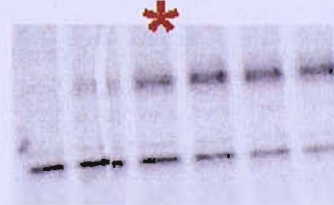
HAΔKDEL



HAΔ11



HAΔ22

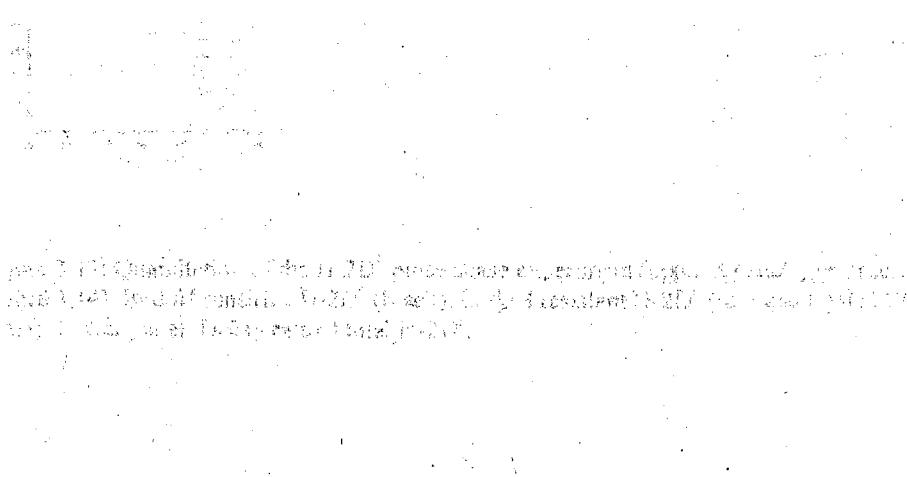


HAΔ34 cl.9

Figure 3.16: Pulse chase analysis to assess the trafficking rate of H-2Db to the cell surface of K42 transfected with c-terminally truncated CRT.

One working model for CRT function has been to recycle inappropriately peptide-loaded MHC class I molecules from the cis-Golgi to the ER using the KDEL receptor thereby slowing their trafficking rate to the cell surface. However, analysis of HAΔKDEL showed that it could also restore slow trafficking (Figure 3.16), suggesting that CRT-mediated retrieval / retention in the ER is not the rate-determining step for class I trafficking. However, the c-terminal truncations of Δ11, Δ22 and Δ34 amino acids failed to slow the trafficking rate, suggesting that this region is important for regulating class I egress from the ER. The failure of HAΔ11 to restore the class I trafficking compared to HAΔKDEL would imply that the class I trafficking rate is determined by an as yet unspecified residue(s) that has so far been defined to the 11 c-terminal amino acids of CRT.

There is a lag period of approximately 40min prior to the onset of degradation for each of the cell lines (Figure 3.17a). The H-2D^b decay rate is not significantly different between the cell lines (Figure 3.17b). Interestingly, H-2D^b appears to start being degraded before the H-2D^b trafficking T^{1/2} of all the cell lines except for K42, HAΔ11, HAΔ22 and HAΔ34, which have a fast trafficking rate. It is therefore possible that this lost material represents poorly-loaded class I that dissociates during egress to the cell surface. The pulse-chase experiment appeared to be too short to see any loss of H-2D^b from K41, which had the slowest trafficking T^{1/2} of all the cell lines, but it is unclear if this is significant compared to the K42 transfectants, so should be extended. The H-2D^b pulse-chase experiment should be repeated in the presence of stabilising peptide to determine how large the pool of otherwise unstable class I molecules are generated within each cell line.



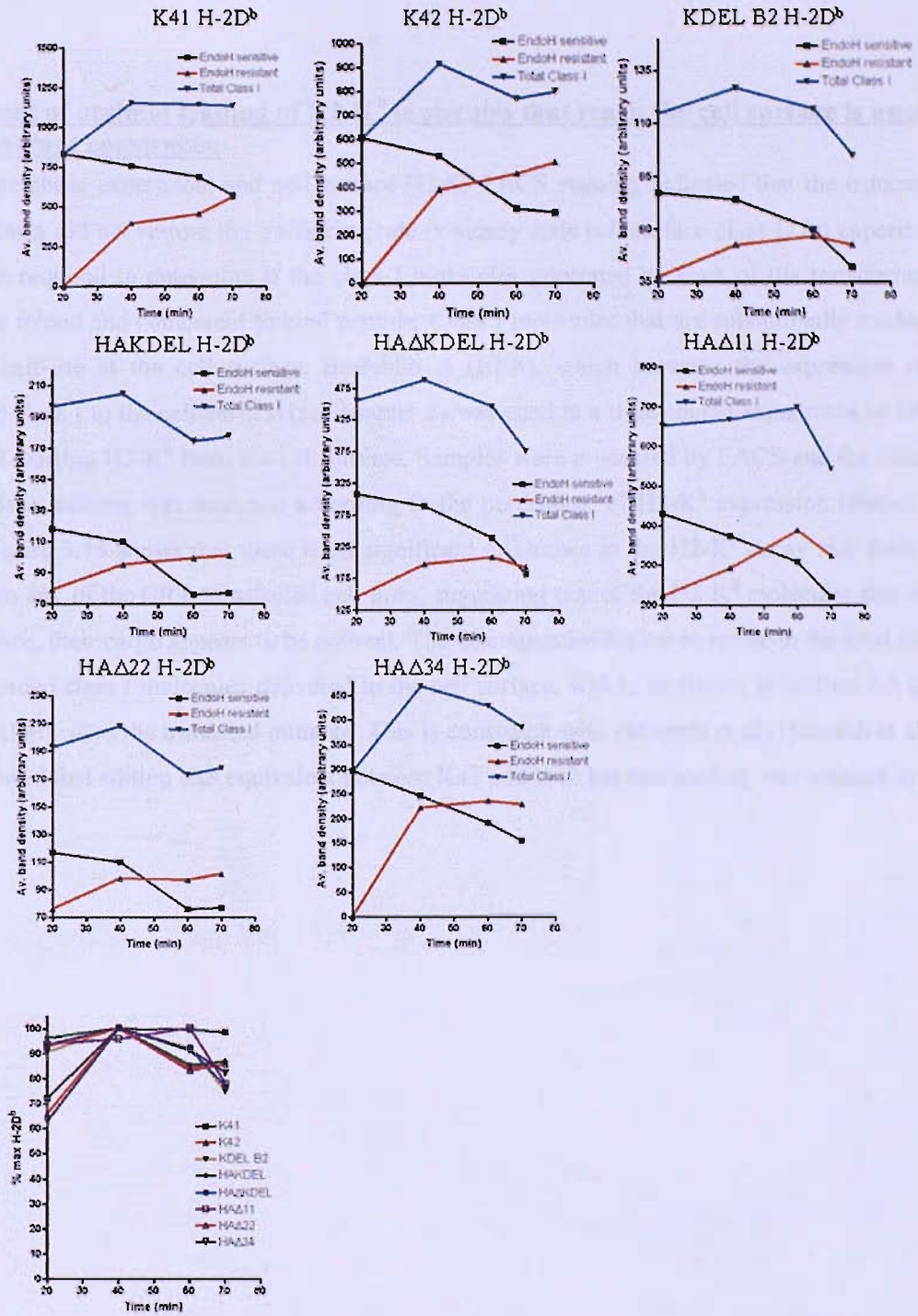


Figure 3.17: Quantitation of the H-2D^b pulse chase experiment (upper 8 panels)(as described in Figure 3.14). EndoH sensitive H-2D^b (black), EndoH resistant H-2D^b (red) and total H-2D^b (blue). Lower panel; Decay rate of total H-2D^b.

3.7 Extent of optimal loading of H2-K^b molecules that reach the cell surface is unaffected in the mutant constructs.

The pulse chase experiment and cell surface H2-K^b FACS staining indicated that the truncated CRT transfectants did not restore the trafficking rate or steady state cell surface class I. An experiment was therefore required to determine if the class I molecules generated by each of the transfectants were correctly folded and competent to bind peptide. Class I molecules that are suboptimally loaded have a shorter half-life at the cell surface. Brefeldin A (BFA), which prevents the expression of newly exported class I to the cell surface (see chapter 2) was used in a time course experiment to follow the decay of existing H2-K^b from the cell surface. Samples were processed by FACS and the reduction in cell surface staining was analysed according to the percentage of H2-K^b expression relative to time 0min. Figure 3.18 shows that there is no significant difference in the H2-K^b decay rate from the cell surface in any of the CRT transfected cell lines, suggesting that of the H2-K^b molecules that reach the cell surface, their cargo appears to be optimal. The discrepancies appear to reside in the total number of stably loaded class I molecules delivered to the cell surface, which, as shown in section 3.5 is greater for HAKDEL than the truncated mutants. This is consistent with Howarth et al (Howarth et al., 2004) who showed that editing was equivalent between K41 and K42 but that loading was reduced in K42.

Figure 3.18 FACS analysis of H2-K^b decay rate from the cell surface. Cells were treated with Brefeldin A (BFA) for 10 minutes and then analysed by FACS. The decay rate of H2-K^b from the cell surface was measured by the percentage of H2-K^b expression relative to time 0min. The results show that there is no significant difference in the H2-K^b decay rate from the cell surface in any of the CRT transfected cell lines.

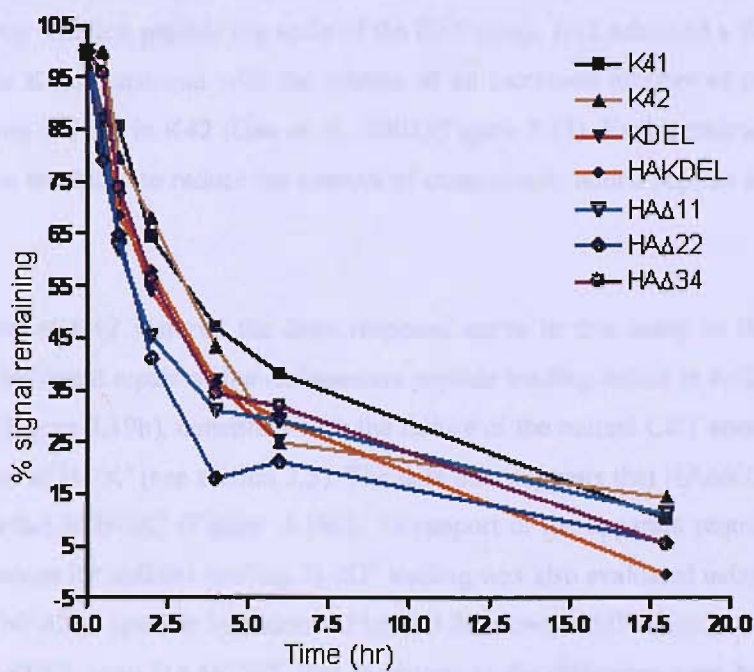
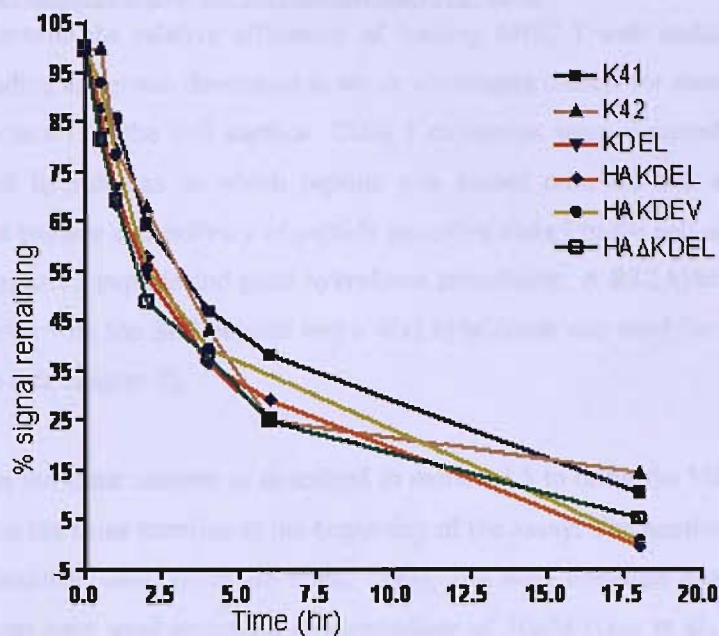


Figure 3.18: H-2K^b expressed on the cell surface by each K42 CRT transfectant has the same stability. This was assessed using BFA (see chapter 2). The graphs present the percentage reduction in MHC I on the cell surface over time using conformation-sensitive antibodies. Upper panel; HAΔKDEL, Lower panel; C-terminally truncated mutants HAΔ11, HAΔ22, HAΔ34.

3.8 Loading of exogenous peptide for presentation to T-cells

In an attempt to determine the relative efficiency of loading MHC I with stabilising peptides, an exogenous peptide loading assay was developed to act as a surrogate marker for measuring the delivery of peptide-receptive class I to the cell surface. Class I molecules were detected quantitatively with peptide-specific T cell hybridomas in which peptide was loaded onto the cell surface. Inefficient loading of endogenous peptide and delivery of peptide receptive class I to the cell surface gives rise to good loading with exogenous peptide and good hybridoma stimulation. A B3Z hybridoma was used to detect H2-K^b in complex with the SL8 peptide and a 4D5 hybridoma was used for H2-D^b in complex with the KAV peptide (see chapter 2).

Cells were prepared in the same manner as described in section 3.5 to bring the MHC I expression of all mutant constructs to the same baseline at the beginning of the assay. The peptide titrations covered physiological concentrations (1nM; (Purbhoo et al., 1998)) and were therefore more appropriate than conventional assays that have used saturating concentrations of 10 μ M (Gao et al., 2002). This assay provided a way to determine if endogenous peptide loading in the K42 transfectants was similar to K41 or more like K42. Over the first peptide log scale of the B3Z assay, K42 achieved a B3Z response 2-3 times greater than for K41, consistent with the release of an increased number of peptide receptive MHC I molecules from the ER in K42 (Gao et al., 2002)(Figure 3.12). Each construct could then be evaluated according to its ability to reduce the amount of exogenously added peptide loaded onto class I relative to K42.

HAKDEL transfection of K42 restored the dose response curve in this assay to that seen in K41 (Figure 3.19a). This indicated repair of the endogenous peptide loading defect in K42. No restoration was seen in HAA11 (Figure 3.19b), consistent with the failure of the mutant CRT constructs to restore cell surface expression of H-2K^b (see section 3.5). The data also suggests that HAAKDEL also fails to restore the loading defect in H-2K^b (Figure 3.19c). In support of the apparent requirement of the c-terminal KDEL sequences for optimal loading, H-2D^b loading was also evaluated using a similar assay utilising a D^b-KAVYNFATM-specific hybridoma. Figure 3.20 shows a difference in the dose response curve comparing HAKDEL with HAAKDEL that is similar to the difference seen between K41 and K42, again consistent with the restoration of optimal loading by KDEL but not by Δ KDEL.

The hybridoma passage number and their general condition can influence the sensitivity of this assay over the lower titration ranges, which can obscure potential shifts between the curves. Although this

assay can be informative, its downfall is that it is totally reliant on the ability of the hybridoma to activate properly according to the number of specific peptide-MHC I molecules it recognises on the cell surface. Therefore, the dose response curves in both the B3Z and 4D5 experiments provide a measure of absolute numbers of peptide-receptive MHC I molecules at the cell surface, not the relative proportion of receptive MHC I molecules. More direct assays of endogenous peptide loading were therefore sought.

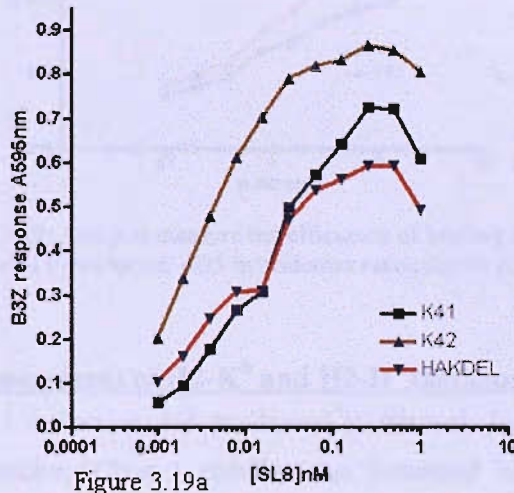


Figure 3.19a

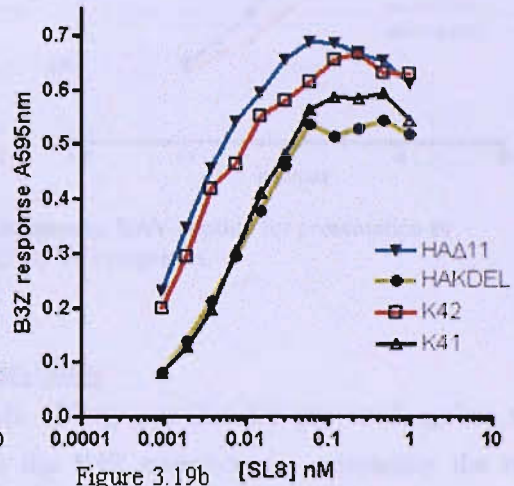


Figure 3.19b

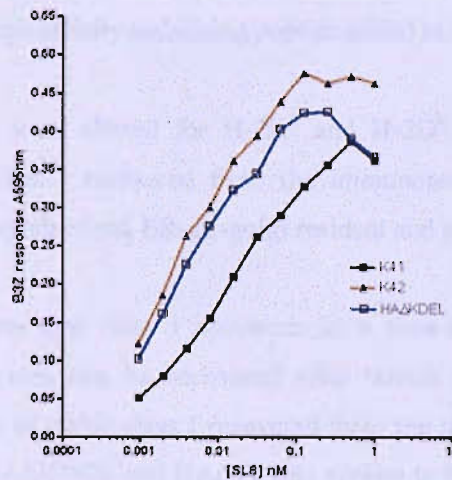


Figure 3.19c

Figure 3.19: Assay to measure the efficiency of loading exogenous SL8 peptide for presentation to B3Z T-cell hybridomas. Inefficient endogenous peptide loading in c-terminal CRT mutants. B3Z hybridomas recognize H-2K^b-SL8 complexes.

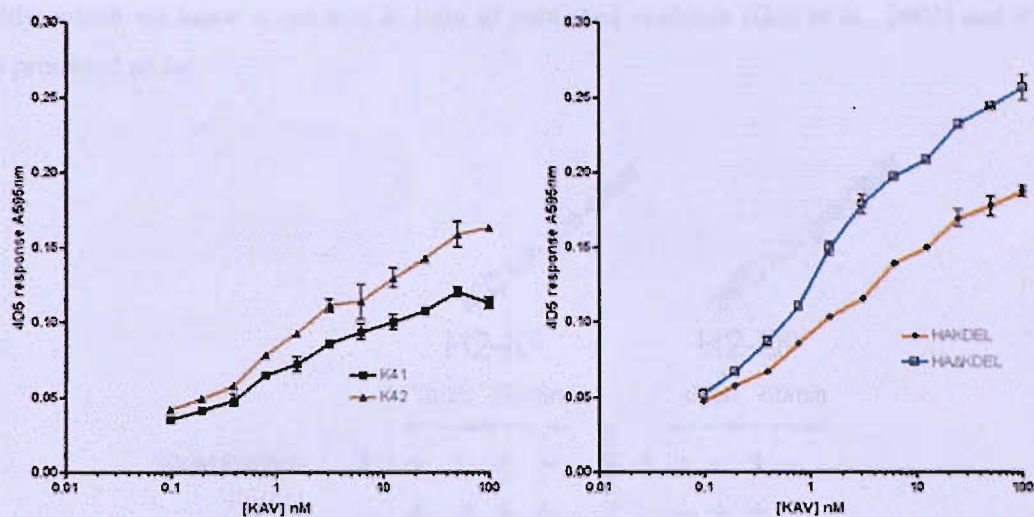


Figure 3.20: Assay to measure the efficiency of loading exogenous KAV peptide for presentation to 4D5 T-cell hybridomas. 4D5 hybridomas recognize H-2D^b-KAV complexes.

3.9 Assessment of H2-K^b and H2-D^b thermostability

Class I molecules that are bound to optimal, high affinity peptides are protected against thermal denaturation. Class I stability was measured in the K42 transfectants, calculating the ratio of recoverable class I immunoprecipitated with a conformational-sensitive H2-K^b or H2-D^b antibody in the presence and absence of a high affinity stabilising peptide added to the cell lysate.

Thermostability conditions were altered for H-2K^b and H-2D^b to 4°C and 26°C respectively to maximise the amount of class I recovered from the immunoprecipitation. Two time points were selected to represent newly synthesized, ER-cis-golgi resident and post-medial golgi class I.

Figures 3.21 and 3.22 show that class I optimizes in a time-dependent manner since a greater proportion of stable molecules can be recovered after 60min compared to 0min. Stability was calculated as the percentage of stable class I recovered from the IP in the absence of peptide (Figure 3.22). H-2K^b stability for HAΔKDEL and HAΔ11 was similar to HAKDEL and K42, suggesting that there is little difference in H-2K^b assembly soon after synthesis. At 60min, the results again show no difference for stable H-2K^b between HAKDEL and K42, making it impossible to determine whether the poorer H-2K^b stability shown by HAΔKDEL and HAΔ11 is significant or not. Equally, H-2D^b stability at both 0 and 60min for HAKDEL, K42 and the two K42 transfectants is no different. Alterations to the current protocol or an increased number of experimental repeats should be made to make this assay more robust, since these results seem to suggest that CRT plays no role in class I

assembly, which we know is not true in light of published evidence (Gao et al., 2002) and from the results presented so far.

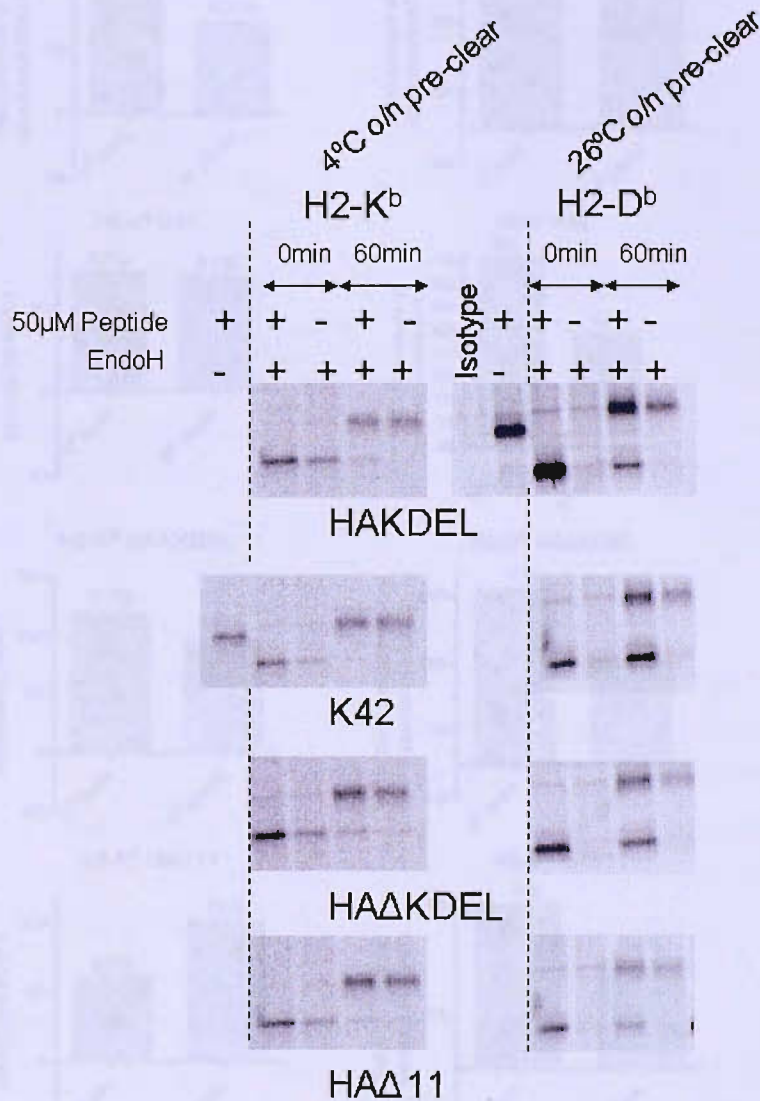


Figure 3.21: Investigating intracellular H-2K^b and H-2D^b loading in c-terminally truncated CRT transfectants using a pulse-chase thermostability experiment. Cells were labeled with ³⁵S-cysteine/methionine for 10min and immediately placed on ice or incubated at 37°C for 60min as described in chapter 2. Cell N-P40 lysates were incubated at 4°C for H-2K^b and 26°C for H-2D^b o/n in the presence or absence of 50µM stabilizing peptide. Immunoprecipitation was performed using Y3 (H-2K^b) or B22 (H-2D^b) antibodies.

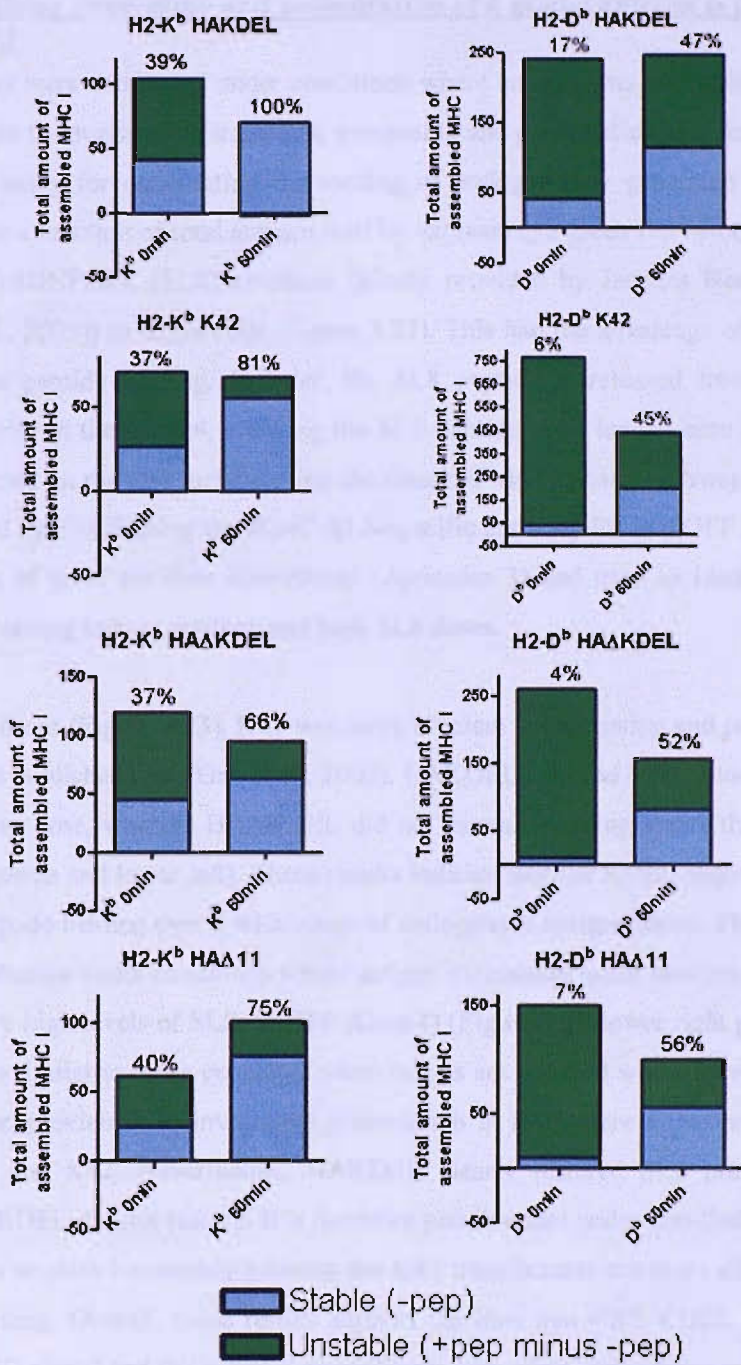


Figure 3.22: Time dependent peptide optimization of H-2K^b and H-2D^b. Quantification of the pulse chase thermostability experiments for H-2K^b and H-2D^b.

3.10 Intracellular processing and presentation of a model antigen is impaired in CRT lacking KDEL

Previous assays were conducted under conditions where antigen was not limiting. A direct assay was therefore sought to investigate intracellular processing and presentation as a function of antigen load. I developed an assay for quantitating the loading of endogenously generated peptide onto H-2K^b in transfectants as a function of total antigen load by expressing a green fluorescent protein (GFP)-tagged ubiquitin (Ub)-SIINFEKL (SL8) chimera (kindly provided by Jacques Neefjes; original reference (Neijssen et al., 2005)) in target cells (Figure 3.23). This had the advantage of being a direct measure of endogenous peptide loading. In brief, the SL8 peptide is released from GFP-ub by ubiquitin hydrolase activity in the cytosol, allowing the SL8 peptide to be loaded onto class I molecules in the ER and presented on the cell surface using the classical MHC class I pathway. Cell surface-presented SL8 is detected by FACS using the H2-K^b-SL8-specific antibody D1 and GFP is used to show the SL8 dose. A series of gates are then constructed (Appendix 3) and used to identify H-2K^b-SL8 surface expression according to low, medium and high SL8 doses.

At all antigen doses (Figure 3.23), K41 was more efficient at processing and presenting SL8 than K42, consistent with published data (Gao et al., 2002). HAKDEL restored MHC I loading over a logarithmic range of antigen dose, whereas HAΔKDEL did not increase loading above that seen for K42 (Figure 3.23 upper 5 panels and lower left). These results indicate that the KDEL sequence of CRT is essential for optimal peptide loading over a wide range of endogenous antigen doses. This assay also allowed us to study presentation under conditions where antigen expression is not limiting, as seen in transfectants expressing very high levels of SL8-ub-GFP (Gate 4) (Figure 3.23 lower right panel). These conditions are likely to be similar to those generated when targets are infected with retroviral viral vectors, which have been used previously to investigate presentation in K42. Here differences are less pronounced between K41 and K42. Nevertheless, HAKDEL clearly restored SL8 presentation albeit partial, whereas HAΔKDEL did not restore. It is therefore possible that under non-limiting peptide conditions, the differences in class I assembly between the K42 transfectants are more difficult to see than when peptide is limiting. Overall, these results support the idea that CRT KDEL is essential for optimal loading of MHC class I and this effect is most clearly seen when endogenous antigen is non-limiting.

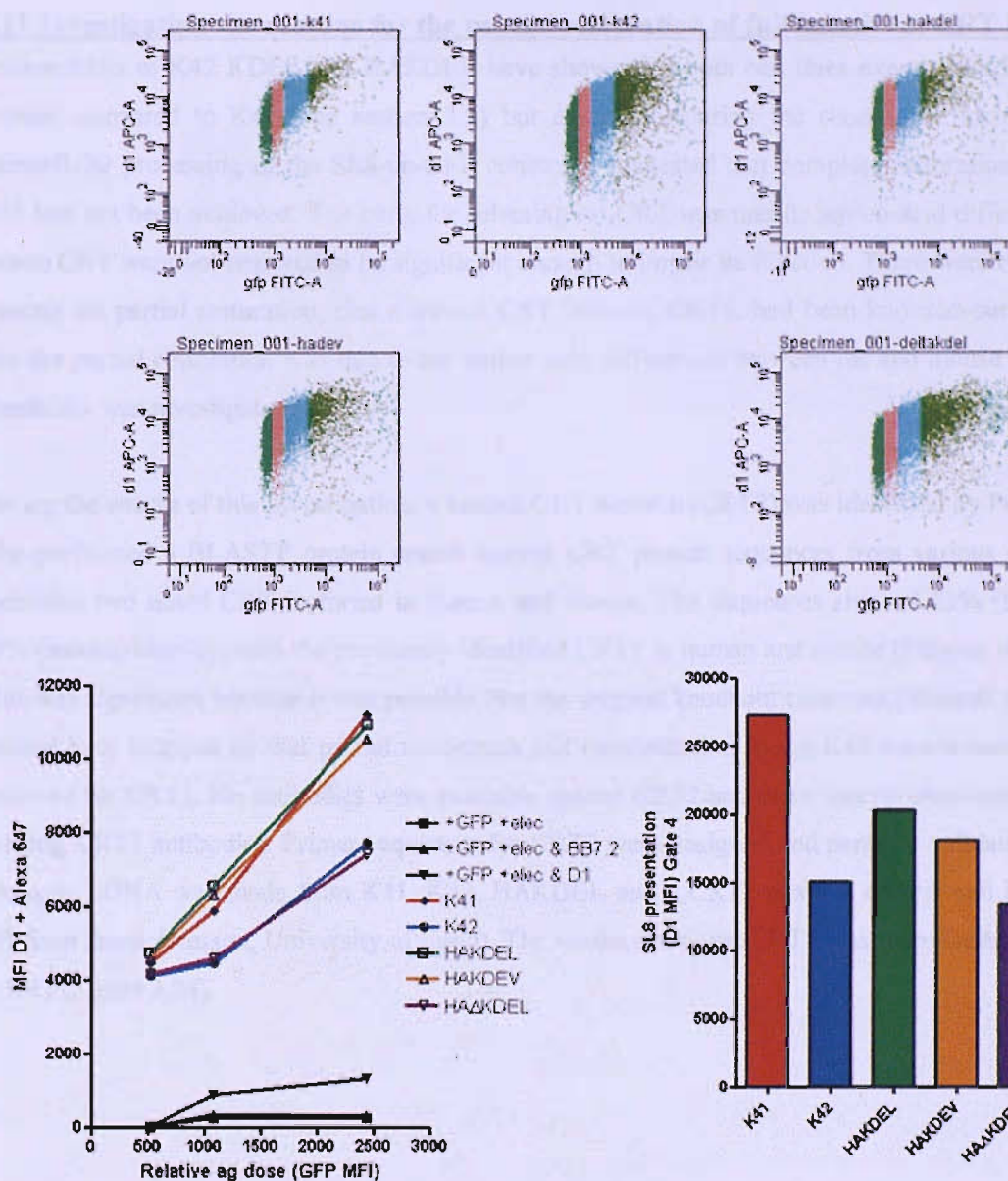


Figure 3.23: Intracellular loading assay FACS plot of H-2Kb-SL8 surface expression (D1 antibody) versus SL8 dose (GFP fluorescence) for c-terminally truncated CRT transfected K42 cells (upper panel). Analysis of D1 staining as a function of antigen load (GFP MFI)(lower left panel; low-medium dose, lower right panel; high dose). Intracellular processing and presentation of SL8 is poor in HAKDEL at all doses. Controls; GFP +elec (secondary antibody only), GFP +elec & BB7.2 (isotype control for D1 antibody), GFP +elec & D1 (no secondary antibody).

3.11 Investigating the reasons for the partial restoration of full length rat CRT in K42.

Immunoblots of K42 KDEL and HAKDEL have shown that both cell lines express similar levels of protein compared to K41 (see section 3.2) but assays comparing the class I trafficking rate and intracellular processing of the SL8-ub-GFP construct, suggested that complete restoration relative to K41 had not been achieved. The basis for selecting rat CRT was that its amino acid differences with mouse CRT were not believed to be significant enough to impair its function. There were two possible reasons the partial restoration; that a second CRT isoform, CRT2, had been knocked-out in K42; or that the partial restoration was due to the amino acid differences between rat and mouse CRT. Each possibility was investigated in turn.

During the course of this investigation, a second CRT isoform (CRT2) was identified by Persson et al. who performed a BLASTP protein search against CRT protein sequences from various species and identified two novel CRT isoforms in human and mouse. The sequences showed 53% (human) and 49% (mouse) identity, with the previously identified CRT1 in human and mouse (Persson et al., 2002). This was significant because it was possible that the original knockout construct (Mesaeli et al., 1999) deleted both isotypes so that partial restoration and reconstitution in the K42 transfectants was only achieved for CRT1. No antibodies were available against CRT2 and there was no cross-reactivity with existing CRT1 antibodies. Primer sequences for CRT2 were designed and partially validated by Anna Åkesson. cDNA was made from K41, K42, HAKDEL and a CRT2-positive control cell line (a kind gift from Anna Åkesson, University of Lund). The results show that CRT2 was reproducibly expressed in K42 (Figure 3.24).



Figure 3.24: CRT2 detection by PCR. cDNA was generated from K41, K42, HAKDEL and a CRT2 control cell line. H₂O was substituted for template in the control, since no CRT2 deficient cell lines were available. A β -actin housekeeping control was run alongside each sample.

Another possibility was in the species differences between rat and mouse. Three adjacent residues in the c-terminus of CRT were identified at residues 407-409 that were different between the species. They were noted previously but were not thought to be significant (see section 3.2). These residues appeared to be lost in the HA Δ 11 transfectant, which failed to restore the MHC I trafficking rate relative to HAKDEL compared to HA Δ KDEL that did restore, suggesting that the c-terminal 11 amino acid residues may play a role in class I processing. A species alignment was expanded to include human and rabbit calreticulin, because they have been commonly documented in the literature (Figure 3.25). Among them, they contained amino acid substitutions at identical sites as those in rat. Although substituted with different amino acids in some cases, the single substitutions appeared conservative. Significantly, each contained different amino acid combinations at positions 407-409 within the acidic c-terminal region comprising; mouse – ESP; rat – DAT; rabbit – AAA; Human – DVP. To investigate this issue, a mouse CRT K42 transfectant (K42mCRT) was obtained from David Williams (University of Toronto) to allow direct comparison.


```

Mus      MLLSVPLLLGLLGLAAADPAIYFKEQFLDGDAMTNRUVESKHKSDFGKFLVSSGKFYGD 60
Rattus  MLLSVPLLLGLLGLAAADPAIYFKEQFLDGDAMTNRUVESKHKSDFGKFLVSSGKFYGDQ 60
Oryctolagus MLLPVPLLLGLLGLAAAEPPVVFKEQFLDGDGWTNRVIESKHKSDFGKFLVSSGKFYGDQ 60
Homo    MLLSVPLLLGLLGLAAAEPAVVFKEQFLDGDGWTNRVIESKHKSDFGKFLVSSGKFYGDE 60
      ***.*****.:.:.;*****.:.:.;*****

Mus      EKDKGLQTSQDARFYALSARFEPFSNKGQTLVVQFTVKHEQNIDCGGGYVKLFPPGGLDQK 120
Rattus  EKDKGLQTSQDARFYALSARFEPFSNKGQTLVVQFTVKHEQNIDCGGGYVKLFPPGGLDQK 120
Oryctolagus EKDKGLQTSQDARFYALSARFEPFSNKGQTLVVQFTVKHEQNIDCGGGYVKLFPPAGLDQK 120
Homo    EKDKGLQTSQDARFYALSASFEPFSNKGQTLVVQFTVKHEQNIDCGGGYVKLFPPNSLDQK 120
      *****.*****.*****.***.

Mus      DMHGDSEYNINFGPDICGPGTKKVHVIFNYKGNVLIINKDIRCKDDEFTHLYTLIVRFPDN 180
Rattus  DMHGDSEYNINFGPDICGPGTKKVHVIFNYKGNVLIINKDIRCKDDEFTHLYTLIVRFPDN 180
Oryctolagus DMHGDSEYNINFGPDICGPGTKKVHVIFNYKGNVLIINKDIRCKDDEFTHLYTLIVRFPDN 180
Homo    DMHGDSEYNINFGPDICGPGTKKVHVIFNYKGNVLIINKDIRCKDDEFTHLYTLIVRFPDN 180
      *****

Mus      TYEVKIDNSQVESGSLEDDWDFLPPKKIKDPDAAKPEDWDERAKIDDPDTSKPEDWDKPE 240
Rattus  TYEVKIDNSQVESGSLEDDWDFLPPKKIKDPDAAKPEDWDERAKIDDPDTSKPEDWDKPE 240
Oryctolagus TYEVKIDNSQVESGSLEDDWDFLPPKKIKDPDASKPEDWDERAKIDDPDTSKPEDWDKPE 240
Homo    TYEVKIDNSQVESGSLEDDWDFLPPKKIKDPDASKPEDWDERAKIDDPDTSKPEDWDKPE 240
      *****:*****

Mus      HIPDPDAKKPEDWDEEMDGEWEPVVIQNPEYKGEWKPRQIDNPDYKGTWIHPEIDNPEYS 300
Rattus  HIPDPDAKKPEDWDEEMDGEWEPVVIQNPEYKGEWKPRQIDNPDYKGTWIHPEIDNPEYS 300
Oryctolagus HIPDPDAKKPEDWDEEMDGEWEPVVIQNPEYKGEWKPRQIDNPDYKGTWIHPEIDNPEYS 300
Homo    HIPDPDAKKPEDWDEEMDGEWEPVVIQNPEYKGEWKPRQIDNPDYKGTWIHPEIDNPEYS 300
      *****

Mus      PDANIYAYDSFAVLGLDLWQVKSGTIFDNFLITNDEAYAEFNGNETMGVTKAAEKQMKDK 360
Rattus  PDANIYAYDSFAVLGLDLWQVKSGTIFDNFLITNDEAYAEFNGNETMGVTKAAEKQMKDK 360
Oryctolagus PDANIYAYDSFAVLGLDLWQVKSGTIFDNFLITNDEAYAEFNGNETMGVTKAAEKQMKDK 360
Homo    PDPSIYAYDNFVGLGLDLWQVKSGTIFDNFLITNDEAYAEFNGNETMGVTKAAEKQMKDK 360
      **..*****.:.:.;*****:*****

Mus      QDEEQRLKEEEEDKKRKEEEAE-DKEDDDDR-DEDEDEDEKDEEEDSFGQAKDEL 416
Rattus  QDEEQRLKEEEEDKKRKEEEAE-DKEDDDDR-DEDEDEDEKDEEEDATGQAKDEL 416
Oryctolagus QDEEQRLKEEEEDKKRKEEEAEDEEEDKDDKEDEDEDEEDKDEEEDAAAGQAKDEL 418
Homo    QDEEQRLKEEEEDKKRKEEEAE-DKEDDEBKDEDEDEDEEDKDEEEDVPGQAKDEL 417
      *****:*****.:.:.;*****.:.:.;*****

```

Figure 3.25: Cross-species CRT alignment. The significant region of interest is thought to reside between residues 407-409, where each species has a unique combination of amino acids. These can be non-conservative differences when compared cross-species. For all alignments the following NCBI protein identification numbers were used: *Mus musculus* (mouse): NP021617; *Rattus norvegicus* (rat): NP071794; *Homo sapiens* (human): NP004334; *Oryctolagus cuniculus* (rabbit); NP001075704.

Intracellular loading of K41, K42, KDEL, HAKDEL and K42mCRT was assessed using the GFP-ub-SL8 construct, which investigated presentation as a function of antigen load. When antigen is limited (Figure 3.26 lower left panel), K42mCRT fully restores intracellular processing and presentation relative to K41, however, KDEL and HAKDEL achieve only partial restoration, consistent with previous results. Under conditions where the antigen dose is very high and unlikely to be limiting (Figure 3.26 lower right panel), K42mCRT and K41 still efficiently present antigen on the cell surface in contrast to KDEL and HAKDEL that present SL8 at comparably to K42. These results suggest that species differences between rat and mouse may account for the partial restoration seen for KDEL and HAKDEL when antigen is non-limiting. Rat CRT appears inhibited in comparison to K42mCRT, which may be due to a function that can be attributed to 3 species-specific c-terminal residues.



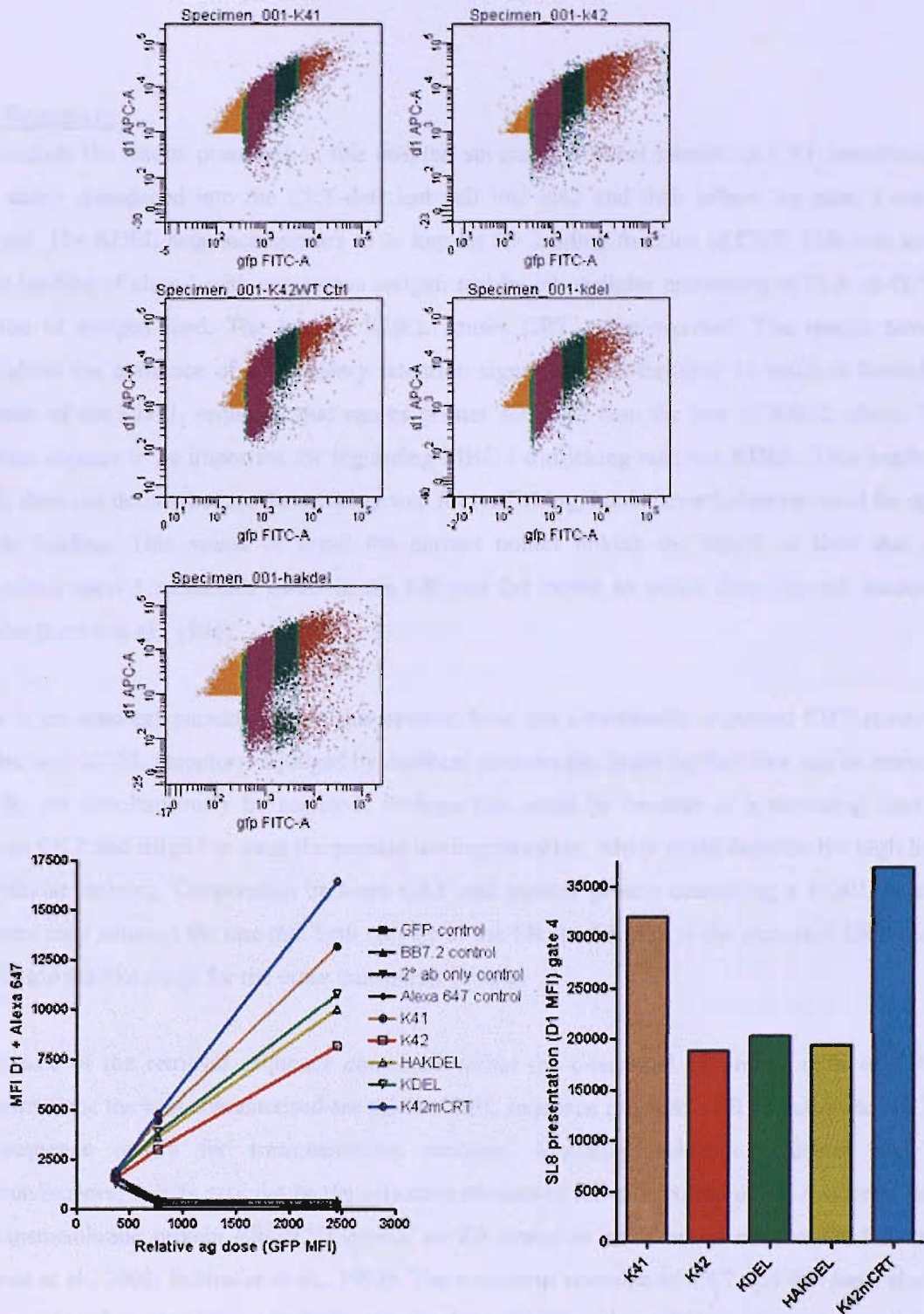


Figure 3.26: Intracellular loading assay FACS plot of H-2Kb-SL8 cell surface presentation. Intracellular processing as a function of antigen load. Complete restoration of intracellular MHC I peptide loading in K42 transfected with mouse CRT compared to K41. Partial restoration in K42 transfected with rat CRT. Low-Medium SL8 dose (lower left panel), High SL8 dose (lower right panel).

3.12 Summary

To conclude the results presented in this chapter, several c-terminal mutant rat CRT constructs have been stably transduced into the CRT-deficient cell line K42 and their effects on class I assembly assessed. The KDEL sequence appears to be key for the loading function of CRT. This was assessed by the loading of class I with exogenous antigen and by intracellular processing of SL8-ub-GFP as a function of antigen load. The loss of KDEL causes CRT to be secreted. The results have also highlighted the existence of a secondary retention signal in the c-terminal 11 residues immediately upstream of the KDEL sequence that causes greater secretion than the loss of KDEL alone. The c-terminus appears to be important for regulating MHC I trafficking rate, not KDEL. This implies that KDEL does not define the rate determining step for trafficking, but is nevertheless required for optimal peptide loading. This seems to break the current notion linking the length of time that newly synthesised class I molecules dwell in the ER and the extent to which they become loaded with peptides (Lewis et al., 1996).

There is an apparent paradox within this system; how can c-terminally truncated CRT mutants co-localise with KDEL receptor; as judged by confocal microscopy; implying that they can be retrieved to the ER, yet simultaneously be secreted? Perhaps this could be because of a persisting interaction between CRT and ERp57 or even the peptide loading complex, which could describe the high level of intracellular staining. Cooperation between CRT and another protein containing a KDEL or similar sequence may enhance the rate that both recycle to the ER. In the case of the truncated CRT mutants, they would act like cargo for the other transporter protein.

The nature of the retrieval sequence contained within the c-terminal 11 amino acids of CRT are unknown since the best characterised are the H/KDEL sequence of soluble ER proteins and KKXX or RR sequence motifs for transmembrane proteins. Mounting evidence indicates that these retention/retrieval motifs may not be the sole determinants of the distribution of ER-residents, because the transmembrane protein ERGIC53 carries an ER retention motif but is not localised to the ER (Monnat et al., 2000; Schindler et al., 1993). The c-terminal domains of CRT and BiP have also been shown to somehow participate in their retention by a KDEL independent mechanism, possibly by a Ca^{2+} -dependent interaction with the reticular matrix (Monnat et al., 2000; Munro and Pelham, 1987; Zagouras and Rose, 1989). Further analysis will need to be performed to confirm the nature of the sequence in the 11 c-terminal residues.

Chapter 4: The CRT C-terminal ER retrieval sequence

4.1 The retention / retrieval mechanism

Pentcheva and Edidin demonstrated that the mutant class I molecule T134K, which fails to interact with the PLC (TAP)(Lewis et al., 1996), enters the secretory pathway prematurely at an ER exit site that is different for wild-type molecules (Pentcheva and Edidin, 2001). In doing so, it appears to bypass the normal quality control that ensures their optimal loading with peptide. The similarities between T134K and K42 would indicate that CRT contributes to class I quality control and the results presented in chapter 3 show a function for the KDEL sequence in this process. CRT might ensure that class I is correctly distributed and placed in close proximity to the PLC, retaining class I molecules within the ER until they are fit for transport to the cell surface. Alternatively, CRT could recycle and retrieve newly synthesised class I molecules that are incompletely loaded from the ERGIC/Golgi to the ER (Hsu et al., 1991). Other glycoproteins have been shown to recycle to the ER by a mechanism mediated by the c-terminal KDEL motif (Pelham, 1989). MHC I molecules do not contain a c-terminal KDEL motif, so if they are recycled, it must be via a recycled binding partner such as CRT. Experiments were undertaken to investigate the potential role of CRT to mediate class I retention or retrieval.

4.1 PLC composition

To determine whether the CRT mutants were efficiently incorporated into the PLC, cells were lysed in digitonin and co-immunoprecipitated with an anti-TAP1 antibody. Immunoprecipitated material was divided into two and fractionated on two identical SDS-PAGE gels and analysed by western blot (Figure 4.1). Digitonin is a mild detergent that preserves the TAP-tapasin interaction (Diedrich et al., 2001). A non-reducing loading buffer was used to elute the proteins from the sepharose beads, because a reducing buffer separated the immunoglobulin used for the co-IP into its heavy and light chain components. The heavy chain migrated at a similar molecular weight to CRT and Erp57, which obscured the western blots and made it difficult to see them. To control for variations in the quantity of protein in the cell lysate prior to the IP, a sample of lysate (labelled supernatant) was run alongside the IP on SDS-PAGE.

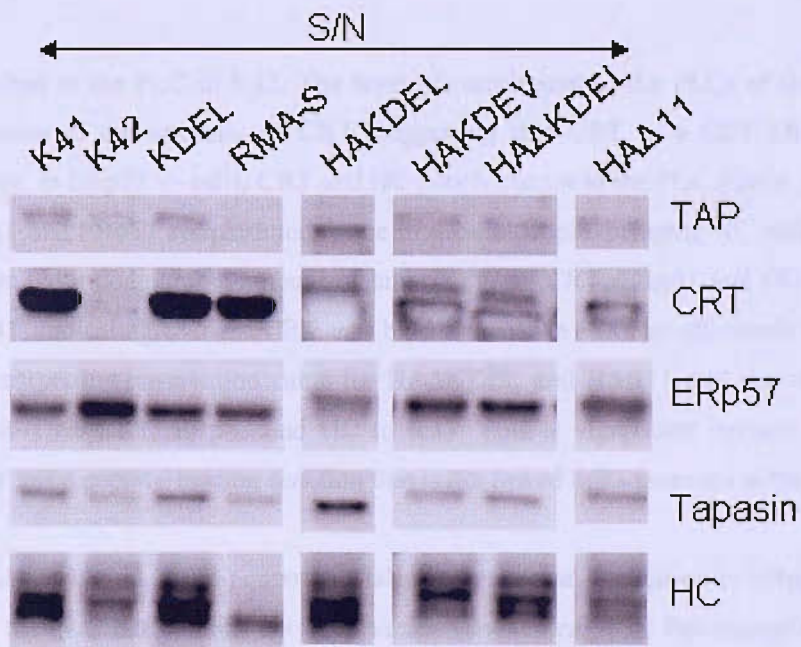


Figure 4.1: The PLC remains intact in c-terminal truncated CRT mutants. A co-immunoprecipitation (co-IP) was performed to determine the composition of the PLC. $15\text{-}20 \times 10^6$ cells were used for the co-IP and the samples split into two SDS-PAGE gels to allow proteins with similar molecular weights to be analysed from the same sample. No alkylation agent was used. RMA-S is a TAP1 deficient cell line and was used as a negative control for the co-IP. Less HC appears to co-IP in the K42 PLC.

The western blot shows that TAP was uniformly immunoprecipitated in each of the cell lines tested. Tapasin was recruited proportionately to TAP in all cell lines confirming it as a component of the “core” TAP complex. All of the K42 transfectants recruited CRT to the PLC. ERp57 is recruited to the K42 PLC but at a reduced level compared to K41, which is different to Gao et al (Gao et al., 2002) but consistent with recent data from Williams et al (personal communication). The reason for this is not clear. Although the quality of the western blot for the mutants is not excellent, it is clear that ERp57 is recruited for all of the mutants.

Despite using non-reducing loading buffer, the background surrounding the ERp57 co-IP band remained but was absent in the cell lysate control lanes. It is possible that scrambled disulphide-bonded ERp57 forms gave rise to the background or that there was cross-reactivity between the ERp57 antibody and a co-IP by-product. N-Ethylmaleimide (NEM) treatment, which alkylates free thiols and should have trapped any scrambled disulphide-bonded forms, did little to decrease the background signal.

HC is poorly recruited to the PLC in K42. The level of recruitment to the PLCs of the mutant CRT transfectants correlates to the intensity of CRT, suggesting that CRT or a CRT-ERp57 conjugate recruits HC. Notably, in ERp57 *-/-* cells, CRT and HC poorly recruit to the PLC (Garbi et al., 2006). It is possible that CRT and ERp57 are recruited to the PLC as a couple, bringing HC with them. KDEL and HAKDEL recruited a comparable amount of tapasin (Tpn), CRT, ERp57 and HC to their PLCs with respect to K41, indicating that rat CRT can bind the mouse PLC as efficiently as autologous murine CRT. The surprising observation came for HA Δ KDEL and HA Δ 11 that showed comparable PLC recruitment of Tpn, CRT, ERp57 and HC to K41. This is significant because it is the first indication that CRT has a peptide-loading function that is not linked to its presence in the PLC.

Recently, Park et al (Park et al., 2006) controversially reported that in addition to ERp57, they could also detect PDI in the PLC but this has not been verified by several labs. For example Kienast et al (Kienast et al., 2007) were unable to show its recruitment to the PLC but a recent paper by Santos et al has since confirmed that it is also present in the PLC of .220.tpn.B8 cell lines (Santos et al., 2007). A TAP1 co-IP was performed on HAKDEL, HAKDEV, HA Δ KDEL and HA Δ 11 cell lysates. Figure 4.2 shows that similar quantities of PDI are recruited to the PLC of each of the cell lines tested. PDI migrates with a similar molecular weight to ERp57 and it is possible that there may be cross-reactivity between ERp57 and the PDI antibody used in the western blot. Alternatively, the PDI band may have

appeared as part of a non-specific precipitation during the co-IP. The composition of the PLC in ERp57^{-/-} cells should be determined to clarify this result.

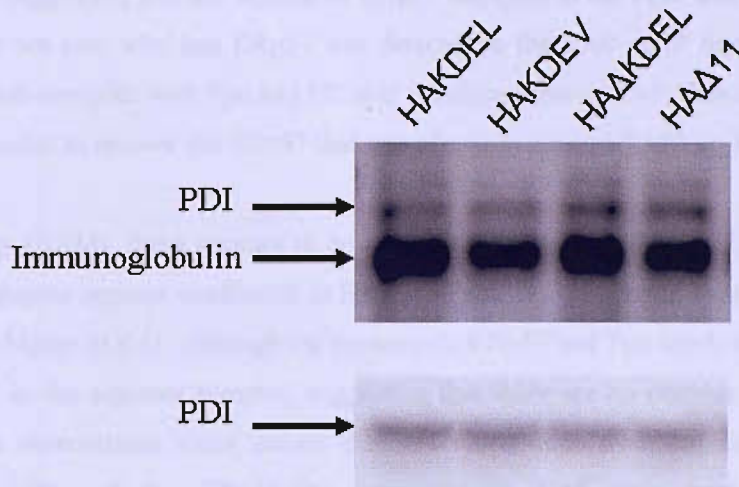


Figure 4.2: PDI assembly with the PLC. An anti-TAP1 PLC co-IP was performed on 20nM PBS pH6.8 NEM-treated cell lysates to determine whether PDI is incorporated into the PLC.

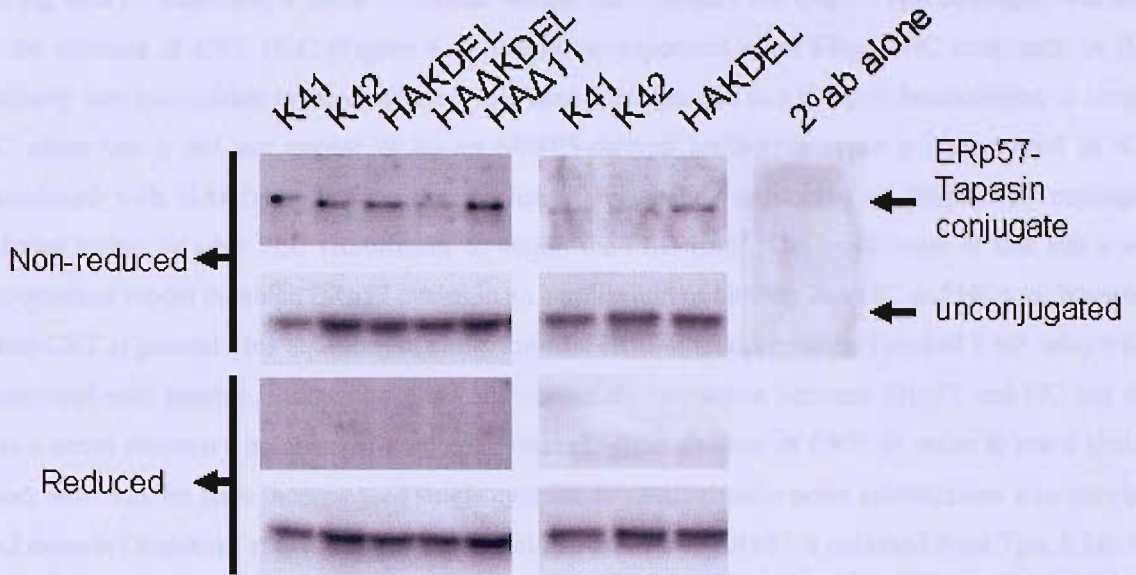
Recent data suggests that Tpn is only functional when bound to ERp57 (Wearsch and Cresswell, 2007), although Tpn has clearly been shown to retain its function in the absence of ERp57 (Chen and Bouvier, 2007). Dick et al. reported that cysteine-95 of Tpn disulphide bonds with cysteine-57 of ERp57 (Dick et al., 2002) and showed that this conjugate was part of the PLC. According to recent observations, this conjugate protects empty peptide-binding grooves of MHC I molecules from $\alpha 2$ disulphide reduction until that protection is provided by the peptide ligand (Kienast et al., 2007). This is thought to ensure that the groove is maintained in a peptide-receptive state while in contact with the PLC. Given the apparent importance of CRT for ERp57 recruitment to the PLC, together with the finding that the truncated CRT transfectants poorly loaded, despite incorporation into the PLC, it was important to determine whether the disulphide conjugation between ERp57 and Tpn was normal in PLC's containing mutant CRT.

Thiol-blocking chemicals were required to preserve the tapasin-ERp57 conjugate (Dick et al., 2002) and NEM was the reagent of choice because it alkylates free thiols irreversibly. NEM conjugate treatment was conducted in tandem with another recently identified reagent called Methyl methanethiosulfonate (MMTS), which has been found to be superior than NEM (Peaper et al., 2005) because it alkylates free thiols with a greater efficiency. It provided a useful tool but had to be used cautiously because it specifically modifies the free thiol groups to dithiomethane (-S-S-CH₃), which

free cysteine residues of proteins can potentially react with, resulting in artificial protein disulphide bond formation (Karala and Ruddock, 2007). Consistent with published work, MMTS could detect the tapasin-ERp57 conjugate more efficiently than NEM (Figure 4.3) but the level of conjugate was unaffected in K42, suggesting that the amount of ERp57 recruited to the PLC was unchanged. In light of this result, I am not sure why less ERp57 was detected in the TAP co-IP from K42. If a pool of ERp57 exists in a sub-complex with Tpn and HC that is independent of TAP, then an anti-Tpn co-IP of K42 cells would predict to recover the ERp57 that was absent in the anti-TAP1 co-IP.

At lower sensitivity (NEM), there appears to be less ERp57-Tpn for HA Δ KDEL, but it is not clear why, since the conjugate appears unaffected in HA Δ 11. The ERp57-detected conjugate (but not Tpn) also appears to run higher in K41, although the monomeric ERp57 and Tpn bands in K41 appear to run at the same height as the adjacent samples, suggesting that there are no obvious differences in their redox state. These observations alone cannot discount redox state from explaining the change in electrophoretic mobility of the ERp57-Tpn conjugate in K41 and should be investigated. Characterisation of the ERp57-Tpn conjugate has already been documented by using rapid acidification of the intracellular environment with trichloroacetic acid (TCA), followed by thiol modification with the alkylating agent 4'-maleimidylstilbene-2,2'-disulfonic acid (AMS) (Antoniou and Powis, 2003). Using this technique, proteins migrate at different molecular weights according to their redox state, which can be detected by western blot.

NEM alkylation



MMTS alkylation

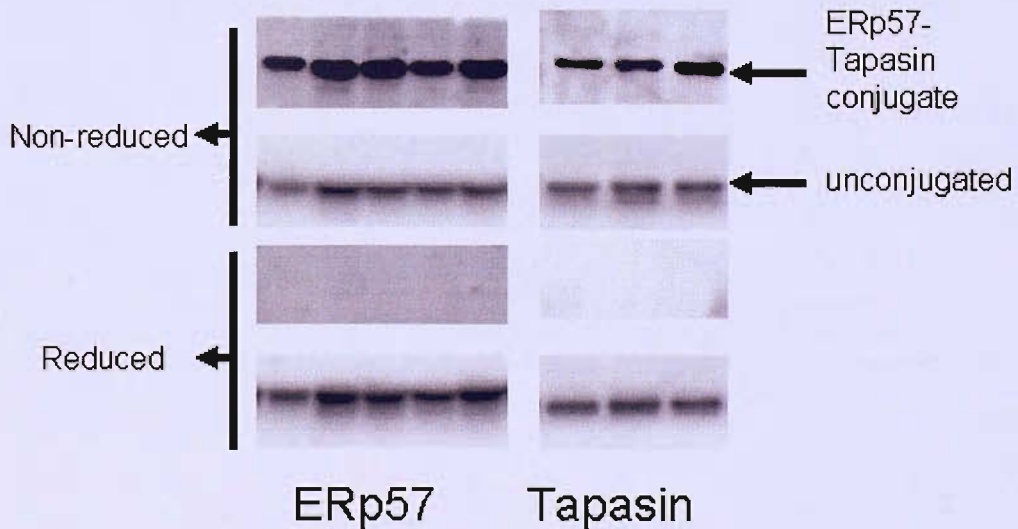


Figure 4.3: NEM and MMTS alkylation of the ERp57-Tpn conjugate. NEM and MMTS alkylation experiments were performed to identify the state of the ERp57-Tpn conjugate in the CRT mutants. MMTS was more efficient at detecting the conjugate than NEM.

During MMTS treatment, a lower molecular weight band beneath the ERp57-Tpn conjugate was seen in the absence of CRT (K42)(Figure 4.4), which corresponded to an ERp57-HC conjugate. A β_2m antibody was unavailable to prove whether this band corresponded to a HC- β_2m heterodimer, or simply HC alone but it did not appear to be an MMTS-derived artifact, because it disappeared in K42 transduced with HAKDEL. It was also unclear if this band represented an ERp57-HC conjugate existing before or after PLC recruitment or within the PLC itself. The implication of this result is a hypothetical model in which ERp57 cycles in an equilibrium of binding free HC and HC β_2m , however, when CRT is present, this equilibrium shifts towards HC β_2m recruitment to Tpn and TAP, where it is assembled with peptide. Studies have already shown an interaction between ERp57 and HC but this was a novel discovery because the conjugate formed in the absence of CRT. In order to see a similar band, other studies have incorporated single cysteine to alanine/serine point substitutions into the class I $\alpha 2$ domain (Antoniou et al., 2007; Kienast et al., 2007). When ERp57 is unbound from Tpn, it has the tendency to reduce HC but my attempts to determine the redox state of HC in complex with Erp57 in these samples were not successful.

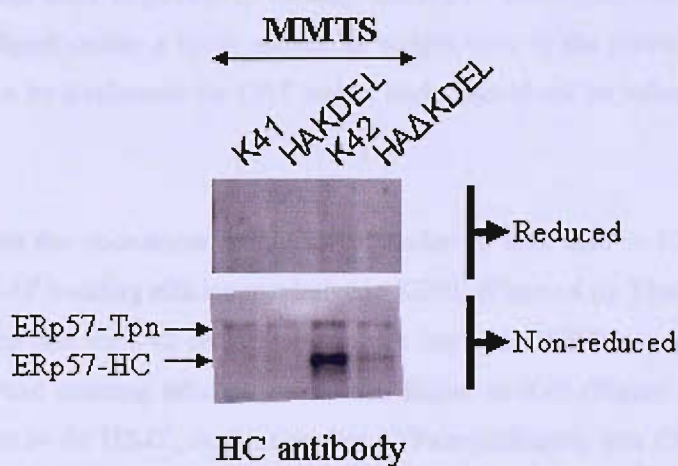
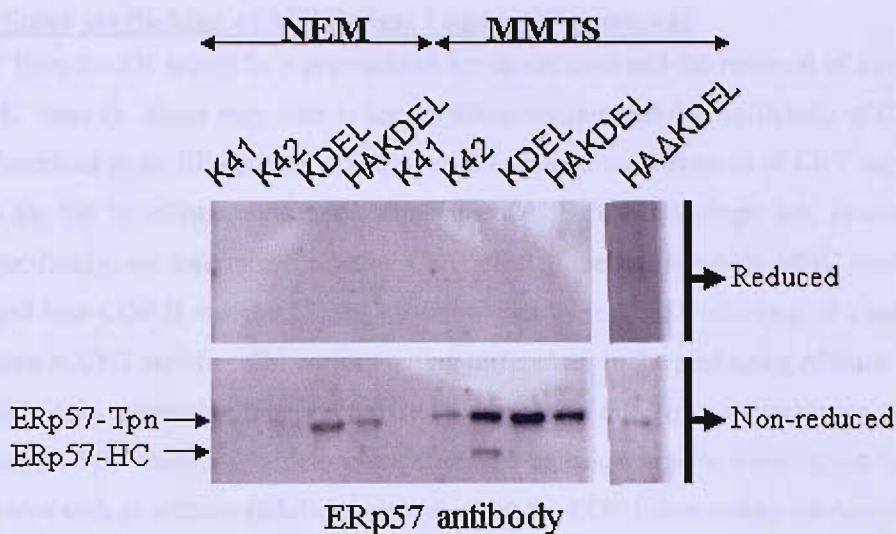


Figure 4.4: An ERp57-HC conjugate forms in the absence of CRT. During ERp57-Tpn alkylation experiments, a lower molecular weight band corresponding to ERp57-HC was identified in K42. This band was less apparent in HAΔKDEL and undetectable in HAKDEL and K41. The ERp57-Tpn band visible on the lower blot is due to a reprobe of the blot.

4.2 Intracellular trafficking of MHC class I and CRT retrieval.

Exit of CRT from the ER would be a prerequisite for its retrieval and the retrieval of associated cargo (such as MHC class I). Since very little is known about the intracellular trafficking of CRT, which is commonly described as an ER-resident protein, we determined the influence of CRT on exit of MHC class I from the ER in collaboration with Mohammed Al Balushi (Springer lab, Jacobs University, Bremen). Specifically, we determined whether CRT affected the rate at which MHC class I molecules were packaged into COP II vesicles. Since we know that the rate of trafficking of class I in K42 is more rapid than in CRT replete cells; corresponding differences in the packaging of class I into COP II vesicles would imply a retention function for CRT; whereas no difference in packaging would imply a retrieval function. The “budding” efficiency of COP II was calculated by working out the fraction of H2-D^b recovered with or without stabilising peptide from the COP II-containing microsomes compared against 50% of the total cell membrane H2-D^b recovered with or without stabilising peptide. Endoglycosidase F₁ (EndoF) was used to positively identify the H2-D^b associated with the COP II vesicles because the enzyme digest causes a lower molecular weight shift of the protein. ATPase is non-glycosylated and should not be a substrate for CRT and as such, should not be influenced by any CRT-mediated retention.

Less H2-D^b was recovered from the microsome immunoprecipitation in K42 than in KDEL (Figure 4.5). K42 also has twice the H2-D^b budding efficiency relative to KDEL (Figure 4.6). This is consistent with the faster H2-D^b trafficking rate for K42 cells. These results imply that CRT may play a role in H2-D^b ER retention. The ATPase budding efficiency was also higher in K42 (Figure 4.7), but the difference was not as significant as for H2-D^b, suggesting that ATPase packaging into COPII vesicles was less dependent on CRT than H2-D^b.

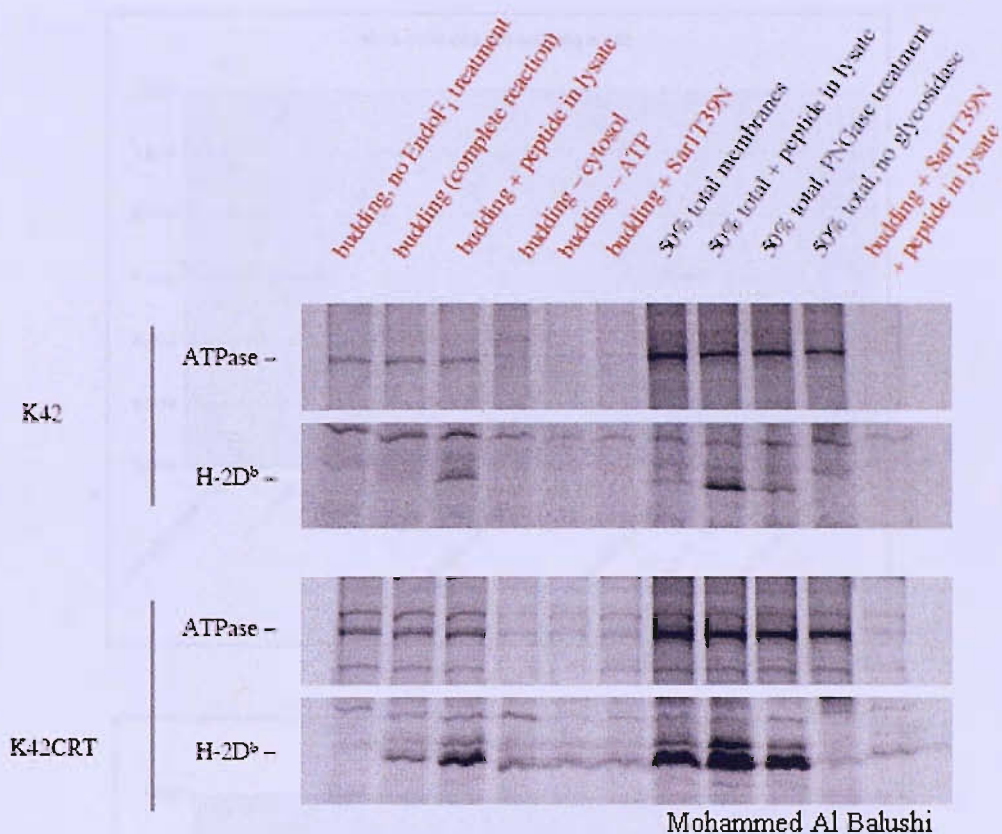
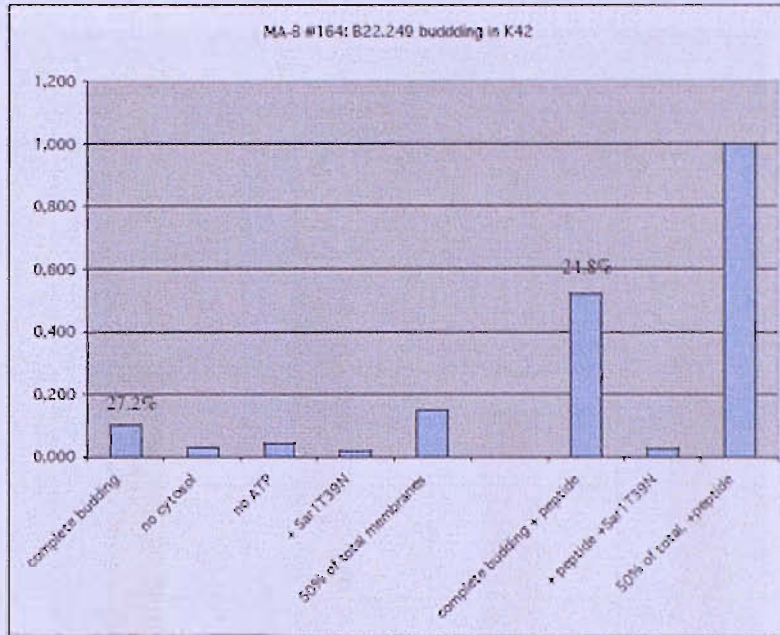
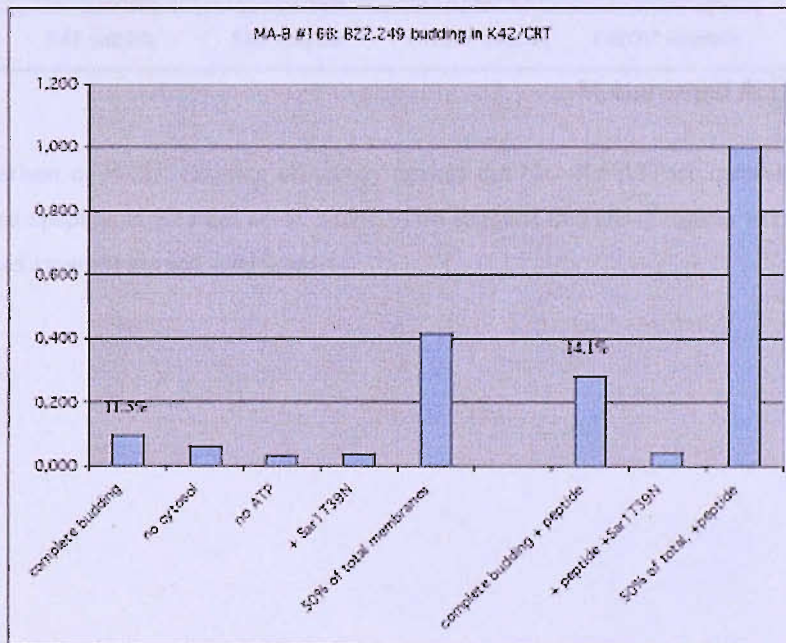


Figure 4.5: H-2D^b leaves the ER in COPII vesicles of K41 at a faster rate than K42 transfected with CRT KDEL. A COP II budding assay was performed to determine whether the inclusion of MHC I into COP II vesicles was different in cells with or without CRT. The “budding efficiency” was calculated by working out the fraction of vesicle budding \pm peptide compared to the 50% of cell membrane isolated MHC I \pm peptide. Vesicle supernatants are indicated in red. All samples were treated with EndoF1 unless otherwise indicated. Na⁺-K⁺-ATPase (alpha subunit) is not glycosylated. The recovery of material is greater in K42CART (KDEL) than in K42, which may be reflective of the different H2-D^b trafficking rates – it is faster in K42 and may have travelled through the COP II enriched microsomes much faster than in KDEL. The control Sar1T39N is a GDP locked form of Sar1 that prevents COPII-dependent ER export (Kuge et al., 1994; Ward and Moss, 2001).

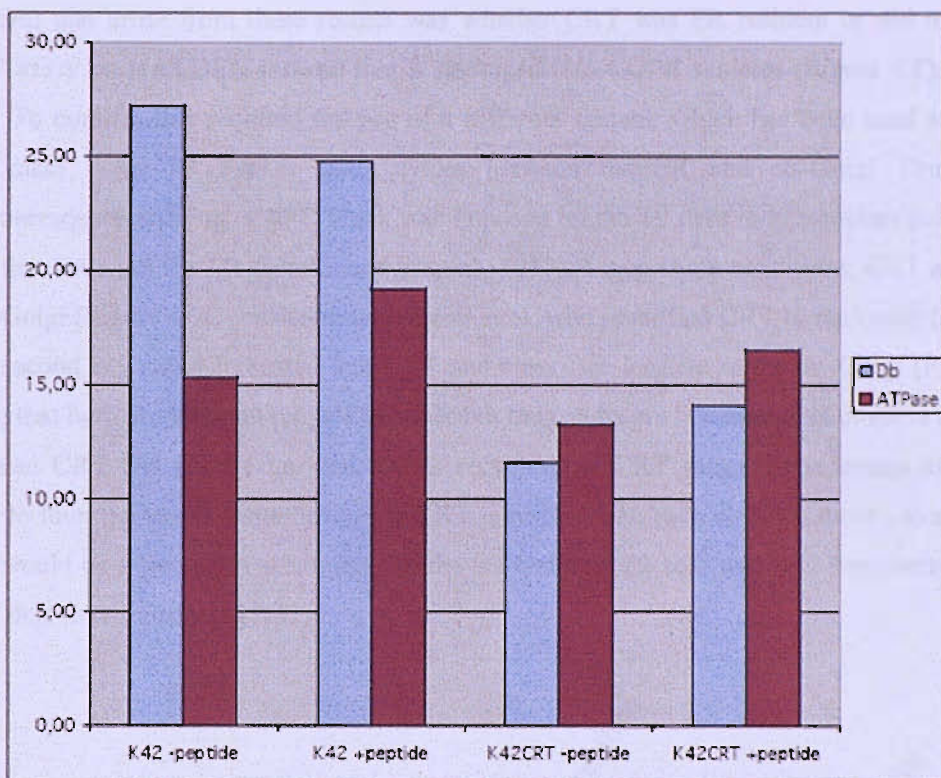


Mohammed Al Balushi



Mohammed Al Balushi

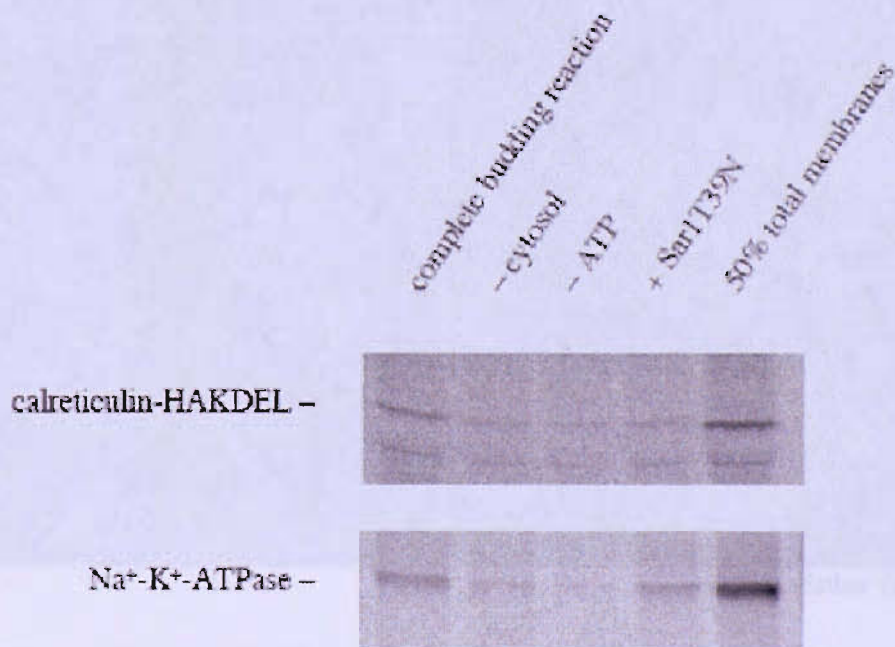
Figure 4.6: The H-2D^b COPII budding efficiency is higher in K42 than K42 transfected with CRT KDEL. Bar graphs showing the budding efficiency in K42 and K42CRT (KDEL) ±peptide (presented as the fraction of 50% of total ±peptide). The budding efficiency is approximately the same with and without peptide. The IP signal strength is normalised against the rightmost column.



Mohammed Al Balushi

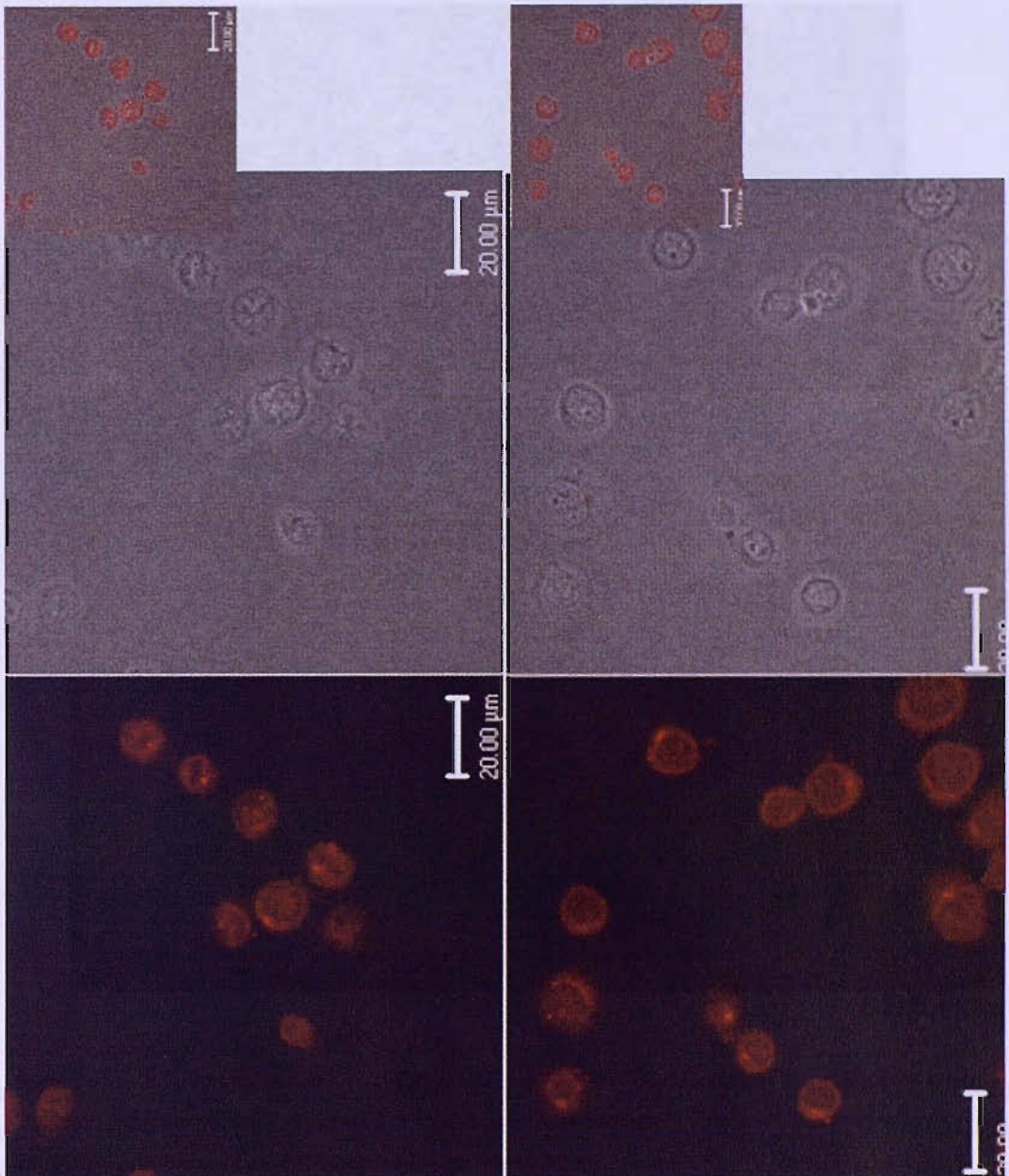
Figure 4.7: Comparison of H-2D^b budding efficiency against the Na⁺-K⁺-ATPase control. H2-D^b budding is greater than ATPase ±peptide in K42 but not in KDEL. This suggests that H2-D^b egress from the ER is faster in K42. The differences ±peptide are not significant.

The question that arose from these results was whether CRT was ER resident or did it recycle. A “budding” assay on HAKDEL showed that it packaged into COPII vesicles (Figure 4.8), suggesting recycling. To confirm this required the use of a different system, which has been used to show that unloaded class I (in T2 TAP^{-/-} cells) cycles between the ER and cis-Golgi. Prior to CRT immunofluorescence staining, a 20°C block was imposed on the T2 cells to accumulate proteins in the cis-Golgi that have left the ER (Matlin and Simons, 1983). Under these conditions, CRT accumulated in the cis-Golgi (Figure 4.9), consistent with Neeli et al. who identified CRT in the Golgi (Neeli et al., 2007). A second key result indicated that CRT and class I co-localise in the cis-Golgi (Figure 4.10), suggesting that both proteins can recycle together but the results are not enough to confirm a functional link between CRT and class I i.e. that HC is recycling as CRT cargo. Experiments are currently underway to investigate this issue further. If CRT is responsible, then at 20°C, more unloaded class I and CRT would be expected to accumulate in the cis-Golgi of T2 cells and K42 transfected with wild type CRT than in untransfected K42.



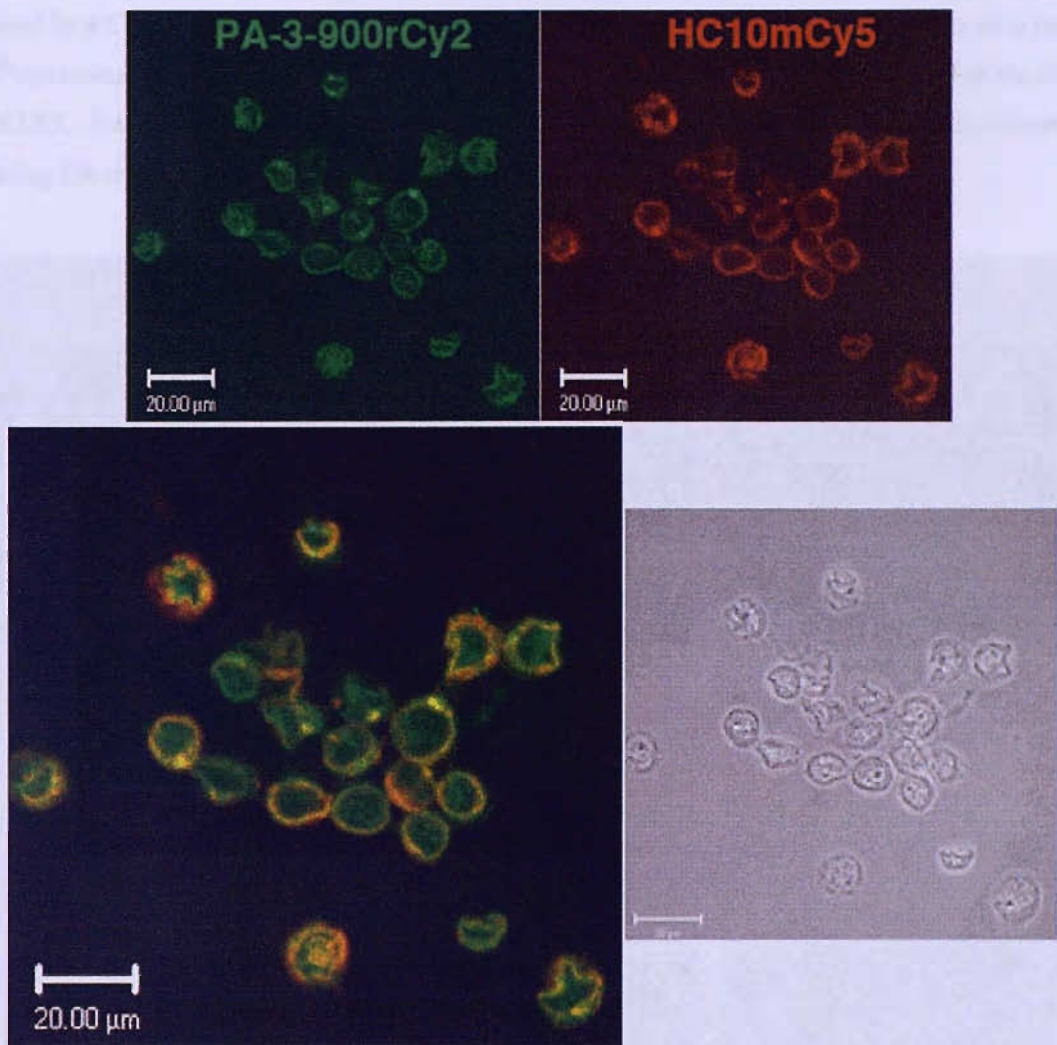
Mohammed Al Balushi

Figure 4.8: CRT is present in COPII vesicles. A COPII budding assay shows that CRT is present in a COPII enriched microsomal fraction.



Esther Ghanem

Figure 4.9: CRT accumulates in the cis-Golgi of T2 cells. CRT labelled in red alongside rabbit serum using Cy3. Punctate patterning of CRT suggesting it accumulates in the secretory pathway. This pattern is less evident in fibroblast cells because the ER labels easily, giving high background.

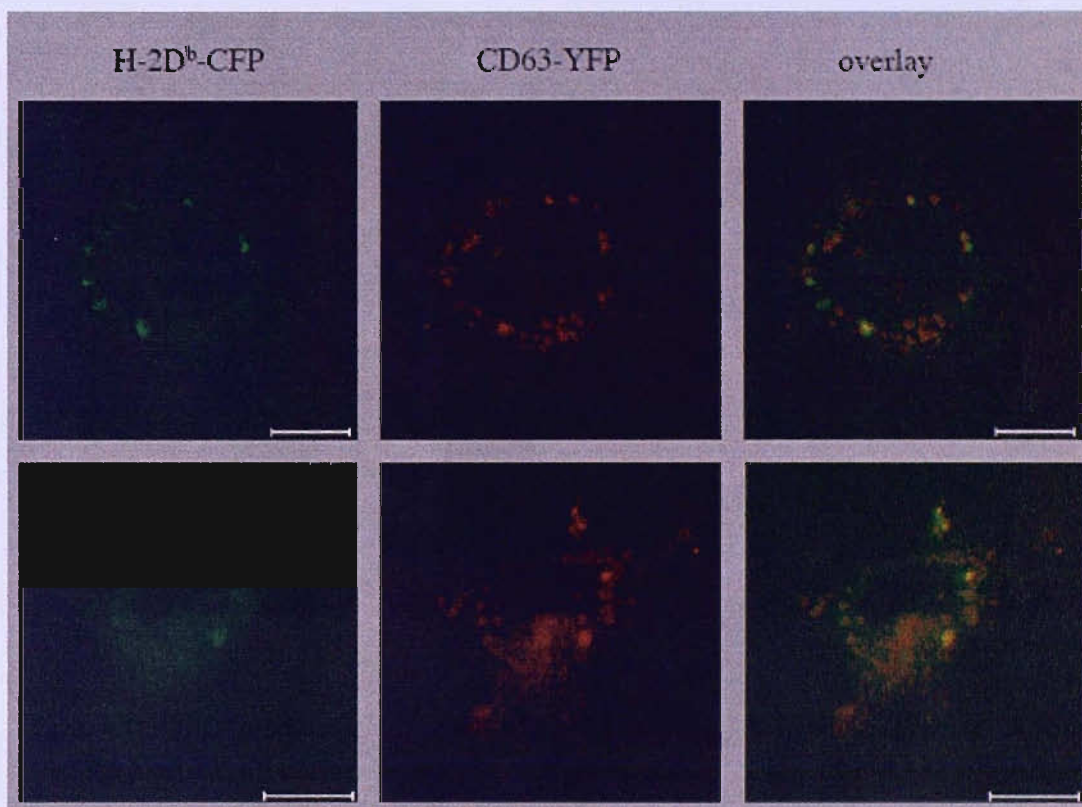


Esther Ghanem

Figure 4.10: CRT and MHC I co-localise at the cis-Golgi of T2 cells. Double immunofluorescence labelling of endogenous CRT in green (Cy2) and HLA-B (Cy5) in T2 cells. A 20°C temperature incubation was imposed to accumulate proteins in the cis-Golgi.

The differences in MHC class I assembly and cell surface expression between CRT deficient and replete cells have been documented (Gao et al., 2002) but it is unclear if this alters the fate of MHC I molecules once they have been internalised back into the cell. Immunofluorescence microscopy showed that endogenous K42 H-2D^b accumulated in intracellular clusters at 37°C that co-localised with the lysosomal marker CD63 (Figure 4.11). H2-D^b accumulation was greater in K42 than K41 (Figure unavailable) suggesting that in the absence of CRT, a large pool of class I are short lived on the cell surface, are poorly loaded with peptide and internalise rapidly. If MHC I accumulation in the lysosome

is caused by a CRT deficiency, further microscopy studies on HAKDEL would predict to see a reduced H-2D^b-lysosomal staining. To ascertain whether CRT is responsible for recycling class I to the ER, the HAAKDEL K42 transfectant should help understand the importance of the KDEL-receptor in mediating ER retrieval of CRT with class I as cargo.



Malgorzata Garstka

Figure 4.11: MHC I expressed in K42 accumulates in the lysosome. K42 cells transfected with CFP-tagged H2-D^b colocalised with a lysosome marker CD63. This pattern of labelling was absent in K41, suggesting that H2-D^b is internalised more rapidly, accumulating in the lysosome. This may also suggest that H2-D^b is not optimised with peptide as well as in K41.

These results indicate that CRT-mediated class I ER retention and potentially recycling MHC I from the cis-Golgi to ER are important for correct peptide-loading. It is unclear whether CRT does this by facilitating class I access to peptide. To determine whether the K42 peptide loading defect could simply be overcome by increasing the endogenous peptide pool, an H2-D^b stabilising peptide was electroporated into K41 and K42 (performed by Malgorzata Garstka). The results show a small rise (15%) of H2-D^b cell surface expression for K42 but not K41 in the presence of peptide, suggesting that

CRT improves peptide access to class I (Figure 4.12). It may do this by increasing the efficiency of class I recruitment to the PLC. However, raising the endogenous pool of peptide induces only a small rise in cell surface class I expression suggesting that it may not be a key role for CRT, which instead may be in class I ER retention or retrieval from the cis-Golgi to the ER.

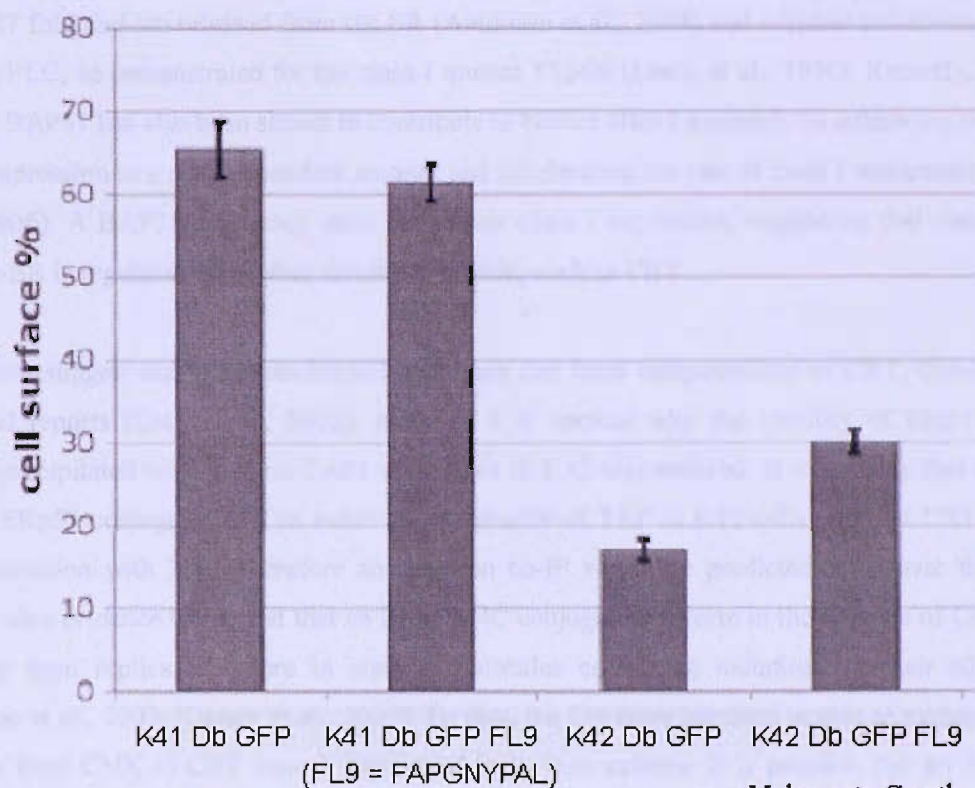


Figure 4.12: Electroporation of high affinity H-2Db stabilizing peptide into K41 and K42 cells.

The aim: to stabilise inefficiently peptide-loaded H2-D^b molecules, which could be detected at the cell surface. Addition of peptide had little impact in K41, but in K42, raised the detection of H2-D^b by 15%.

4.3 Summary

These results appear to uncouple PLC assembly from class I optimisation, suggesting that CRT performs a loading function that is independent of its ability to bind and recruit HC to the PLC. This recruitment does not appear to require the KDEL or 11 c-terminal amino acids of CRT.

The results are consistent with CRT both retaining class I to the ER and retrieving them from the cis-Golgi. H2-D^b has a faster budding efficiency in K42 than KDEL, suggesting that CRT operates to retain class I in the ER. However, CRT also appears to bud from the ER in COP II vesicles and

accumulate with class I in the cis-Golgi of T2 cells at 20°C, suggesting a retrieval role too. The class I peptide-loading defect in K42 cannot be completely overcome by raising the pool of endogenous class I-binding peptide, suggesting that CRT-mediated class I ER retention or retrieval from the cis-Golgi may be more significant a role for CRT than simply improving class I access to peptide.

MHC class I assembly appears to be limited by two steps; the rate that MHC class I alleles such as HLA-B27 fold and are released from the ER (Antoniou et al., 2004) and whether the alleles assemble with the PLC, as demonstrated for the class I mutant T134K (Lewis et al., 1996). Recently, the cargo receptor BAP31 has also been shown to contribute to human class I assembly by enhancing cell surface class I expression in a dose dependent manner and accelerating the rate of class I maturation (Ladasky et al., 2006). A BAP31 deficiency does not impair class I expression, suggesting that class I egress from the ER is regulated by another candidate protein, such as CRT.

The results suggest that a tapasin-ERp57 conjugate can form independently of CRT, consistent with published reports (Dick et al., 2002), however it is unclear why the quantity of ERp57 that co-immunoprecipitated with the anti-TAP1 antibodies in K42 was reduced. It is possible that a separate pool of ERp57 conjugated to Tpn exists independently of TAP in K42 cells and that CRT stabilises their interaction with TAP; therefore an anti-Tpn co-IP would be predicted to recover the ERp57. There is also evidence to suggest that an ERp57-HC conjugate can form in the absence of CRT, which has only been replicated before in class I molecules containing mutations in their $\alpha 2$ domains (Antoniou et al., 2007; Kienast et al., 2007). To date, the literature has been unable to explain how HC transfers from CNX to CRT once it has bound to its β_2m subunit. It is possible that an ERp57-HC conjugate may provide a better substrate for CRT to bind than to HC alone either because CRT can bind both proteins independently of one another or that ERp57 changes the redox state of the HC to make it a better substrate for CRT to bind.

The intensity of CRT correlated with level of recruitment of HC to the PLCs of the mutant CRT transfectants, suggesting that CRT or a CRT-ERp57 conjugate recruits HC. In ERp57 $-/-$ cells, CRT and HC poorly recruit to the PLC (Garbi et al., 2006), suggesting that cooperation between CRT and ERp57 may be important for HC recruitment to the PLC. It is unclear if ERp57 and CRT may also cooperate in other aspects of class I assembly. Analysis of the CRT $-/-$ and ERp57 $-/-$ cells has also been unable to establish whether the interaction between CRT and ERp57 is requisite for both to function normally.

Chapter 5: the ERp57-binding and glycan binding sites

5.1 The CRT binding site for ERp57

CRT is an ER resident chaperone and together with CNX and ERp57, forms part of the CNX/CRT chaperone system that operates to assist protein folding and quality control within the ER. All 3 chaperones are found within the MHC class I pathway. This chapter investigates the role of CRT and its association with ERp57 to understand if this is an important requirement for CRT to function in class I assembly.

As discussed in section 1, CRT and ERp57 are thought to be tightly linked with respect to MHC class I assembly, since impaired HC recruitment to the PLC and poor MHC class I assembly are common to both CRT *-/-* and ERp57 *-/-* cells (Gao et al., 2002; Garbi et al., 2006)(David Williams, personal communication). ERp57 *-/-* cells also recruit less CRT to the PLC, suggesting a mechanism whereby Tpn may first engage ERp57 through its C95 disulphide bond (Dick et al., 2002). CRT and HC might then be recruited to the PLC through ERp57. Tpn is already known to be an important component for MHC class I peptide optimisation (Chen and Bouvier, 2007; Howarth et al., 2004; Wearsch and Cresswell, 2007) and although the above CRT and ERp57 studies have shown both to be important for class I assembly, they were unable to determine whether CRT and ERp57 need only be present, or are reliant on their ability to interact with one another to fulfil their chaperone and redox isomerise functions (see chapter 1). If the CRT-ERp57 interaction was important for class I assembly, then poorer class I assembly and peptide loading would be expected to occur if it was disrupted. It is also possible that the effects on class I assembly might be expected to mirror those documented in the CRT and ERp57 *-/-* studies.

The ERp57 binding site for CRT has been mapped to residues 225-251, which form the tip of the P-domain (Frickel et al., 2002). The P-domain is highly conserved, with the exception of the *Saccharomyces cerevisiae* homolog, Cne1p (de Virgilio et al., 1993; Parlati et al., 1995). Mutational analysis of the CRT-ERp57 binding site was undertaken by Micha Häuptle (Appendix 4), Helenius Laboratory, Zurich), who substituted the Cne1p P-domain tip sequence into the CRT P-domain from EDWDEEMD > SWWKELMH, on the basis that as ERp57 is absent in yeast, any evolutionary pressure keeping the ERp57 binding site intact in Cne1p would be lost. The studies used recombinant residues 189-288 of the mutant CRT P-domain and ERp57, which were expressed and purified from *Escherichia coli*. Cross-linking studies, Enzyme-Linked ImmunoSorbent Assays (performed by Micha Häuptle) and Isothermal Titration Calorimetry (performed by Llian Jelesarov, University of

Zurich)(Appendix 4) verified that the CRT P-domain failed to bind ERp57. A restriction digest was then used to insert the ERp57-binding defective CRT P-domain into the full-length CRT sequence (Δ EB; Eva Frickel, Helenius Laboratory, Zurich). I inserted an HA-tag immediately upstream of the KDEL sequence of the ERp57-binding defective CRT mutant to help improve its detection (HA Δ EB) (Figure 5.1). On the strength of the results published by Frickel et al. (Frickel et al., 2002) and the mutational analysis on the CRT-ERp57 binding site, no further binding assays were performed on HA Δ EB to verify that it failed to bind ERp57. HA Δ EB was expressed in K42 cells using the cmv-bip-NGFR retroviral vector and HA Δ EB expression was confirmed by western blot. HA Δ EB expression and was comparable to HAKDEL, but it ran slightly lower on the gel (Figure 5.2). The HA Δ EB sequence had already been confirmed by DNA sequencing, so it is possible that the amino acid substitutions in the P-domain tip influenced its electrophoretic mobility relative to HAKDEL.

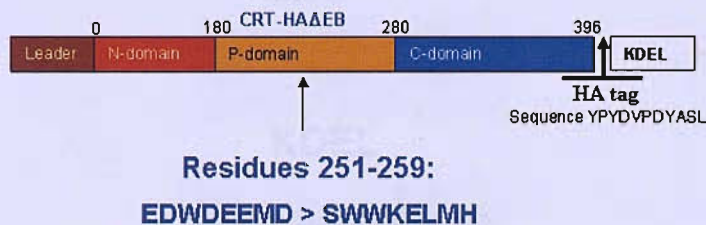


Figure 5.1: Schematic of the ERp57-binding defective rat CRT mutant HA Δ EB

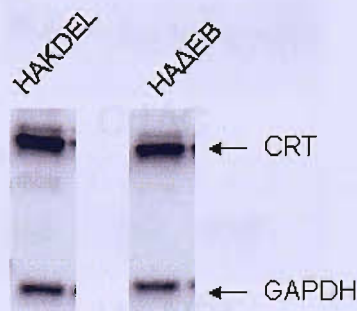


Figure 5.2: Expression of HA Δ EB is comparable to HAKDEL. The housekeeping gene, GAPDH was used as a loading control to compare CRT expression between the transfected cells.

The level of HA Δ EB secretion into the surrounding cell culture media was measured to provide a simple indirect measurement of protein accumulation over time and test whether the P-domain modifications impaired its ability to be retained / retrieved to the ER. K41, KDEL and HAKDEL were used as wild type controls to compare HA Δ EB (Figure 5.3), which appeared no different, suggesting that CRT retention is not a consequence of ERp57-binding but because of its own KDEL and c-terminal sequence.

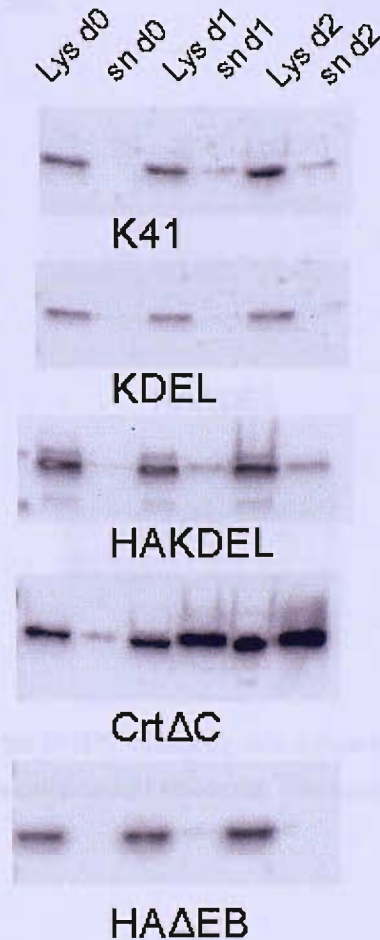


Figure 5.3: HA Δ EB is not secreted. Cell lysate and cell culture media were collected over a two day period and probed for CRT. This was compared against a secreted CRT control cell line Crt Δ C (see section 3) and wild type K41, KDEL and HAKDEL K42 transfectants.

5.2 MHC I assembly is impaired in ERp57-binding defective CRT cell lines

For the same reasons as described in section 3.6, the effect of HA Δ EB on MHC class I trafficking was investigated. H-2D^b was studied because it has slow overall trafficking, permitting a window of approximately 40-50min between HAKDEL and K42. HA Δ EB failed to restore H2-D^b trafficking relative to HAKDEL (Figure 5.4), which was similar to the trafficking rate observed for the c-terminally truncated CRT mutants, suggesting that CRT cooperation with ERp57 is also required to achieve the appropriate trafficking rate.

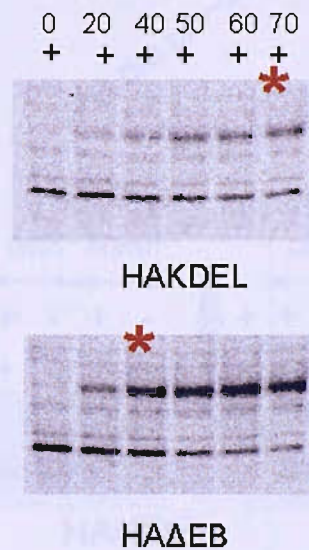


Figure 5.4: HA Δ EB does not restore the H-2D^b trafficking rate compared to HAKDEL. Asterisks represent the time taken for 50% of the H2-D^b to acquire EndoH resistance. This suggests that the CRT-ERp57 interaction is important for MHC I trafficking.

If correct MHC I assembly requires ERp57 bound to CRT, then MHC class I should be more thermostable in HAΔEB than HAKDEL. The total amount of MHC I recovered by IP with and without stabilizing peptide should indicate how good the construct is at assisting peptide loading. An EndoH digest discriminates between the MHC I thermostability at either the ER-Cis-Golgi or cis-Golgi-cell surface compartments. A smaller quantity of H2-K^b and H2-D^b was recovered from an HAΔEB IP than HAKDEL after either a 4°C or 26°C overnight temperature incubation, indicating that MHC class I is more unstable in HAΔEB (Figure 5.5).

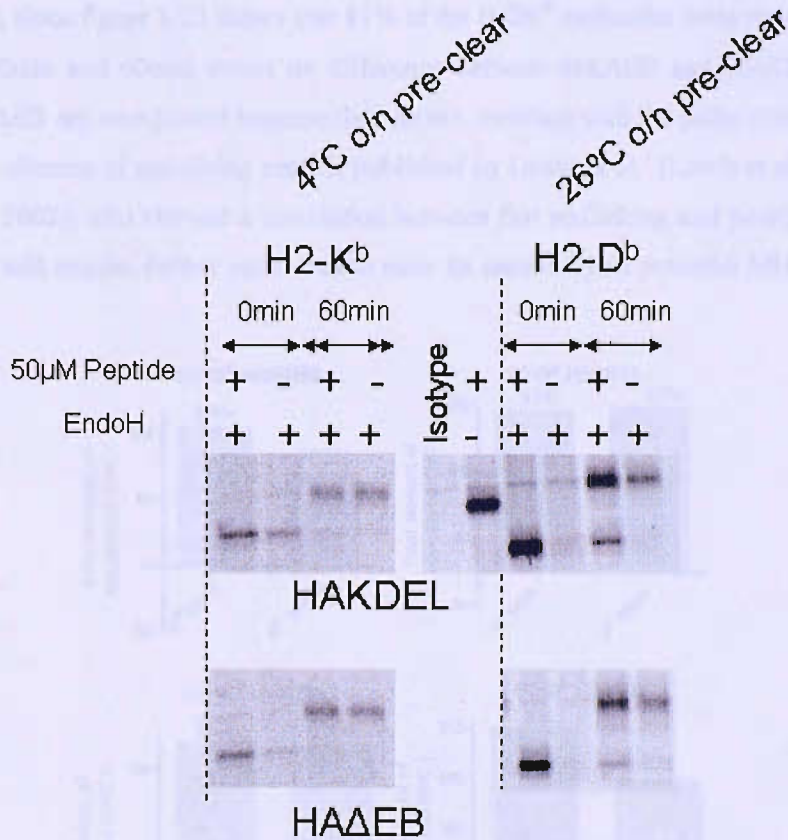


Figure 5.5: Investigating intracellular H-2K^b and H-2D^b loading in HAKDEL and HA^ΔEB using a pulse-chase thermostability experiment. Results show a peptide-induced and time-dependent stabilization of MHC class I molecules over 60min. A greater quantity of H2-D^b is immunoprecipitated relative to H2-K^b. The overnight thermostability experiment was performed at 4°C for H2-K^b and 26°C for H2-D^b.

MHC class I stability was calculated as the percentage of stable class I recovered from the IP in the absence of peptide and is written above each histogram (Figure 5.6) The amount of stable MHC class I recovered in the absence of stabilizing peptide increases with time for both alleles in both cells, suggesting that peptide optimization is time-dependent. Less H2-K^b is stable in HAΔEB after 60min than H2-D^b, suggesting that K^b is more sensitive to defects in MHC class I processing machinery than D^b. H2-K^b stability in HAΔEB is similar to HAKDEL at time 0min, suggesting that there is no difference in H2-K^b folding immediately after synthesis. At 60min, the results show that 100% of the H-2K^b molecules are recovered from HAKDEL compared to 85% in HAΔEB. It is not clear whether this is significant, since figure 3.23 shows that 81% of the H-2K^b molecules were recovered in K42. H-2D^b stability at 0min and 60min shows no difference between HAΔEB and HAKDEL. The results obtained for HAΔEB are unexpected because they do not correlate with the pulse chase experiments in the presence and absence of stabilising peptide published by Lewis et al. (Lewis et al., 1996) and Gao et al (Gao et al., 2002), who showed a correlation between fast trafficking and poorly loaded HCβ₂m. This experiment will require further optimisation raise its sensitivity to potential MHC class I loading defects.

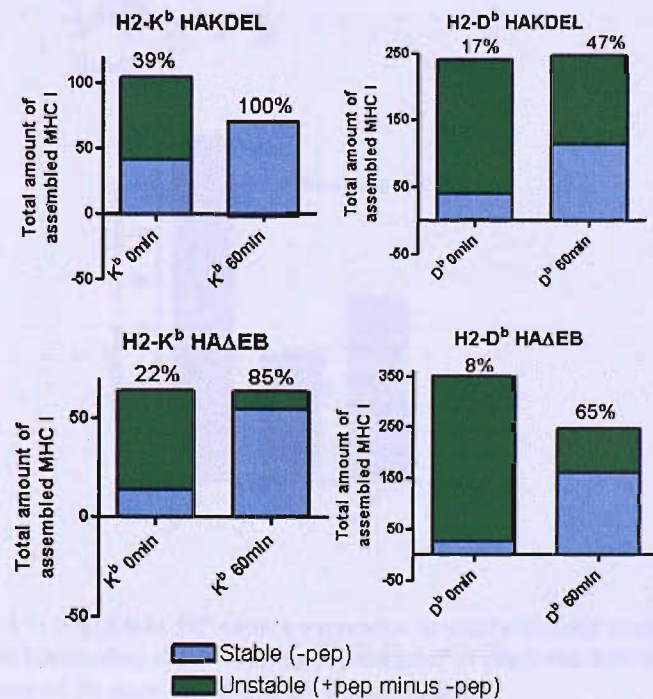


Figure 5.6: Quantitation of the pulse chase thermostability experiments for H-2K^b and H-2D^b on HAΔEB. Figures above each column represent the % stable MHC I molecules (calculated from MHC I recovered from IP in absence of peptide). Endogenous peptide loading improves with time.

To determine the effects of HAΔEB on class I cell surface expression, H-2K^b was analysed by FACS. Cells were prepared in the same way as described in section 3.5. Figure 5.7 shows that transfection of K42 cells with HAKDEL, increases H-2K^b surface expression by a factor of 3. H-2K^b expression in HAΔEB is slightly higher than in K42, but the difference is not significant given that no statistical test was performed. This suggests that defects in ERp57-CRT binding impair MHC class I assembly and cell surface presentation.

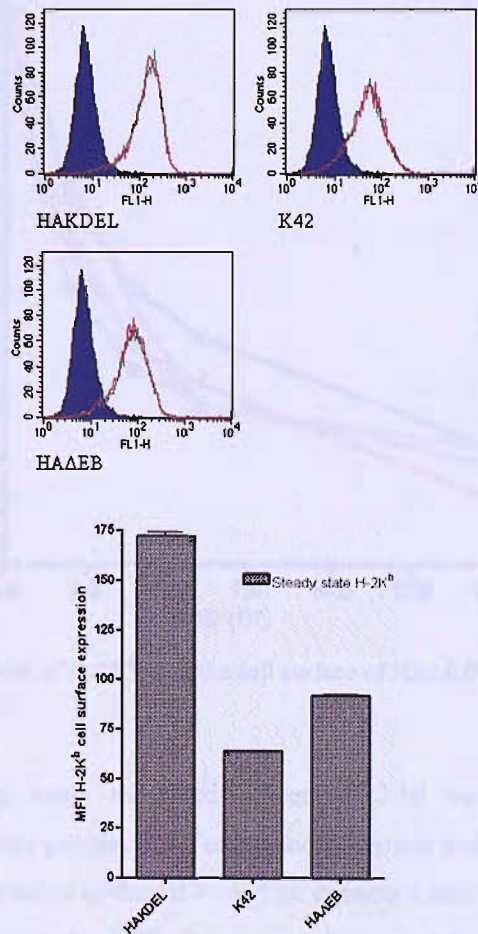


Figure 5.7: HAΔEB H-2K^b surface expression is poorly restored relative to HAKDEL according to FACS analysis performed in duplicate. Red and green are duplicates of the same cell line as are the error bars.

MHC class I trafficking and cell surface expression were not restored in HAΔEB. To determine if the class I molecules generated by HAΔEB were correctly folded and competent to bind peptide (described in section 3.7), BFA was used in a time course experiment to follow the decay of H-2K^b molecules from the cell surface (Figure 5.8). The results show that H-2K^b decay in HAΔEB is not significantly different from K41, K42 or HAKDEL, suggesting that K^b is still able to bind endogenous peptide at the cell surface with equal affinity to wild type CRT.

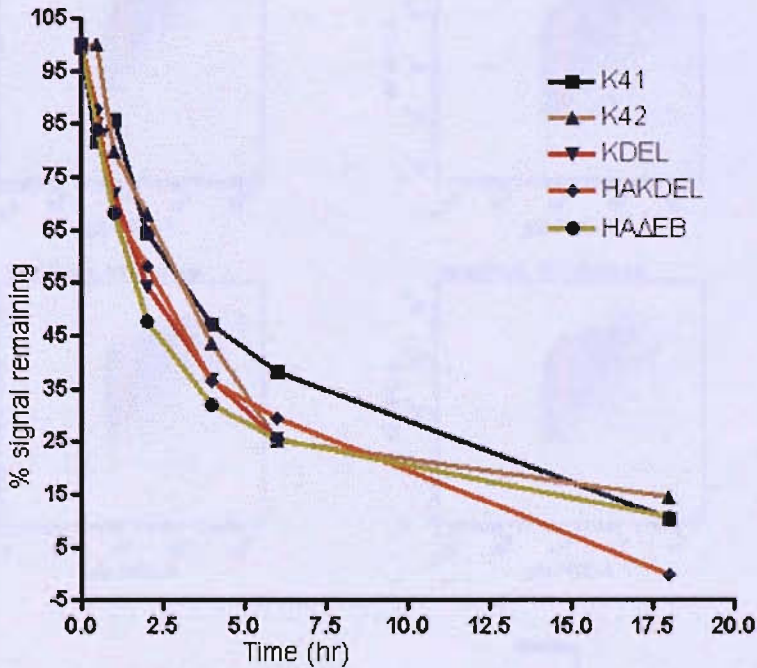


Figure 5.8: Percentage loss of H-2K^b from the cell surface of HAΔEB occurs at the same rate as K41 following BFA treatment

The intracellular loading assay described in section 3.10 was used to provide a more direct measurement of intracellular processing of endogenous peptide within HAΔEB as a function of antigen load. Following electroporation of the GFP-ub-SL8 construct into the target cells, four antigen “dose” gates were constructed using the GFP fluorescence (Figure 5.9 upper 4 panels). A D1 SL8-H2-K^b specific antibody was used to detect the SL8 presented on the cell surface. The mean D1 fluorescence was calibrated and plotted against the GFP dose. Figure 5.9 (lower 2 panels) shows that HAΔEB does not restore loading with respect to HAKDEL. This result is clearest with an intermediate SL8 load but the difference is still evident at high SL8 loads (Figure 5.9 lower right panel). HAΔEB presents slightly more SL8 than K42, suggesting that it can partially restore antigen processing and presentation. The difference between HAΔEB and HAKDEL decreases with lower SL8 loads, suggesting that the SL8 dose is too limited and beneath the sensitivity of the assay to reveal any intracellular loading

deficiencies. When the antigen is close to saturation, K41 is the most efficient cell line at presenting SL8 and K42 is the least. HAKDEL presents SL8 less efficiently than K41. HAΔEB is unable to restore comparable levels of SL8 presentation relative to HAKDEL, suggesting that the interaction between CRT and ERp57 is important for MHC class I assembly.

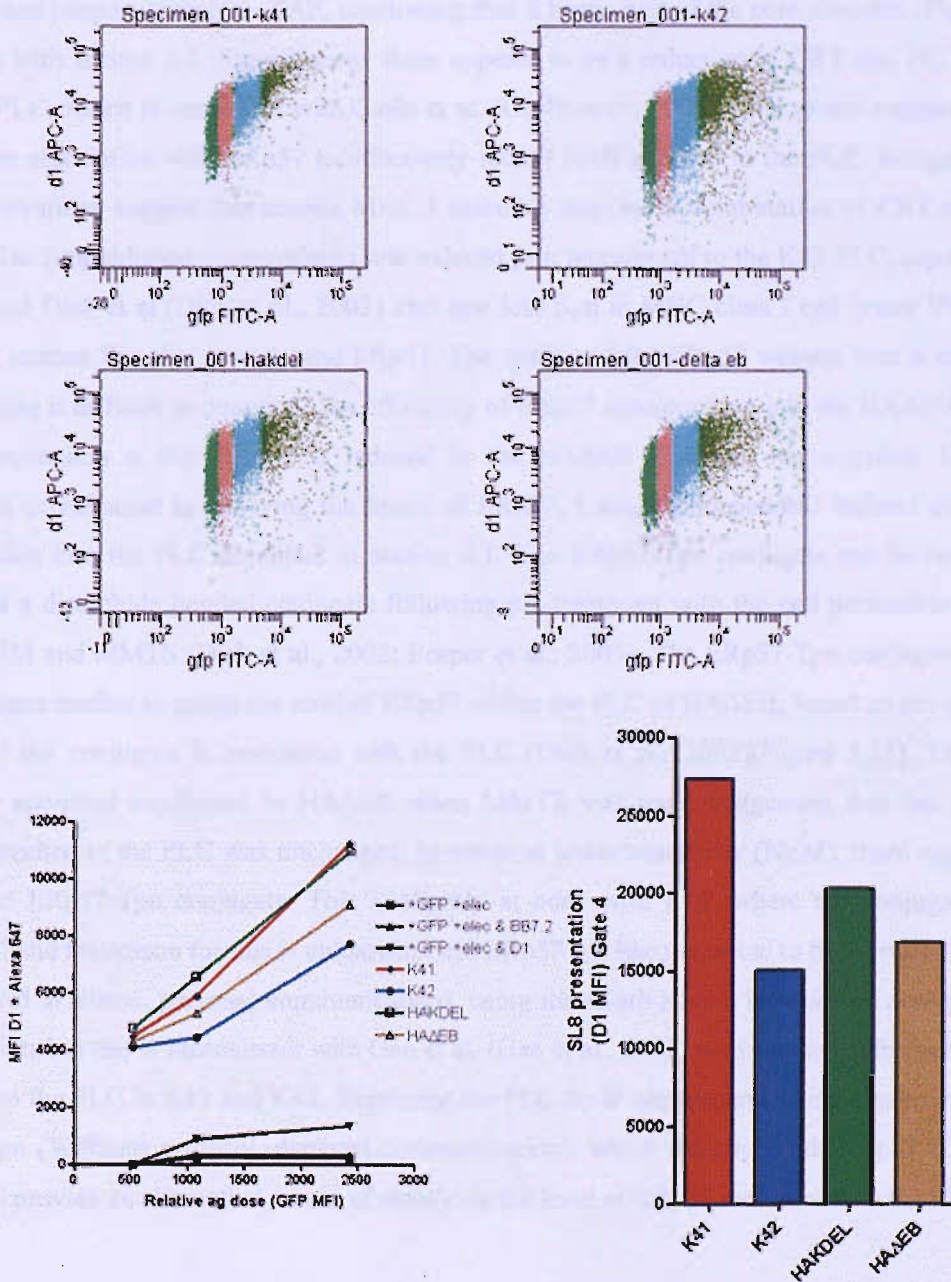


Figure 5.9: Intracellular loading assay FACS plot of H-2Kb-SL8 versus SL8 dose (upper 4 panels). Partial restoration of intracellular antigen processing in HAΔEB at low-medium (lower left panel) and high (lower right panel) SL8 doses.

5.3 PLC recruitment is impaired in ERp57-binding defective CRT cell lines

To determine whether HAΔEB was efficiently recruited into the PLC assembly, a co-IP was performed and examined through immunoblotting using the same protocol described in section 4.1 and chapter 2. The western blot shows that TAP is uniformly immunoprecipitated in HAKDEL and HAΔEB. Tpn is also recruited proportionately to TAP, confirming that it forms part of the core complex (Figure 5.11), consistent with section 4.1. Significantly, there appears to be a reduction in CRT and HC within the HAΔEB PLC, which is consistent with Garbi et al. (Garbi et al., 2006). This would suggest that CRT requires an association with ERp57 to effectively recruit itself and HC to the PLC. Intriguingly, two other observations suggest that correct MHC I assembly requires a combination of CRT and ERp57 activity. Gao (unpublished observations) saw reduced β_2m recruitment to the K42 PLC, consistent with less HC and Dick et al (Dick et al., 2002) also saw less β_2m in MHC class I cell lysate IPs of C95A tapasin; a mutant Tpn that cannot bind ERp57. The quality of the ERp57 western blot is consistently poor, making it difficult to quantitate the efficiency of ERp57 incorporation into the HAΔEB PLC. The overall impression is that ERp57 is reduced in the HAΔEB PLC but not negative. Due to the difficulties experienced in resolving the levels of ERp57, I sought independent indirect evidence for incorporation into the PLC described in section 4.1. The ERp57-Tpn conjugate can be resolved and trapped as a disulphide bonded conjugate following pre-treatment with the cell permeable alkylating agents NEM and MMTS (Dick et al., 2002; Peaper et al., 2005). The ERp57-Tpn conjugate was used as a surrogate marker to gauge the level of ERp57 within the PLC of HAΔEB, based on the assumption that all of the conjugate is associated with the PLC (Dick et al., 2002)(Figure 5.12). The level of conjugate appeared unaffected in HAΔEB when MMTS was used, suggesting that the amount of ERp57 recruited to the PLC was unchanged, however at lower sensitivity (NEM), there appears to be less of the ERp57-Tpn conjugate. This is slightly at odds with K42, where the conjugate appears unaffected and the reason for this is unknown. Less ERp57 has been reported to be recruited to the K42 PLC (David Williams, personal communication), using the relative band intensity of non-quantitative western blots but this is inconsistent with Gao et al. (Gao et al., 2002) who saw no difference in ERp57 recruited to the PLC in K41 and K42. Repeating the PLC co-IP experiments using a primary antibody against Tpn (Williams protocol, personal communication), which directly binds ERp57 (Dick et al., 2002) will provide an alternative means of clarifying the level of ERp57 recruitment to the PLC.

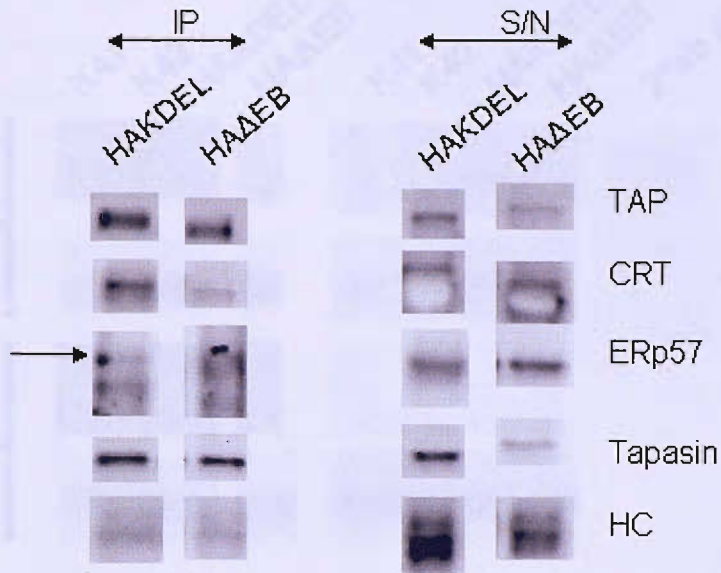


Figure 5.10: anti-Tap1 antibody co-IP of the HAΔEB PLC. Cells were lysed in 1% digitonin containing the co-IP antibody and samples were analysed by immunoblot of each member of the PLC. Tpn band intensity is proportionate to TAP, indicating that it is part of the “core” complex. HC and CRT recruitment to the PLC is impaired in HAΔEB. Results for ERp57 are poor, but suggest that it is present.

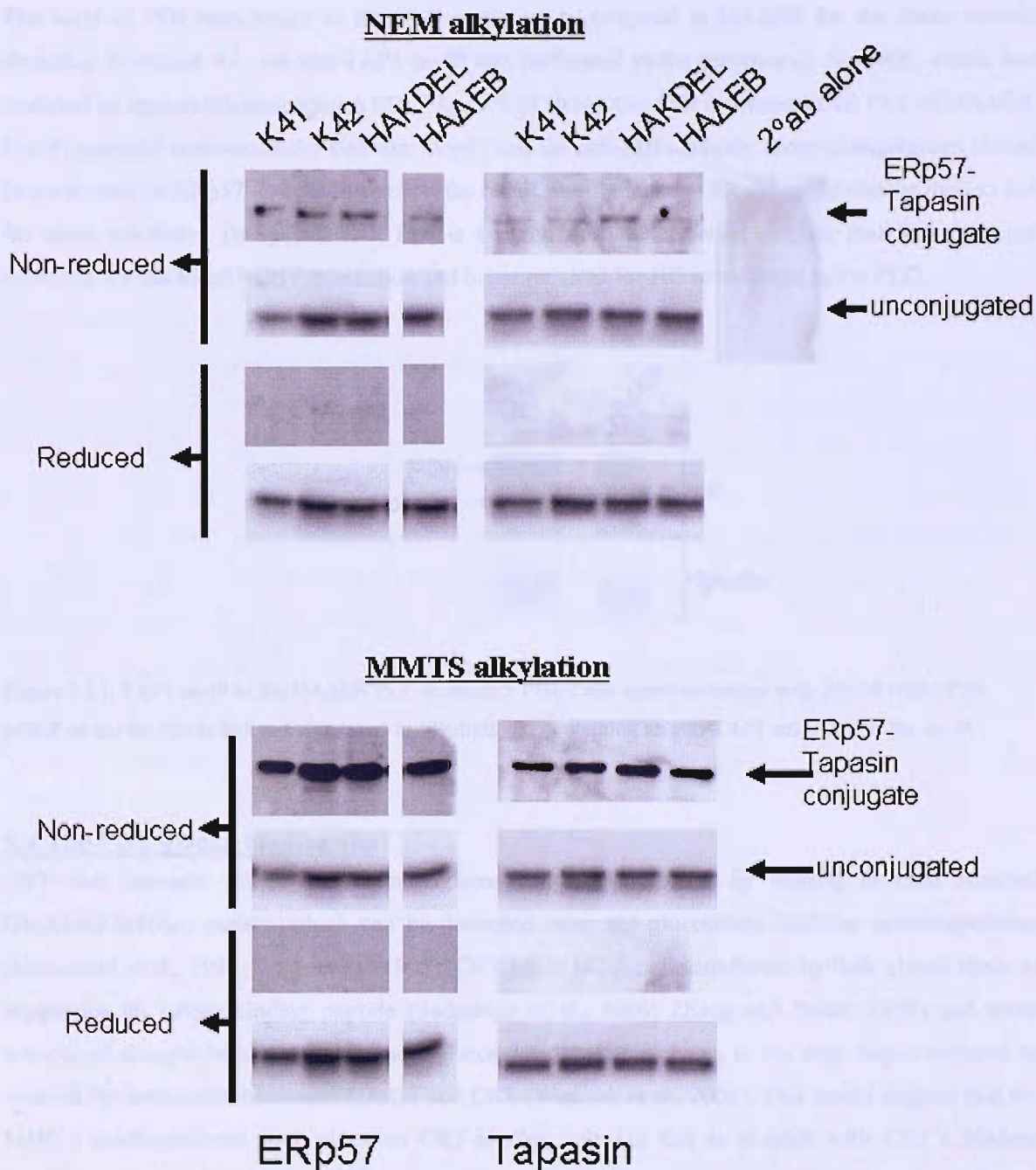


Figure 5.11: Trapping of the ERp57-Tpn conjugate from HAΔEB cell lysates. This acted as a surrogate marker for ERp57 within the PLC using the alkylating agents NEM and MMTS. MMTS appears to trap the ERp57-Tpn conjugate more efficiently than NEM. The results suggest little difference in the amount of conjugate in HAΔEB compared to the controls. This indirectly suggests that levels of ERp57 in the PLC are similar to wild type.

The level of PDI recruitment to the PLC was also investigated in HAΔEB for the same reasons described in section 4.1. An anti-TAP1 co-IP was performed in the presence of digitonin, which was analysed by immunoblotting against PDI. Figure 5.13 shows that PDI is present in the PLC of HAΔEB. Due to potential cross-reactivity between ERp57 and the anti-PDI antibody, a repeat experiment should be performed on ERp57 ^{-/-} cells to confirm the result. Purified mouse ERp57 could also be used to test for cross reactivity. To speculate, if PDI is present, the results would suggest that PDI does not substitute for the ERp57-CRT interaction and is not required for HC recruitment to the PLC.

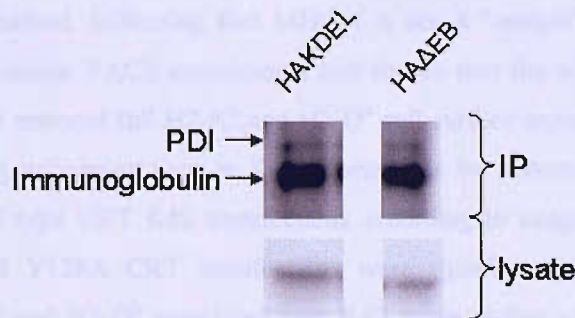


Figure 5.12: TAP1 co-IP of the HAΔEB PLC to identify PDI. Cells were pre-treated with 20mM NEM PBS pH6.8 on ice for 20min before being lysed in 1% digitonin containing an anti-TAP1 antibody for the co-IP.

5.4 The CRT glycan binding site

CRT also interacts with N-linked monoglucosylated glycoproteins by binding to their attached Glc₁Man₉GlcNAc₂ moiety, which can be disrupted using the glucosidase inhibitor castanospermine (Hammond et al., 1994; Wada et al., 1995). CRT binds HC-β₂m heterodimers by their glycan chain at asparagine 86 before binding peptide (Sadasivan et al., 1996; Zhang and Salter, 1998) and some schools of thought believe that the monoglucosylated MHC I glycan is the only factor required to mediate the interaction between HLA-B8 and CRT (Wearsch et al., 2004). This would suggest that the MHC I conformational state plays no CRT-binding role but this is at odds with CRT's binding specificity for HC-β₂m in the MHC I processing pathway (Sadasivan et al., 1996; Zhang and Salter, 1998), which suggests that protein conformation may also be important for CRT to recognize its substrate. It is possible that CRT could indirectly recognize polypeptide conformation via UGGT in the CNX/CRT folding cycle but protein-protein interactions between CRT, CNX and their substrates have been reported (Ihara et al., 1999; Saito et al., 1999). Glycan-independent CRT binding was investigated using two glycan-binding-defective CRT point mutants. These were used in preference to castanospermine, because it is non-specific and would also impair CNX function.

The CRT glycan binding site was mapped by the Williams group in Toronto and Kapoor et al (Kapoor et al., 2004). They mutated different residues within the CRT glycan-binding region to create mutants that failed to show sugar-mediated binding to monoglucosylated residues. Two K42 cell lines transfected with CRT containing a mutation of either D to A at position 317 or Y to A at position 128 were generated by this lab. They saw similar expression of the mutants in K42 relative to wild type CRT in K41 by western blot. A CRT IP of radiolabeled lysates showed that the D317A and Y128A CRT transfectants associate with fewer substrates than wild type CRT. However, many mutant CRT-substrate interactions remained, indicating that MHC I is not a "unique" substrate for the glycan-binding-deficient CRT mutants. FACS experiments had shown that the wild type CRT, D317A and Y128A CRT transfectants restored full H2-K^b and H2-D^b cell surface expression in K42 compared to K41. The peptide loading deficiency seen in K42 appeared to be restored relative to K41 for both D317A, Y128A and wild type CRT K42 transfectants according to exogenous peptide stabilization experiments. D317A and Y128A CRT transfectants were equally capable of slowing the rapid trafficking rate for H2-K^b and H2-D^b associated with K42 down to that of K41. D317A and Y128A CRT was also present in the PLC at a similar abundance to K41 according to CRT western blots of anti-tapasin IPs. The overall PLC composition appeared similar when isolated from wild type versus glycan-binding-deficient CRT transfectants according to western blots against TAP, Tpn, ERp57, HC, β_2m and CRT (Ireland, Brockmeier, Howe, Elliott, Williams submitted).

I measured the processing and presentation capacity of these mutants using the GFP-ub-SL8 to investigate the intracellular loading efficiency of D317A and Y128A CRT (Figure 5.13 upper and lower panels). The poor intracellular loading associated with K42 was restored to K41 in wild type, Y128A CRT and D317A CRT transfectants. The results are consistent with CRT being able to recruit HC independently of its monoglucosylated glycan.

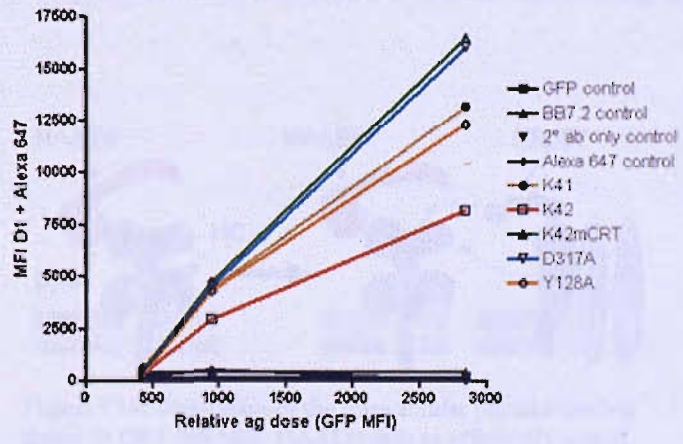
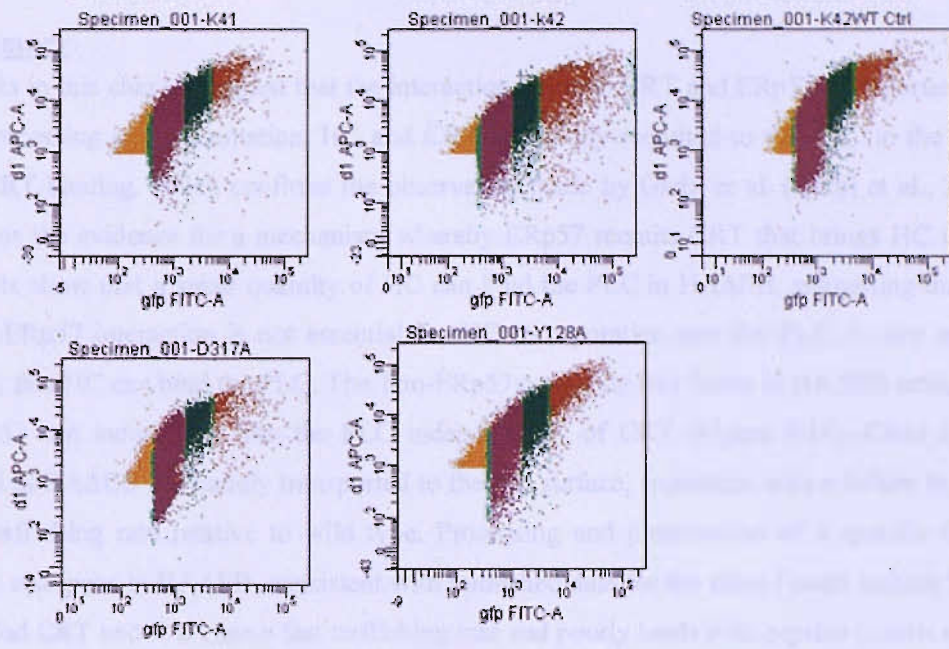


Figure 5.13: Intracellular loading efficiency of the glycan-binding defective CRT mutants using the GFP-ub-SL8 assay. Lower panel: Quantitation of SL8-H2-Kb cell surface expression (MFI D1 + Alexa 647) versus the relative SL8 dose (as measured by GFP fluorescence). Intracellular loading is unaffected in glycan-binding-defective CRT transfectants.

5.5 Summary

The results in this chapter suggest that the interaction between CRT and ERp57 is important for MHC class I processing and presentation. HC and CRT are poorly recruited to the PLC in the absence of ERp57-CRT binding, which confirms the observation made by Garbi et al. (Garbi et al., 2006). This strengthens the evidence for a mechanism whereby ERp57 recruits CRT that brings HC to the PLC. The results show that a small quantity of HC can bind the PLC in HAΔEB, suggesting that although the CRT-ERp57 interaction is not essential for HC incorporation into the PLC, it may enhance the efficiency that HC can bind the PLC. The Tpn-ERp57 conjugate still forms in HAΔEB cells, indicating that ERp57 can incorporate into the PLC independently of CRT (Figure 5.14). Class I molecules expressed in HAΔEB are rapidly transported to the cell surface, consistent with a failure to restore the correct trafficking rate relative to wild type. Processing and presentation of a specific endogenous antigen is also poor in HAΔEB, consistent with published data for the class I point mutant T134K that fails to bind CRT and TAP, has a fast trafficking rate and poorly loads with peptide (Lewis et al., 1996; Lewis et al., 1998). The HAΔEB confirms that the PLC is a rate determining step in class I peptide-loading.

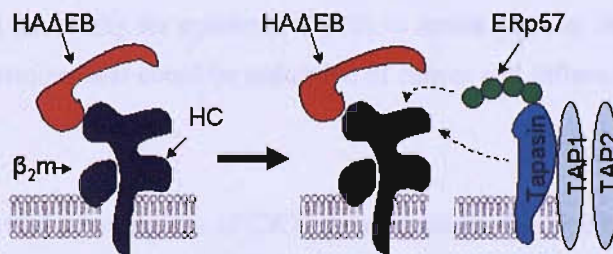


Figure 5.14: Illustration of the intracellular peptide-loading defect in CRT HAΔEB. HAΔEB fails to efficiently recruit MHC I to the PLC.

Results of two CRT glycan-binding defective point mutants and their effects on MHC I processing and presentation have also been presented in this chapter. CRT appears to be capable of recruiting HC to the PLC independently of its monoglucosylated glycan, suggesting that this is polypeptide mediated. Endogenous peptide processing and presentation in K42 cells transfected with glycan-binding defective CRT appears to be restored relative to wild type, suggesting that oligosaccharide binding by CRT is not essential for efficient class I assembly.

Chapter 6: Discussion

MHC I HC is synthesized by the ribosome and co-translationally inserted into the ER where it binds a coordinated series of chaperones to assist correct protein folding. HC is post-translationally modified by folding and disulphide bond rearrangement, where it acquires a conformation that can bind β_2m . Following HC assembly with β_2m , peptide binding places the MHC I molecules in a competent state to leave the ER (Lewis et al., 1996). CRT is a central chaperone in MHC I folding and although CRT may not participate in selecting optimal peptides for class I molecules (Howarth et al., 2004), this study has isolated specific regions of CRT that are required to ensure that antigen is presented efficiently on the cell surface. CRT needs to bind ERp57 to recruit MHC class I molecules into the PLC, however the KDEL sequence is essential for optimal peptide loading. Optimisation therefore appears to require two components; catalysed peptide exchange mediated by Tpn in the PLC and KDEL-mediated retention / retrieval of class I molecules to the ER that have failed to acquire their optimum peptide. Failure to correctly assemble class I molecules in the PLC may influence the peptide repertoire reaching the cell surface. In the absence of a retention / retrieval mechanism, an increased number of peptide-receptive class I molecules may be expected to be released into the secretory pathway. This would have the consequence of limiting the ability for cytotoxic T-cells to detect peptides derived from viral proteins or alternate peptide repertoires that could be indicative of cancer and influence the size of the immune response.

This study has characterised three regions of CRT: the c-terminus, the binding site with the disulphide oxidoreductase ERp57 and its glycan binding site and assessed their effects on MHC I processing and presentation. The results support a model whereby CRT's c-terminus, KDEL sequence and ERp57 binding site, but not CRT's glycan-binding site, are obligatory for efficient MHC I antigen presentation. Efficient MHC I assembly with the PLC is also shown to require an interaction between CRT and ERp57 (summarised in Figure 6.1).

To investigate KDEL-mediated ER retention / retrieval of MHC I molecules, a truncated CRT mutant missing the KDEL sequence was generated and transfected into the CRT-deficient cell line K42. This cell line (HA Δ KDEL) loaded MHC class I molecules inefficiently with intracellular antigen but importantly, HA Δ KDEL restored the trafficking speed of the MHC I allele H-2D^b to the cell surface with respect to the control cell line HAKDEL. These two observations appear to uncouple the class I trafficking rate as a surrogate marker for the quality of peptide loading, breaking the current notion

originally suggested by Lewis et al. (Lewis et al., 1996). MHC I molecules also became incorporated into the PLC, suggesting that efficient MHC class I assembly can be uncoupled from formation of the PLC. Indeed, MHC I molecules leave the ER in COPII vesicles faster in K42 compared to K42 transfected with CRT, suggesting that CRT retains MHC I molecules in the ER. It is currently unclear whether CRT promotes further rounds of MHC I assembly with the PLC or alternatively slows the rate of MHC I association with ER exit sites. CRT is also present in COPII vesicles and has been shown in this and other studies to co-localise with the cis-Golgi (Neeli et al., 2007), indicating that CRT is not uniquely resident in the ER. Further investigation will be required to determine whether MHC I molecules recycle to the ER as CRT cargo, but it is possible that CRT may perform a role in both MHC I retention and retrieval to the ER.

To characterise whether the interaction between CRT and the disulphide isomerase ERp57 plays a role in efficient MHC I assembly, a CRT P-domain mutant was constructed to disrupt the CRT-ERp57 interaction (HAΔEB). Efficient MHC I antigen presentation was shown to require an interaction between CRT and ERp57. The ERp57-binding mutant did not restore the trafficking rate of MHC I from the ER with respect to wild type, suggesting the trafficking rate is influenced by the interaction between CRT and ERp57. Furthermore, MHC I assembled inefficiently with the PLC in HAΔEB, consistent with the phenotypes published in the ERp57 *-/-* and CRT *-/-* cell lines (Gao et al., 2002; Garbi et al., 2006)(Williams, personal communication). These findings suggest that CRT and ERp57 function cooperatively in MHC I antigen presentation.

To investigate the importance of CRT's glycan binding site on MHC I assembly, a glycan-binding defective CRT mutant construct was transfected into K42 and characterised. MHC I recruitment to the PLC and peptide-binding was completely restored relative to K41, suggesting that polypeptide-polypeptide interactions make a significant contribution to CRT function in MHC I assembly. This appears to be inconsistent with another group who reported on an *in vitro* study where the glycan was found to be essential for CRT function and that CRT substrate specificity was independent of protein conformation (Wearsch et al., 2004). The multi-protein interactions with CRT to form the PLC in the *in vivo* system used in this study may account for the differences with the Wearsch study. Protein conformation and polypeptide residues appear to be important for CRT-substrate binding, which might account for CRTs binding specificity for HCβ_{2m} (Sadasivan et al., 1996; Zhang and Salter, 1998) and ability to interact with non-glycosylated proteins (Saito et al., 1999). There are suggestions that polypeptide-polypeptide binding may reside within the CRT P-domain (Peterson and Helenius, 1999;

Vassilakos et al., 1998). To date, the specific polypeptide-binding region within the P-domain has not been isolated or characterised.

A further interesting finding of this study showed that the c-terminal truncation of 11 amino acids (HA Δ 11) failed to restore the MHC I trafficking rate from the ER compared to the control HAKDEL and HA Δ KDEL which did. Since formation of the PLC was apparently unaffected in HA Δ 11, it is possible that the as yet unknown sequence in HA Δ 11 participates in MHC I retention / retrieval to the ER.

Construct	Nature of CRT mutation	PLC Assembly	MHC I Trafficking rate from ER	GFP-ub-SL8 MHC I antigen presentation
K41	Wild type (WT)	Good	Slow	Good
K42	CRT -/-	Less HC	Fast	Poor
HAKDEL	K42 transfected with WT rat CRT	Good	Slow	Good
HAΔKDEL	loss of KDEL	Good	Slow	Poor
HAΔ11	loss of 11 c-terminal amino acids	Good	Fast	Poor
HAΔEB	ERp57-binding mutant	Less CRT and HC	Fast	Poor

Figure 6.1: Construct summary; effects on MHC I antigen processing and presentation. Details listed in green are comparable to wild type; red show deficiencies in MHC I assembly.

K42 transfected with rat CRT restored MHC class I assembly relative to K42 (albeit partially), however autologous murine CRT was required to fully restore wild type MHC I assembly. Comparison between the results obtained from the other CRT mutants used in this study and CRT sequence analysis across several species defined a 3-mer candidate amino acid sequence within the c-terminal 11 amino acids that was unique to each species. This suggests the three amino acid differences influence MHC I assembly and also appear to play a role in MHC I ER retention / retrieval (see section 3.11).

The published results and those presented here indicate that CRT is not obligatory for MHC class I to assemble with the PLC but binding is clearly reduced when either CRT (Gao et al., 2002) or ERp57 (Garbi et al., 2006) are absent. This study has also shown that MHC I cannot assemble efficiently with the PLC when CRT is prevented from binding ERp57. This implies that an exclusive interaction between CRT and Erp57 may be obligatory for MHC class I molecules to efficiently assemble with

Tpn and TAP to form the PLC. A novel finding of the current study indicates that increased detection of the ERp57-HC conjugate occurs in the absence of CRT and does not need to be artificially trapped as described in other studies (Kienast et al., 2007; Santos et al., 2007; Wearsch and Cresswell, 2007). It is not clear from these results if the increased detection of ERp57-HC in the absence of CRT resulted from a prolonged interaction between ERp57 and HC or whether the ERp57-HC conjugate was transient but simply more abundant. It is possible that if the interaction between ERp57 and HC is transient in nature, CRT may assist ERp57 and MHC I assembly with the PLC, since CRT can bind ERp57 (Oliver et al., 1999) independently of MHC I (Harris et al., 1998).

The PLC is thought to facilitate class I peptide optimization by exchanging low affinity, fast off-rate peptides for ones with a high affinity and slower off-rate and Tpn is thought to be the key protein responsible for this process (Howarth et al., 2004; Williams et al., 2002). Recently, the exclusive role for Tpn in peptide optimization has been questioned in light of evidence to suggest that this role is performed by a Tpn-ERp57 conjugate (Wearsch and Cresswell, 2007), although another recent study demonstrated that the peptide editing function was performed by Tpn alone (Chen and Bouvier, 2007). Chen and Bouvier showed that Tpn only functions when conjugated to MHC I via a leucine zipper domain *in vitro*, so it may be that ERp57 bridges Tpn and HC. The Tpn-ERp57 conjugate is clearly important for MHC class I expression in light of evidence from a Tpn mutant engineered to have an alanine at residue 95 instead of a cysteine, which cannot bind ERp57 (Dick et al., 2002). Instead of optimization, ERp57 may therefore assist in class I assembly by recruiting class I to the PLC (Garbi et al., 2006)(present study), thereby bringing class I into closer proximity to Tpn for peptide optimization.

MHC class I mutants such as T134K share a similar phenotype to class I molecules expressed in CRT deficient cells because the class I mutants bypass association with the PLC including CRT and TAP (Lewis and Elliott, 1998). Both systems have impaired antigen presentation, consistent with an inability to properly optimise the peptide. Within this study, H2-K^b and -D^b expressed in the c-terminal truncated CRT transfectant cell lines have retained the ability to bind the PLC, however the reduction in class I HC able to bind the PLC in K42 and HAΔEB suggests that CRT and ERp57 cooperate to stabilize the interaction between class I, TAP and Tpn. It is possible that the lower quantity of HC isolated from the anti-TAP1 PLC co-immunoprecipitation for K42 and HAΔEB represents a lower rate of HC translation, but this seems unlikely, since these results are consistent with Garbi et al (Garbi et al., 2006), experiments performed by David Williams (personal communication) and castanospermine (a glucosidase inhibitor that prevents the generation of mono-glucosylated glycans, the substrate for

CRT) treatment (Lewis and Elliott, 1998; Sadasivan et al., 1996), which impairs class I interaction with TAP.

What seem clear from the results presented for the c-terminal truncated CRT mutants is that peptide loading can be inefficient despite HC assembly with the PLC. This suggests that inefficient MHC I antigen presentation in HA Δ KDEL may either be due to an impaired function in the PLC or the absence of an off-PLC quality control (QC) step. This could be in MHC I retention in the ER or retrieval from the cis-Golgi, consistent with the proposed function of the CRT c-terminus.

It is also possible that other proteins may possess a role in MHC I antigen assembly off the PLC. For example, the BAP31 cargo protein that contains a c-terminal KKXX ER-retrieval motif and may also contribute to class I QC, since it has been linked with raising class I cell surface expression in a dose-dependent manner (Ladasky et al., 2006). Tpn also possesses a KKXX motif which may implicate it in a possible role in MHC I antigen presentation off the PLC.

It is possible that MHC I folding could undertake the following model (Figure 6.2). Following HC assembly with β_2m , the HC β_2m dimer remains bound to ERp57. The interaction between HC β_2m and ERp57 is transient and may readily dissociate, favouring association with CRT to stabilize the HC β_2m -ERp57 conjugate. Most HC β_2m molecules are then assembled with the core PLC complex comprising Tpn and TAP for peptide optimization. Once class I molecules are bound to the PLC, Tpn is thought to function by stabilizing class I molecules in a peptide-receptive conformation (Elliott, 1997) by rotating the class I α_2 -1 helix outward (Zacharias and Springer, 2004), which weakens the binding affinity of peptide in the groove and shift a pre-existing equilibrium between an “open” and “closed” groove form; the open form being one that is peptide receptive and the closed is “stably” bound (Williams et al., 2002). ERp57 and PDI may facilitate class I peptide-loading by altering the redox state of the peptide-binding groove. It is thought that Tpn-independent MHC I alleles are unable rotate the α_2 -1 helix to as large an open conformation as Tpn-dependent alleles (Zacharias and Springer, 2004), giving independent MHC I alleles a more rigid structure, which offers more stability and consequently, the continued ability to transition between “open” and “closed” states to bind peptide. Once bound to low off-rate peptides, MHC I molecules are released from the ER. CRT may act like a folding sensor to recognize the flexibility of MHC I molecules, which would be predicted to increase with higher off-rate peptides and retain them in the ER. Alternatively, UGGT which has been described as a folding sensor by recognizing exposed protein moieties of glycosylated proteins (Gahmberg and Tolvanen, 1996), may be responsible for class I-peptide quality control, and re-glycosylate class I molecules so that they become substrate for CRT to bind and return to the PLC.

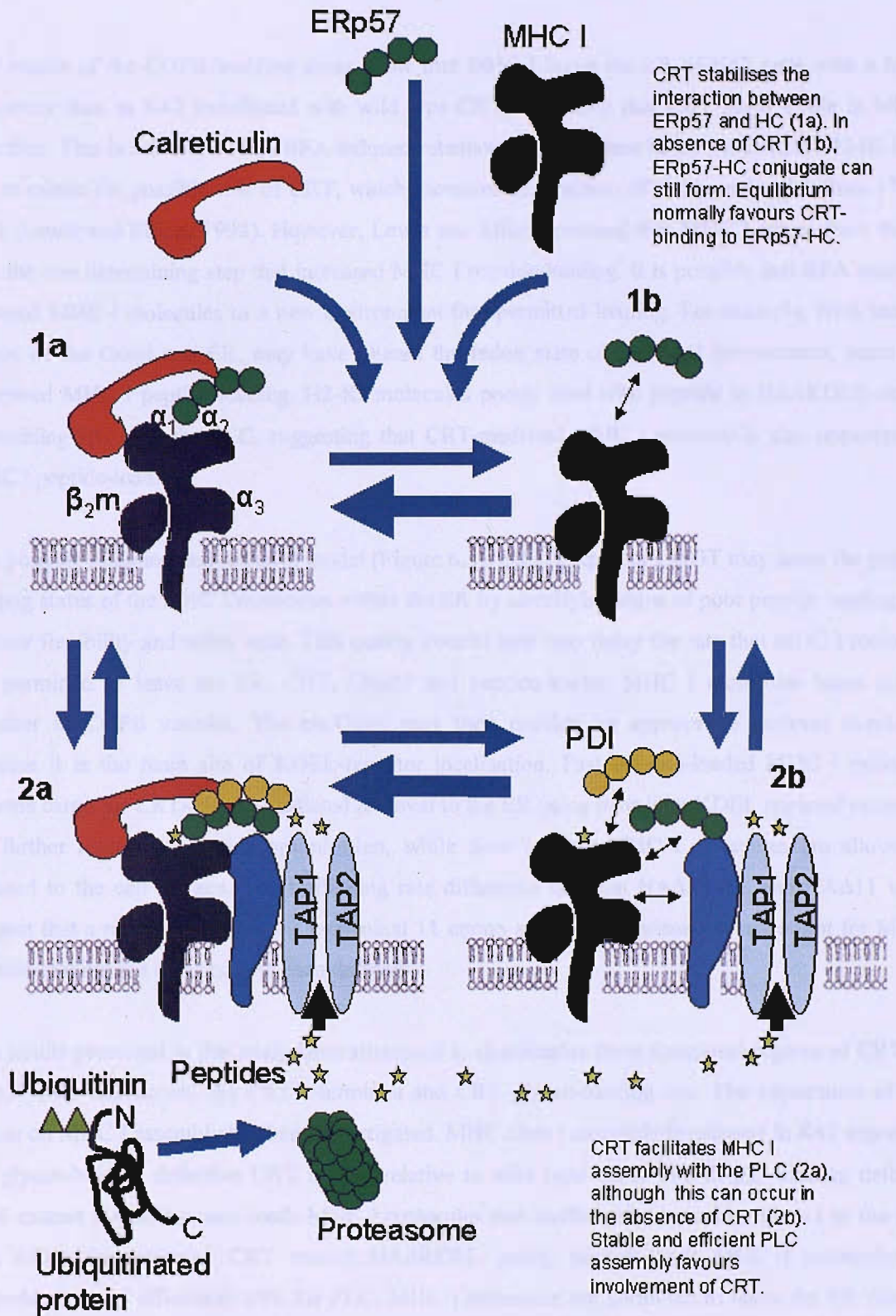


Figure 6.2: Peptide binding complex assembly model.

The results of the COPII budding assay show that MHC I leave the ER of K42 cells with a higher efficiency than in K42 transfected with wild type CRT, indicating that CRT plays a role in MHC I retention. This is consistent with BFA-induced retention of the mutant MHC I molecule T134K in the ER to mimic the possible role of CRT, which increases the fraction of stable molecules from 17% to 67% (Lewis and Elliott, 1998). However, Lewis and Elliott assumed that MHC I egress from the ER was the rate determining step that increased MHC I peptide-loading. It is possible that BFA treatment exposed MHC I molecules to a new environment that permitted loading. For example, BFA-induced fusion of the Golgi and ER, may have altered the redox state of the local environment, permitting improved MHC I peptide-loading. H2-K^b molecules poorly load with peptide in HAΔKDEL despite assembling HC with the PLC, suggesting that CRT-mediated MHC I retrieval is also important for MHC I peptide-loading.

In a possible retention and retrieval model (Figure 6.3), CRT, ERp57 or UGGT may sense the peptide-loading status of the MHC I molecules within the ER by identifying signs of poor peptide loading such as their flexibility and redox state. This quality control step may delay the rate that MHC I molecules are permitted to leave the ER. CRT, ERp57 and peptide-loaded MHC I molecules leave the ER together in COPII vesicles. The cis-Golgi may then provide an appropriate retrieval checkpoint because it is the main site of KDEL-receptor localisation. Fast off-rate-loaded MHC I molecules become cargo for CRT-ERp57-mediated retrieval to the ER using their joint KDEL retrieval sequences for further rounds of peptide optimisation, while slow off-rate MHC I molecules are allowed to proceed to the cell surface. The trafficking rate difference between HAΔKDEL and HAΔ11 would suggest that a residue(s) within the c-terminal 11 amino acids is also somehow important for MHC I peptide-loading but it has not yet been defined.

The results presented in this study have attempted to characterize three functional regions of CRT; the ERp57-CRT interaction, the CRT c-terminus and CRT glycan-binding site. The importance of each region on MHC I assembly has been investigated. MHC class I assembly is restored in K42 expressing the glycan-binding defective CRT mutant relative to wild type CRT. The ERp57-binding defective CRT mutant HAΔEB poorly loads MHC I molecules and inefficiently assembles class I to the PLC. The c-terminal truncated CRT mutant HAΔKDEL poorly peptide-loads MHC I molecules but assembles class I efficiently with the PLC. MHC I molecules are permitted to leave the ER faster in CRT deficient cells compared to CRT replete cells. These results indicate that the interaction between CRT and ERp57 as well as the CRT KDEL motif are essential for efficient MHC I assembly with antigen.

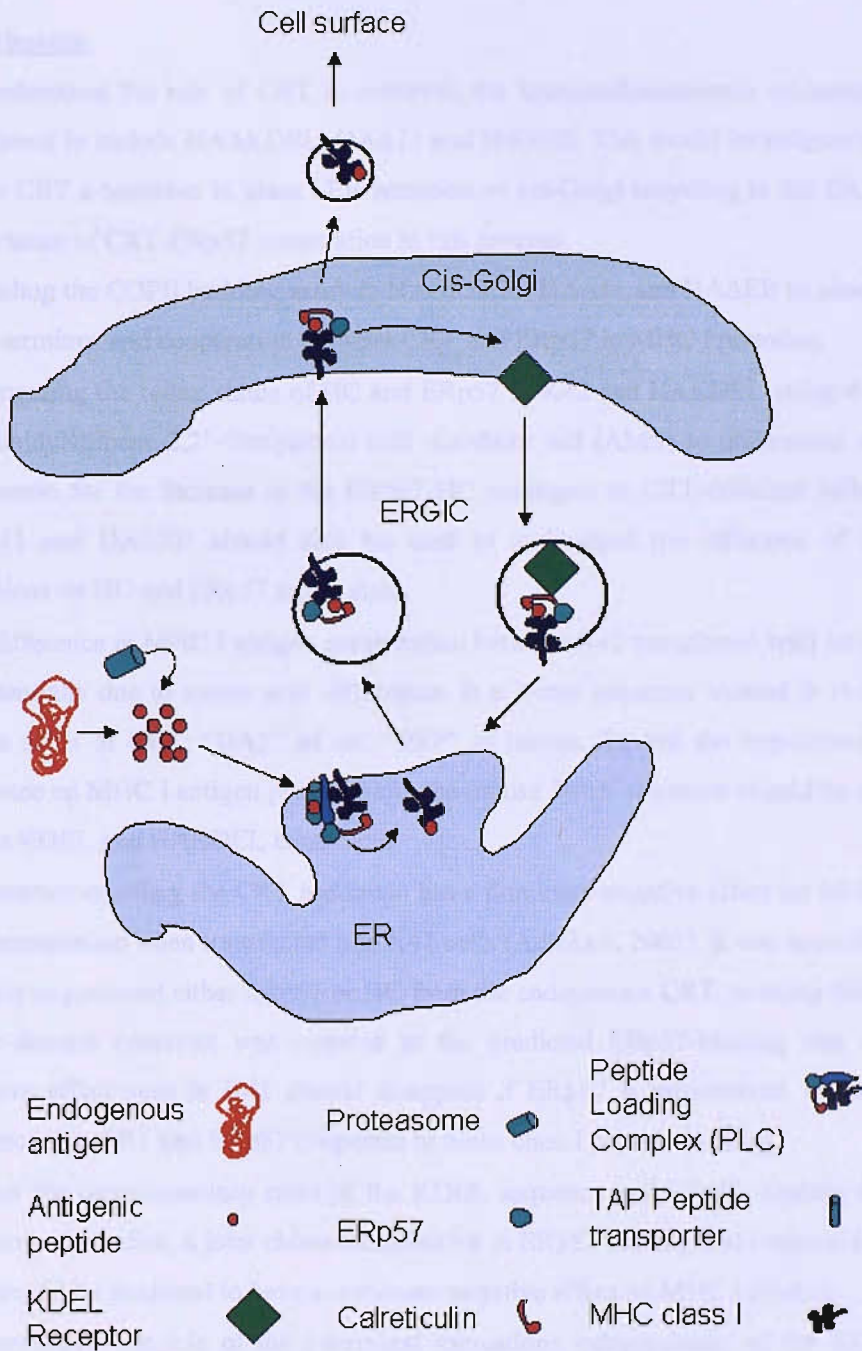
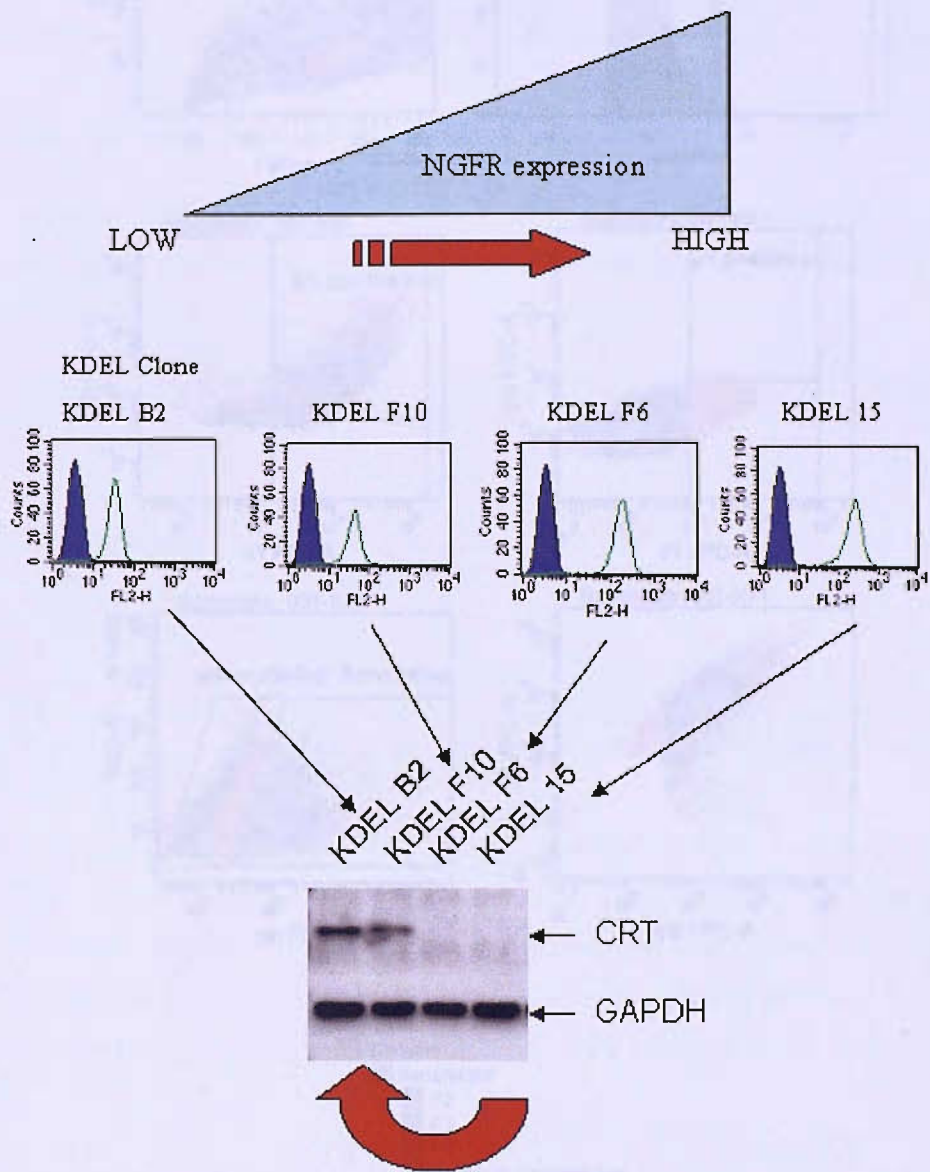


Figure 6.3: MHC I retention / retrieval model. CRT-ERp57 or UGGT cooperate to sense peptide loading status of MHC I molecules within the ER and remain bound to MHC I during transport to cis-Golgi. Fast off-rate peptide-loaded MHC I molecules retrieved by CRT-ERp57 for further rounds of peptide optimisation using the KDEL-receptor. Slow off-rate peptide-loaded MHC I are allowed to proceed to the cell surface.

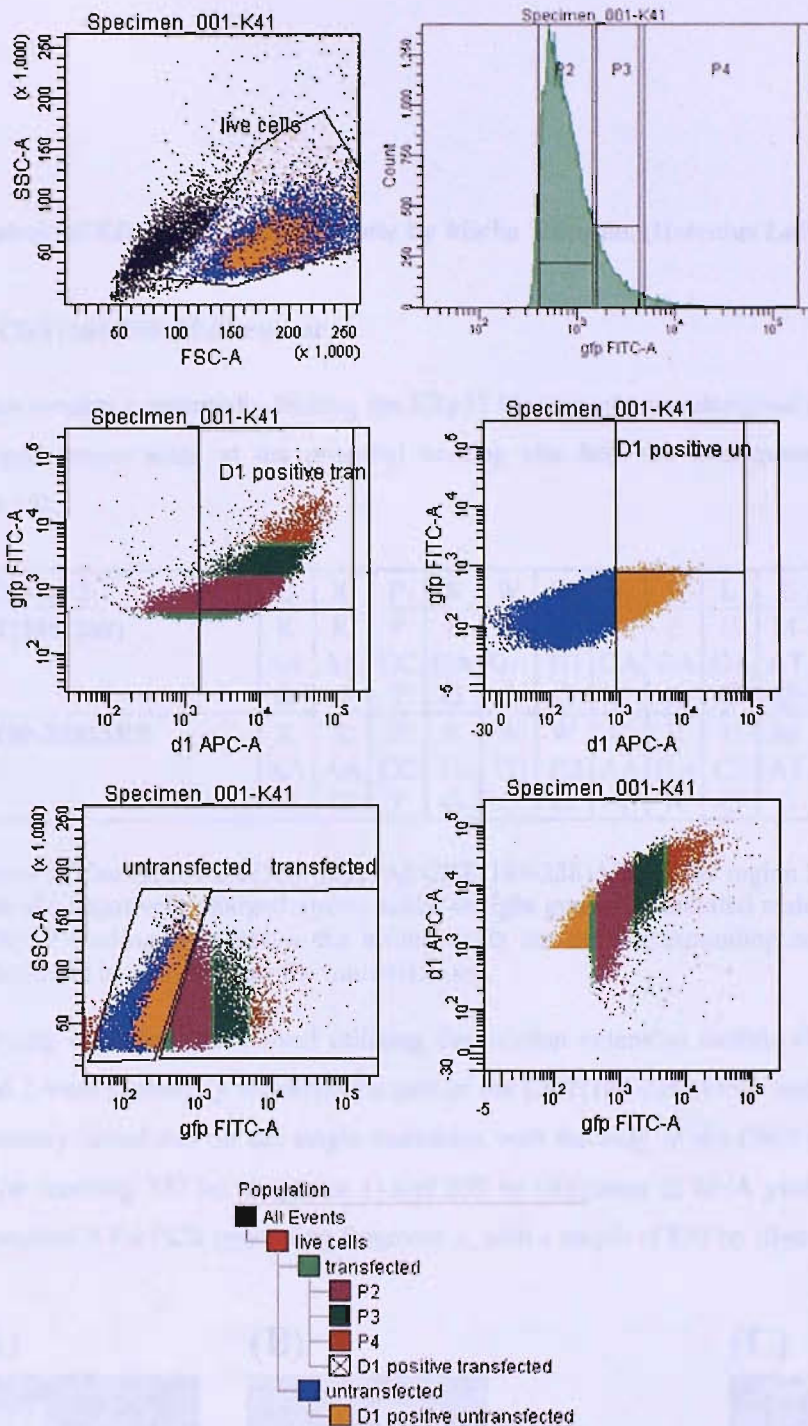
Future experiments.

- To understand the role of CRT in retrieval, the immunofluorescence microscopy should be broadened to include HAΔKDEL, HAΔ11 and HAΔEB. This would investigate the importance of the CRT c-terminus in class I ER retention or cis-Golgi recycling to the ER as well as the importance of CRT-ERp57 cooperation in this process.
- Extending the COPII budding assay to HAΔKDEL, HAΔ11 and HAΔEB to identify the role of the c-terminus and cooperation between CRT and ERp57 in MHC I retention.
- Investigating the redox status of HC and ERp57 in K42 and HAKDEL using 4-acetamido-4'-maleimidylstilbene-2,2'-disulphonic acid disodium salt (AMS) to understand whether this is the reason for the increase in the ERp57-HC conjugate in CRT-deficient cells. HAΔKDEL, HAΔ11 and HAΔEB should also be used to understand the influence of different CRT mutations on HC and ERp57 redox state.
- The difference in MHC I antigen presentation between K42 transfected with rat or mouse CRT is potentially due to amino acid differences in a 3-mer sequence located in the c-terminal 11 amino acids of CRT; "DAT" of rat; "ESP" in mouse. To test the importance of the 3-mer sequence on MHC I antigen presentation, the mouse 3-mer sequence should be substituted into the rat KDEL and HAKDEL constructs.
- A construct encoding the CRT p-domain has a dominant-negative effect on MHC I processing and presentation when transfected into K41 cells (Adhikari, 2002). It was speculated that the p-domain sequestered either ERp57 or HC from the endogenous CRT, creating this phenotype. If the p-domain construct was mutated at the predicted ERp57-binding site, the dominant-negative effect seen in K41 should disappear if ERp57 is sequestered, supporting existing evidence that CRT and ERp57 cooperate to assist class I peptide-loading.
- To test the complementary roles of the KDEL sequence and ERp57 binding site on MHC I antigen presentation, a joint chimaera defective in ERp57 binding and retrieval transfected into K41 would be predicted to have a dominant-negative effect on MHC I loading
- To investigate the role of the c-terminal truncations independently of the KDEL sequence, additional c-terminal CRT mutant constructs should include the KDEL motif.
- To use the in vitro assay system described by Wearsch et al (Wearsch and Cresswell, 2007) to characterize the function of each CRT mutant used in this study on PLC subcomplex assembly.
- To characterize the effect of the CRT mutants on the folding of other published CRT substrates other than MHC I. For example influenza haemagglutinin (Hebert et al., 1997) or Semliki forest virus proteins E1 or p62 (Molinari and Helenius, 1999).



Appendix 2

Results showing the inverse correlation between CRT and Δ NGFR expression. Consequently, CRT expression of each transfected K42 clone was screened by immunoblot.



Appendix 3

FACS plot set-up for the GFP-ub-SL8 intracellular loading assay. Step 1; Gate correct cell population according to forward and side scatter. Divide GFP histogram into three gates. Using a GFP versus APC dot plot, use the controls to insert an additional gate to distinguish the transfected from untransfected cells. “D1 positive untransfected” defines cells expressing low-GFP but are positively transfected.

Appendix 4

Mutational analysis of ERP57-CRT binding site by Micha Häuptle, (Helenius Laboratory, Zurich)

Cloning of the CRT(189-288) Δ EB mutant

A CRT P-domain construct potentially lacking the ERp57 binding site was designed by changing five negatively charged amino acids at the potential binding site into the corresponding residues of Cne1p32 (figure 35).

Cne1p32	Q	K	P	S	W	W	K	E	L	E	H	G	E	W
CRT(189-288)	K	K	P	E	D	W	D	E	E	M	D	G	E	W
	AA	AA	CC	GA	GA	TG	GA	GA	GA	AT	GA	GG	GA	TG
	G	G	T	G	C	G	C	A	G	G	T	A	G	G
CRT(189-288)ΔEB	K	K	P	S	W	W	K	E	L	M	H	G	E	W
	AA	AA	CC	TC	TG	TG	AA	GA	CT	AT	CA	GG	GA	TG
	G	G	T	G	G	G	A	A	G	G	T	A	G	G

Fig. 35: Alignment of Cne1p32, CRT(188-289) and CRT(189-288) Δ EB in the region 231-244 of CRT. Shown in red are the negatively charged amino acids, in light green the mutated residues to eliminate the potential ERp57 binding site. Below the amino acids are the corresponding nucleotide triplets labeled in dark blue and in turquoise for the mutated bases.

This cloning challenge was solved utilizing the overlap extension method (Ho et al., 1989). Fragments 1 and 2 were created by amplifying a part of the CRT(189-288) DNA template with PCR, which simultaneously introduces all ten single mutations with the help of the DNA primers Ebdel F and Ebdel B. The resulting 337 bp (fragment 1) and 259 bp (fragment 2) DNA pieces were purified and used as a template in the PCR generating fragment 3, with a length of 559 bp (figure 36).

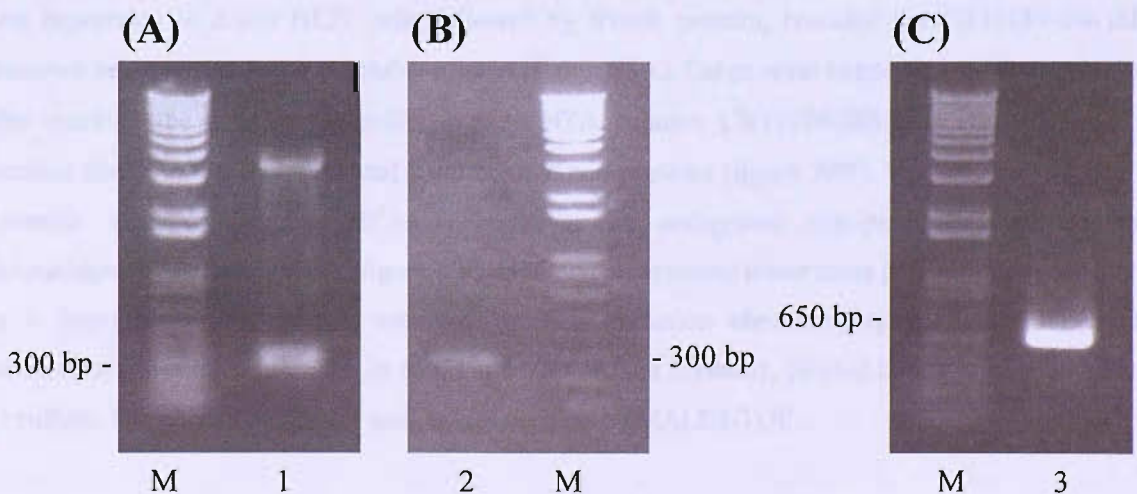


Fig. 36: PCR products on 1% agarose gels: Fragment 1 (A; lane 1), fragment 2 (B; lane 2) and fragment 3 (C; lane 3) were analyzed on a 1% agarose gel. 1 kb plus DNA ladder (M) was used as standard. All DNA pieces corresponded well to the calculated mass. The additional band in (A) lane 1 corresponds to the amplified CRT(189-289) template.

Fragment 3 was purified before and after restriction digestion with BamH I and EcoR I (figure 37A). The resulting 351 bp sticky end DNA fragment was then cloned into a pRSET-miniT expression vector and transformed into *E.coli* for replication. The generated plasmid was recovered by the miniprep procedure (Macherey-Nagel). Analytical restriction digestion was carried out to ensure the presence of the insert in the vector (figure 37B). Sequencing identified one picked clone as the correct CRT(189-288) Δ EB mutant.

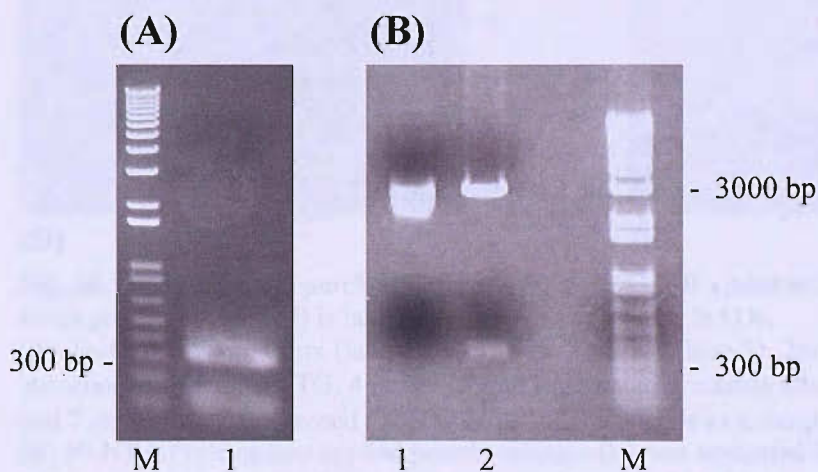


Fig. 37: 1% agarose gels of preparative (A) and analytical (B) BamH I and EcoR I restriction digestion. Fragment 3 (A; lane 1) appears at 350 kb as expected, band below represents one of the two restriction byproducts. Untreated (B; lane 1) and digested expression vector show the expected pattern. The lower band in B, lane 2 represents the excised insert.

Expression and purification of CRT(189-288) Δ EB

Test expression in *E.coli* BL21 cells followed by french pressing revealed the CRT(189-288) Δ EB construct being expressed as a soluble protein (figure 38A). Large scale expression products obtained after cracking the cells were applied to a Ni-NTA column. CRT(189-288) Δ EB containing an N-terminal histidine tag was separated from other *E.coli* proteins (figure 38B). The tag was cleaved by thrombin digestion (figure 38C). To remove the undigested side-product, anion-exchange chromatography was performed (figure 38D). Finally, an apparent lower mass polypeptide suspected to be a degradation product was removed by size exclusion chromatography (figure 38E). This purification procedure, described in detail in Materials and Methods, yielded 20 mg pure protein from 3 l culture. The correct molecular weight was verified by MALDI-TOF.

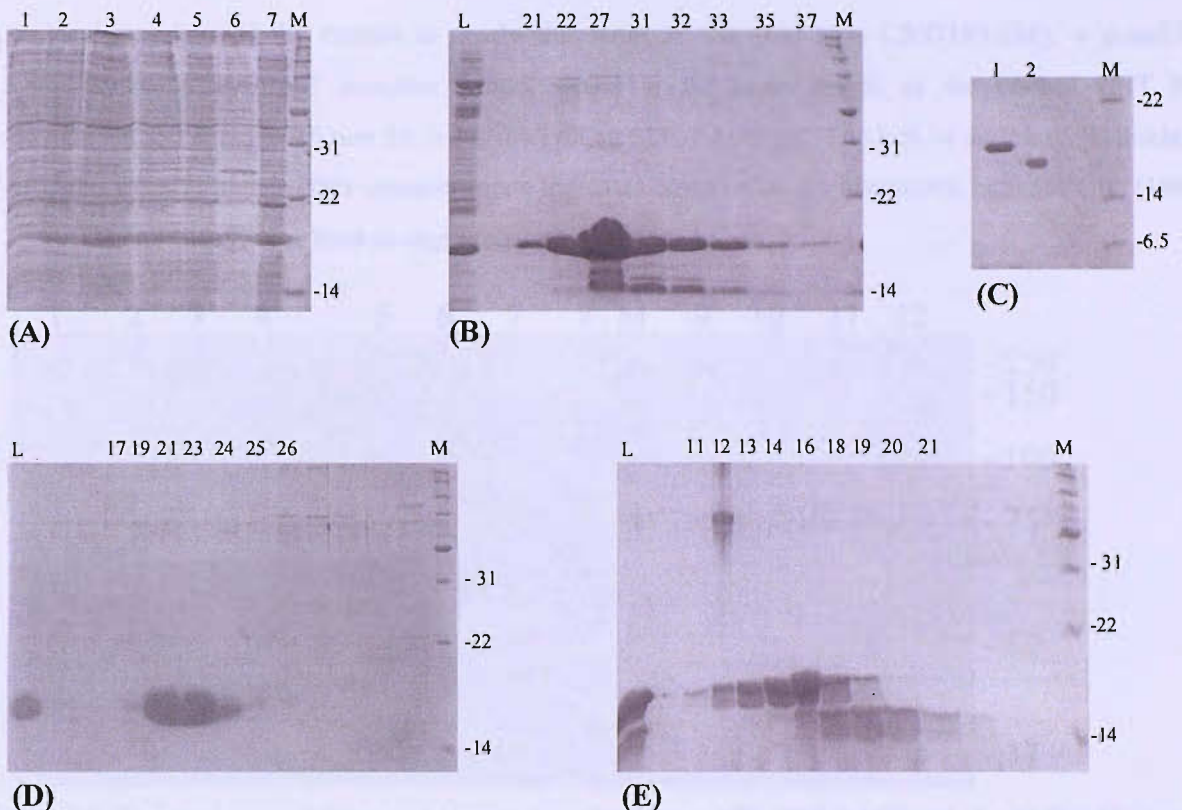


Fig. 38: Expression and purification of CRT(189-288) Δ EB visualized on 15% SDS-PAGE gels. Broad range protein marker (M) is labeled on the right of all gels in kDa.

(A) Test expression: 0 hrs (lane 1), 1 hr (lane 2), 2 hrs (lane 3), 3hrs (lane 4) and 4hrs (lane 5) after induction with 1 mM IPTG. 4 hrs pellet and supernatant fractions after cell rupture are shown in lane 6 and 7 respectively. Expressed CRT(189-288) Δ EB is visible as a sharp band at approximately 17 kDa.

(B) Ni-NTA Purification: applied protein solution (L) was separated into different fractions (labeled on the top of the gel). CRT(189-288) Δ EB in fractions 21-33 was pooled and processed further. A collection of all purification chromatograms is added in the Appendix.

(C) Thrombin cleavage of CRT(189-288) Δ EB: The correct molecular weight of the undigested (lane 1; 17 kDa) and the processed (lane 2; 16 kDa) protein was visualised.

(D) CRT(189-288) Δ EB was loaded (L) on a monoQ column for anion exchange chromatography. Fractions 18-24 (labeled on the top of the gel) containing the desired protein were pooled and used further.

(E) Final purification by size exclusion chromatography: Mixture of CRT(189-288) Δ EB and suspected degradation product (L) was separated. Pure P-domain mutant was obtained by pooling fractions 13-15 (labeled on the top of the gel).

Studies on CRT(189-288) Δ EB

Crosslinking experiments

As a first interaction investigation CRT(189-288) Δ EB was attempted cross-linked to ERp57. The homobifunctional agent DSG was handled in the same way as during the Cne1p32 studies. Since the

molecular weight of the mutant is nearly the same as the wild type CRT(189-288), a possible CRT(189-288) Δ EB/ERp57 complex would appear at the same height as the control CRT P-domain/ERp57 complex (figure 39, red arrow) on an SDS-PAGE gel. The lack of such a cross-linking products even at higher DSG concentrations indicates clearly that the interaction between CRT(189-288) Δ EB and ERp57 is at least strongly reduced.

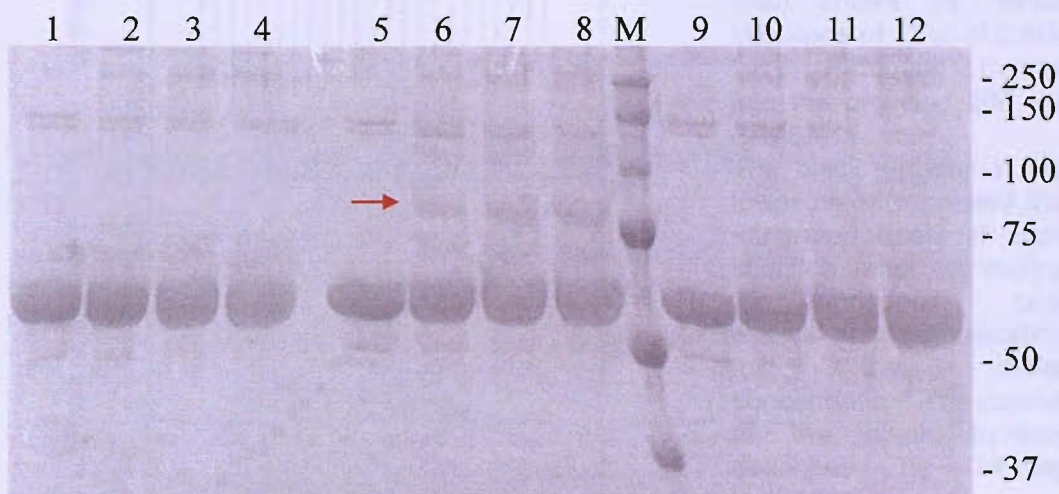


Fig. 39: Chemical cross-linking experiment visualized on a 15% SDS-PAGE gel. 5 μ M ERp57 alone (lanes 1-4), together with 5 μ M CRT(189-288) (lanes 5-8) or with 5 μ M CRT(189-288) Δ EB (lanes 9-12) was incubated with different amounts of DSG (lanes 1, 5 and 9 without, lanes 2, 6 and 10 with 0.5 mM, lanes 3, 7 and 11 with 1 mM and lanes 4, 8 and 12 with 1.5 mM). The band that appears at 77 kDa (red arrow), is assumed to be the 1:1 complex between ERp57 and CRT(189-288). No similar complex could be detected in the case of CRT(189-288) Δ EB with ERp57.

Isothermal titration calorimetry

Performance and analysis of the ITC was done by Dr. Ilian Jelezarov under the same conditions as for Cne1p32. The top part of figure 41 shows that the experiment worked optimally: The microinjections caused regular heat changes extending from a straight baseline. But the integrated, corrected and normalized curved did not show a typical binding isotherm. Thus, like the cross-linking experiment described above, this result also indicates the at least strongly reduced interaction of the CRT(189-288) Δ EB mutant with ERp57.

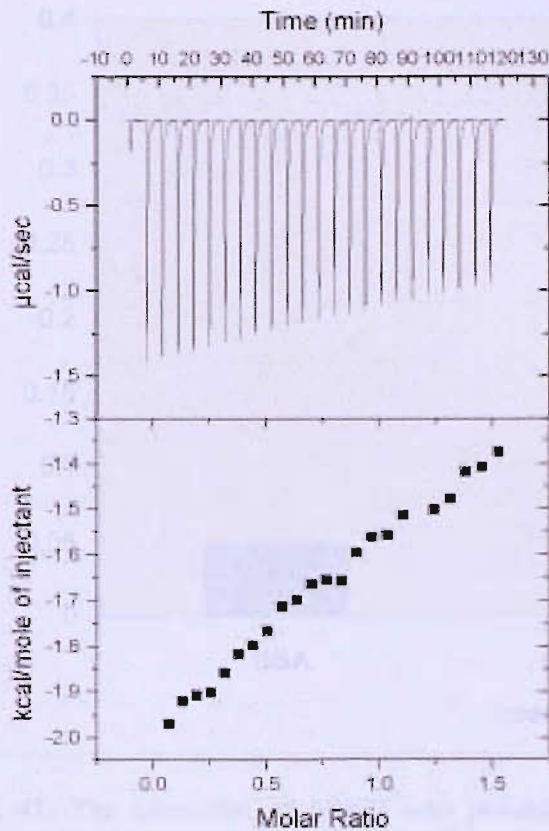


Fig. 40: ITC performed on ERp57 and CRT(189-288) Δ EB: The recorded binding heat (ΔH) diagram (top) shows 24 micro-injections of 12 μ l of 2 mM CRT P-domain mutant into the provided 200 μ M ERp57.

The black squares in the lower panel represent the integrated heats at each injection after correcting for nonspecific heat effects and normalization for the molar concentration. The course of the black squares describes no binding isotherm.

Interaction studies by ELISA

In order to define the strongly reduced or even non-existing binding between CRT(189-288) Δ EB and ERp57 more quantitatively, ELISA was performed. Different CRT P-domain constructs were coated into the wells of an ELISA plate and then the interaction was probed with biotinylated ERp57 at a concentration of 2.5 μ M. The resulting absorbance at 405 nm was measured after a developing time of 30 minutes.

CRT(189-288) Δ EB binding reached with a measured absorbance of 0.046 ± 0.008 just a little more than 10% of the CRT(189-288)/ERp57 control complex value and was thus in the range of BSA, which was used as a negative control protein. It can be concluded from this immunosorbent assay that binding of CRT(189-288) Δ EB to ERp57 is substantially reduced if not abolished as compared to the wild type protein. Since this is the third experiment showing no binding, it can be concluded that CRT(189-288) Δ EB most probably constitutes a negative binding mutant.

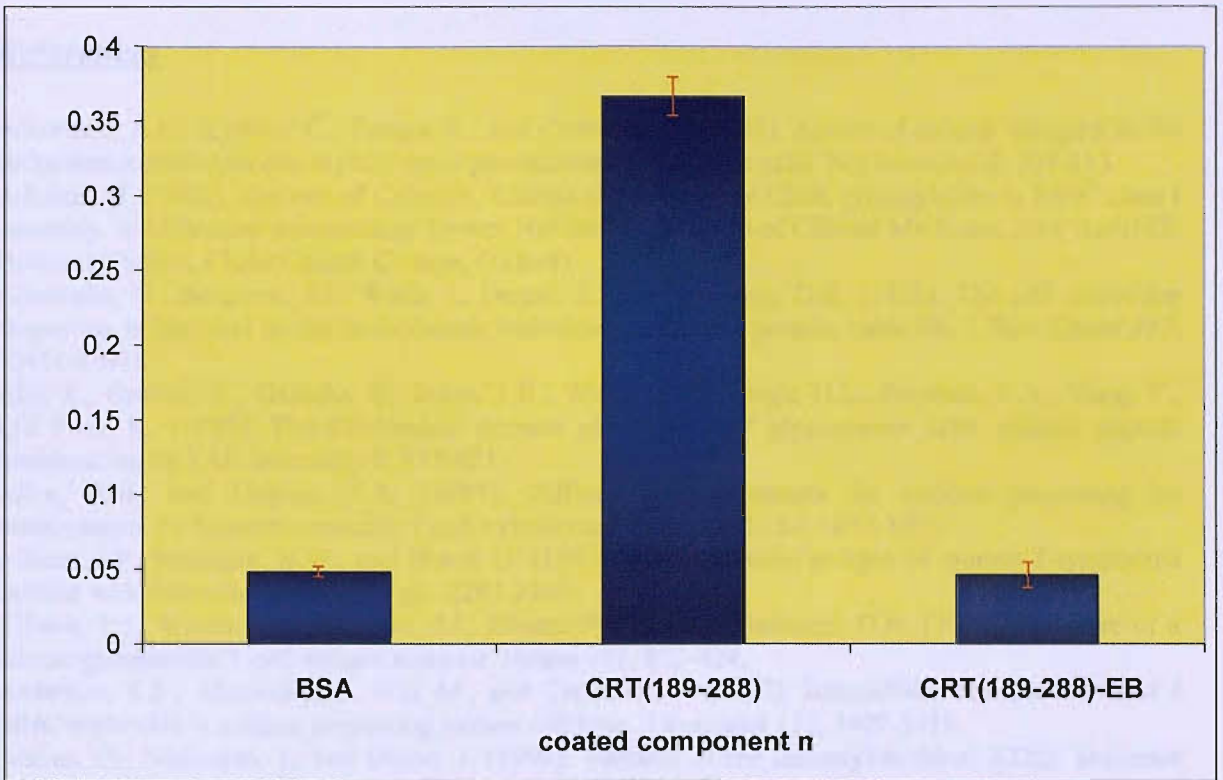


Fig. 41: The interaction of ERp57 with possible binding partners studied by ELISA. The data presented in the graph are average values of triplicates. The experiment was repeated three times with comparable results. Standard deviations are given with orange error bars. Binding of the developing agents to coated protein ligands in the absence of biotinylated ERp57 was subtracted from each value.

References

- Ackerman, A.L., Kyritsis, C., Tampe, R., and Cresswell, P. (2005). Access of soluble antigens to the endoplasmic reticulum can explain cross-presentation by dendritic cells. *Nat Immunol* **6**, 107-113.
- Adhikari, R. (2002). The role of Calnexin, Calreticulin and Heavy Chain glycosylation in MHC class I assembly. In Molecular Immunology Group, Nuffield Department of Clinical Medicine, John Radcliffe Hospital (Oxford, Christ Church College, Oxford).
- Ahluwalia, N., Bergeron, J.J., Wada, I., Degen, E., and Williams, D.B. (1992). The p88 molecular chaperone is identical to the endoplasmic reticulum membrane protein, calnexin. *J Biol Chem* **267**, 10914-10918.
- Ahn, K., Gruhler, A., Galocha, B., Jones, T.R., Wiertz, E.J., Ploegh, H.L., Peterson, P.A., Yang, Y., and Fruh, K. (1997). The ER-luminal domain of the HCMV glycoprotein US6 inhibits peptide translocation by TAP. *Immunity* **6**, 613-621.
- Allen, P.M., and Unanue, E.R. (1984). Differential requirements for antigen processing by macrophages for lysozyme-specific T cell hybridomas. *J Immunol* **132**, 1077-1079.
- Allison, J.P., McIntyre, B.W., and Bloch, D. (1982). Tumor-specific antigen of murine T-lymphoma defined with monoclonal antibody. pp. 2293-2300.
- Allison, T.J., Winter, C.C., Fournie, J.J., Bonneville, M., and Garboczi, D.N. (2001). Structure of a human gammadelta T-cell antigen receptor. *Nature* **411**, 820-824.
- Anderson, K.S., Alexander, J., Wei, M., and Cresswell, P. (1993). Intracellular transport of class I MHC molecules in antigen processing mutant cell lines. *J Immunol* **151**, 3407-3419.
- Andres, D., Dickerson, I., and Dixon, J. (1990). Variants of the carboxyl-terminal KDEL sequence direct intracellular retention. *J. Biol. Chem.* **265**, 5952-5955.
- Anthony L. Defranco, R.M.L., Miranda Robertson (2007). 4-3 Adaptive Immunity and the Detection of Infection by T Lymphocytes. In *Immunity; The Immune Response in Infectious and Inflammatory Disease* (Published in print in association with Oxford University Press and Sinauer Associates).
- Antoniou, A.N., Ford, S., Alphey, M., Osborne, A., Elliott, T., and Powis, S.J. (2002). The oxidoreductase ERp57 efficiently reduces partially folded in preference to fully folded MHC class I molecules. *Embo J* **21**, 2655-2663.
- Antoniou, A.N., Ford, S., Taurog, J.D., Butcher, G.W., and Powis, S.J. (2004). Formation of HLA-B27 homodimers and their relationship to assembly kinetics. *J Biol Chem* **279**, 8895-8902.
- Antoniou, A.N., and Powis, S.J. (2003). Characterization of the ERp57-Tapasin Complex by Rapid Cellular Acidification and Thiol Modification. *Antioxidants & Redox Signaling* **5**, 375-379.
- Antoniou, A.N., Santos, S.G., Campbell, E.C., Lynch, S., Arosa, F.A., and Powis, S.J. (2007). ERp57 interacts with conserved cysteine residues in the MHC class I peptide-binding groove. *FEBS Lett* **581**, 1988-1992.
- Arendt, C.S., and Hochstrasser, M. (1997). Identification of the yeast 20S proteasome catalytic centers and subunit interactions required for active-site formation. *Proc Natl Acad Sci U S A* **94**, 7156-7161.
- Babbitt, B.P., Allen, P.M., Matsueda, G., Haber, E., and Unanue, E.R. (1985). Binding of immunogenic peptides to Ia histocompatibility molecules. *Nature* **317**, 359-361.
- Bakke, O., and Dobberstein, B. (1990). MHC class II-associated invariant chain contains a sorting signal for endosomal compartments. *Cell* **63**, 707-716.
- Baksh, S., and Michalak, M. (1991). Expression of calreticulin in *Escherichia coli* and identification of its Ca²⁺ binding domains. *J Biol Chem* **266**, 21458-21465.
- Bangia, N., and Cresswell, P. (2005). Stoichiometric tapasin interactions in the catalysis of major histocompatibility complex class I molecule assembly. *Immunology* **114**, 346-353.
- Bangia, N., Lehner, P.J., Hughes, E.A., Surman, M., and Cresswell, P. (1999). The N-terminal region of tapasin is required to stabilize the MHC class I loading complex. *Eur J Immunol* **29**, 1858-1870.

- Barber, L.D., Patel, T.P., Percival, L., Gumperz, J.E., Lanier, L.L., Phillips, J.H., Bigge, J.C., Wormwald, M.R., Parekh, R.B., and Parham, P. (1996). Unusual uniformity of the N-linked oligosaccharides of HLA-A, -B, and -C glycoproteins. *J Immunol* *156*, 3275-3284.
- Beissbarth, T., Sun, J., Kavathas, P.B., and Ortmann, B. (2000). Increased efficiency of folding and peptide loading of mutant MHC class I molecules. *Eur J Immunol* *30*, 1203-1213.
- Benham, A.M., Cabibbo, A., Fassio, A., Bulleid, N., Sitia, R., and Braakman, I. (2000). The CXXCXXC motif determines the folding, structure and stability of human Ero1-Lalpha. *Embo J* *19*, 4493-4502.
- Beninga, J., Rock, K.L., and Goldberg, A.L. (1998). Interferon-gamma can stimulate post-proteasomal trimming of the N terminus of an antigenic peptide by inducing leucine aminopeptidase. *J Biol Chem* *273*, 18734-18742.
- Bergeron, J.J., Brenner, M.B., Thomas, D.Y., and Williams, D.B. (1994). Calnexin: a membrane-bound chaperone of the endoplasmic reticulum. *Trends Biochem Sci* *19*, 124-128.
- Beutler, B. (2004). Inferences, questions and possibilities in Toll-like receptor signalling. *Nature* *430*, 257-263.
- Bjorkman, P.J., Saper, M.A., Samraoui, B., Bennett, W.S., Strominger, J.L., and Wiley, D.C. (1987a). The foreign antigen binding site and T cell recognition regions of class I histocompatibility antigens. *Nature* *329*, 512-518.
- Bjorkman, P.J., Saper, M.A., Samraoui, B., Bennett, W.S., Strominger, J.L., and Wiley, D.C. (1987b). Structure of the human class I histocompatibility antigen, HLA-A2. *Nature* *329*, 506-512.
- Bouvier, M., and Stafford, W.F. (2000). Probing the three-dimensional structure of human calreticulin. *Biochemistry* *39*, 14950-14959.
- Breier, A., and Michalak, M. (1994). 2,4,6-Trinitrobenzenesulfonic acid modification of the carboxyl-terminal region (C-domain) of calreticulin. *Molecular and cellular biochemistry* *130*, 19-28.
- Brocke, P., Garbi, N., Momburg, F., and Hammerling, G.J. (2002). HLA-DM, HLA-DO and tapasin: functional similarities and differences. *Curr Opin Immunol* *14*, 22-29.
- Brown, J.H., Jardetzky, T.S., Gorga, J.C., Stern, L.J., Urban, R.G., Strominger, J.L., and Wiley, D.C. (1993). Three-dimensional structure of the human class II histocompatibility antigen HLA-DR1. *Nature* *364*, 33-39.
- Burnet, M. (1959). Auto-immune disease. II. Pathology of the immune response. *Br Med J* *5154*, 720-725.
- Cadwell, K., and Coscoy, L. (2005). Ubiquitination on nonlysine residues by a viral E3 ubiquitin ligase. *Science* *309*, 127-130.
- Carreno, B.M., Solheim, J.C., Harris, M., Stroynowski, I., Connolly, J.M., and Hansen, T.H. (1995). TAP associates with a unique class I conformation, whereas calnexin associates with multiple class I forms in mouse and man. *J Immunol* *155*, 4726-4733.
- Cerundolo, V., Alexander, J., Anderson, K., Lamb, C., Cresswell, P., McMichael, A., Gotch, F., and Townsend, A. (1990). Presentation of viral antigen controlled by a gene in the major histocompatibility complex. *Nature* *345*, 449-452.
- Chan, N.L., and Hill, C.P. (2001). Defining polyubiquitin chain topology. *Nature structural biology* *8*, 650-652.
- Chen, M., and Bouvier, M. (2007). Analysis of interactions in a tapasin/class I complex provides a mechanism for peptide selection. *Embo J* *26*, 1681-1690.
- Chen, M., Stafford, W.F., Diedrich, G., Khan, A., and Bouvier, M. (2002). A characterization of the lumenal region of human tapasin reveals the presence of two structural domains. *Biochemistry* *41*, 14539-14545.
- Chen, Y., Holcomb, C., and Moore, H. (1993). Expression and Localization of Two Low Molecular Weight GTP-Binding Proteins, Rab8 and Rab10, by Epitope Tag
10.1073/pnas.90.14.6508. *PNAS* *90*, 6508-6512.

- Chicz, R.M., Urban, R.G., Lane, W.S., Gorga, J.C., Stern, L.J., Vignali, D.A., and Strominger, J.L. (1992). Predominant naturally processed peptides bound to HLA-DR1 are derived from MHC-related molecules and are heterogeneous in size. *Nature* 358, 764-768.
- Chien, Y.H., Gascoigne, N.R., Kavaler, J., Lee, N.E., and Davis, M.M. (1984). Somatic recombination in a murine T-cell receptor gene. *Nature* 309, 322-326.
- Chow, A.Y., and Mellman, I. (2005). Old lysosomes, new tricks: MHC II dynamics in DCs. *Trends in immunology* 26, 72-78.
- Ciechanover, A. (1994). The ubiquitin-proteasome proteolytic pathway. *Cell* 79, 13-21.
- Clark, R., and Kupper, T. (2005). Old meets new: the interaction between innate and adaptive immunity. *J Invest Dermatol* 125, 629-637.
- Coulombe, P., Rodier, G., Bonneil, E., Thibault, P., and Meloche, S. (2004). N-Terminal ubiquitination of extracellular signal-regulated kinase 3 and p21 directs their degradation by the proteasome. *Molecular and cellular biology* 24, 6140-6150.
- Cox, A.L., Skipper, J., Chen, Y., Henderson, R.A., Darrow, T.L., Shabanowitz, J., Engelhard, V.H., Hunt, D.F., and Slingluff, C.L., Jr. (1994). Identification of a peptide recognized by five melanoma-specific human cytotoxic T cell lines. *Science* 264, 716-719.
- Cresswell, P., Ackerman, A.L., Giodini, A., Peaper, D.R., and Wearsch, P.A. (2005). Mechanisms of MHC class I-restricted antigen processing and cross-presentation. *Immunol Rev* 207, 145-157.
- Cromme, F.V., Airey, J., Heemels, M.T., Ploegh, H.L., Keating, P.J., Stern, P.L., Meijer, C.J., and Walboomers, J.M. (1994a). Loss of transporter protein, encoded by the TAP-1 gene, is highly correlated with loss of HLA expression in cervical carcinomas. *J Exp Med* 179, 335-340.
- Cromme, F.V., van Bommel, P.F., Walboomers, J.M., Gallee, M.P., Stern, P.L., Kenemans, P., Helmerhorst, T.J., Stukart, M.J., and Meijer, C.J. (1994b). Differences in MHC and TAP-1 expression in cervical cancer lymph node metastases as compared with the primary tumours. *British journal of cancer* 69, 1176-1181.
- David, V., Hochstenbach, F., Rajagopalan, S., and Brenner, M.B. (1993). Interaction with newly synthesized and retained proteins in the endoplasmic reticulum suggests a chaperone function for human integral membrane protein IP90 (calnexin). *J Biol Chem* 268, 9585-9592.
- de Virgilio, C., Burckert, N., Neuhaus, J.M., Boller, T., and Wiemken, A. (1993). CNE1, a *Saccharomyces cerevisiae* homologue of the genes encoding mammalian calnexin and calreticulin. *Yeast (Chichester, England)* 9, 185-188.
- Dembic, Z., Haas, W., Weiss, S., McCubrey, J., Kiefer, H., von Boehmer, H., and Steinmetz, M. (1986). Transfer of specificity by murine [alpha] and [beta] T-cell receptor genes. *Nature* 320, 232-238.
- Deverson, E.V., Gow, I.R., Coadwell, W.J., Monaco, J.J., Butcher, G.W., and Howard, J.C. (1990). MHC class II region encoding proteins related to the multidrug resistance family of transmembrane transporters. *Nature* 348, 738-741.
- Dick, T.P., Bangia, N., Peaper, D.R., and Cresswell, P. (2002). Disulfide bond isomerization and the assembly of MHC class I-peptide complexes. *Immunity* 16, 87-98.
- Diedrich, G., Bangia, N., Pan, M., and Cresswell, P. (2001). A Role for Calnexin in the Assembly of the MHC Class I Loading Complex in the Endoplasmic Reticulum. *J Immunol* 166, 1703-1709.
- Doherty, P., and Zinkernagel, R. (1975). H-2 compatibility is required for T-cell-mediated lysis of target cells infected with lymphocytic choriomeningitis virus. *J. Exp. Med.* 141.2.502. *J. Exp. Med.* 141, 502-507.
- Donaldson, J.G., Finazzi, D., and Klausner, R.D. (1992). Brefeldin A inhibits Golgi membrane-catalysed exchange of guanine nucleotide onto ARF protein. *Nature* 360, 350-352.
- Edry, E., and Melamed, D. (2004). Receptor editing in positive and negative selection of B lymphopoiesis. *J Immunol* 173, 4265-4271.
- Ellgaard, L., Molinari, M., and Helenius, A. (1999). Setting the standards: quality control in the secretory pathway. *Science* 286, 1882-1888.

- Ellgaard, L., Riek, R., Herrmann, T., Guntert, P., Braun, D., Helenius, A., and Wuthrich, K. (2001). NMR structure of the calreticulin P-domain. *Proc Natl Acad Sci U S A* 98, 3133-3138.
- Elliott, T. (1997a). How does TAP associate with MHC class I molecules? *Immunol Today* 18, 375-379.
- Elliott, T. (1997b). Transporter associated with antigen processing. *Advances in immunology* 65, 47-109.
- Elliott, T., Cerundolo, V., Elvin, J., and Townsend, A. (1991a). Peptide-induced conformational change of the class I heavy chain. *Nature* 351, 402-406.
- Elliott, T.J., Cerundolo, V., Ohlen, C., Ljunggren, H.G., Karre, K., and Townsend, A. (1991b). Antigen presentation and the association of class-I molecules. *Acta Biol Hung* 42, 213-229.
- Falk, K., Rotzschke, O., and Rammensee, H.G. (1990). Cellular peptide composition governed by major histocompatibility complex class I molecules. *Nature* 348, 248-251.
- Falk, K., Rotzschke, O., Stevanovic, S., Jung, G., and Rammensee, H.G. (1991). Allele-specific motifs revealed by sequencing of self-peptides eluted from MHC molecules. *Nature* 351, 290-296.
- Fearon, D.T., and Locksley, R.M. (1996). The instructive role of innate immunity in the acquired immune response. *Science* 272, 50-53.
- Ferrari, D.M., and Soling, H.D. (1999). The protein disulphide-isomerase family: unravelling a string of folds. *Biochem J* 339 (Pt 1), 1-10.
- Finlay D, C.V. (1991). Ubiquitination. *Annual Review of Cell Biology* 7, 25-69.
- Fliegel, L., Burns, K., MacLennan, D.H., Reithmeier, R.A., and Michalak, M. (1989). Molecular cloning of the high affinity calcium-binding protein (calreticulin) of skeletal muscle sarcoplasmic reticulum. *J Biol Chem* 264, 21522-21528.
- Frangoulis, B., Park, I., Guillemot, F., Severac, V., Auffray, C., and Zoorob, R. (1999). Identification of the Tapasin gene in the chicken major histocompatibility complex. *Immunogenetics* 49, 328-337.
- Frickel, E.M., Riek, R., Jelesarov, I., Helenius, A., Wuthrich, K., and Ellgaard, L. (2002). TROSY-NMR reveals interaction between ERp57 and the tip of the calreticulin P-domain. *Proc Natl Acad Sci U S A* 99, 1954-1959.
- Fruh, K., Ahn, K., Djaballah, H., Sempe, P., van Endert, P.M., Tampe, R., Peterson, P.A., and Yang, Y. (1995). A viral inhibitor of peptide transporters for antigen presentation. *Nature* 375, 415-418.
- Fruh, K., and Yang, Y. (1999). Antigen presentation by MHC class I and its regulation by interferon gamma. *Curr Opin Immunol* 11, 76-81.
- Gadola, S.D., Moins-Teisserenc, H.T., Trowsdale, J., Gross, W.L., and Cerundolo, V. (2000). TAP deficiency syndrome. Clinical and experimental immunology 121, 173-178.
- Gahmberg, C.G., and Tolvanen, M. (1996). Why mammalian cell surface proteins are glycoproteins. *Trends Biochem Sci* 21, 308-311.
- Gao, B., Adhikari, R., Howarth, M., Nakamura, K., Gold, M.C., Hill, A.B., Knee, R., Michalak, M., and Elliott, T. (2002). Assembly and antigen-presenting function of MHC class I molecules in cells lacking the ER chaperone calreticulin. *Immunity* 16, 99-109.
- Garbi, N., Tanaka, S., Momburg, F., and Hammerling, G.J. (2006). Impaired assembly of the major histocompatibility complex class I peptide-loading complex in mice deficient in the oxidoreductase ERp57. *Nat Immunol* 7, 93-102.
- Garcia, K.C., and Adams, E.J. (2005). How the T cell receptor sees antigen--a structural view. *Cell* 122, 333-336.
- Gay, N.J., and Keith, F.J. (1991). Drosophila Toll and IL-1 receptor. *Nature* 351, 355-356.
- Geier, E., Pfeifer, G., Wilm, M., Lucchiari-Hartz, M., Baumeister, W., Eichmann, K., and Niedermann, G. (1999). A giant protease with potential to substitute for some functions of the proteasome. *Science* 283, 978-981.
- Glickman, M.H., Rubin, D.M., Coux, O., Wefes, I., Pfeifer, G., Cjeka, Z., Baumeister, W., Fried, V.A., and Finley, D. (1998). A subcomplex of the proteasome regulatory particle required for ubiquitin-conjugate degradation and related to the COP9-signalosome and eIF3. *Cell* 94, 615-623.
- Goldsby Richard A., K.T.J., Osbourne Barbara A., Kuby Janis (2003). *Immunology* 5th edition.

Greenwood, R., Shimizu, Y., Sekhon, G.S., and DeMars, R. (1994). Novel allele-specific, post-translational reduction in HLA class I surface expression in a mutant human B cell line. *J Immunol* *153*, 5525-5536.

Haglund, K., Di Fiore, P.P., and Dikic, I. (2003). Distinct monoubiquitin signals in receptor endocytosis. *Trends Biochem Sci* *28*, 598-603.

Haglund, K., and Dikic, I. (2005). Ubiquitylation and cell signaling. *Embo J* *24*, 3353-3359.

Hammer, G.E., Gonzalez, F., Champsaur, M., Cado, D., and Shastri, N. (2006). The aminopeptidase ERAAP shapes the peptide repertoire displayed by major histocompatibility complex class I molecules. *Nat Immunol* *7*, 103-112.

Hammerling, G.J., Rusch, E., Tada, N., Kimura, S., and Hammerling, U. (1982). Localization of allodeterminants on H-2Kb antigens determined with monoclonal antibodies and H-2 mutant mice. *Proc Natl Acad Sci U S A* *79*, 4737-4741.

Hammond, C., Braakman, I., and Helenius, A. (1994). Role of N-linked oligosaccharide recognition, glucose trimming, and calnexin in glycoprotein folding and quality control. *Proc Natl Acad Sci U S A* *91*, 913-917.

Harris, M.R., Lybarger, L., Myers, N.B., Hilbert, C., Solheim, J.C., Hansen, T.H., and Yu, Y.Y.L. (2001). Interactions of HLA-B27 with the peptide loading complex as revealed by heavy chain mutations. *Int. Immunol.* *13*, 1275-1282.

Harris, M.R., Yu, Y.Y.L., Kindle, C.S., Hansen, T.H., and Solheim, J.C. (1998). Calreticulin and Calnexin Interact with Different Protein and Glycan Determinants During the Assembly of MHC Class I. *J Immunol* *160*, 5404-5409.

Haskins, K., Kubo, R., White, J., Pigeon, M., Kappler, J., and Marrack, P. (1983). The major histocompatibility complex-restricted antigen receptor on T cells. I. Isolation with a monoclonal antibody. *J Exp Med* *157*, 1149-1169.

Haugejorden, S., Srinivasan, M., and Green, M. (1991). Analysis of the retention signals of two resident luminal endoplasmic reticulum proteins by in vitro mutagenesis. *J. Biol. Chem.* *266*, 6015-6018.

Hayday, A.C., Saito, H., Gillies, S.D., Kranz, D.M., Tanigawa, G., Eisen, H.N., and Tonegawa, S. (1985). Structure, organization, and somatic rearrangement of T cell gamma genes. *Cell* *40*, 259-269.

Hebert, D.N., Zhang, J.X., Chen, W., Foellmer, B., and Helenius, A. (1997). The number and location of glycans on influenza hemagglutinin determine folding and association with calnexin and calreticulin. *J Cell Biol* *139*, 613-623.

Hedrick, S.M., Cohen, D.I., Nielsen, E.A., and Davis, M.M. (1984a). Isolation of cDNA clones encoding T cell-specific membrane-associated proteins. *Nature* *308*, 149-153.

Hedrick, S.M., Nielsen, E.A., Kavaler, J., Cohen, D.I., and Davis, M.M. (1984b). Sequence relationships between putative T-cell receptor polypeptides and immunoglobulins. *Nature* *308*, 153-158.

Heemels, M.T., Schumacher, T.N., Wonigeit, K., and Ploegh, H.L. (1993). Peptide translocation by variants of the transporter associated with antigen processing. *Science* *262*, 2059-2063.

Helenius, A., and Aebi, M. (2004). ROLES OF N-LINKED GLYCANS IN THE ENDOPLASMIC RETICULUM. *Annual Review of Biochemistry* *73*, 1019-1049.

Helms, J.B., and Rothman, J.E. (1992). Inhibition by brefeldin A of a Golgi membrane enzyme that catalyses exchange of guanine nucleotide bound to ARF. *Nature* *360*, 352-354.

Hengel, H., Koopmann, J.O., Flohr, T., Muranyi, W., Goulmy, E., Hammerling, G.J., Koszinowski, U.H., and Momburg, F. (1997). A viral ER-resident glycoprotein inactivates the MHC-encoded peptide transporter. *Immunity* *6*, 623-632.

Herberg, J.A., Sgouros, J., Jones, T., Copeman, J., Humphray, S.J., Sheer, D., Cresswell, P., Beck, S., and Trowsdale, J. (1998). Genomic analysis of the Tapasin gene, located close to the TAP loci in the MHC. *Eur J Immunol* *28*, 459-467.

Hildebrand, W.H., Turnquist, H.R., Prilliman, K.R., Hickman, H.D., Schenk, E.L., McIlhaney, M.M., and Solheim, J.C. (2002). HLA class I polymorphism has a dual impact on ligand binding and chaperone interaction. *Hum Immunol* 63, 248-255.

Hill, A., Jugovic, P., York, I., Russ, G., Bennink, J., Yewdell, J., Ploegh, H., and Johnson, D. (1995). Herpes simplex virus turns off the TAP to evade host immunity. *Nature* 375, 411-415.

Hisamatsu, H., Shimbara, N., Saito, Y., Kristensen, P., Hendil, K.B., Fujiwara, T., Takahashi, E., Tanahashi, N., Tamura, T., Ichihara, A., and Tanaka, K. (1996). Newly identified pair of proteasomal subunits regulated reciprocally by interferon gamma. *J Exp Med* 183, 1807-1816.

Ho, S.N., Hunt, H.D., Horton, R.M., Pullen, J.K., and Pease, L.R. (1989). Site-directed mutagenesis by overlap extension using the polymerase chain reaction. *Gene* 77, 51-59.

Howarth, M., Williams, A., Tolstrup, A.B., and Elliott, T. (2004). Tapasin enhances MHC class I peptide presentation according to peptide half-life. *Proc Natl Acad Sci U S A* 101, 11737-11742.

Hsu, V.W., Yuan, L.C., Nuchtern, J.G., Lippincott-Schwartz, J., Hammerling, G.J., and Klausner, R.D. (1991). A recycling pathway between the endoplasmic reticulum and the Golgi apparatus for retention of unassembled MHC class I molecules. *J Biol Chem* 266, 441-444.

Ihara, Y., Cohen-Doyle, M.F., Saito, Y., and Williams, D.B. (1999). Calnexin discriminates between protein conformational states and functions as a molecular chaperone in vitro. *Molecular cell* 4, 331-341.

Ikeda, K., Sannoh, T., Kawasaki, N., Kawasaki, T., and Yamashina, I. (1987). Serum lectin with known structure activates complement through the classical pathway. *J Biol Chem* 262, 7451-7454.

Janeway, C.A., Jr. (1989). Approaching the asymptote? Evolution and revolution in immunology. *Cold Spring Harb Symp Quant Biol* 54 Pt 1, 1-13.

Joly, E., Le Rolle, A.F., Gonzalez, A.L., Mehling, B., Stevens, J., Coadwell, W.J., Hunig, T., Howard, J.C., and Butcher, G.W. (1998). Co-evolution of rat TAP transporters and MHC class I RT1-A molecules. *Curr Biol* 8, 169-172.

Kapoor, M., Ellgaard, L., Gopalakrishnapai, J., Schirra, C., Gemma, E., Oscarson, S., Helenius, A., and Suroli, A. (2004). Mutational analysis provides molecular insight into the carbohydrate-binding region of calreticulin: pivotal roles of tyrosine-109 and aspartate-135 in carbohydrate recognition. *Biochemistry* 43, 97-106.

Karala, A.R., and Ruddock, L.W. (2007). Does s-methyl methanethiosulfonate trap the thiol-disulfide state of proteins? *Antioxid Redox Signal* 9, 527-531.

Karttunen, J., Sanderson, S., and Shastri, N. (1992). Detection of rare antigen-presenting cells by the lacZ T-cell activation assay suggests an expression cloning strategy for T-cell antigens. *Proc Natl Acad Sci U S A* 89, 6020-6024.

Kaufman, J., Milne, S., Gobel, T.W., Walker, B.A., Jacob, J.P., Auffray, C., Zoorob, R., and Beck, S. (1999). The chicken B locus is a minimal essential major histocompatibility complex. *Nature* 401, 923-925.

Kelly, A., Powis, S.H., Kerr, L.-A., Mockridge, I., Elliott, T., Bastin, J., Uchanska-Ziegler, B., Ziegler, A., Trowsdale, J., and Townsend, A. (1992). Assembly and function of the two ABC transporter proteins encoded in the human major histocompatibility complex. *Nature* 355, 641-644.

Kerscher, O., Felberbaum, R., and Hochstrasser, M. (2006). Modification of proteins by ubiquitin and ubiquitin-like proteins. *Annu Rev Cell Dev Biol* 22, 159-180.

Khanna, N.C., Tokuda, M., and Waisman, D.M. (1986). Conformational changes induced by binding of divalent cations to calregulin. *J Biol Chem* 261, 8883-8887.

Kienast, A., Preuss, M., Winkler, M., and Dick, T.P. (2007). Redox regulation of peptide receptivity of major histocompatibility complex class I molecules by ERp57 and tapasin. *Nat Immunol* 8, 864-872.

Kirkpatrick, D.S., Denison, C., and Gygi, S.P. (2005). Weighing in on ubiquitin: the expanding role of mass-spectrometry-based proteomics. *Nature cell biology* 7, 750-757.

Kisselev, A.F., Akopian, T.N., and Goldberg, A.L. (1998). Range of sizes of peptide products generated during degradation of different proteins by archaeal proteasomes. *J Biol Chem* 273, 1982-1989.

- Klappa, P., Hawkins, H.C., and Freedman, R.B. (1997). Interactions between protein disulphide isomerase and peptides. *Eur J Biochem* 248, 37-42.
- Klappa, P., Ruddock, L.W., Darby, N.J., and Freedman, R.B. (1998). The b' domain provides the principal peptide-binding site of protein disulfide isomerase but all domains contribute to binding of misfolded proteins. *Embo J* 17, 927-935.
- Kleijmeer, M.J., Kelly, A., Geuze, H.J., Slot, J.W., Townsend, A., and Trowsdale, J. (1992). Location of MHC-encoded transporters in the endoplasmic reticulum and cis-Golgi. *Nature* 357, 342-344.
- Kloetzel, P.M. (2004). The proteasome and MHC class I antigen processing. *Biochim Biophys Acta* 1695, 225-233.
- Kuge, O., Dascher, C., Orci, L., Rowe, T., Amherdt, M., Plutner, H., Ravazzola, M., Tanigawa, G., Rothman, J.E., and Balch, W.E. (1994). Sar1 promotes vesicle budding from the endoplasmic reticulum but not Golgi compartments. *J Cell Biol* 125, 51-65.
- Ladasky, J.J., Boyle, S., Seth, M., Li, H., Pentcheva, T., Abe, F., Steinberg, S.J., and Edidin, M. (2006). Bap31 enhances the endoplasmic reticulum export and quality control of human class I MHC molecules. *J Immunol* 177, 6172-6181.
- Lehner, P.J., Karttunen, J.T., Wilkinson, G.W., and Cresswell, P. (1997). The human cytomegalovirus US6 glycoprotein inhibits transporter associated with antigen processing-dependent peptide translocation. *Proc Natl Acad Sci U S A* 94, 6904-6909.
- Lehner, P.J., Surman, M.J., and Cresswell, P. (1998). Soluble tapasin restores MHC class I expression and function in the tapasin-negative cell line .220. *Immunity* 8, 221-231.
- Lemaitre, B., Nicolas, E., Michaut, L., Reichhart, J.M., and Hoffmann, J.A. (1996). The dorsoventral regulatory gene cassette spatzle/Toll/cactus controls the potent antifungal response in *Drosophila* adults. *Cell* 86, 973-983.
- Lemke, H., Hammerling, G.J., and Hammerling, U. (1979). Fine specificity analysis with monoclonal antibodies of antigens controlled by the major histocompatibility complex and by the Qa/TL region in mice. *Immunol Rev* 47, 175-206.
- Lewis, J.W., and Elliott, T. (1998). Evidence for successive peptide binding and quality control stages during MHC class I assembly. *Curr Biol* 8, 717-720.
- Lewis, J.W., Neisig, A., Neefjes, J., and Elliott, T. (1996). Point mutations in the alpha 2 domain of HLA-A2.1 define a functionally relevant interaction with TAP. *Curr Biol* 6, 873-883.
- Lewis, J.W., Sewell, A., Price, D., and Elliott, T. (1998). HLA-A*0201 presents TAP-dependent peptide epitopes to cytotoxic T lymphocytes in the absence of tapasin. *Eur J Immunol* 28, 3214-3220.
- Lewis, M.J., and Pelham, H.R. (1990). A human homologue of the yeast HDEL receptor. *Nature* 348, 162-163.
- Li, S., Paulsson, K.M., Chen, S., Sjogren, H.-O., and Wang, P. (2000). Tapasin Is Required for Efficient Peptide Binding to Transporter Associated with Antigen Processing. *J. Biol. Chem.* 275, 1581-1586.
- Li, S., Paulsson, K.M., Sjogren, H.-O., and Wang, P. (1999). Peptide-bound Major Histocompatibility Complex Class I Molecules Associate with Tapasin before Dissociation from Transporter Associated with Antigen Processing. *J. Biol. Chem.* 274, 8649-8654.
- Li, Z., Stafford, W.F., and Bouvier, M. (2001). The metal ion binding properties of calreticulin modulate its conformational flexibility and thermal stability. *Biochemistry* 40, 11193-11201.
- Lian, R.H., Freeman, J.D., Mager, D.L., and Takei, F. (1998). Role of conserved glycosylation site unique to murine class I MHC in recognition by Ly-49 NK cell receptor. *J Immunol* 161, 2301-2306.
- Lindquist, J.A., Hammerling, G.J., and Trowsdale, J. (2001). ER60/ERp57 forms disulfide-bonded intermediates with MHC class I heavy chain. *Faseb J* 15, 1448-1450.
- Lippincott-Schwartz, J., Yuan, L., Tipper, C., Amherdt, M., Orci, L., and Klausner, R.D. (1991). Brefeldin A's effects on endosomes, lysosomes, and the TGN suggest a general mechanism for regulating organelle structure and membrane traffic. *Cell* 67, 601-616.
- Lowe, J., Stock, D., Jap, B., Zwickl, P., Baumeister, W., and Huber, R. (1995). Crystal structure of the 20S proteasome from the archaeon *T. acidophilum* at 3.4 Å resolution. *Science* 268, 533-539.

Macer, D.R., and Koch, G.L. (1988). Identification of a set of calcium-binding proteins in reticuloplasm, the luminal content of the endoplasmic reticulum. *J Cell Sci* 91 (Pt 1), 61-70.

Majoul, I., Straub, M., Hell, S.W., Duden, R., and Soling, H.D. (2001). KDEL-cargo regulates interactions between proteins involved in COPI vesicle traffic: measurements in living cells using FRET. *Dev Cell* 1, 139-153.

Malarkannan, S., Gonzalez, F., Nguyen, V., Adair, G., and Shastri, N. (1996). Alloreactive CD8+ T cells can recognize unusual, rare, and unique processed peptide/MHC complexes. *J Immunol* 157, 4464-4473.

Malissen, M., Malissen, B., and Jordan, B.R. (1982). Exon/intron organization and complete nucleotide sequence of an HLA gene. *Proc Natl Acad Sci U S A* 79, 893-897.

Marusina, K., Iyer, M., and Monaco, J.J. (1997). Allelic variation in the mouse Tap-1 and Tap-2 transporter genes. *J Immunol* 158, 5251-5256.

Matlin, K.S., and Simons, K. (1983). Reduced temperature prevents transfer of a membrane glycoprotein to the cell surface but does not prevent terminal glycosylation. *Cell* 34, 233-243.

McBlane, J.F., van Gent, D.C., Ramsden, D.A., Romeo, C., Cuomo, C.A., Gellert, M., and Oettinger, M.A. (1995). Cleavage at a V(D)J recombination signal requires only RAG1 and RAG2 proteins and occurs in two steps. *Cell* 83, 387-395.

McCauliffe, D.P., Lux, F.A., Lieu, T.S., Sanz, I., Hanke, J., Newkirk, M.M., Bachinski, L.L., Itoh, Y., Siciliano, M.J., Reichlin, M., and et al. (1990). Molecular cloning, expression, and chromosome 19 localization of a human Ro/SS-A autoantigen. *The Journal of clinical investigation* 85, 1379-1391.

McDevitt, H.O., and Tyan, M.L. (1968). Genetic control of the antibody response in inbred mice. Transfer of response by spleen cells and linkage to the major histocompatibility (H-2) locus. *J Exp Med* 128, 1-11.

Medzhitov, R., and Janeway, C.A., Jr. (2002). Decoding the patterns of self and nonself by the innate immune system. *Science* 296, 298-300.

Mesaeli, N., Nakamura, K., Zvaritch, E., Dickie, P., Dziak, E., Krause, K.-H., Opas, M., MacLennan, D.H., and Michalak, M. (1999). Calreticulin Is Essential for Cardiac Development. *J. Cell Biol.* 144, 857-868.

Meuer, S.C., Fitzgerald, K.A., Hussey, R.E., Hodgdon, J.C., Schlossman, S.F., and Reinherz, E.L. (1983). Clonotypic structures involved in antigen-specific human T cell function. Relationship to the T3 molecular complex. *J Exp Med* 157, 705-719.

Michalak, M., Milner, R.E., Burns, K., and Opas, M. (1992). Calreticulin. *Biochem J* 285 (Pt 3), 681-692.

Molinari, M., and Helenius, A. (1999). Glycoproteins form mixed disulphides with oxidoreductases during folding in living cells. *Nature* 402, 90-93.

Molinari, M., and Helenius, A. (2000). Chaperone selection during glycoprotein translocation into the endoplasmic reticulum. *Science* 288, 331-333.

Momburg, F., Roelse, J., Hammerling, G.J., and Neefjes, J.J. (1994a). Peptide size selection by the major histocompatibility complex-encoded peptide transporter. *J Exp Med* 179, 1613-1623.

Momburg, F., Roelse, J., Howard, J.C., Butcher, G.W., Hammerling, G.J., and Neefjes, J.J. (1994b). Selectivity of MHC-encoded peptide transporters from human, mouse and rat. *Nature* 367, 648-651.

Monaco, J.J., Cho, S., and Attaya, M. (1990). Transport protein genes in the murine MHC: possible implications for antigen processing. *Science* 250, 1723-1726.

Monaco, J.J., and McDevitt, H.O. (1984). H-2-linked low-molecular weight polypeptide antigens assemble into an unusual macromolecular complex. *Nature* 309, 797-799.

Monaco, J.J., and McDevitt, H.O. (1986). The LMP antigens: a stable MHC-controlled multisubunit protein complex. *Hum Immunol* 15, 416-426.

Monnat, J., Neuhaus, E.M., Pop, M.S., Ferrari, D.M., Kramer, B., and Soldati, T. (2000). Identification of a Novel Saturable Endoplasmic Reticulum Localization Mechanism Mediated by the C-Terminus of a Dictyostelium Protein Disulfide Isomerase. *Mol. Biol. Cell* 11, 3469-3484.

Morjana, N.A., and Gilbert, H.F. (1991). Effect of protein and peptide inhibitors on the activity of protein disulfide isomerase. *Biochemistry* 30, 4985-4990.

Munro, S., and Pelham, H.R. (1987). A C-terminal signal prevents secretion of luminal ER proteins. *Cell* 48, 899-907.

Neefjes, J., Gottfried, E., Roelse, J., Gromme, M., Obst, R., Hammerling, G.J., and Momburg, F. (1995). Analysis of the fine specificity of rat, mouse and human TAP peptide transporters. *Eur J Immunol* 25, 1133-1136.

Neeli, I., Siddiqi, S.A., Siddiqi, S., Mahan, J., Lagakos, W.S., Binas, B., Gheyi, T., Storch, J., and Mansbach, C.M., II (2007). Liver Fatty Acid-binding Protein Initiates Budding of Pre-chylomicron Transport Vesicles from Intestinal Endoplasmic Reticulum. pp. 17974-17984.

Neijssen, J., Herberths, C., Drijfhout, J.W., Reits, E., Janssen, L., and Neefjes, J. (2005). Cross-presentation by intercellular peptide transfer through gap junctions. *Nature* 434, 83-88.

Neisig, A., Wubbolts, R., Zang, X., Melief, C., and Neefjes, J. (1996). Allele-specific differences in the interaction of MHC class I molecules with transporters associated with antigen processing. *J Immunol* 156, 3196-3206.

Noiva, R., Freedman, R.B., and Lennarz, W.J. (1993). Peptide binding to protein disulfide isomerase occurs at a site distinct from the active sites. *J Biol Chem* 268, 19210-19217.

Nossner, E., and Parham, P. (1995). Species-specific differences in chaperone interaction of human and mouse major histocompatibility complex class I molecules. *J Exp Med* 181, 327-337.

Oettinger, M.A., Schatz, D.G., Gorka, C., and Baltimore, D. (1990). RAG-1 and RAG-2, adjacent genes that synergistically activate V(D)J recombination. *Science* 248, 1517-1523.

Ohlen, C., Bejarano, M.T., Gronberg, A., Torsteinsdottir, S., Franksson, L., Ljunggren, H.G., Klein, E., Klein, G., and Karre, K. (1989). Studies of sublines selected for loss of HLA expression from an EBV-transformed lymphoblastoid cell line. Changes in sensitivity to cytotoxic T cells activated by allostimulation and natural killer cells activated by IFN or IL-2. *J Immunol* 142, 3336-3341.

Oliver, J.D., Roderick, H.L., Llewellyn, D.H., and High, S. (1999). ERp57 functions as a subunit of specific complexes formed with the ER lectins calreticulin and calnexin. *Mol Biol Cell* 10, 2573-2582.

Orino, E., Tanaka, K., Tamura, T., Sone, S., Ogura, T., and Ichihara, A. (1991). ATP-dependent reversible association of proteasomes with multiple protein components to form 26S complexes that degrade ubiquitinated proteins in human HL-60 cells. *FEBS Lett* 284, 206-210.

Ortmann, B., Androlewicz, M.J., and Cresswell, P. (1994). MHC class I/beta 2-microglobulin complexes associate with TAP transporters before peptide binding. *Nature* 368, 864-867.

Ortmann, B., Copeman, J., Lehner, P.J., Sadasivan, B., Herberg, J.A., Grandea, A.G., Riddell, S.R., Tampe, R., Spies, T., Trowsdale, J., and Cresswell, P. (1997). A critical role for tapasin in the assembly and function of multimeric MHC class I-TAP complexes. *Science* 277, 1306-1309.

Parham, P., and Brodsky, F.M. (1981). Partial purification and some properties of BB7.2. A cytotoxic monoclonal antibody with specificity for HLA-A2 and a variant of HLA-A28. *Hum Immunol* 3, 277-299.

Park, B., Lee, S., Kim, E., and Ahn, K. (2003). A single polymorphic residue within the peptide-binding cleft of MHC class I molecules determines spectrum of tapasin dependence. *J Immunol* 170, 961-968.

Park, B., Lee, S., Kim, E., Cho, K., Riddell, S.R., Cho, S., and Ahn, K. (2006). Redox regulation facilitates optimal peptide selection by MHC class I during antigen processing. *Cell* 127, 369-382.

Parlati, F., Dignard, D., Bergeron, J.J., and Thomas, D.Y. (1995). The calnexin homologue *cnx1+* in *Schizosaccharomyces pombe*, is an essential gene which can be complemented by its soluble ER domain. *Embo J* 14, 3064-3072.

Paul, P., Rouas-Freiss, N., Khalil-Daher, I., Moreau, P., Riteau, B., Le Gal, F.A., Avril, M.F., Dausset, J., Guillet, J.G., and Carosella, E.D. (1998). HLA-G expression in melanoma: a way for tumor cells to escape from immunosurveillance. *Proc Natl Acad Sci U S A* 95, 4510-4515.

Peaper, D.R., Wearsch, P.A., and Cresswell, P. (2005). Tapasin and ERp57 form a stable disulfide-linked dimer within the MHC class I peptide-loading complex. *Embo J* 24, 3613-3623.

- Peh, C.A., Burrows, S.R., Barnden, M., Khanna, R., Cresswell, P., Moss, D.J., and McCluskey, J. (1998). HLA-B27-restricted antigen presentation in the absence of tapasin reveals polymorphism in mechanisms of HLA class I peptide loading. *Immunity* 8, 531-542.
- Pelham, H.R. (1989). Control of protein exit from the endoplasmic reticulum. *Annu Rev Cell Biol* 5, 1-23.
- Pentcheva, T., and Edidin, M. (2001). Clustering of peptide-loaded MHC class I molecules for endoplasmic reticulum export imaged by fluorescence resonance energy transfer. *J Immunol* 166, 6625-6632.
- Persson, S., Rosenquist, M., and Sommarin, M. (2002). Identification of a novel calreticulin isoform (Crt2) in human and mouse. *Gene* 297, 151-158.
- Peterson, J., and Helenius, A. (1999). In vitro reconstitution of calreticulin-substrate interactions. *J Cell Sci* 112, 2775-2784.
- Porgador, A., Yewdell, J.W., Deng, Y., Bennink, J.R., and Germain, R.N. (1997). Localization, quantitation, and in situ detection of specific peptide-MHC class I complexes using a monoclonal antibody. *Immunity* 6, 715-726.
- Powis, S.J. (1997). Major histocompatibility complex class I molecules interact with both subunits of the transporter associated with antigen processing, TAP1 and TAP2. *Eur J Immunol* 27, 2744-2747.
- Powis, S.J., Townsend, A.R.M., Deverson, E.V., Bastin, J., Butcher, G.W., and Howard, J.C. (1991). Restoration of antigen presentation to the mutant cell line RMA-S by an MHC-linked transporter. 354, 528-531.
- Purbhoo, M.A., Sewell, A.K., Klenerman, P., Goulder, P.J., Hilyard, K.L., Bell, J.I., Jakobsen, B.K., and Phillips, R.E. (1998). Copresentation of natural HIV-I agonist and antagonist ligands fails to induce the T cell receptor signaling cascade. *Proc Natl Acad Sci U S A* 95, 4527-4532.
- Rigney, E., Kojima, M., Glithero, A., and Elliott, T. (1998). A Soluble Major Histocompatibility Complex Class I Peptide-binding Platform Undergoes a Conformational Change in Response to Peptide Epitopes. *J. Biol. Chem.* 273, 14200-14204.
- Rock, K.L., and Goldberg, A.L. (1999). Degradation of cell proteins and the generation of MHC class I-presented peptides. *Annu Rev Immunol* 17, 739-779.
- Rosenthal, A.S., and Shevach, E.M. (1973). FUNCTION OF MACROPHAGES IN ANTIGEN RECOGNITION BY GUINEA PIG T LYMPHOCYTES: I. REQUIREMENT FOR HISTOCOMPATIBLE MACROPHAGES AND LYMPHOCYTES
10.1084/jem.138.5.1194. *J. Exp. Med.* 138, 1194-1212.
- Rudensky, A., Preston-Hurlburt, P., Hong, S.C., Barlow, A., and Janeway, C.A., Jr. (1991). Sequence analysis of peptides bound to MHC class II molecules. *Nature* 353, 622-627.
- Sadasivan, B., Lehner, P.J., Ortmann, B., Spies, T., and Cresswell, P. (1996). Roles for calreticulin and a novel glycoprotein, tapasin, in the interaction of MHC class I molecules with TAP. *Immunity* 5, 103-114.
- Saeki, Y., Tayama, Y., Toh-e, A., and Yokosawa, H. (2004). Definitive evidence for Ufd2-catalyzed elongation of the ubiquitin chain through Lys48 linkage. *Biochem Biophys Res Commun* 320, 840-845.
- Saito, H., Kranz, D.M., Takagaki, Y., Hayday, A.C., Eisen, H.N., and Tonegawa, S. (1984). Complete primary structure of a heterodimeric T-cell receptor deduced from cDNA sequences. *Nature* 309, 757-762.
- Saito, Y., Ihara, Y., Leach, M.R., Cohen-Doyle, M.F., and Williams, D.B. (1999). Calreticulin functions in vitro as a molecular chaperone for both glycosylated and non-glycosylated proteins. *Embo J* 18, 6718-6729.
- Samelson, L.E., Harford, J.B., and Klausner, R.D. (1985). Identification of the components of the murine T cell antigen receptor complex. *Cell* 43, 223-231.
- Santos, S.G., Campbell, E.C., Lynch, S., Wong, V., Antoniou, A.N., and Powis, S.J. (2007). Major histocompatibility complex class I-ERp57-tapasin interactions within the peptide-loading complex. *J Biol Chem* 282, 17587-17593.

- Schatz, D.G., Oettinger, M.A., and Baltimore, D. (1989). The V(D)J recombination activating gene, RAG-1. *Cell* *59*, 1035-1048.
- Schindler, R., Itin, C., Zerial, M., Lottspeich, F., and Hauri, H.P. (1993). ERGIC-53, a membrane protein of the ER-Golgi intermediate compartment, carries an ER retention motif. *Eur J Cell Biol* *61*, 1-9.
- Schmidtke, G., Kraft, R., Kostka, S., Henklein, P., Frommel, C., Lowe, J., Huber, R., Kloetzel, P.M., and Schmidt, M. (1996). Analysis of mammalian 20S proteasome biogenesis: the maturation of beta-subunits is an ordered two-step mechanism involving autocatalysis. *Embo J* *15*, 6887-6898.
- Schrag, J.D., Bergeron, J.J., Li, Y., Borisova, S., Hahn, M., Thomas, D.Y., and Cygler, M. (2001). The Structure of calnexin, an ER chaperone involved in quality control of protein folding. *Molecular cell* *8*, 633-644.
- Schubert, U., Anton, L.C., Gibbs, J., Norbury, C.C., Yewdell, J.W., and Bannink, J.R. (2000). Rapid degradation of a large fraction of newly synthesized proteins by proteasomes. *Nature* *404*, 770-774.
- Schumacher, T.N., Kantesaria, D.V., Heemels, M.T., Ashton-Rickardt, P.G., Shepherd, J.C., Fruh, K., Yang, Y., Peterson, P.A., Tonegawa, S., and Ploegh, H.L. (1994). Peptide length and sequence specificity of the mouse TAP1/TAP2 translocator. *J Exp Med* *179*, 533-540.
- Serwold, T., Gonzalez, F., Kim, J., Jacob, R., and Shastri, N. (2002). ERAAP customizes peptides for MHC class I molecules in the endoplasmic reticulum. *Nature* *419*, 480-483.
- Shastri, N., Schwab, S., and Serwold, T. (2002). Producing nature's gene-chips: the generation of peptides for display by MHC class I molecules. *Annu Rev Immunol* *20*, 463-493.
- Shepherd, J.C., Schumacher, T.N., Ashton-Rickardt, P.G., Imaeda, S., Ploegh, H.L., Janeway, C.A., Jr., and Tonegawa, S. (1993). TAP1-dependent peptide translocation in vitro is ATP dependent and peptide selective. *Cell* *74*, 577-584.
- Siggs, O.M., Makaroff, L.E., and Liston, A. (2006). The why and how of thymocyte negative selection. *Curr Opin Immunol* *18*, 175-183.
- Sim, R.B., and Reid, K.B. (1991). C1: molecular interactions with activating systems. *Immunol Today* *12*, 307-311.
- Smith, K.J., Reid, S.W., Stuart, D.I., McMichael, A.J., Jones, E.Y., and Bell, J.I. (1996). An altered position of the alpha 2 helix of MHC class I is revealed by the crystal structure of HLA-B*3501. *Immunity* *4*, 203-213.
- Smith, M.J., and Koch, G.L. (1989). Multiple zones in the sequence of calreticulin (CRP55, calregulin, HACBP), a major calcium binding ER/SR protein. *Embo J* *8*, 3581-3586.
- Sonnichsen, B., Fullekrug, J., Nguyen Van, P., Diekmann, W., Robinson, D., and Mieskes, G. (1994). Retention and retrieval: both mechanisms cooperate to maintain calreticulin in the endoplasmic reticulum. *J Cell Sci* *107*, 2705-2717.
- Spies, T., Cerundolo, V., Colonna, M., Cresswell, P., Townsend, A., and DeMars, R. (1992). Presentation of viral antigen by MHC class I molecules is dependent on a putative peptide transporter heterodimer. *Nature* *355*, 644-646.
- Spiliotis, E.T., Pentcheva, T., and Edidin, M. (2002). Probing for membrane domains in the endoplasmic reticulum: retention and degradation of unassembled MHC class I molecules. *Mol Biol Cell* *13*, 1566-1581.
- Stoltze, L., Schirle, M., Schwarz, G., Schroter, C., Thompson, M.W., Hersh, L.B., Kalbacher, H., Stevanovic, S., Rammensee, H.G., and Schild, H. (2000). Two new proteases in the MHC class I processing pathway. *Nat Immunol* *1*, 413-418.
- Sugita, M., and Brenner, M.B. (1994). An unstable beta 2-microglobulin: major histocompatibility complex class I heavy chain intermediate dissociates from calnexin and then is stabilized by binding peptide. *J Exp Med* *180*, 2163-2171.
- Tang, B., Wong, S., Low, S., and Hong, W. (1992). Retention of a type II surface membrane protein in the endoplasmic reticulum by the Lys-Asp-Glu-Leu sequence. *J. Biol. Chem.* *267*, 7072-7076.
- Thompson, C.B. (1995). New insights into V(D)J recombination and its role in the evolution of the immune system. *Immunity* *3*, 531-539.

Thomson, S.P., and Williams, D.B. (2005). Delineation of the lectin site of the molecular chaperone calreticulin. *Cell stress & chaperones* *10*, 242-251.

Thrower, J.S., Hoffman, L., Rechsteiner, M., and Pickart, C.M. (2000). Recognition of the polyubiquitin proteolytic signal. *Embo J* *19*, 94-102.

Tolstrup, A.B., Duch, M., Dalum, I., Pedersen, F.S., and Mouritsen, S. (2001). Functional screening of a retroviral peptide library for MHC class I presentation. *Gene* *263*, 77-84.

Townsend, A., Elliott, T., Cerundolo, V., Foster, L., Barber, B., and Tse, A. (1990). Assembly of MHC class I molecules analyzed in vitro. *Cell* *62*, 285-295.

Townsend, A., Ohlen, C., Bastin, J., Ljunggren, H.G., Foster, L., and Karre, K. (1989). Association of class I major histocompatibility heavy and light chains induced by viral peptides. *Nature* *340*, 443-448.

Trowsdale, J., Hanson, I., Mockridge, I., Beck, S., Townsend, A., and Kelly, A. (1990). Sequences encoded in the class II region of the MHC related to the 'ABC' superfamily of transporters. *Nature* *348*, 741-744.

Turner, M.J., Sowders, D.P., DeLay, M.L., Mohapatra, R., Bai, S., Smith, J.A., Brandewie, J.R., Taurog, J.D., and Colbert, R.A. (2005). HLA-B27 misfolding in transgenic rats is associated with activation of the unfolded protein response. *J Immunol* *175*, 2438-2448.

Turnquist, H.R., Thomas, H.J., Prilliman, K.R., Lutz, C.T., Hildebrand, W.H., and Solheim, J.C. (2000). HLA-B polymorphism affects interactions with multiple endoplasmic reticulum proteins. *Eur J Immunol* *30*, 3021-3028.

Uebel, S., Kraas, W., Kienle, S., Wiesmuller, K.-H., Jung, G., and Tampe, R. (1997). Recognition principle of the TAP transporter disclosed by combinatorial peptide libraries
10.1073/pnas.94.17.8976. *PNAS* *94*, 8976-8981.

Uebel, S., and Tampe, R. (1999). Specificity of the proteasome and the TAP transporter. *Curr Opin Immunol* *11*, 203-208.

van Bleek, G.M., and Nathenson, S.G. (1991). The structure of the antigen-binding groove of major histocompatibility complex class I molecules determines specific selection of self-peptides. *Proc Natl Acad Sci U S A* *88*, 11032-11036.

van den Elsen, P., Shepley, B.A., Cho, M., and Terhorst, C. (1985). Isolation and characterization of a cDNA clone encoding the murine homologue of the human 20K T3/T-cell receptor glycoprotein. *Nature* *314*, 542-544.

Van Kaer, L., Ashton-Rickardt, P.G., Ploegh, H.L., and Tonegawa, S. (1992). TAP1 mutant mice are deficient in antigen presentation, surface class I molecules, and CD4-8+ T cells. *Cell* *71*, 1205-1214.

Vassilakos, A., Michalak, M., Lehrman, M.A., and Williams, D.B. (1998). Oligosaccharide binding characteristics of the molecular chaperones calnexin and calreticulin. *Biochemistry* *37*, 3480-3490.

Velarde, G., Ford, R.C., Rosenberg, M.F., and Powis, S.J. (2001). Three-dimensional structure of transporter associated with antigen processing (TAP) obtained by single Particle image analysis. *J Biol Chem* *276*, 46054-46063.

Wada, I., Imai, S., Kai, M., Sakane, F., and Kanoh, H. (1995). Chaperone function of calreticulin when expressed in the endoplasmic reticulum as the membrane-anchored and soluble forms. *J Biol Chem* *270*, 20298-20304.

Wada, I., Rindress, D., Cameron, P.H., Ou, W.J., Doherty, J.J., 2nd, Louvard, D., Bell, A.W., Dignard, D., Thomas, D.Y., and Bergeron, J.J. (1991). SSR alpha and associated calnexin are major calcium binding proteins of the endoplasmic reticulum membrane. *J Biol Chem* *266*, 19599-19610.

Walker, K.W., and Gilbert, H.F. (1997). Scanning and escape during protein-disulfide isomerase-assisted protein folding. *J Biol Chem* *272*, 8845-8848.

Wang, H., Capps, G., Robinson, B., and Zuniga, M. (1994). Ab initio association with beta 2-microglobulin during biosynthesis of the H-2Ld class I major histocompatibility complex heavy chain promotes proper disulfide bond formation and stable peptide binding. *J. Biol. Chem.* *269*, 22276-22281.

- Ward, B.M., and Moss, B. (2001). Visualization of intracellular movement of vaccinia virus virions containing a green fluorescent protein-B5R membrane protein chimera. *Journal of virology* 75, 4802-4813.
- Ware, F.E., Vassilakos, A., Peterson, P.A., Jackson, M.R., Lehrman, M.A., and Williams, D.B. (1995). The molecular chaperone calnexin binds Glc1Man9GlcNAc2 oligosaccharide as an initial step in recognizing unfolded glycoproteins. *J Biol Chem* 270, 4697-4704.
- Wearsch, P.A., and Cresswell, P. (2007). Selective loading of high-affinity peptides onto major histocompatibility complex class I molecules by the tapasin-ERp57 heterodimer. *Nat Immunol* 8, 873-881.
- Wearsch, P.A., Jakob, C.A., Vallin, A., Dwek, R.A., Rudd, P.M., and Cresswell, P. (2004). MHC class I molecules expressed with monoglucosylated N-linked glycans bind calreticulin independently of their assembly status. *J. Biol. Chem.*, M401721200.
- Wentworth, P., Jr., McDunn, J.E., Wentworth, A.D., Takeuchi, C., Nieva, J., Jones, T., Bautista, C., Ruedi, J.M., Gutierrez, A., Janda, K.D., *et al.* (2002). Evidence for antibody-catalyzed ozone formation in bacterial killing and inflammation. *Science* 298, 2195-2199.
- Wenzel, T., Eckerskorn, C., Lottspeich, F., and Baumeister, W. (1994). Existence of a molecular ruler in proteasomes suggested by analysis of degradation products. *FEBS Lett* 349, 205-209.
- Williams, A., Peh, C.A., and Elliott, T. (2002a). The cell biology of MHC class I antigen presentation. *Tissue Antigens* 59, 3-17.
- Williams, A.P., Peh, C.A., Purcell, A.W., McCluskey, J., and Elliott, T. (2002b). Optimization of the MHC class I peptide cargo is dependent on tapasin. *Immunity* 16, 509-520.
- Wolbink, G.J., Brouwer, M.C., Buysmann, S., ten Berge, I.J., and Hack, C.E. (1996). CRP-mediated activation of complement in vivo: assessment by measuring circulating complement-C-reactive protein complexes. pp. 473-479.
- Wright, C.A., Kozik, P., Zacharias, M., and Springer, S. (2004). Tapasin and other chaperones: models of the MHC class I loading complex. *Biol Chem* 385, 763-778.
- Yanagi, Y., Yoshikai, Y., Leggett, K., Clark, S.P., Aleksander, I., and Mak, T.W. (1984). A human T cell-specific cDNA clone encodes a protein having extensive homology to immunoglobulin chains. *Nature* 308, 145-149.
- Yewdell, J.W., and Bennink, J.R. (1999). IMMUNODOMINANCE IN MAJOR HISTOCOMPATIBILITY COMPLEX CLASS I RESTRICTED T LYMPHOCYTE RESPONSES. *Annual Review of Immunology* 17, 51-88.
- Yu, Y.Y., Turnquist, H.R., Myers, N.B., Balendiran, G.K., Hansen, T.H., and Solheim, J.C. (1999). An extensive region of an MHC class I alpha 2 domain loop influences interaction with the assembly complex. *J Immunol* 163, 4427-4433.
- Zacharias, M., and Springer, S. (2004). Conformational flexibility of the MHC class I alpha1-alpha2 domain in peptide bound and free states: a molecular dynamics simulation study. *Biophysical journal* 87, 2203-2214.
- Zagouras, P., and Rose, J.K. (1989). Carboxy-terminal SEKDEL sequences retard but do not retain two secretory proteins in the endoplasmic reticulum. *J Cell Biol* 109, 2633-2640.
- Zhang, Q., and Salter, R.D. (1998). Distinct Patterns of Folding and Interactions with Calnexin and Calreticulin in Human Class I MHC Proteins with Altered N-Glycosylation. *J Immunol* 160, 831-837.
- Zinkernagel, R.M. (2003). On natural and artificial vaccinations. *Annu Rev Immunol* 21, 515-546.
- Zinkernagel, R.M., and Doherty, P.C. (1974). Restriction of in vitro T cell-mediated cytotoxicity in lymphocytic choriomeningitis within a syngeneic or semiallogeneic system. *Nature* 248, 701-702.